BULLETIN 101

GEOLOGIC FIELD TRIPS in WESTERN OREGON and SOUTHWESTERN WASHINGTON

PUBLISHED BY
STATE OF OREGON
DEPARTMENT OF GEOLOGY AND MINERAL INDUSTRIES

FOR THE
GEOLOGICAL SOCIETY OF AMERICA, CORDILLERAN MEETING
CORVALLIS, OREGON, MARCH 1980

STATE OF OREGON
DEPARTMENT OF GEOLOGY AND MINERAL INDUSTRIES
1069 State Office Building
Portland, Oregon 97201

BULLETIN 101

GEOLOGIC FIELD TRIPS IN WESTERN OREGON AND SOUTHWESTERN WASHINGTON

Keith F. Oles, J. Granville Johnson, Alan R. Niem, & Wendy A. Niem
Editors

Alan R. Niem, Wendy A. Niem, Edward M. Taylor, Herbert G. Schlicker
Field Trip Committee Co-chairmen

for the

GEOLOGICAL SOCIETY OF AMERICA
Cordilleran Section Meeting
Corvallis, Oregon   March 1980

CONTENTS

PREFACE

The geology of the Pacific Northwest is not only varied, but its expression in the landscape is a major factor in the scenic beauty of this region. Much is known about the geology of the Northwest, but much more remains to be studied and interpreted. The papers and field trip guides in this text reflect recent and continuing geologic research and will contribute to our understanding of the history of this region.

The areas and subject matter covered in the articles describe nine field trips which range from southwestern Washington to the southern Oregon Coast; these accounts emphasize the Paleogene rocks of the Coast Range and its structural aspects along with articles on the Neogene rocks, structure, and geomorphology of the Oregon Cascades. The article by Komar and others on beach processes along the present Oregon coast perhaps highlights the fact that the Cenozoic evolution of the Northwest involved a dynamic and evanescent coastline which faced a shrinking Pacific Ocean.

This guidebook is being issued in conjunction with the 76th annual meeting of the Cordilleran Section of the Geological Society of America. We hope that the text will not only benefit those earth scientists attending the field trips, but also will be an invaluable guide to the interested layman or geologist who, independently at a later date, will visit the same localities.

The editors wish to take this opportunity to thank the many geologists who have expended time and effort to produce the several field trips and the accompanying texts and illustrations. Their willingness to share their research is deeply appreciated. Our thanks go also to Alan R. Niem, Wendy A. Niem, Edward M. Taylor, and Herbert G. Schlicker, the co-chairmen of the Field Trip Committee. For more than a year they have been organizing this sequence and it is because of their work that this interesting and varied spectrum of geological field trips is possible. Special thanks are extended to Beverly F. Vogt, Geologist-Editor of the Oregon Department of Geology and Mineral Industries, for her efforts in the publication of this guidebook.

K. F. Oles and J. G. Johnson

Cover photograph: view northwest across Oregon State University campus to east flank of Coast Range.

VOLCANIC AND VOLCANICLASTIC ROCKS ON THE EAST FLANK OF THE CENTRAL CASCADE RANGE TO THE DESCHUTES RIVER, OREGON

Edward M. Taylor
Department of Geology
Oregon State University

INTRODUCTION

A calc-alkalic volcanic arc has been intermittently active during the last 10-15 m.y. along the eastern part of the central Cascade Range in Oregon. The late Pleistocene record of this volcanic activity is well preserved on the crest of the High Cascades; the best exposed record of early Pleistocene, Pliocene, and late Miocene Cascade volcanism is found in volcanic and volcaniclastic deposits on the east flank of the range and in the adjacent Deschutes Basin. In the following discussion, structural, stratigraphic, and magmatic features of the Western Cascade, High Cascade, and Deschutes Basin subprovinces are described and their interrelationships are briefly summarized.

Central High Cascade Province

The central High Cascade Range in Oregon is chiefly a Pleistocene volcanic platform of overlapping basalt and basaltic andesite lava flows whose aggregate thickness is generally unknown but probably exceeds 4,000 feet locally. This platform is elongate north-south and is 20-30 miles wide. A typical volcano of the platform is a broad shield of light-colored, vesicular basaltic andesite with a cinder cone core that has been invaded by plugs and radial dikes. Pleistocene examples exposed in cross-section by glacial erosion include Sphinx Butte south of Separation Creek canyon, Deer Butte north of Lost Creek canyon, and Bald Peter east of Jefferson Creek canyon; a perfectly preserved Holocene example is Belknap Crater on the McKenzie Pass summit. Some of the basaltic andesite volcanoes developed large composite structures reaching 10,000 feet elevation on a shield base 10 miles wide. Examples include The Husband, North Sister, Mount Washington, and Three Fingered Jack. In contrast, many volcanoes of the platform were active for only a brief time and produced small cinder cones with or without narrow lobes of lava. Holocene examples abound; they include Yapoah Cone, Twin Craters, and Sims Butte near McKenzie Pass, and Nash Crater, Lost Lake Cones, and Blue Lake Crater near Santiam Pass. Pleistocene cinder cones are no less abundant but they are not as well preserved. Examples of glaciated remnants of Pleistocene cones include Bluegrass Butte, Condon Butte, and Scott Mountain near McKenzie Pass and Maxwell Butte, Hoodoo Butte, and Cache Mountain near Santiam Pass.

A systematic temporal inhomogeneity exists within the High Cascade platform. Early Pleistocene lavas were predominantly high-alumina olivine tholeiites in vesicular, thin, widespread units, commonly with pronounced diktytaxitic textures. Later Pleistocene lavas were predominantly high-alumina basaltic andesites in thick, platy units, generally with pilotaxitic textures. The early basalts crop out in greater abundance and variety along the western and eastern margins of the platform and in the walls of deeply glaciated canyons; however, identical basalts do occur at higher levels. Later basaltic andesites cover most of the platform but they are also found at lower stratigraphic levels. Examples of early basalts are well exposed along the west margin of the platform at Cupola Rock in Lost Creek canyon, in cuts of Highway 126 north of Trailbridge Reservoir, and in the valley of Hackleman Creek west of Fish Lake. Early basalts along the east margin of the platform are widespread in the upper Metolius River valley and in the vicinity of Sisters.

A systematic spacial inhomogeneity also exists within the High Cascade platform. West of Bend, in the vicinity of South Sister, silicic volcanic rocks are interbedded with and rest upon the mafic platform rocks. A silicic highland of some 15 miles breadth was produced by the development of rhyolite, rhyodacite, and dacite domes surrounded by andesite, dacite, and rhyodacite lavas and ash-flow tuffs. Most of this highland is mantled by mafic cinder cones and lavas of the Triangle Hill group and by composite volcanoes such as Broken Top. Examples of interbedded andesites, dacites, and rhyodacite lavas are common in upper Squaw Creek and Tumalo Creek canyons. Two units of black andesitic ash-flow tuff (Century Drive Tuff and Shevlin Park Tuff) and one unit of pink, devitrified, dacite ash-flow tuff (Desert Spring Tuff) were erupted from the highland and are well exposed west of Bend. Two rhyodacite ash-flow tuffs (Tumalo Tuff and Lava Island Tuff) and one extensive lapilli-fall pumice deposit (Bend Pumice) of High Cascade origin are also exposed near Bend but were probably erupted from a vent south of the silicic highland.

South Sister volcano is chiefly andesite with minor dacite and rhyodacite. Broken Top (east of South Sister) is basaltic andesite with minor interbedded dacite and rhyodacite lavas and small-volume ash-flow tuffs. Middle Sister (north of South Sister) is basalt with minor basaltic andesite, andesite, dacite, and rhyodacite. South Sister and nearby volcanoes are relatively late products of long-continued, compositionally diverse, and localized silicic magmatism.

In summary, the central High Cascade Range is not the simple Pliocene-Pleistocene belt of andesite volcanoes commonly depicted in geology textbooks; instead, it is a broad Pleistocene platform of mafic composition in which open-textured basaltic lavas were at first predominant, then became subordinate to basaltic andesite. Silicic magma has invaded this platform throughout its development but only in isolated regions.

Deschutes Basin Province

The eastern margin of the central High Cascade platform is marked by a very irregular contact with the late Miocene and Pliocene Deschutes Formation. Early platform intracanyon lavas extend as much as 5 miles east of the Cascade foothills and isolated Pleistocene volcanoes of basalt and basaltic andesite rest on Pliocene rocks of the Deschutes Basin. Examples of High Cascade intracanyon lavas occur in lower Metolius River canyon, Deep Canyon, and near Squaw Creek, Bull Flat, and Tumalo Creek between Sisters and Bend. Isolated volcanoes of High Cascade affinity include Squaw Back Ridge, Long Butte, and Pilot Butte and Awbrey Butte near Bend.

The Deschutes Formation contains stream-deposited silt, sand, and gravel, andesitic-to-rhyodacitic ash-flow and ash-fall tuffs, and interbedded basalt flows. The basaltic lavas were erupted from cinder cones and fissure vents within the Deschutes Basin but the epiclastic and volcaniclastic rocks were chiefly of Cascade provenance. Close to the Cascades, the formation becomes thicker, basaltic andesite lavas predominate, and the volcaniclastic rocks become discontinuous interbeds. Indicators of transport direction within the volcaniclastic sediments point eastward. Deschutes Formation source volcanoes were coincident with, or not far removed from the High Cascade axis. One deeply dissected remnant of an andesitic Deschutes Formation source volcano is located at the bend of Metolius River, 12 miles east of Mount Jefferson.

Strata of the Deschutes Formation between Warm Springs and Bend are generally flat-lying except where they are offset by north-northwest-trending normal faults of small displacement. These faults are part of the Brothers-Sisters Fault Zone and are best exposed in cross-section along cuts of Highway 126 in Deep Canyon east of Sisters. The Deschutes Formation is unconformably underlain by folded and faulted basalts of the mid-Miocene Columbia River Group on the north and by silicic domes, lavas, and tuffaceous rocks on the south, variously ascribed to Clarno and John Day Formations of early Tertiary age.

Parts of the High Cascade - Deschutes Formation contact are fault controlled. This is especially obvious at the west base of the Green Ridge escarpment, a 20-mile-long-north-south fault block in which upper Deschutes Formation rocks rise 2,000 feet above the east edge of the High Cascade platform. K-Ar ages of rocks on the crest of Green Ridge and of lavas emplaced against the base of the scarp indicate that faulting occurred during the interval 2.5 to 4.5 m.y. ago (Armstrong and others, 1975). A closely related but much less spectacular feature is the Tumalo Fault between Sisters and Bend. The Tumalo Fault can be traced without interruption for 15 miles; north and south segments extend its length another 10 miles. Parts of the Tumalo Fault were reactivated during the Pleistocene.

Green Ridge probably marks the east flank of a prominent Pliocene volcanic complex. North and south of Green Ridge the trace of a major fault is obscure; isolated hills of Deschutes Formation are surrounded by lavas of the platform and a previously existing fault-controlled topography appears to have been extensively eroded and almost completely buried.

A correct interpretation of the east-margin fault system is of great significance in understanding High Cascade and Deschutes Basin geology. My interpretation can be summarized as follows:

1. Deschutes Formation basaltic andesite lavas, andesite lavas, and ash-flow tuffs were derived from volcanoes near the present High Cascade axis and flowed eastward into the Deschutes Basin more than 4.5 m.y. ago. Rock units desposted by this process have been traced from Green Ridge to the Deschutes River. They reveal a continuous, gentle eastward dip of only 1-2 degrees. Therefore, Green Ridge cannot represent a tilted-up fault block. It is, instead, a remnant of stable eastern Cascade foothills and its rocks still rest on an initial paleoslope.

2. The maximum age yet obtained by radiometric dating of central High Cascade platform rocks is 3.9 m.y. Therefore, Deschutes Formation rocks and source volcanoes must lie beneath the Cascade platform and displacement of the east-margin fault system probably exceeds (and might greatly exceed) 3,000 feet.

3. If Green Ridge has not been displaced upward relative to the Deschutes Basin, the Cascade axis has been displaced downward. This presumably occurred about 4.5 m.y. ago, terminating deposition of Deschutes Formation rocks.

Is it possible that a whole range of Pliocene composite volcanoes foundered and was buried beneath the Pleistocene High Cascade platform? Such an interpretation is strongly suggested by available field evidence. With appropriate informality, this hypothetical assemblage of volcanic rocks might be called the "Plio-Cascades."

East Margin of the Central Western Cascade Province

Stratigraphic and structural relationships at the western margin of the central High Cascade platform are obscured by more extensive erosion, thicker alluvial cover, and more luxuriant vegetation than along the eastern margin. However, striking similarities are evident. Isolated Pleistocene volcanoes of basalt and basaltic andesite occur in the Western Cascades at least 20 miles west of the platform. Examples include Harter Mountain, a cinder cone and flow near Quartzville, and Battle Ax Mountain. Early High Cascade platform basalts occur as intracanyon lavas in the adjacent Western Cascades. Examples include diktytaxitic basalts of Foley Ridge in the canyon of McKenzie River and similar rocks in the canyon of North Santiam River.

Rocks of the Western Cascades adjacent to the central High Cascade platform are predominantly late Miocene and Pliocene mafic lavas (Armstrong and others, 1975; Sutter, 1978) with subordinate ash-flow tuffs and silicic volcanic domes. These rocks have been included in the Sardine Formation by Peck and others (1964) but should be assigned to the Outerson Formation of Thayer (1937). They are equivalent in lithology and age to the Deschutes Formation. They are generally flat-lying except where they are offset by northwest-trending normal faults of small displacement. Although many units of the Outerson Formation were vented along the eastern edge of the Western Cascades, several andesitic ash-flow tuffs and one basaltic andesite ash-flow tuff appear to have moved westward from

Plio-Cascade volcanoes. Examples of Outerson Formation rocks can be seen along the south-to-north crestline of mountains which includes Frissell Point, Bunchgrass Mountain, Browder Ridge, Iron Mountain, Echo Mountain, Crescent Mountain, Three Pyramids, and Coffin Butte.

Outerson Formation rests with angular and/or erosional unconformity upon a complex and poorly exposed assemblage of moderately deformed, altered, silicic volcaniclastic rocks with subordinate lavas and intrusive bodies. These rocks are part of the Sardine Formation. Examples of pre-Outerson rocks are best seen west of the Frissell Point-Coffin Butte crestline in canyons tributary to McKenzie River and South, Middle, and North Santiam Rivers. Many of these rocks have been assigned K-Ar ages between 14 and 20 m.y. by Sutter (1978).

Although field evidence is still inconclusive, it is likely that the eastern part of the central Western Cascades was displaced several thousand feet down on the east side of a north-south fault system during the interval 4 to 5 m.y. ago. Outerson Formation rock units exceed 3,000 feet in thickness and are approximately horizontal in attitude along the Frissell Point - Coffin Butte crestline. In the east face of a 30-mile-long deeply eroded north-south escarpment, they "sky-out" over the younger High Cascade platform. A major fault has been found at the base of this escarpment in a few places. For example, in the vicinity of Belknap Hot Springs, rocks on the crestline west of the fault are 6.2 m.y. old; rocks of the same age east of the fault occur 2,000 feet lower (Armstrong and others, 1975). Throughout its length, this fault system has been obscured by glaciation of the escarpment and by lavas of the High Cascade platform deposited against the base of the escarpment.

If it can be demonstrated that the High Cascade axis was displaced downward along marginal boundary faults relative to the Deschutes Basin and Western Cascades during the interval 3 to 4.5 m.y. ago, the High Cascade platform should be viewed as a Pleistocene fill within a Pliocene graben. On the basis of my own limited experience, I believe that this condition prevailed north at least as far as Mount Adams and south at least as far as Crater Lake, but was not necessarily continuous in time or space. It is likely that such a structure, 20 miles wide, would subside along many fractures, chiefly trending north-south. Intragraben faults could have served as channelways for ascending magma. This might explain why volcanoes on the High Cascade platform commonly occur within long north-south alignments and why volcanoes adjacent to the platform tend not to do so. The early flood of gas-rich diktytaxitic basalts might be related to unusually rapid ascent of magma during a time of relative crustal tension. Correspondingly, the later dominance of basaltic andesite might reflect a slower ascent and greater opportunity for evolution of magmas.

Considerable evidence now suggests that a broad calc-alkaline volcanic field consisting of Deschutes Formation, "Plio-Cascades," and Outerson Formation rocks covered the eastern half of the central Cascade Range during late Miocene and Pliocene time. If it is assumed that a subduction system was responsible for this volcanism, it might also be assumed that the subduction process became inactive or modified approximately 4.5 m.y. ago. This might have led to relaxation of the crust, subsidence along the volcanic axis, less frequent ascent of andesite-dacite magmas from more restricted, residual reservoirs, and much increased outpouring of basaltic magma from relatively shallow levels, probably associated more with Basin and Range magmatism than with a subduction system. However, it is easy to propose models. Testing their validity will require years of intense effort on many fronts.

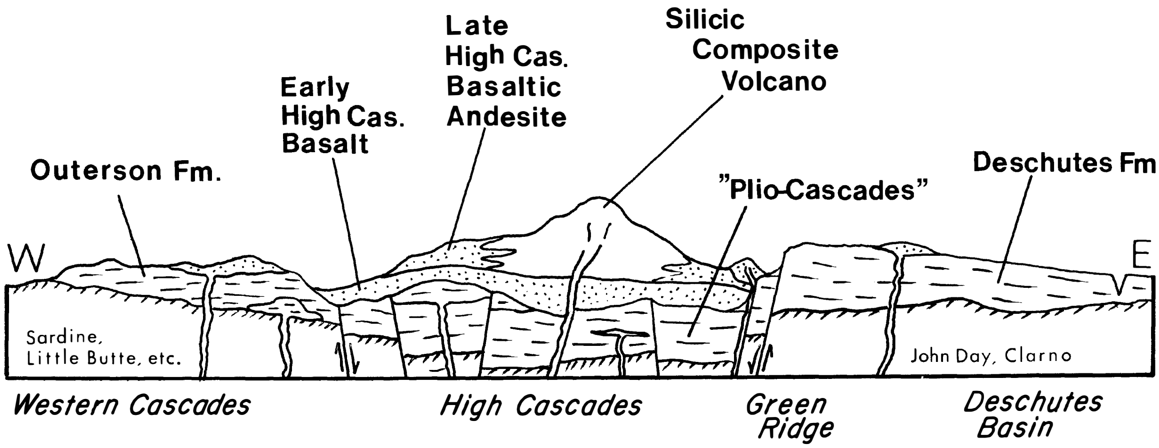

FIGURE 1. DIAGRAMMATIC CROSS SECTION OF THE CENTRAL CASCADES OF OREGON.

FIELD TRIP ITINERARY

Because of the extremely variable weather, snow cover, and road conditions that exist on the Cascade east slope in springtime and the consequent likelihood of last-minute changes in route, a detailed geologic road guide will not be given. The following is an itinerary of the regions to be traversed and the features to be studied.

First Day

Leg 1. Corvallis to Santiam Pass via Highways 34 and 20. A few brief stops will be made west of Tombstone Summit to examine several ash-flow tuffs of the Sardine and Outerson Formations. Many are extensively weathered and consist of little but clay; others contain plutonic xenoliths; some are of mafic composition.

Leg 2. Santiam Pass to Sisters. Air-fall tuffs and mafic lavas of the Green Ridge escarpment will be examined. A logging road ascends the escarpment from a point near Metolius River Bridge 99 and will be used if it is accessible. A clear day on Green Ridge will afford spectacular views of the High Cascades from Mt. Hood to Three Sisters.

Leg 3. Sisters to Tumalo State Park via Highway 126 and secondary roads leading south. Lavas and ash-flow tuffs of the uppermost Deschutes Formation will be examined in the west wall of Deep Creek Canyon along Highway 126. Early High Cascade intracanyon lavas and ash-flow tuffs will be examined in outcrops along Fryrear, Tumalo Reservoir, and Johnson roads.

Leg 4. Tumalo State Park to Century Drive. Cross sections of four ash-flow tuffs and one pumice lapilli-fall deposit of High Cascade origin will be studied in quarries and canyon walls northwest, west, and southwest of Bend. The most complete exposures of ash-flow units in vertical section will be seen in privately owned active quarries where permission to trespass must be obtained.

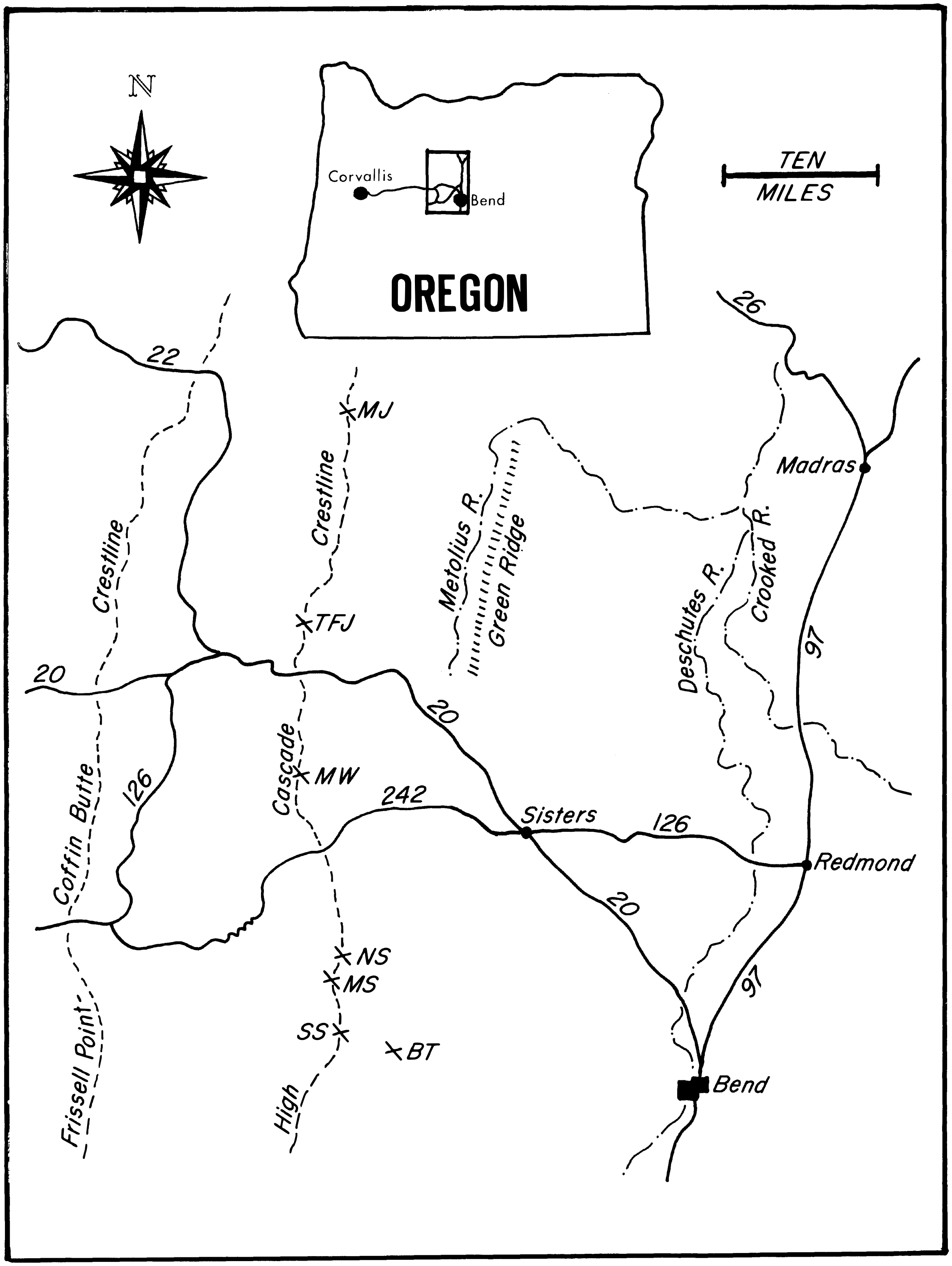

FIGURE 2. INDEX MAP.

Second Day

Leg 5. Bend to Helmholtz Road west of Redmond. A spectacular and enigmatic lahar will be examined in the east wall of Deschutes River canyon, 2.5 miles north of Highway 126.

Leg 6. Tethrow Buttes to Lower Bridge. Ash-flow tuffs, air-fall tuffs, and diatomite beds of the Deschutes Formation will be examined in roadcuts and canyon walls near Lower Bridge.

Leg 7. Lower Bridge to Pelton Dam, nonstop via Highway 97. Route will provide views and mid-Tertiary rhyolite domes (such as Juniper Butte) and volcaniclastic rocks (Smith Rocks) north of Redmond. Where Highway 26 descends into Deschutes River canyon north of Madras, the Deschutes Formation rimrock basalts will be seen to overlie a section of Deschutes Formation volcaniclastic rocks, Columbia River Group lavas, and John Day Formation tuffs. Lower Deschutes Formation tuffs will be studied in the vicinity of Pelton Dam.

Leg 8. Pelton Dam to summit of Round Butte and south to Deschutes Canyon viewpoint. Several picturesque and instructive vantage points will afford excellent views of the central Deschutes Basin and its fill of volcaniclastic rocks from Green Ridge on the west to Ochoco foothills on the east.

Leg 9. Crooked River and Deschutes River arms of Round Butte Dam Reservoir. Volcaniclastic rocks of the best exposed and most accessible section of the Deschutes Formation will be examined in road cuts between Cove Palisades State Park and Lower Desert (tableland west of Deschutes River canyon).

Leg 10. If road conditions are favorable, leg 10 will follow Fly Creek - Green Ridge logging roads to Highway 20 and on to Corvallis. Otherwise, leg 10 will retrace Highways 97, 126, and 20 to Corvallis.

PALEOGENE STRATIGRAPHY AND STRUCTURE ALONG THE KLAMATH BORDERLAND, OREGON

Ewart M. Baldwin, University of Oregon, and
Rauno Perttu, Bear Creek Mining Co.

Introduction

The Paleogene strata were deposited in a mobile belt bordering the continental margin at a time deformation in the Klamath Mountains influenced rate of sedimentation and distribution of lithologies and formations. Most of the sediments came from the Klamath Highland filling a tectonically active basin.

Baldwin (1974, 1975) summarized Paleogene stratigraphic units with a generalized map showing known distribution of units with suggested paleoshorelines. He reviewed geologic work done prior to those dates and the present summary refers largely to work done later.

Perttu (1976) named and described the Canyonville fault zone along the northern Klamath borderland and discussed movement in relation to sedimentation in the Dutchman Butte area. Simpson and Cox (1977) proposed clockwise rotation of 50-70 degrees of the southern Coast Range. Miles (1977) furnished micropaleontological data which aid in refining age assignments. Gandera (1977) mapped the Lorane Siltstone and revised contacts between the Spencer and Flournoy formations west of Eugene.

Baldwin (1974, 1975) divided the Umpqua Formation of Diller (1898) into the Roseburg, Lookingglass, and Flournoy Formations and elevated the Umpqua to group status. He assigned all of the volcanics and the thick flysch-like beds to the Roseburg Formation. Nearly all Roseburg contacts are faulted and it is only in Elk Valley and along the West Branch of Cow Creek that beds assigned to the Roseburg may be seen resting unconformably upon the Dothan Formation. The volcanic rocks are absent at these localities. The Roseburg was closely folded and reverse-faulted during plate movements at the end of the early Eocene.

The Lookingglass Formation, with a thick basal conglomerate, the Bushnell Rock Member, representing onlapping seas grades upward to sandstone and siltstone, the Tenmile Member. An upper offlapping massive pebbly sandstone and conglomerate, present on Tenmile Butte and along Olalla Creek, is called the Olalla Creek Member (Baldwin, 1974) (Figures 4,6).

The Flournoy Formation is generally disconformable where its basal sandstone rests upon older formations. The basal sandstone, the Whitetail Ridge Member, grades upward into thin-bedded sandstone and siltstone, the Camas Valley Member. The Lorane Siltstone and beds at Sacchi Beach south of Cape Arago are correlated with the Camas Valley Member of the Flournoy.

Baldwin (1975) restricted the Tyee Formation to the center of the southern Coast Range where it rests unconformably upon older formations. The unit thins northward and grades upward into the Elkton Siltstone which in turn is overlain by the offlapping sands of the Bateman Formation.

The Coaledo Formation occupies a north trending basin in the Coos Bay area west of the central part of the Coast Range. It is unconformable upon older units where they are in contact and it is not known to be in contact with the Tyee or Elkton Formations which are restricted to the central part of the range. The Spencer Formation, which correlates with the Coaledo, is unconformable upon older units in the Corvallis and Eugene areas.

The late Eocene Bastendorff Formation, made up largely of siltstone and shale, is overlain abruptly but conformably by tuffaceous sandstone of the Tunnel Point Formation

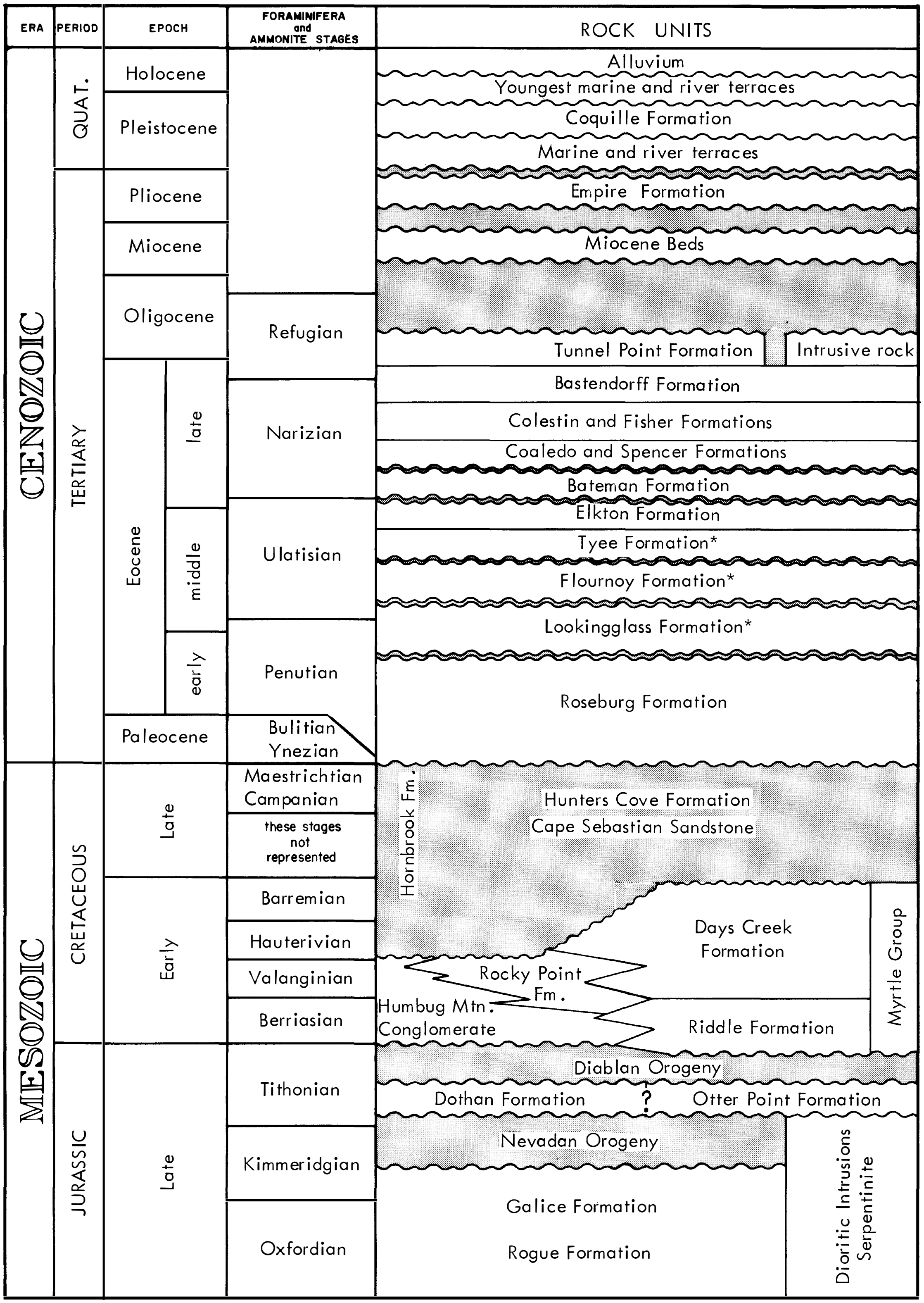

*For discussion of members see text

Table 1. Stratigraphic column for southwestern Oregon (From Baldwin 1974)

in the Coos Bay area. The Tunnel Point Formation has usually been assigned to the early Oligocene but Armentrout (1973) places it in the late Eocene.

The Fisher Formation composed largely of fragmental volcanic material is overlain by and possibly interfingers with the tuffaceous beds of the Eugene Formation. The Fisher Formation occupies approximately the same position as the Bastendorff Formation and the Eugene Formation is considered to be equivalent to the Tunnel Point Formation and latest Eocene.

Plate movements preceeding and accompanying Paleogene deposition had a profound effect on character and distribution of the sedimentary units. Perttu (1976; p. 49-52) summarized geologic events as follows:

"In Late Jurassic time, trench and slope sediments were deposited on a subducting sea floor of 'western Rogue' (the volcanics in the block along Mule Creek assigned by some to the Rogue Formation). The sediments and volcanics of the Otter Point Formation accumulated near the trench, while the Dothan Formation sediments probably accumulated on the slope and possibly locally on the shelf."

"The Otter Point and Dothan sediments were probably deformed as they accumulated as well as after deposition, because of continued underthrusting along the continental margin. Before the deposition of the Myrtle Group, the 'western Rogue' seafloor was obducted relative to the Otter Point and Dothan formations. Possibly some of the volcanic blocks in the Otter Point Formation were derived from the 'western Rogue Formation' during its obduction."

"Shortly after deposition and initial deformation of the Otter Point and Dothan formations and obduction of the 'western Rogue,' right-lateral faulting began along the Canyonville fault zone. The faulting probably offset two active trench segments."

"As a result of the right-lateral faulting, the Canyonville fault zone locally formed the latest Jurassic and Early Cretaceous shoreline. Along and near the shoreline, the Myrtle Group sediments were deposited as near shore and probably locally as nonmarine fluvial-deltaic sediments. Right-lateral movement along the zone, as well as regional subduction in the offset trench segments, with accompanying deformation, continued, possibly sporadically, deforming the Myrtle Group rocks."

"By Lookingglass time, the right-lateral movement along the Canyonville fault zone was replaced by vertical movement. Regionally, southeast to northwest compressive deformation parallel to the pre-Tertiary was ending, possibly because subduction along the continental margin was ending locally or because in Roseburg and Lookingglass time, the subduction zone in western Oregon was shifted westward to a position west of the present shoreline. A possible fix on the timing of the proposed westward stepping of subduction would be: Roseburg time, active subduction; Lookingglass time, westward stepping of subduction and end of associated compressive deformation; Flournoy and Tyee time, northward building of deltaic deposits across a now inactive shelf and slope."

An alternate explanation by Perttu of the Canyonville fault zone is that it may represent a rotated southern extension of the Straight Creek fault in Washington (Misch, 1966; Tabor and Frizzell, 1979). Simpson and Cox (1977) proposed up to 70 degrees clockwise rotation of southwest Oregon. If the Canyonville fault is rotated back to its proposed original orientation, with accompanying closing of proposed Basin and Range extension, the fault becomes generally northerly in trend and lies approximately on projection of the Straight Creek fault. Directions and times of movement and relative magnitudes of offset are similar on the faults. After rotation back to the presumed original orientation for the Canyonville fault, the Mesozoic lithologies cut by the Canyonville fault are subparallel to similar lithologies cut by the Straight Creek fault. If the two faults were originally continuous, then the setting and lithologies of the Canyonville fault suggest that it may have been trending at a low angle across a continental shelf and slope in a somewhat similar manner to the Denali-Fairweather fault of today.

Stratigraphy

Roseburg Formation

The Roseburg Formation is exposed primarily on either side of the southern Coast Range south of Drain and Coos Bay. It contains several thousand feet of pillow and brecciated basalt, tuff, and interbedded lenses of sedimentary rock deposited beneath the sea. The basalt is confined to the lower part of the formation. The upper part is made up of a thick section of turbidites with minor amounts of conglomerate and blocks of blueschist and greenstone as wild flysch near Bridge and along the East Fork of the Coquille River.

Two Roseburg sections have been plotted although thickness is only tentative. One along the North Fork of the Umpqua River starts a few hundred feet west of the Frear Bridge and extends westward toward Roseburg. If not repeated this section would contain several thousand feet of extrusive volcanic rock and a few lenses of sedimentary rock. It is possible that the volcanic section is duplicated by imbricate faulting. Some of the sedimentary interbeds seem to be clear depositional during extrusion. Although pillow lavas are particularly common along the North Fork of the Umpqua, basalt near Drain and along Hayhurst road appears to be subaerial extrusions. In an island arc some extrusions would be submarine and others subaerial. Above the volcanic unit is a thick sedimentary section exposed along US I-5 south of the Red Hill anticline to the vicinity of Oakland (Figure 3). The exposures are intermittent but, if the dips are projected, as much as 8,000 feet may be present. Silt and mudstone are common in the lower part and graded sandstone beds are present and form ridges and the narrows in the valley just north of the northern turnoff from I-5 to Oakland.

Another section is exposed along State Highway 42 between Coquille and Myrtle Point. At least 2,000 feet of basalt is present without the base being exposed. Then assuming relatively continuous dips to the southeast past the areas of poor exposure as much as 8,000 feet of sedimentary rock could also be present. In both the Umpqua River and Highway 42 sections the top is eroded or faulted off so that one cannot determine the original thickness, but 15,000 feet seems to be a reasonable estimate for the formation in some places.

A logging road constructed in the Sutherlin Creek drainage revealed approximately 2,000 feet of siltstone, sandstone and fine-pebble conglomerate. These beds are not turbidites and appear to be shelf deposits unlike other sections of the Roseburg Formation. They appear to be overlain to the southeast by the volcanic unit but this may be a thrust along the Bonanza Fault. If beneath the thrust then the sedimentary section at the head of Sutherlin Creek may be a facies of the Roseburg but if actually below the basalt it could be a new stratigraphic unit.

Most of the fossil evidence points to a Penutian, early Eocene age, for the Roseburg Formation although earlier assignments have ranged into the Paleocene. Miles (1977) examined the microfaunas and found no evidence for a Paleocene age. The Roseburg was probably deposited on an oceanic plate as it was being subducted. The beds were closely folded and perhaps are duplicated by faulting.

Lookingglass Formation

The Lookingglass Formation was named by Baldwin (1974). One section is exposed along the south side of Lookingglass Valley where the name was derived, but a better section lies along Tenmile Creek where approximately 5,000 feet is exposed. The basal member is made up of 800-1,000 feet of conglomerate which is exposed in Bushnell Rock and along the ridge paralleling the north side of Highway 42 from Alexander Butte to the point it is unconformably overlain by the Flournoy Formation west of Tenmile Creek. This is the Bushnell Rock Member.

The conglomerate is overlain by a thick section of thinly bedded sandstone and siltstone which underlies the valley east of the Tenmile Post Office. It is called the

Tenmile Member. This member may thin or almost pinch out to the south where the congomerate coming from the Klamath Highlands predominates.

The uppermost part of the Lookingglass Formation in the Camas Valley, Bone Mountain and Sitkum quadrangles is a massive sandstone and conglomerate, perhaps representing deposition in an offlapping sea. This member caps Tenmile Butte but is thicker and coarser along Olalla Creek near the mouth of Coarse Gold Creek and is called the Olalla Creek Member.

Perttu (1976) suggested that repeated movement along a shear zone, which he named the Canyonville fault zone, governed the outpouring of Eocene sediments probably coupled with periodic uplift of the Klamath block. The zone with a pre-Lookingglass movement of 40 km or more borders the northern Klamaths and extends eastward along Cow Creek then divides into several faults in the southern part of the Dixonville quadrangle which was mapped by Seeley (1974). Thus nearest to the Klamaths there is more conglomerate and northward an increase in siltstone. According to Perttu (1976; p. 35) "Before Lookingglass time, and possibly before Roseburg time, extensive right-lateral faulting characterized the zone. Right-lateral faulting was followed by down-to-the-north faulting in Lookingglass, and possibly into post-Lookingglass time. During Riddle and Days Creek time and again in early to middle Eocene time, the Canyonville fault zone formed the southern shoreline of a marine embayment."

The Lookingglass Formation is represented by infaulted blocks of the Bushnell Rock Member along Cow Creek. In Lookingglass Valley and northward to the south side of Woodruff Mountain the formation strikes northwestward and disappears beneath the Tyee escarpment. The formation is present in the Powers quadrangle at Gaylord, near Powers, and along upper Salmon Creek and the head of the Sixes River, and in the Bandon quadrangle along Bear Creek. It may be present in some of the deep wells in the center of the Coast Range but does not crop out north of Bandon and Woodruff Mountain.

Although the Lookingglass deposition followed severe deformation and erosion of the Roseburg, both contain a Penutian microfossil assemblage. This indicates rapid tectonic movements with accompanying deformation and erosion of the underlying Roseburg beds occurred before deposition of the massive basal conglomerate of the Lookingglass. At least locally, the basal conglomerate was involved in Roseburg-style deformation, which died off before or during deposition of the overlying members.

Flournoy Formation

The Flournoy Formation was named by Baldwin (1974) for Flournoy Valley which is drained by Lookingglass Creek. It rests unconformably upon the Roseburg in places where the Lookingglass is missing north of Bushnell Rock and along the north edge of Lookingglass Valley. The lower part of the formation is mostly sandstone which appears to be near-shelf deposits in its type area. Along the western and northern parts of the basins it is composed of more distinctly graded beds of sandstone and siltstone and may represent a position farther out on the shelf. White Tail Ridge, east of Lookingglass Creek, is made up of the basal sand and is the type section of the White Tail Ridge Member. The sandstone grades rapidly upward into thin-bedded sandstone and siltstone with the siltstone dominant in the upper part. The more argillaceous beds crop out in the upper part of the Flournoy Valley section and in Camas Valley where they have been designated as the Camas Valley Member. The siltstone is unconformable beneath the rim of Tyee sandstone at the Signal Creek Lookout west of Camas Valley. It also crops out in the Middle Fork of the Coquille River and Rock Creek beneath and on both sides of Bone Mountain and intermittently beneath the Tyee Formation just west of Sitkum and in the north Fork of the Coquille River.

The White Tail Ridge Member of the Flournoy Formation underlies the Tyee sandstone at the head of Big Creek where the Camas Valley Member is missing. The two formations may be told apart by the dissimilar types of bedding present. The Flournoy bedding is graded whereas the Tyee is nongraded, crossbedded and contains much more massive sandstone and less amounts of siltstone. At this point on the ridge between Big Creek and the East Fork of the Coquille at Sitkum, the Tyee strikes northward to Brewster Rock, Coos Mountain, and Gold and Silver Falls whereas the Flournoy strikes northwesterly and the Camas Valley Member is present unconformably beneath the Tyee Formation. The graded beds in the Coos Bay area west of Coos Mountain are Flournoy. They exhibit steeper dips than those of the Tyee and may be traced northward past Reedsport, Siltcoos Lake, into the central Coast Range along the Siuslaw, Alsea and Yaquina rivers where they have been previously mapped as Burpee and then later as Tyee.

Small areas of Flournoy sedimentary beds crop out along the coast in Fourmile Creek drainage, along Bear Creek, and the Coquille River just west of the Lampa mine. Baldwin has traced the Flournoy beds nearly to Sacchi Beach and he correlates the beds at Sacchi Beach with the Flournoy Formation. Microfossils from Sacchi Beach do not differ enough from either the Camas Valley Member of the Flournoy or the Elkton Siltstone to be diagnostic. Deposition was evidently rapid enough that evolutionary changes were not significant and the faunas may respond more to sedimentary facies than evolutionary changes in the relatively short time involved.

The Tyee is not known to crop out along the coast whereas the Flournoy is traceable very close to Sacchi Beach. There appears to have been a pre-Tertiary peninsula or barrier on the west side of the basin as far north as Bandon and possibly even farther north. This appears to have been a positive area against which the Eocene formations lapped from the east. Some formations are missing because of erosion, or perhaps because they never extended that far westward. Baldwin suggests that the Tyee Formation never extended to the coast at Coos Bay or southward.

Dott (1966) has the Sacchi Beach beds conformable with the overlying Coaledo beds and suggests that deposition was generally continuous. From a regional viewpoint this is the only place in western Oregon where an unconformity is not placed at the base of the late Eocene formations such as the Cowlitz, Nestucca, Spencer and Coaledo. It would be rather coincidental if Sacchi Beach were the only place that they conform. If Baldwin is correct that the Tyee, Elkton and Batemen Formations are missing then there should be a major unconformity between the beds at Sacchi Beach and the Coaledo even though they may be parallel.

On the basis of micropaleontological data the Flournoy Formation is placed in the Ulatisian.

Lorane Siltstone

The Lorane Siltstone was first described as a member of the Spencer Formation (Vokes and others, 1951). It was mapped and described separately by Gandera (1977). It was correlated with the upper part of the Flournoy Formation by Baldwin (1975) where it underlies the Spencer Formation in Eugene and Cottage Grove quadrangles. Similar beds crop out in places in the Corvallis quadrangle near the top of the Flournoy Formation.

The formation is made up of siltstone which contains abundant microfossils in places. Areas underlain by Lorane are usually valleys because the formation is more easily eroded than the nearby Spencer and Flournoy Formations. Baldwin (1975) considers the Lorane to be equivalent to the Camas Valley Member of the Flournoy and the beds at Sacchi Beach and it is assigned an Ulatisian age.

Tyee Formation

The Tyee Formation has been described by many writers. Unfortunately much that has been written is confusing as the beds of the Flournoy Formation have been described with it. The Tyee Formation gets its name from Tyee Mountain northwest of Roseburg (Diller, 1898). Baldwin has traced the base of the formation from Tyee Mountain to the south end of the basin where it stands above the Rogue River at Bald Mountain Lookout and then northward along the western edge of the basin through Coquille and Coos river drainages. The formation is unconformable upon all the older Eocene formations and at Hanging Rock it laps against the Jurassic Rogue Formation.

Lovell (1969) noted that the Tyee south of a line between Coos Bay and Elkton was massive and not notably a turbidite but toward the north into the central Coast Range it contained thinner but more definitely graded beds. The writer agrees that the Tyee at its type area and farther south is more massive, contains less silt, and in places contains crossbedded sandstone with conglomerate and coal and that farther north the beds thin somewhat, lose their coal content and become more graded but does not extend them far north of Elkton. The graded beds Lovell and other authors refer to are assigned to the underlying Flournoy Formation. Both sandstone units are micaceous and were likely derived from the Klamaths to the south. They differ in stratigraphic position and in environment of deposition for the Flournoy is a turbidite and the Tyee generally deposited in shallow water nearer to shore. The Flournoy basin was far more extensive than that of the Tyee Formation and folding and faulting of the Flournoy preceded Tyee deposition.

Fossils are not numerous in the Tyee Formation but several prominent megafossil localities occur near the contact of the Tyee and overlying Elkton and they have been compared with the Domengine of California. Microfossils are Ulatisian.

Elkton Formation

The Elkton Formation was originally named the Elkton Siltstone Member of the Tyee Formation by Baldwin (1961) but later workers have treated it as a formation. It represents a shift in sedimentation toward more argillaceous beds both upward and to the north. The Elkton is made up of approximately 3,000 feet of siltstone with lenses of massive sandstone which resemble the Tyee Formation with which the formation is apparently conformable and gradational. Good exposures are present along Lutsinger, Rader and Waggoner creeks.

Microfossils are abundant and most authorities place it within the Ulatisian or lower Narizian Stages.

Bateman Formation

The Bateman Formation was named by Baldwin (1974) for the Bateman Lookout. It occupies the central part of the southern Coast Range south of Elkton and it appears there is no significant break in Tyee, Elkton, and Bateman deposition. The Bateman apparently represents an offlapping depositional environment. The Bateman sandstone is similar to the Tyee in mineral content. The beds are cross-bedded, current-sorted deposits, such as occur in shallow deltaic conditions. Coaly beds are present. Uplift and erosion apparently preceded encroachment of the Coaledo and Spencer seaways.

Both mega and microfossils are fairly rare but those present appear to be more closely associated with the Tyee than the Coaledo Formation.

Coaledo Formation

The Coaledo Formation occupies a distinct basin along the west side of the Coast Range. The formation contains a lower sandstone member overlain by a middle siltstone member and capped by an upper sandstone member. The three members total approximately 6,000 feet. The lower and upper sandstone members are made up of deltaic deposits and exhibit channeling, crossbedding and much variation in lithology. Pebbly sandstone is present in places as is considerable intraformational conglomerate. Coal is present in both sandstone members but is more common in the upper Coaledo.

The formation rests unconformably upon all the older Cenozoic formations with the exception of the Tyee, Elkton and Bateman Formations which are missing in the Coos Bay area. Within the city limits of Bandon, the formation appears to lap against pre-Tertiary beds in the western positive area.

The thickness of the members is not uniform. Along the eastern margin the formation seems to thin and the middle silty member seems to thin even more, probably because of interfingering with sandstone close to the old shoreline. The contacts between members are probably gradational throughout the basin.

Spencer Formation

The Spencer Formation is present along the western margin of the Cascades from the central Anlauf quadrangle northward along the western edge of the Willamette Valley (Figure 2).

The Spencer beds appear to be near-shore current-sorted deposits without noticeable grading. The Spencer contains micaceous feldspathic sandstone with minor siltstone near the base but alternating beds of sandstone and siltstone appear higher in the formation. The Spencer may be derived largely from erosion of the Flournoy and Tyee Formations. The Spencer rests unconformably upon the older formations as indicated by the pre-Spencer erosion of the underlying Lorane Siltstone. In fact, the Cowlitz, Spencer and Coaledo beds are unconformable throughout western Oregon and only Dott (1966) proposes that the Coaledo and underlying beds at Sacchi Beach are conformable. This relationship has been discussed previously in the discussion of the Flournoy Formation. The Spencer Formation is overlain by fragmental volcanic material of the Fisher Formation which interfingers with the flows in the Anlauf and Glide areas.

Megafossils are abundant in the Spencer Formation and these have been compared with the Cowlitz Formation of Washington and the Tejon Stage of the West Coast Eocene. Microfossils are present in the Spencer and Coaledo Formations and both are assigned to the Narizian Stage.

Fisher Formation

The Fisher Formation is made up of pyroclastic material which crops out from a point west of Junction City south into the Anlauf area where it interfingers with basalt flows. The formation has been described by Hoover (1963) in the Anlauf quadrangle. Flora in the Fisher indicate that it is largely late Eocene but may extend into the early Oligocene.

Bastendorff Formation

Eocene shale 2,900 feet thick crops out at Bastendorff Beach, its type section, on the west limb of the South Slough Syncline near Coos Bay. Abundant microfossils have been examined and assigned to the late Eocene by nearly all workers although some have considered the uppermost part to be Oligocene.

Tunnel Point Formation

The Bastendorff Formation is overlain by tuffaceous sandstone of the Tunnel Point Formation at its type section near the east end of Bastendorff Beach. The transition is abrupt but apparently conformable. The upper part of the formation has been eroded but 800 feet is exposed in Tunnel Point, the only known section. Megafossils are similar to those in the Eugene Formation and Armentrout (1973) places both formations entirely within the late Eocene.

Eugene Formation

The Eugene Formation is present under the southernmost part of the Willamette Valley from Cottage Grove northward along the west edge of the Coburg Hills to the Salem area. The formation contains tuffaceous sandstone and siltstone and may interfinger with volcanics of the western Cascades to the east. The Eugene fauna has been studied by Hickman (1969) who considers it early Oligocene but Armentrout (1973) places it entirely within the late Eocene.

References

Armentrout, J. M., 1973, Molluscan paleontology and biostratigraphy of the Lincoln Creek Formation late Eocene-Oligocene southwestern Washington: Univ. Washington doctoral thesis, 478 p., unpub.

Baldwin, E. M., 1961, Geologic map of the lower Umpqua River area, Oregon: U.S. Geol. Survey Map OM 204.

______, 1973, Geologic map of Coos County: Oregon Dept. Geology and Mineral Industries Bull. 80.

Baldwin, E. M., 1974, Eocene stratigraphy of southwestern Oregon: Oregon Dept. Geology and Mineral Industries Bull. 80, 40 p.
_____, 1975, Revision of the Eocene stratigraphy of southwestern Oregon: Paleogene symposium and selected technical papers, AAPG, SEPM and SEG Ann. Meeting, Long Beach, California, Editors, Weaver, D.W., Hornaday, G.R., and Tipton, Ann. p. 49-64.
_____, and Hess, P. D., 1971. Geology of the Powers quadrangle, Oregon: Oregon Dept. Geology and Mineral Industries, GMS-4.
_____, and Howell, P. W., 1949, The Long Tom, a former tributary of the Siuslaw River: Northwest Sci., v. 23, p. 112-24.
Cornell, J. H., III, 1971, Geology of the northwest quarter of the Canyonville quadrangle, Oregon: Univ. Oregon master's thesis, 64 p., unpub.
Diller, J. S., 1898, Roseburg folio, Oregon: U. S. Geol. Survey, Geol. Atlas of U.S., Folio no. 49.
_____, 1915, Guidebook of the western United States, Pt. D, The Shasta Route and Coast Line: U. S. Geol. Survey Bull. 614, 142 p.
_____, and Kay, G. F., 1924, Riddle folio, Oregon: U. S. Geol. Survey, Geol. Atlas of U.S. Folio no. 218.
Dott, R. H., Jr., 1966, Eocene deltaic sedimentation at Coos Bay, Oregon: Jour. Geol., v. 74, no. 4, p. 373-420.
Gandera, W. E., 1977, Stratigraphy of the middle to late Eocene formations of the southwestern Willamette valley, Oregon: Univ. Oregon master's thesis, 75 p, unpub.
Haq, Z. N., 1975, Geology of the northwest quarter of the Roseburg quadrangle, Oregon: Univ. Oregon master's thesis, 75 p., unpub.
Hickman, C. J., 1969, The Oligocene marine molluscan fauna of the Eugene Formation, Oregon: Oregon Museum Nat. Hist. Bull. 16, 112 p.
Hoover, L., 1963, Geology of the Anlauf and Drain quadrangles, Douglas and Lane counties, Oregon: U. S. Geol. Survey Bull. 1122-D, 62 p.
Johannesen, N. P., 1972, The geology of the northeastern quarter of the Bone Mountain quadrangle, Oregon: Univ. Oregon master's thesis, 98 p., unpub.
Lovell, J.T.B., 1969, Tyee Formation:Undeformed turbidites and their lateral equivalents, mineralogy and paleogeography: Geol. Soc. America Bull., v. 80, no. 1, p. 9-22.
Miles, G. A., 1977, Planktonic foraminifera of the lower Tertiary Roseburg, Lookingglass, and Flournoy formations, southwest Oregon: Univ. Oregon doctoral thesis, 359 p., unpub.
Misch, P., 1966, Tectonic evolution of the northern Cascades of Washington State: Can. Inst. Min. Met. Spec. Vol. 8, p. 101-148.
Perttu, R. K., 1976, Structural geology of the northeast quarter of the Dutchman Butte quadrangle, Oregon: Portland State Univ. master's thesis, 60 p., unpub.
Peterson, N. V., 1957, The geology of the southwestern third of the Camas Valley quadrangle, Oregon: Univ. Oregon master's thesis, 89 p., unpub.
Seeley, W. O., 1974, Geology of the southeastern quarter of the Dixonville quadrangle, Oregon: Univ. Oregon master's thesis, 77 p., unpub.
Simpson, R. W., and Cox, A., 1977, Paleomagnetic evidence for tectonic rotation of the Oregon Coast Range: Geology, v. 5, p. 585-589.
Tabor, R. W., and Frizzell, V. A., 1979, Tertiary movement along the southern segment of the Straight Creek fault and its relation to the Olympic-Wallowa lineament in the central Cascades, Washington: Geol. Soc. America, abstract, v. 11, no. 3, p. 131.
Trigger, J. K., 1966, Geology of the south-central part of the Sitkum quadrangle, Coos County, Oregon: Univ. Oregon master's thesis, 79 p., unpub.
Vokes, H. E., Myers, D. A., and Hoover, Linn, 1954, Geology of the west central border area of the Willamette Valley, Oregon: U.S. Geol. Survey Oil and Gas Inv. Map OM-150.
_____, Snavely, P. D., Jr., and Myers, D. A., 1951, Geology of the southern and southwestern border areas of the Willamette Valley, Oregon: U.S. Geol. Survey Oil and Gas Inv. Map OM-150.

ROAD LOG

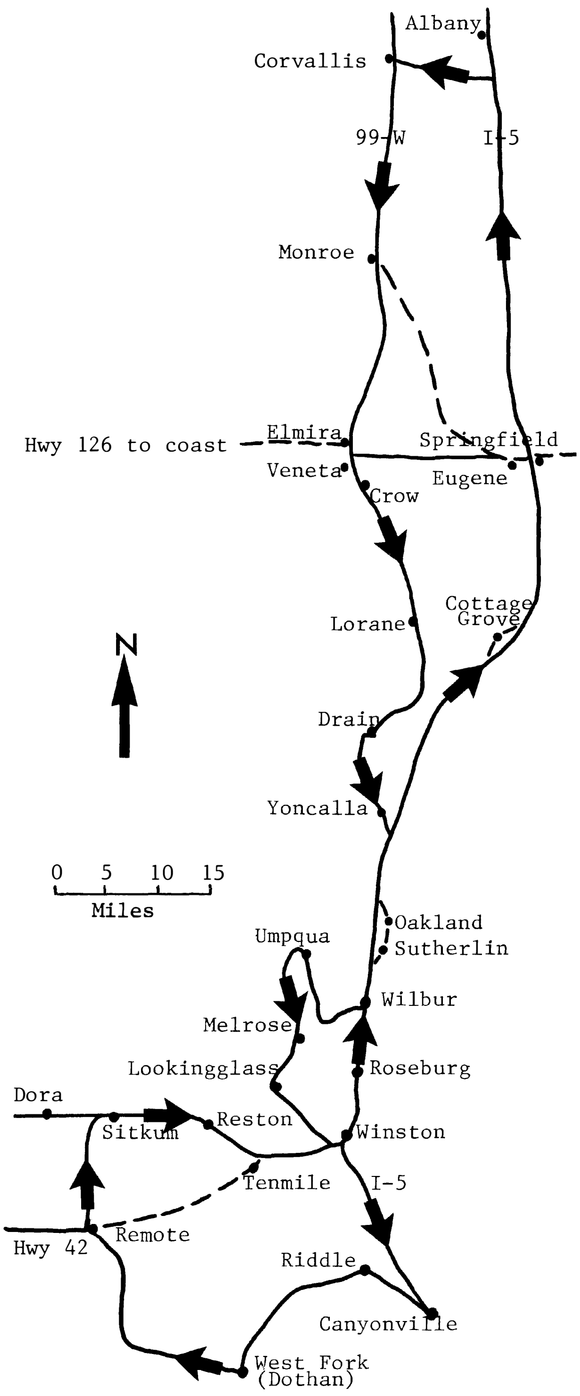

Figure 1

Assemble in the Parking lot at Wilkinson Hall, Oregon State Campus then proceed along 27th to Monroe, then right to 4th and southward along 99W.

00.0 Corner of Wilkinson Hall. The geology of the Corvallis area is described by Vokes, Myers and Hoover (1954). Corvallis is located on alluvial covered Spencer sedimentary rocks and separated from the Siletz River volcanics in the highlands to the west by a prominent fault.

01.6 The Philomath road turns to the right and the Marys River bridge is just ahead. Country Club hill to the west is made up of Spencer beds. Marys Peak will be on the western skyline for several miles. It is capped by a gabbroic sill.

08.7 At Greenberry a road leads to the west to Alsea. The valley is covered by alluvium, the lower slopes expose Spencer beds but the top of the hill is capped by a gabbro sill.

10.4 Winkle Butte is located to the east. It is composed of Oligocene sandstone with a small intrusive body. The sedimentary rock is probably equivalent to the Eugene Formation.

12.0 The highway is upon alluvium but the low ridge that trends approximately S. 70 W. is held up by a dike that reaches from the alluvium to Green Mountain, a larger intrusive body.

17.0 The road to Glenbrook goes to the right (west) and the Long Tom River parallels the highway to the east. The ridge to the southwest (west of Monroe) is formed by a gabbroic intrusive into the Spencer Formation.

17.9 North Monroe city limits. A brick factory utilizing local clay is to the east.

18.6 Highway 99 W turns eastward across the Long Tom River but the traverse continues southward on the Territorial Road which is also known as the Applegate Trail. The hills ahead on the west are of Spencer capped by a gabbroic sill.

23.2 Ferguson Creek bridge. The area south of here to a point south of Lorane has been mapped by Gandera (1977). He showed the areal extent of the Lorane Siltstone.

24.4 Cox Butte road goes eastward.

24.9 Cox Butte cemetery is on the east side of the road. The east side of the butte is made up of Fisher Formation resting on Spencer beds which crop out along the main road.

25.2 Bear Creek bridge. Upper Bear Creek is the pirated branch of the Long Tom River. The former valley parallels Highway 36 (Baldwin and Howell, 1949).

25.45 The High Pass road leads to Blachly to the west and to Junction City to the east.

27.25 Join Highway 36 and turn left for a short distance through Cheshire. The hill ahead is Spencer Formation intruded by gabbroic dikes.

27.5 After going through Cheshire turn right (south). The Spencer Formation crops out along this road.

28.5 Roadcut at slight turn is where Vokes and others (1951) reported Spencer fossils.

29.4 The tuffaceous beds to the right are probably still a part of the Spencer Formation but they resemble the Fisher Formation in lithology and texture. To the east is an intrusive body that has been quarried and the pit is partly filled with refuse.

30.1 Road junction in Franklin by churches and grange hall (Fig. 2).

31.5 Kirk road runs eastward along the north side of Richardson Butte. The butte is made up of Spencer beds cut by an east dipping gabbroic sill which crops out near the west end of Fern Ridge dam. Hills to the west are thin-bedded Flournoy beds which are more silty than usual (Gandera, 1977).

32.6 Road eastward to Fern Ridge dam along the south side of Richardson Butte.

33.6 Fern Ridge Reservoir is located to the east. The road is on Pleistocene terrace material to a point south of Veneta.

36.9 Elmira High School is located on the left.

37.1 Highway 26 (also known as Route F) goes west from this point and the Long Tom River bridge is just ahead. The road westward is on Pleistocene alluvium for several miles, then as the valley narrows weathered Flournoy beds are exposed. Just beyond Noti fresher outcrops of Flournoy sandstone crop out. The Long Tom River formerly followed Poodle Creek to its junction with Coyote Creek and Noti Creek before turning westward following Wildcat Creek to the Siuslaw River (Baldwin and Howell, 1949) (Fig. 2).

38.0 Road junction with road to Eugene to the east. The railroad and Veneta lie just ahead. The area is underlain by Pleistocene terrace deposits which are weathered and eroded to rolling topography.

- - - - - - - - - - - - - - - - - - - - - -

Geology Building, University of Oregon. Proceed to Franklin Blvd., then westward on 11th Avenue without turning to Veneta. The city of Eugene is located on alluvium and the Eugene Formation of late Eocene-early Oligocene age cut in places by dikes and sills (Vokes, Snavely and Myers, 1951) (Fig. 2).

00.0 Back of Geology building.

03.9 Bailey Hill road goes to the south. Wallace Butte is on the north (right). It is made of weathered Eugene sandstone which was processed for foundry sand and aolin

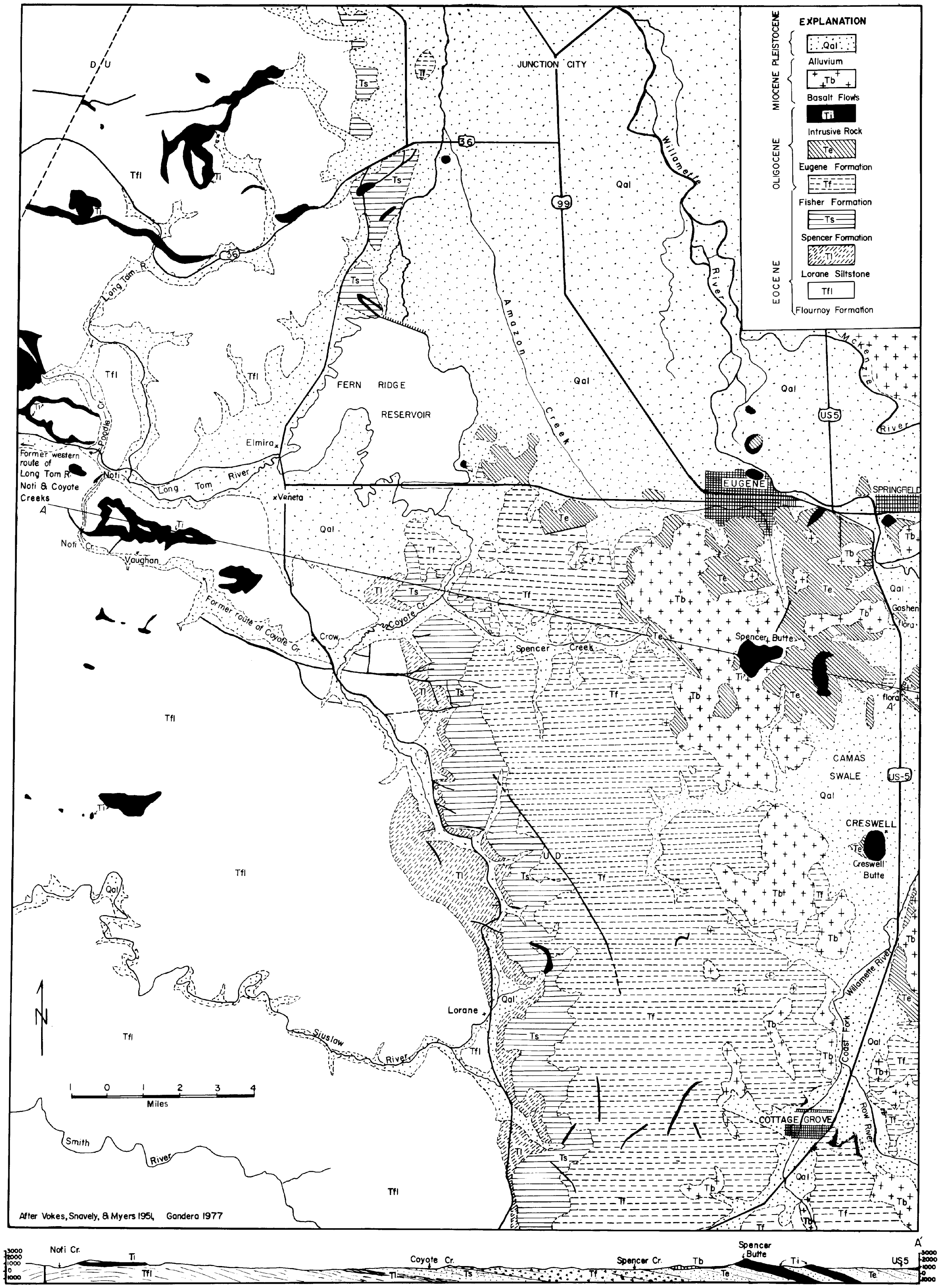

Figure 2. Geologic map of the Eugene area.

during World War II. The pit is located at the west end of the butte. Turn at this point then follow Stewart Avenue to the pond that fills the sand pit.

05.2 Beltline road goes to the right. It is alluvium nearby but the concealed Eugene-Fisher contact is near here and should be found in the hills to the south (Fig. 2).

07.0 Greenhill road leads northward to the airport and southward to the Crow road.

07.7 Railroad overpass. Vokes and others (1951) show the Eugene beds faulted against the Fisher Formation to the north and also to the south.

09.5 Fisher Butte quarry is located to the right in a hill that has been largely removed for crushed rock. The Fisher Formation is said to have derived its name from this butte. Most of the Fisher Formation is made up of pyroclastic material but there are a few vents, flows and dikes.

10.2 Coyote Creek bridge and southeast corner of Fern Ridge reservoir.

11.4 Central road leads to the southwest to Crow over alluvium then Flournoy beds. Perkins Peninsula to the right has a small outcrop of Spencer near the waterline.

14.4 Across Pleistocene alluvium that has been weathered and eroded. This is the junction with the Territorial Road and traverse from Corvallis. Proceed southward through Veneta.

- - - - - - - - - - - - - - - -

38.0 (See traverse from Corvallis)- This is the Eugene turnoff. Proceed southward through Veneta.

40.8 End of alluvium and starting up the hill in Flournoy beds.

41.9 Crest of the hill in Flournoy Formation.

42.6 Crow store with Central road from left and road to Vaughan and westward to the right. The road to Vaughan and Noti crosses an imperceptible pass over which Coyote Creek used to flow into Noti Creek. There are several gabbroic intrusions between Vaughn and Noti where the valley narrows considerably but otherwise the valley is cut in Flournoy beds (Fig. 2).

43.5 Crow road junction which leads back to Eugene. The traverse proceeds southward.

43.8 Wolf Creek road to the right leads to the Oxbow on the Siuslaw River and over the Oxbow burn to Smith River and to the coast at Reedsport. The road exposes only Flournoy beds. A dike to the right of this junction has been quarried showing Flournoy along the walls and the dike crops out at the back end. It has been partially filled during nearby logging.

46.0 Doane Road goes to the left toward Eugene. At the top of the hill it crosses a prominent dike that runs for miles through the Flournoy, Lorane, Spencer and Fisher Formations. It has been quarried to the west and now presents a series of pits (Fig. 2).

47.3 The location of the old Hadleyville school and turnoff to the left of the Briggs Hill Road. Flournoy makes up the hills on both sides of the Briggs Hill junction but the open valley ahead both up Briggs Hill Road and to the south is carved in the Lorane Siltstone.

48.5 A narrow dike, perhaps 8-10 feet thick, crops out on the point just south of a barn on the left (east).

50.6 Gillespie Corners and the Lorane Road lead back to Eugene on the east. A dike cuts

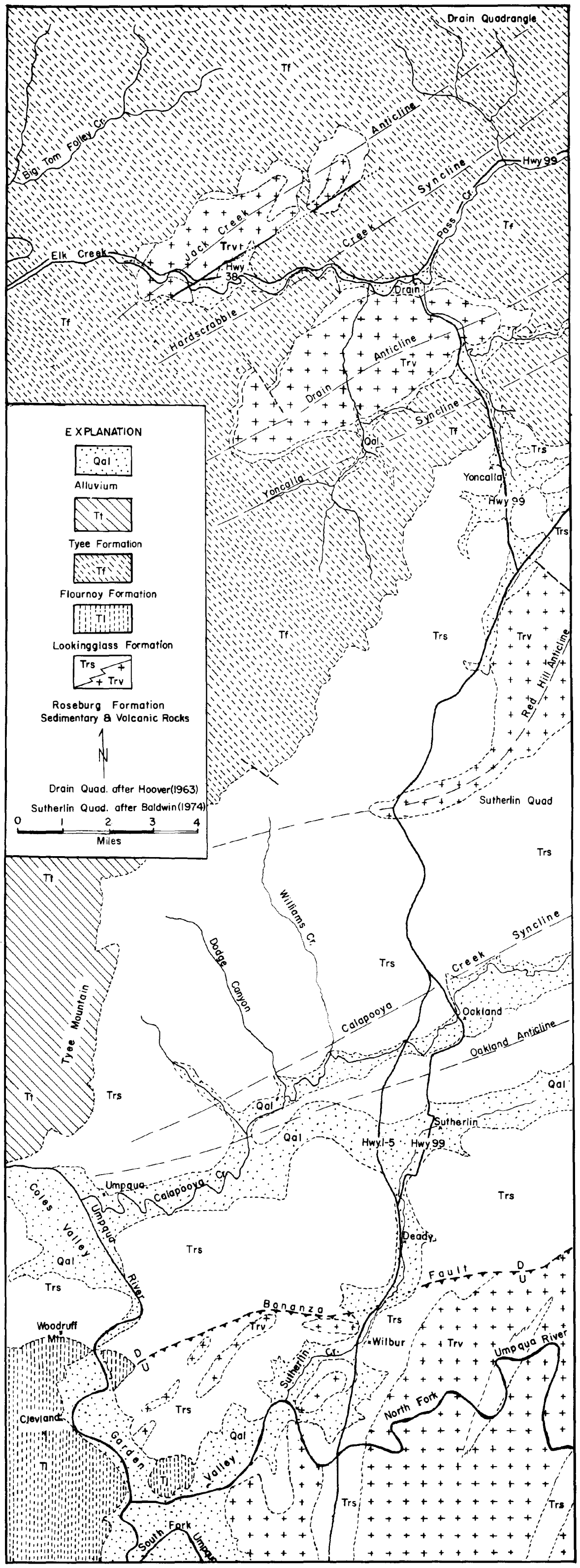

Figure 3. Geology of the Drain and Sutherlin quadrangles.

the Spencer beds 1½ miles to the east but the main road south is still in Lorane beds.

53.1 Haw road to the east. If one goes up Haw road Lorane gives way to Spencer then about 2 miles to the east the road crosses a fault into the Fisher (see Fig. 2).

53.9 Summit of pass between Coyote and Siuslaw drainage. Pass is present here because of a dike which cuts the Lorane beds. Relatively fresh Lorane may be seen next to the dike.

56.5 In Lorane at the road junction with the Siuslaw River road. It is all Flournoy beds to the west and Lorane beds beneath the valley east of Lorane.

57.7 Leaving the alluvium and starting to climb hill. The pavement ends.

58.8 Summit which is in weathered Flournoy beds.

62.9 Seeley Creek joins Pheasant Creek and all beds exposed are Flournoy.

63.7 Old Highway 99 with the present highway .3 mile ahead.

64.2 Good outcrops of graded Flournoy sandstone are exposed in the road cuts.

67.1 Sand Creek bridge and good outcrops of Flournoy sandstone crop out here and for a few miles.

68.4 The road to the right goes to Smith River through Flournoy beds.

70.6 Main road junction in Drain. Roseburg basalt crops out in south edge of town and in the narrow valley to the south along Highway 99. Good exposures of graded Flournoy crop out along the highway that leads to the coast. Continue westward.

71.7 Hayhurst road leads southward. Turn left and cross Elk Creek and beyond the alluvium the traverse enters the Roseburg Formation. Some tuffaceous sedimentary beds are on top of basalt which makes up the narrow valley to the south. No pillows were observed and the flow structure indicates probable subaerial extrusion. The Anlauf and Drain quadrangles were mapped by Hoover (1963)(Fig. 3).

73.6 Basalt is present along the road but a large quarry at creek mouth to the west shows subaerial basalt flows.

76.0 Skelly road goes to the right. Flournoy beds are exposed up the road. Turn toward Yoncalla.

77.8 Summit in Flournoy beds but Hoover (1963) shows the contact just east of the summit with Roseburg (Umpqua) beds. The Roseburg is thinner bedded sandstone and siltstone and lacks the mica and plant fragments common in the Flournoy and Tyee formations.

80.8 Intersection with Highway 99 in Yoncalla.

83.6 Intersection with U.S. Highway I-5. The Red Hill anticline lies to the east. Basalt quarries may be seen from here and overlying tuffaceous beds dip northwestward away from the center of the anticline (Fig. 3).

89.4 The highway crosses the plunging end of the Red Hill anticline with Turkey Hill to the southwest. Basalt, which appears to have some pillow structures, is exposed in the center.

89.8 Black siltstone dipping 39-35 degrees southeastward is the base of a thick homoclinal section. Although considerable distances are unexposed there may be as much as 8,000 feet of sedimentary rock if a fairly constant dip is assumed.

93.0 Long area without exposures then cuts of graded Roseburg sandstone and siltstone.

93.4 Turnoff to Oakland and the south end of high cuts of graded Roseburg beds.

94.3 Overpass across the highway is near the center of a syncline.

95.3 Calapooya Creek bridge. The beds ahead dip northwesterly. The tree-covered ridge on the skyline to the west is the Tyee escarpment.

96.2 Top of the Oakland anticline is in graded Roseburg beds. The beds gradually roll over and dip gently southeastward. The structure is asymmetrical with steeper beds on the northwest.

98.7 After passing by the western edge of Sutherlin take the first overpass south and cross over I-5 to Highway 99 on the east and follow the signs to Wilbur. Proceed southward paralleling main highway.

100.1 Thin-bedded dark gray Roseburg beds crop out along I-5. At the east end of road to the east at Deady siding there is a quarry that produced sandstone for the old bank building in Sutherlin and reputedly for the old State Capitol building that burned in Salem.

102.5 North limits of Wilbur with Coles Valley road to the west. The hill east of Wilbur is made up of basalt-pebble conglomerate which rests on basalt. The conglomerate seems to be of local derivation and is considered to be a part of the Roseburg, perhaps formed near an island soon after extrusion.

102.9 Turn west on Garden Valley road and go under Highway I-5. If one continues south on Highway 99 a few yards, a road to the east leads along the north bank of the North Fork of the Umpqua River to Glide. Pillow basalt is common along the road to Glide.

105.1 Mouth of Sutherlin Creek and turn to the right paralleling the Umpqua River.

105.6 Point above the river exposes angular basaltic breccia in a large channel which is possibly a submarine slump deposit. It is overlain by ripple-marked sandstone. Finer grained siltstone is present along the west edge of the channel.

107.0 Pillow basalt is present in a small outcrop near the top of the terrace.

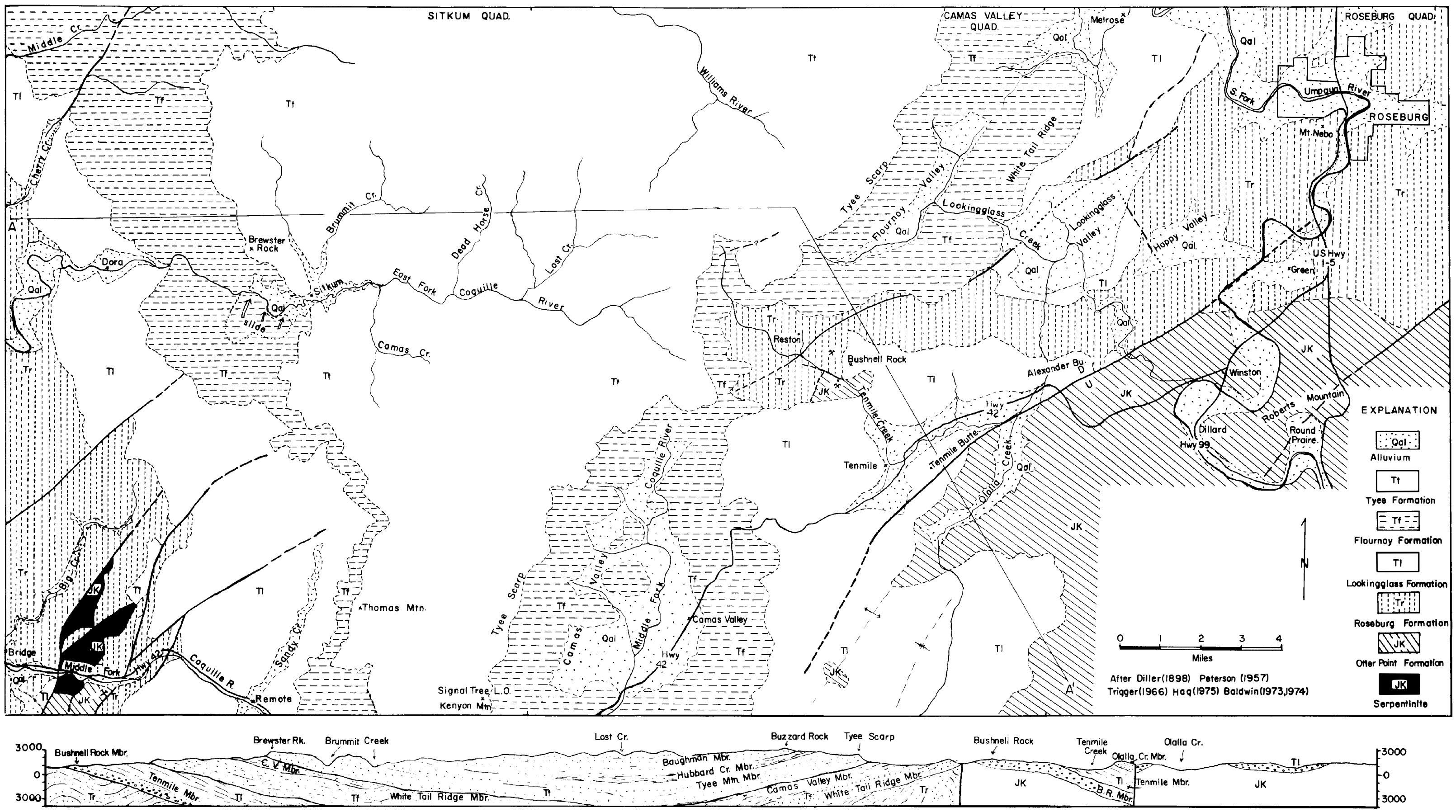

Figure 4. Geology of the area between Roseburg and East Fork of the Coquille River.

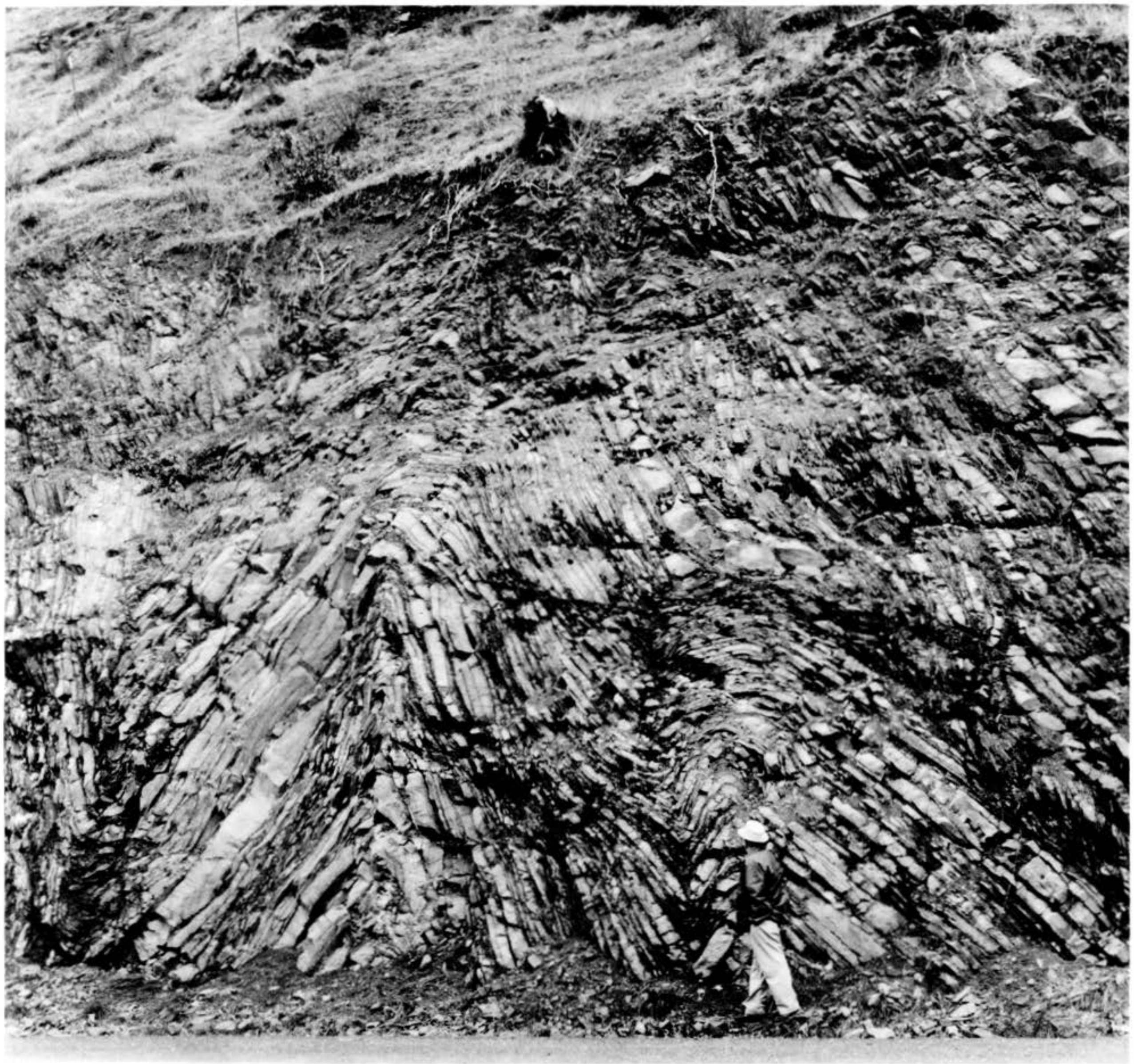

Figure 5. Closely folded Roseburg beds along the north side of the Umpqua River north of Woodruff Mountain. (mileage 113.0)

107.7 Road 31A goes to the left to Roseburg but proceed straight ahead passing by the north edge of Coyote Hill.

108.1 Conglomerate of the Bushnell Rock Member of the Lookingglass Formation is present along the road and underlies the south-dipping beds of Lookingglass in Coyote Hill. This is the first Lookingglass outcrop encountered and the contact continues west under alluvium to a point near Woodruff Mountain (Fig. 3).

109.1 Road junction but bear to the right. Basalt in the hills near the junction show that the traverse is back into the Roseburg Formation.

110.4 Cleveland Rapids road leads to the left with graded Roseburg sandstone and siltstone cropping out in the nearby cuts.

111.4 Massive sandstone ahead and to the right near a small creek doesn't fit with the steep beds just seen. We are nearing the Bonanza thrust and these beds may be thrust Roseburg sandstone or onlapping Lookingglass beds.

113.0 The river swings close to the road at the end of a long cut showing closely folded thin-bedded Roseburg beds (Fig. 5). The graded beds are closely folded and in places slightly thrust. These beds may be just beneath the Bonanza thrust which projects into the vicinity.

115.6 Thin-bedded Roseburg beds are exposed in Calapooya Creek. Note Tyee Mountain ahead to the northwest where the name for the Tyee Formation was derived. The large valley is called Coles Valley.

116.0 Bridge over Calapooya Creek with thin-bedded Roseburg beds exposed, particularly at low water. At the road junction ahead turn left to the bridge over the Umpqua. The relocated Umpqua store and post office is about ½ mile to the east of this junction. Dips in the Roseburg do not conform with those of the more gently dipping Tyee sandstone higher on the mountain.

116.5 North end of Umpqua River bridge and the mouth of Calapooya Creek. This was the location of the old Umpqua store and post office. Thin-bedded Roseburg beds are exposed along the river. Farther downstream near the first bend a dike protrudes from the north bank. Before reaching the Tyee some sandstone beds of intermediate texture and composition may be Flournoy between the Roseburg and the Tyee formations.

117.5 Turn left at the road junction. The road ahead goes along the south bank of the river to Hubbard Creek which is flowing in a valley cut in the silty Hubbard Creek Member of the Tyee Formation. A small knob along the Hubbard Creek road about 3/4 mile from this junction is the location of the Coles Valley well started by Douglas County residents and deepened by Union Oil Co. It went approximately 7,500 feet and reputedly encountered steeply dipping beds.

118.6 Coles Valley cemetery is on the point to the right. Steeply dipping Roseburg beds crop out in the hill back of the cemetery and strike southwestward beneath the Tyee scarp.

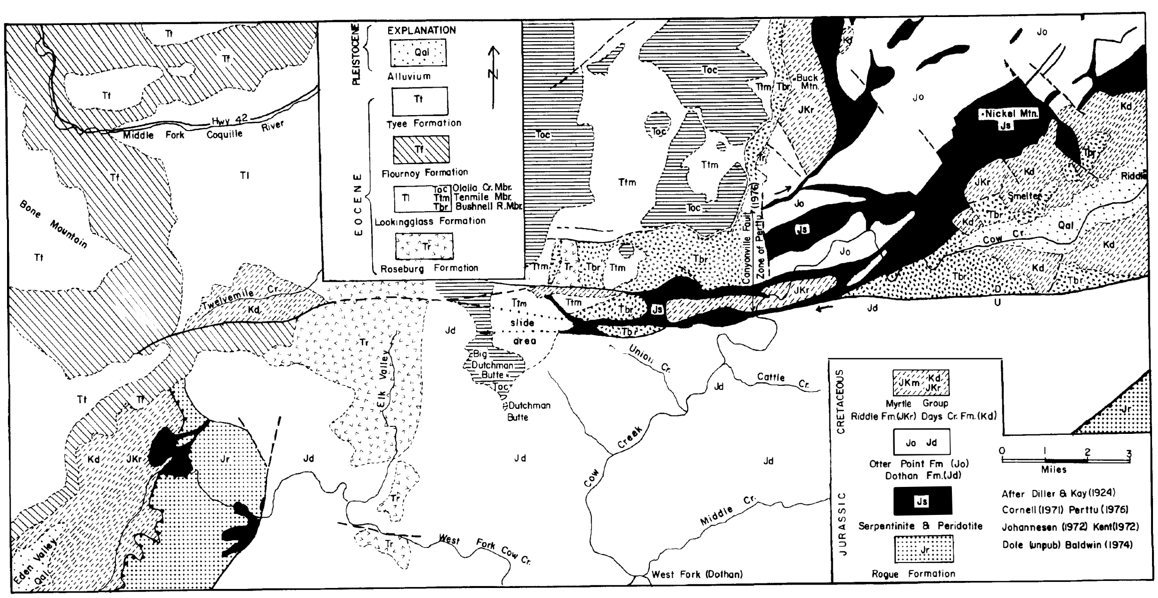

Figure 6. Geology of the Cow Creek area along the Canyonville fault zone.

119.6 Joelson road goes toward the scarp but steeply dipping Roseburg beds are exposed at junction.

120.5 The Bureau of Land Management road to the west climbs to the top of the Tyee scarp. It goes past landslide depressions near the base of the scarp. Woodruff Mountain to the left has steep dipping Roseburg beds along the river. However, massive conglomerate on the south side of the mountain may be onlapping basal Lookingglass. The Lookingglass beds along the south edge of Woodruff Mountain strike westerly and disappear beneath the Tyee escarpment. They do not crop out to the north.

121.5 Woodruff road on south side of Woodruff Mountain cuts bedded conglomerate of the Bushnell Rock Member of the Lookingglass Formation. The hill ahead is also Lookingglass.

122.9 Heydon road goes to right and the old Cleveland school (renovated for housing) is to the left with Cleveland cemetery just ahead. Cleveland rapids, in the river, is a short distance to the east.

123.4 Cleveland Hill road to the right is a short cut to Melrose but continue to the left paralleling the river.

125.8 The North Fork of the Umpqua River joins opposite this point with Lookingglass beds along the road.

127.7 Melrose store and road junction with traverse turning to the right. The Melrose well, started in Lookingglass, is located a short distance to the left (east) opposite the school. It was begun by local residents.

128.4 Top of the hill. Beds are coarse sandstone with some fine conglomerate.

128.7 Doerner road leads to the Tyee escarpment and goes past the former site of the Landers L.O. along the rim (burned) and to the Baughman L.O. near the head of Hubbard Creek. Beds under the lookout form the upper, Baughman Member, of the Tyee Formation and Hubbard Creek occupies the less resistant Hubbard Creek Member of the Tyee.

129.5 Turn to the right at this road junction.

131.7 The Doerner road cutoff goes to the right. The coarse sandstone ahead should be near the base of the Flournoy Formation. We cross a low divide into Flournoy Valley. The beds form a gentle dipslope from White Tail Ridge, the basal member of the Flournoy, to the valley which is carved largely in the Camas Valley Member. The Tyee Formation overlies siltstone of the Camas Valley Member without notable discordance.

135.8 Turn to the left at this road junction and proceed down Lookingglass Creek through the White Tail Ridge sandstone member of the Flournoy. The road to Reston goes to the right across the creek and then westward.

138.2 Road junction with the road to the right leading to Tenmile but continue straight ahead to Lookingglass. The roadcuts beyond this junction appear to be in Roseburg which implies that it is in fault contact with the Lookingglass which makes up the southern part of the valley. Near this point the Lookingglass may have been removed and the Flournoy rests directly on the Roseburg as it does just east of Reston. The valley in general is covered by alluvium.

139.5 Lookingglass store and post office at road junction. Turn right toward Brockway.

140.3 Beyond Lookingglass the valley floor is covered by alluvium. A well near this road junction penetrated the Tenmile Member of the Lookingglass. At junction turn left toward Brockway.

141.5 Small quarry in conglomerate to the left is in the Bushnell Rock Member of Lookingglass near its top where it grades upward into the Tenmile Member. The pebbles, by their variety of compositions and textures, show that they were derived from the Klamath Highlands. A few fossils have been found here. Beyond this point the massive conglomerate in places rests on steeply bedded Roseburg.

142.6 Happy Valley junction with traverse continuing to the right south across Lookingglass Creek. Lookingglass conglomerate forms ridge to the north but Roseburg flows and sedimentary beds underly valley. Happy Valley is underlain by Roseburg flows and sedimentary beds.

142.9 Cuts just south of the creek have pillow lavas and interbedded vertical sedimentary beds. The beds are overlain to the south by Lookingglass conglomerate in Alexander Butte and to the north by the same conglomerate that rims the south side of Lookingglass Valley. It undoubtedly joined in an anticline which went over the steep beds and flows at this cut. This should prove the existence of a profound orogeny at the end of the early Eocene when the Roseburg Formation was closely folded probably as a subducting oceanic plate compressed the strata against the continent. The tops of the folds were eroded prior to the arrival of the onlapping basal conglomerate of the Lookingglass Formation.

143.5 Bridge over Lookingglass Creek which is just beyond turnoff at Swan road which leads to Alexander Butte (also called Swan Butte). Basalt is present both up and down stream.

143.9 Long low cut showing mostly alluvium. Near the center sheared serpentinite is present along a prominent fault that drops the Roseburg against pre-Tertiary beds. The relationship is difficult to see because of alluvium covering outcrop. This fault goes through the Wild Life Safari and may be termed the "Wildlife Safari Fault."

144.2 Light gray feldspathic massive sandstone by Clear Tree Drive. Bedding is very difficult to determine. This facies is assigned to the Otter Point Formation and is called the "Hoover Hill facies" for it also crops out in Hoover Hill to the west. Although this rock type is not proved to be Otter Point it seems to be a part of that complex unit. Similar lithology has been found at Sugarloaf Mountain in the Powers quadrangle by Baldwin and Hess (1971).

150.0 Turn right toward Brockway.

150.8 Brockway is located at junction with Highway 42. Proceed south toward Dillard. The beds are pre-Tertiary near here.

151.9 Kent Creek with all Otter Point beds between Brockway and here.

152.2 Bridge over the South Fork of the Umpqua River where traverse joins Highway 99. Turn right proceeding generally southward past the large Roseburg Lumber Company mill. All the beds beneath the alluvium are assigned to the Otter Point Formation of Late Jurassic age.

154.9 Cross the South Fork of the Umpqua and proceed across alluvial flat southward.

155.8 Round Valley, a large cutoff meander, is across the river to the left.

156.3 Road to the left crosses the river to the freeway but continue southward on Highway 99.

156.8 High cuts of Otter Point sedimentary rock crop out along the highway.

158.7 Entering freeway and still in Otter Point beds.

160.5 Boomer Hill road leaves to the right. A greenstone hummock just ahead looks like a detached block of Rogue Formation but may be greenstone of the Otter Point Formation.

161.6 Serpentinite in a very high cut. It is cut by several diorite dikes.

161.7 Entering the Riddle Formation which is the older of the Myrtle Group. The Riddle Formation is made up of well rounded and sorted chert-pebble conglomerate and some sandstone and siltstone. It is overlain by the Days Creek Formation, the upper part of the Myrtle Group. The Riddle is Juro-Cretaceous whereas the Days Creek is Early Cretaceous. The Riddle continues along the highway beyond the turnoff to Myrtle Creek.

163.7 Cross the railroad onto Missouri Bottom, an alluvial flat, and onto the Riddle Folio (Diller and Kay, 1924).

167.1 Turnoff to Riddle to the right (west). Nickel Mountain is north of Riddle but continue southward on Highway I-5.

168.1 High cuts of steeply dipping beds and volcanic rock which are probably a part of the Otter Point.

168.6 South Fork of the Umpqua bridge just beyond turnoff to Gazley.

171.5 Turnoff into Canyonville and junction with road to Riddle just ahead. The first day's traverse ends at this point. Drive into Canyonville. The traverse resumes at this point tomorrow.

\- - - - - - - - - - - - - -

171.5 The point where the turnoff from I-5 meets the Canyonville to Riddle road. Proceed toward Riddle. Canyon Mountain to the south is made up of the Rogue Formation which has been thrust northwesterly over the Dothan Formation. The Rogue was deformed with the Galice Formation during the Late Jurassic Nevadan Orogeny but thrusting came later and may have continued until the end of the late Eocene.

174.8 Good exposures of Riddle conglomerate and sandstone are present in the cuts.

176.5 Cow Creek bridge is ahead and the Glenbrook loop road goes to the west along the south side of Cow Creek. We proceed through Riddle to the main Cow Creek road which runs along the north side of the valley. Diller and Kay (1924) mapped the Riddle as Knoxville and the Days Creek as Horsetown. The northwestern corner of the Caynonville quadrangle west of Riddle has been mapped by Cornell (1971).

177.3 Main Cow Creek road and the traverse turns left (west) (Fig. 6).

180.3 Nickel Smelter road turns to the right but we cross railroad and continue west up the valley. The smelter obtains its ore from the top of Nickel Mountain and is processed by the Hanna Nickel Co.

180.8 Glennbrook loop road joins from the south side of Cow Creek. Continue westward.

181.4 Thin-bedded sedimentary beds in creek may be Days Creek. Any Umpqua of Diller and Kay seems to be the Lookingglass and these beds do not fit in unless they are a part of the Roseburg Formation and beneath the Lookingglass.

182.3 A small rapids and falls dropping over massive beds of conglomerate coincide with a decided narrowing of the valley. This is a good place for examining the pebbles of the Bushnell Rock Member derived from the Klamath Highlands a short distance to the south. The traverse enters the Conyonville Fault zone described by Perttu (1976).

183.6 After passing more conglomerate the road enters serpentinite.

184.6 Greenstone surrounded by serpentinite which may be a part of the Otter Point Formation.

186.5 Doe Creek road with bridge over Cow Creek just ahead. Cross bridge and enter sheared dark sedimentary rock of the Otter Point Formation. We are on the edge of the Dutchman Butte quadrangle mapped by Dole (unpub.) and the northeastern quarter mapped by Perttu (1976).

186.7 Serpentinite.

189.1 Quarry in steep dipping Riddle conglomerate. On the mountain side to the north one can see the poorer sorted, more gently dipping Lookingglass conglomerates. This is in the Canyonville fault zone (Fig. 6) and blocks of several formations are displaced by the movement.

192.9 Small quarry at the mouth of Cattle Creek exposes deformed Dothan sandstone and siltstone. The formation is well indurated, jointed and made up of dark gray to almost black sandstone and siltstone. Continue in Dothan all the way to West Branch for road is south of the major fault.

194.5 Union Creek road crosses bridge to the north. One can either go to Dutchman Butte or turn north into Olalla Creek drainage (Fig. 6) by the Union Creek road. Continue westward along Cow Creek.

197.2 Darby Creek enters Cow Creek from north side.

199.2 There is quite a bit of pink chert from the Dothan Formation in the creek.

200.5 West Fork Station and the location of Dothan Post Office which was established in 1896 and abandoned in 1942 (McArthur, Oregon Geographic Names). This is the source of the name Dothan given by Diller and the type section is presumably in this area. Cross the creek and continue westward along the West Branch of Cow Creek.

203.1End of county road at Honeysuckle Creek turnoff. Continue westward in Dothan beds.

204.5 Bobby Creek and the road to Marial goes off to the left but traverse continues ahead.

205.3 Dutchman Butte and Slaughter Creek road to right but continue ahead in Dothan.

208.0 Turn right up hill on Elk Valley road. Massive basal Roseburg conglomerate crops out at turn.

210.9 Coarse basal Roseburg conglomerate. The pebbles are more locally derived than those in the Lookingglass Formation.

211.8 Take Elk Valley road to the right. There is conglomerate up the hill to the north but Dothan beds crop out below the road.

212.0 Road junction in Dothan beneath Roseburg. The traverse bears to the left.

213.1 Gulch with fresh outcrop in quarry in Roseburg conglomerate just ahead.

215.5 Turn right into Elk Valley. Elk Valley is underlain by Roseburg sandstone and siltstone above the basal conglomerate and less resistant to erosion.

217.1 Summit between Elk Valley and Twelvemile Creek. The outcrops are Roseburg sandstone.

217.5 Side road goes to the left in saddle but continue toward Twelvemile Creek. The beds are mostly Roseburg sandstone with some layers of conglomerate.

218.0 Bold outcrop of Roseburg sandstone and conglomerate dipping northward 30-35 degrees.

219.7 Dice Creek Road. The hillside north of the creek is Bushnell Rock Member of the Lookingglass Formation. There is probably a fault separating the Roseburg and the Lookingglass along the valley.

219.9 Mouth of Dice Creek and bridge over Twelvemile Creek. A quarry in the Bushnell Rock Member of the Lookingglass is situated here. Johannesen (1972) mapped Days Creek beds a short distance up Twelvemile Creek where the Lookingglass Formation rests directly upon the Days Creek Formation (Fig. 6).

220.3 The beginning of the Tenmile Member of the Lookingglass Formation which is made up mostly of siltsone and thin-bedded sandstone.

221.3 Beds of conglomerate near bridge over Twelvemile Creek are of the overlying off-lapping Olalla Creek Member of the Lookingglass Formation. All the beds from here to Highway 42 are assigned to the Olalla Creek Member. The Tenmile Member may thin near the fault zone.

221.9 Boulder Creek access road goes to the right exposing Olalla Creek conglomerate.

223.8 Bridge over Bridge Creek with most outcrops of conglomerate. Note that landslides are common on the northwest-dipping slopes.

225.1 Bridge over the Middle Fork of the Coquille River with Highway 42 just ahead. The traverse goes west along Highway 42 and the roadcuts show Olalla Creek Member beds.

226.0 Bridge over Middle Fork of the Coquille to the south bank whereas the old highway follows the north bank past the mouth of Bear Creek. Small fossil logs are present just east of Bear Creek along the old highway.

226.9 Bridge over Middle Fork to north bank still in Olalla Creek Member of the Lookingglass.

228.9 Slate Creek comes in to the river from the south. There have been many slides into the river and any long pools tend to be back of landslide dams. Some large landslide blocks of sandstone are present in the river.

229.7 Coos-Douglas county line.

230.9 This is the approximate base of the Flournoy Formation which is made up of graded beds unlike the deltaic Olalla Member of the Lookingglass. No conglomerate has been found in the Flournoy beds near this place. Bridge over the Middle Fork is just ahead.

231.4 Bone Mountain road goes up the hill to the south. Bone Mountain is capped by Tyee.

232.8 The road crosses the river to the north side. At this point we are approximately on the axis of the Coast Range syncline. The Flournoy beds have become more silty and between the river and the base of the Tyee high on the slopes of Bone Mountain the section is dominantly silt equivalent to the Camas Valley Member of the Flournoy Formation (Fig. 4).

233.7 Rock Creek road goes to the right and highway crosses river to the south bank. The beds along here are sandstone equivalent to the White Tail Ridge member of the Flournoy Formation.

233.9 Bridge over the river back to the north side. The old highway joins from the right. If one walks the old highway back toward the mouth of Rock Creek silty beds have produced foraminifera.

235.1 The road has passed the base of the Flournoy sandstone into the Tenmile Member of the Lookingglass which underlies the valley of Sandy Creek ahead. No beds of the Olalla Creek Member of the Lookingglass are known on this side of the Coast Range syncline.

235.5 Remote store on Tenmile Member of the Lookingglass.

235.8 Sandy Creek bridge with road junction just ahead. Turn right and proceed up Sandy Creek on road to Sitkum. Ahead if one proceeds west on Highway 42 the valley narrows as it enters the top of the Bushnell Rock Member. Conglomerate and massive sandstone with coaly layer continues to a point about 200 yards west of Frenchie Creek where it rests unconformably upon the Roseburg Formation. The Bushnell Rock Member is not as massive a conglomerate as it is in most places but instead is made up of beds of conglomerate interspersed with massive sandstone and occasional coaly beds.

238.4 Cross Sandy Creek to the east side. All in Tenmile Member siltstone along the road.

239.9 Just crossed Sandy Creek to west bank and turn up the hill westward leaving the old road. The road proceeds up a dip slope near the top of the Bushnell Rock Member.

242.3 Near the top of the hill coaly streaks are visible in sandstone. Across Sandy Creek valley to the east the Tyee of Thomas Mountain is resting on a thin section of eroded Flournoy sandstone.

244.0 The new road crosses the old Sandy-Big Creek road in saddle and proceed northward up ridge.

245.0 This point is near the base of the Flournoy sandstone which has overlapped the Tenmile Member onto the top of the Bushnell Rock Member.

245.8 Graded bedded Flournoy sandstone which was deposited by turbidity currents in a vastly different environment than that of the Lookingglass beds nearby.

246.5 Approximate base of the Tyee Formation. The Tyee is massive, crossbedded sandstone which contains plant fragments. Near its base in this area it is not graded and it tends to be coarser than the Flournoy beds. This contact was first identified by Trigger (1966) who mapped the area between here and Highway 42.

246.6 Quarry in Tyee at the top of the mountain. Coalified pieces of logs and limbs are present.

246.7 Weaver Road and the traverse turns to the left and continues toward Sitkum. The Flournoy beds strike westward with the upper silty beds being present whereas the Tyee continues to strike to the north toward Brewster Rock. This is perhaps the best place to demonstrate the magnitude of the unconformity at the base of the Tyee and to demonstrate that the Tyee and Flournoy are two different formations.

248.6 A prominent cliff of basal Tyee is to the right and the Flournoy beds crop out beneath.

248.9 Large landslide to the west which dammed Lake Sitkum (now filled). Brewster Rock to the north which formerly had the Forest Lookout is near the base of the Tyee Formation. The Tyee beds dip gently to the Sitkum store. Silty beds of the Camas Valley Member of the Flournoy Formation crop out along the north shore of the old lake west of the old Sitkum store.

251.5 Traverse crosses the landslide, the bridge over the East Fork of the Coquille river and at this point joins the Coos Bay Wagonroad which is the pioneer road between Roseburg and Coos Bay. We turn left to Dora to see the basal part of the Flournoy but if time does not permit the traverse, one could go east from this point.

254.3 Flournoy beds are exposed at the mouth of China Creek. However, if one goes up

China Creek silty beds of the Camas Valley Member are encountered beneath the Tyee Formation.

255.2 Tenmile Member of the Lookingglass Formation but if one looks back the massive sandstone of the basal Flournoy, the White Tail Ridge Member, forms bold cliffs. This cliff of massive sandstone was taken to be the base of the Tyee Formation at one time. The Flournoy overlies the Tenmile Member without the Olalla Creek Member being present on this side of the Coast Range syncline.

256.2 The Dora Store is situated on the siltstone beds of the Tenmile Member of the Lookingglass. West of Dora the basal conglomerate (Bushnell Rock Member) is quite thin to almost missing for the member thins rapidly away from the Canyonville fault zone.

- - - - - - - - - - - - - - -

260.8 Back to the sampe point as 251.8 at bridge over East Fork of the Coquille at foot of slide.

261.0 Brewster Valley is a filled landslide-dammed lake similar to that of Loon Lake and Triangle Lake. Siltstone in the upper part of the Flournoy Formation crops out along the road paralleling the valley.

262.3 Old Sitkum store now abandoned and road up Brummit Creek. The cliffs of Tyee are visible up Brummit Creek and the base is a very short distance west of the store building.

264.5 Camas Creek Road goes across river to south.

265.3 This point is the approximate head of the lake fill. The hills are all Tyee sandstone.

265.6 Coaly beds in nearly flat Tyee is exposed in cut.

266.6 Road has crossed to south side and a 10-15 foot waterfall drops over massive Tyee.

267.9 Dead Horse Creek enters across the river from the north. We are passing more small falls and rapids tumbling over massively bedded Tyee sandstone.

268.4 Lost Creek enters from the north side of the valley and beds are in massive Tyee sandstone.

273.0 Lane-Douglas county line. Continue eastward paralleling river.

274.3 The road that goes south from this point reaches Highway 42 and is all in Tyee beds.

275.2 This is the summit. An old road goes to the north and if one could see eastward through the trees conglomerate in Bushnel Rock dips southward off Roseburg beds and flows. The equivalent limb is missing on the north side and the Flournoy Formation rests directly upon the Roseburg Formation. Considerable folding and erosion preceded deposition of the Flournoy Formation.

276.1 Road to the left and this is the approximate base of the Tyee but landslide blocks and deep soil make determination difficult.

276.8 Busenbark County Park in landslide material but the silty Camas Valley Member of the Flournoy is exposed in the cuts just below.

277.8 Burnt Ridge road leads to the left and graded steeply dipping Roseburg beds strike southwestward beneath the Flournoy and Tyee Formations. If one goes up the Burnt Ridge road a short distance the canyon narrows as the basal sands of the Flournoy are encountered, then it widens out in the Camas Valley Member. Near the top of the hill one enters the Tyee Formation. It is difficult to determine the base of the Tyee for it seems to be siltier than usual and may contain reworked Flournoy siltstone.

279.3 This road junction is the approximate location of Reston which was a stage stop on the old Roseburg to Coos Bay road. Turn right down Tenmile Creek. The small isolated hill to the right is made up of thin-bedded Roseburg.

280.0 Trace of a major fault that cuts the Roseburg Formation. Sheared rock about 100 feet wide has produced a slump zone that the county has tried to hold by dumping large rock. There may be some lateral slip along this fault which affects only the Roseburg and is overlapped to the west by the Flournoy and Tyee Formations without known offset. This same fault may offset the Lookingglass along the north side of Lookingglass Valley.

280.6 The road to the left leads to a rock quarry in Roseburg basalt.

281.0 A quarry on the left side of road is in vertical pillow basalt. It has been abandoned and partly filled but conglomerate and sandstone beyond the basalt are still visible. This vertical section strikes beneath gently dipping Bushnell Rock conglomerate. A fault must parallel the creek for west of the creek crop out Otter Point beds. The deformation took place at the end of the early Eocene for the Lookingglass rests unconformably upon both.

281.6 Enter basal conglomerate but pre-Tertiary crops out on floor of valley to the east and a quarry in greenstone produced crushed rock in that vicinity.

283.5 Road crosses the creek. Conglomerate along the road grades rapidly into sandstone. The valley widens quickly for the transition zone is narrow and the Tenmile Member is ahead.

283.9 Junction with Highway 42 which is located a short distance east of the Tenmile store. Tenmile Butte south across the creek is capped by sandstone and conglomerate of the Olalla Creek Member but the broad Tenmile Creek Valley eastward paralleling the highway is carved in the soft Tenmile Member of the Lookingglass.

285.4 Porter Creek bridge. Porter Creek cuts through the Bushnell Rock Member in a narrow canyon which exposes the conglomerate. Nearly vertical Roseburg sedimentary rock and flows crop out north of the conglomerate.

287.4 Lookingglass Creek into which Tenmile Creek flows. Conglomerate makes up the south-dipping slope to the north.

287.4 The point just past the road to Olalla is made up of Bushnell rock conglomerate. Just east of the point at this mileage the traverse crosses the "Wildlife Safari Fault" and enters the Otter Point Formation. Alexander Butte to the north is set off by Lookingglass Creek Valley to the west and the Wildlife Safari fault cutting off the conglomerate to the east. It is the eastern end of the limb of basal Lookingglass.

289.3 Road to the right goes past Hoover Hill which is made up of the light gray feldspathic sandstone assigned to the Otter Point and encountered earlier north of Brockway (see mileage 144.2).

291.5 Brockway road junction but traverse proceeds eastward toward Winston.

292.3 The bridge over the mouth of Lookingglass Creek just before it enters the South Fork of the Umpqua River. All the rock is Otter Point overlain by alluvium.

293.2 Joining with old Highway 99 in Winston and traverse proceeds to the north (left).

294.3 Bridge over the South Fork of the Umpqua. The small hill to the left north of the river is made up of massive "Hoover Hill facies." The hill to the right with watertank high on point yielded some garnetiferous blue schist which has been carried away by collectors.

295.9 After crossing the overpass a fault places the Roseburg Formation on the north against pre-Tertiary beds.

296.5 After crossing over US Highway I-5 proceed to the north. Roseburg basalt crops out along the road and on the hillside east of highway.

297.5 South turnoff to Roseburg. Roseburg sedimentary beds are interfingered with flows. The bridge over the river is just ahead and basalt crops out along the road north of the bridge.

298.9 Beginning of outcrops of pillow basalt which continue almost continuously past fairgrounds to Harvard Avenue exit.

300.9 Very high cut in Roseburg basalt at the east end of Mt. Nebo just before Harvard Avenue turnoff into Roseburg.

301.7 South end of bridge over South Fork of the Umpqua.

306.0 Many of the hills in and around Roseburg are made up of basalt but the valleys tend to be carved in interbeds. This point is the bridge over the North Fork of the Umpqua River at Winchester where both basalt by the dam and sediments at the west side of the south abutment are a part of the Roseburg Formation. Umpqua Community college is situated on the first prominent bend on the north side of the river above the dam. It is underlain by pillow basalt.

308.8 Sutherlin Creek overpass on I-5 crosses our traverse of the previous day.

309.0 High cuts in severely deformed Roseburg which is situated near the trace of the Bonanza fault. Near here the fault may be high angle reverse rather than a thrust fault.

313.5 After passing thin-bedded dark sand and siltstone along the highway we reach the point under the overpass where we left the highway the previous day (mileage 98.7).

- - - - - - - - - - - - - - -

The highway as far as the turnoff to Yoncalla is covered by the log of yesterday. See mileage 98.7- I-5 overpass south of Sutherlin to 80.8 at intersection of I-5 and Highway 99 near Yoncalla.

- - - - - - - - - - - - - - -

331.6 Same as 90.8, the intersection of I-5 and Highway 99 south of Yoncalla. Follow I-5.

334.1 A low drainage divide with west-dipping cuesta in Roseburg sedimentary beds to the northwest and a dip slope on basaltic flank of the Red Hill anticline to the southeast.

334.7 A dike cuts the Roseburg Formation to the west.

335.5 This is the approximate contact between the Flournoy and the Roseburg Formations. The contact is unconformable and the Lookingglass Formation which should be between is missing. Scott Valley is carved largely in the Roseburg beds. The Flournoy beds can be seen along the north side of the valley cropping out in the grassy slope. The road east through Scott Valley goes past the basalt in the north end of the Red Hill anticline, through a thin Flournoy section, the Spencer and Fisher Formations and passes north of Hobart Butte before reaching the Coast Fork of the Willamette (Hoover, 1963).

336.1 Bridge over Elk Creek just south of an excellent outcrop of Flournoy beds.

340.8 Drainage divide at the top of a hill. Slides from the east have blocked the highway several times. The rock is Flournoy sandstone and siltstone but it seems to be more deeply weathered than usual at this point.

342.7 Highway junction with turnoff to Drain, Elkton and the coast. All the exposures along here are part of the Flournoy Formation.

344.4 Flournoy sandstone which is composed largely of graded beds of micaceous sandstone crop out along the highway.

344.7 A dike crops out to the east near the old railroad siding of Comstock. The Comstock fauna of Turner (1938) and others came from or near the north edge of the dike when the highway cuts were fresher. The fauna included *Venericardia* and *Turritella.*

345.8 Base of the Spencer Formation is exposed where pebbly tuffaceous sandstone disconformably rests on Lorane siltstone which is gradational down into the Flournoy Formation. Although formerly correlated with the Elkton Siltstone by Baldwin (1961) it seems better to assign the Lorane to the Camas Valley Member of the Flournoy Formation which is a little older than the Elkton Formation.

346.0 A coaly bed is exposed on the east side of the highway. This is near the top of the Spencer Formation of Vokes, Snavely, and Myers (1951).

346.8 The Comstock flora was collected from a railroad cut opposite this point along the highway. The fossil leaves were obtained near the base of the Fisher Formation and are probably latest Eocene, possibly early Oligocene.

348.6 Road to the left over overpass is old Highway 99 which leads to Cottage Grove. The rock approaching and at the intersection is purplish tuff and tuffaceous sandstone of the Fisher Formation. A landslide area on the east side has been somewhat stabilized by dumping rock.

349.2 Hawley Road overpass is the approximate location of the divide between the Willamette and Umpqua rivers. This divide has an imperceptible north slope and appears to have been caused by piracy and reversal of flow into Pass Creek. Diller (1915) proposed that the Umpqua River flowed into the Willamette at one time and was captured by a shorter swifter flowing coastal stream that caused reversal of drainage along what is now Pass Creek.

351.6 Bridge over the Coast Fork of the Willamette River. Mostly Fisher beds crop out to the east.

354.1 Tuffaceous sedimentary beds of the Fisher Formation crop out along the edge of Cottage Grove.

355.0 Turnoff to Cottage Grove (west), Dorena Dam (east) and the Bohemia mining district (east).

355.4 Row River bridge on I-5.

358.0 South entrance to rest area on the east side of the highway.

363.1 This is the junction to Creswell on the west side with Creswell Butte, a diorite site which is located just south of the town. Outcrops may be seen where Highway 99 cuts the lower part of the slope. The main highway has been on an alluvial fill of the Coast Fork of the Willamette River. The older highway, Highway 99, follows the western margin of the valley and goes through basalt flows and tuffaceous sedimentary rocks. The hills to the east are made up of flows and tuffaceous sedimentary rock.

365.3 Between Creswell junction and this point the highway is crossing a terrace of older alluvium which is capped by thoroughly weathered alluvium. Just ahead is a large depression called Camas Swale whose floor is covered by relatively recent gravels and sand probably laid down when the Coast Fork of the Willamette made a circular bend later cut off. The peak to the north and west is Spencer Butte, a diorite intrusive in the form of an east-dipping sill.

366.7 The Goshen flora was collected from the old highway cut where the road rounded a small hill at the west end of an overpass over I-5.

369.1 Intersection with highway from Willamette Summit. The small hill by intersection just before crossing the railroad yielded a late Oliogocene flora which is listed by Roland W. Brown in Vokes, Snavely and Myers (1951). The rock is probably in the upper part of the Eugene Formation.

369.4 The tuffaceous sedimentary rock to the west and a short distance north of overpass has been sliding toward I-5. Many yards have been removed and rock is piled at the toe of the slide in an effort to stop movement.

370.9 Just north of an overpass a high slope on the west shows columnar basaltic intrusive rock cutting the Eugene Formation. Between here and Judkins Point several dikes intrude the Eugene. The intrusive rock may be of early Miocene age and related to the Little Butte volcanics.

372.7 The traverse leaves the main highway and turns westward beneath I-5 to Judkins Point which is a basaltic east-dipping sill.

373.7 North side of the Geology Building on the University of Oregon campus.

\- - - - - - - - - - - - -

Instead of turning westward past Judkins Point into Eugene the main highway proceeds northward over the alluvial covered valley to the bridge over the McKenzie River opposite Armitage Park. Just across the river and to the east is a quarry in an intrusive body which cuts the Eugene Formation. The intrusive comes up as a dike, then becomes parallel to the Eugene beds as a sill. The highway parallels the face of the Coburg Hills which may be a faultline scarp. The fault may be located near the highway. Low hills, such as West Point Hill, and othersjust east of the highway, may be exhumed sills in the Eugene Formation. The upper part of the scarp is capped by basalt flows of possible early Miocene age. The Eugene beds are found only at the base of the scarp and presumably crop out beneath the younger volcanics. Most of the hills near the highway south of the Corvallis turnoff are intrusive basaltic bodies. The highway from I-5 to Corvallis crosses the alluvial floor of the Willamette valley.

\- - - - - - - - - - - - - -

FIELD TRIP NO. 3

GEOLOGY OF THE WEST-CENTRAL PART OF THE OREGON COAST RANGE

BY

P. D. Snavely, Jr., N. S. MacLeod, H. C. Wagner, and D. L. Lander
U.S. Geological Survey, Menlo Park, California

March 1980

Frontispiece. View to the south from Otter Crest (Stop 1A) showing ring dikes (r) and radial dikes (rad) of Cape Foulweather Basalt that intrude sandstone and siltstone of the middle Miocene Astoria Formation. Yaquina Head on the skyline is one of the former eruptive centers of Cape Foulweather Basalt.

GEOLOGY OF THE WEST-CENTRAL PART OF THE OREGON COAST RANGE[1]

The tectonic, depositional, and magmatic history of Cenozoic sedimentary and volcanic rocks of western Oregon and the adjacent continental margin is interpreted as having been molded by episodic interactions between the Pacific and North American plates (Snavely and MacLeod, 1977; Snavely and others, 1979). In the Coast Range and on the inner continental shelf more than 7000 meters of Tertiary sedimentary and volcanic rocks accumulated in a marginal basin on a lower to middle Eocene oceanic crust. The route of this field trip traverses a representative section of Tertiary rocks in the central part of the Oregon Coast Range (fig. 1); these rocks in part form the basis for interpreting the Tertiary geologic history.

A thorough discussion of the formations that crop out in the central part of the Oregon Coast Range is not presented in this report as the Tertiary geology of this region has been described fully in previous recent field trip guidebooks by Snavely, MacLeod, and Rau (1969) and by MacLeod and Snavely (1973). Their outcrop areas are shown on detailed geologic maps of the field trip area that have recently been published (Snavely and others, 1976a, b, c). In addition, Snavely and MacLeod (1971) and Lund (1972) give descriptions of the coastal geology, and Braislin, Hastings, and Snavely (1971), Snavely Pearl, and Lander (1977), and Snavely, Wagner, and Lander (1979) summarize the general geology of the adjacent continental shelf.

The oldest rocks exposed in the Oregon Coast Range are pillow lavas, breccias, and interbedded basaltic sedimentary rocks of early and middle Eocene age (fig. 2). In this part of the Coast Range they are referred to the Siletz River Volcanics (Snavely and Baldwin, 1948; Snavely and others, 1968); correlative volcanic units in Oregon and Washington are shown in the correlation chart (fig. 3). These tholeiitic basalts have compositions similar to those of oceanic ridges with low K_2O and TiO_2 (Table 1, col. 1; Snavely and others, 1968) and have similar rare earth elements (REE) patterns. In places, as in the Ball Mountain area (fig. 1), the tholeiitic basalts are overlain by breccias, lapilli tuffs, and pillow lavas of alkalic basalt with interbedded fossiliferous basaltic sandstone and conglomerate. A few flows at the top of the sequence are subaerial. Sills and filled lava tubes are common in this part of the sequence. This upper part of the Siletz River Volcanics is inferred to have been erupted to form oceanic islands and seamounts that were distributed randomly on the ridge basalt (Snavely and MacLeod, 1977).

Basalts that form the Siletz River Volcanics are interpreted to be oceanic crust that accreted onto the continental margin at the time when subduction jumped from east of the Coast Range to the present continental margin. Absence of older rocks in the Coast Range and the relatively thin 16 km crust (Berg and others, 1966) are consistent with this interpretation. However, ultramafic rocks typical of ophiolite sequences have not been found.

A deep marginal basin formed east of the new locus of underthrusting on the newly accreted lower to middle Eocene oceanic crust. More than 2000 meters of turbidite sandstone of the Tyee Formation (figs. 4, 5) (Snavely and others, 1964), and siltstone of the Yamhill Formation (Baldwin and others, 1955) were deposited in middle and early late Eocene time. The Tyee Formation underlies most of the eastern part of the map area (fig. 1) and forms most of the axial part of the Coast Range for a distance of 150 km south to the Klamath Mountains. Source direction, shown by flute and groove casts (arrows on fig. 1), and lithologic characteristics of the sandstone indicate a Klamath provenance. Near Ball Mountain, where the Tyee rests on the truncated surface of a seamount of the Siletz River Volcanics, the Tyee is less than 300 m thick; north of the seamount the Tyee

[1]This report is preliminary and has not been edited or reviewed for conformity with Geological Survey standards and nomenclature.

thickens and interfingers laterally with deep-water marine hemipelagic siltstone of the lower part of the Yamhill Formation. In the map area (fig. 1), the Tyee Formation grades upward into marine siltstone with minor glauconitic sandstone of the Yamhill Formation. Stratigraphic correlatives of the Tyee Formation of middle Eocene (Ulatisian) age and the Yamhill Formation of late middle to early late Eocene (Ulatisian and early Narizian) age are shown in the correlation chart (fig. 3).

In late middle or early late Eocene time, transform faulting is interpreted to have occurred between the Pacific and North American plates. Dextral slip on the continental shelf juxtaposed an early Eocene graywacke sequence on the west against the early to middle Eocene Siletz River Volcanics on the east. This dextral fault (fig. 6, fault A on section) is marked by a linear magnetic anomaly on the inner continental shelf shown on the aeromagnetic map published by the U.S. Geological Survey (1970). This anomaly extends from latitude 45°N (just north of cross section, fig. 6) southward to latitude 43°15'N near Coos Bay. On the inner shelf and onshore near the coast, broad high-amplitude magnetic anomalies typical of terrane underlain by Eocene basalt occur east of the gradient. In contrast, the area west of the linear gradient is magnetically "quiet." West of the gradient a sequence of more than 2000 meters of micaceous arkosic wacke and interbedded siltstone of early Eocene age was penetrated in the Pan Am P-0112 and the Union Fulmar P-0130 (see index map, fig. 6) test wells 90 and 180 km south of the cross section (Snavely and others, 1977, 1979). Foraminifera and nannofossils indicate that this wacke is of early Eocene (Penutian Stage) age and was deposited in a bathyal environment (W. W. Rau and David Bukry, written communs., 1979).

Inasmuch as the wacke and the basalt have been juxtaposed from Coos Bay to the line of the cross section along this transcurrent fault, a dextral separation of about 200 km is required. The original site of deposition for the lower Eocene wacke, therefore, must have been in coastal northern California or farther south.

An episode of plate convergence and underthrusting, which began in mid-late Eocene time, had a locus of underthrusting (fig. 6, Fault B on cross section) that probably lay west of the transcurrent fault boundary. Regional uplift accompanied this period of underthrusting and produced a marked regional angular unconformity at the base of upper Eocene strata in the Oregon and Washington Coast Ranges and on the continental shelf. Also, during this time the earlier deep marginal basin in the present site of the Coast Ranges was segmented into a number of shallow shelf basins. In the map area a regional unconformity separates the Tyee and Yamhill Formations from the overlying Nestucca Formation (Snavely and Vokes, 1949) of latest Eocene age.

In latest Eocene to late middle Miocene time, a period inferred to have been dominated by extension appears to have occurred in the inner shelf area. Several elongate north-trending deep marginal basins were formed and basalt was erupted near the present coastline during both late Eocene and middle Miocene times; gabbro sills were intruded in the late Oligocene. The upper Eocene Yachats Basalt (Snavely and MacLeod, 1974) was erupted from several major centers in the Cape Perpetua-Heceta Head area and at Cascade Head along the eastern margin of a deep marginal basin on the inner shelf. An analysis of the subsurface stratigraphy in the test well drilled on the southern part of the Oregon continental shelf (Snavely and others, 1977) and interpretation of U.S. Geological Survey 24-channel seismic reflection profiles indicates that volcaniclastic sediments and lesser amounts of lapilli-tuff and breccia were deposited throughout this basin. These units thin westward against the middle Eocene mid-shelf high and do not extend west of the former zone of transcurrent faulting.

The Yachats volcanic rocks were erupted from many local vents in the Cape Perpetua-Heceta Head area to form low shield-like accumulations composed largely of subaerial basalt flows 4 to 8 meters thick. Pillow basalt and tuff breccia and marine basaltic conglomerate and sandstone are present at the base and along the fringes of the volcanic piles indicating that the basalts were initially erupted on a shallow shelf. Correlative volcanic rocks crop out along the lower part of the Siletz River in the northwestern part of the map area and at Cascade Head. Upper Eocene volcanic sequences also comprise the upper part of the Tillamook Volcanics of Warren, Norbisrath, and Grivetti (1945).

Typically, the volcanic rocks near Yachats consist of porphyritic basalt and basaltic andesite that are quartz normative and characterized by a relatively high alkali, alumina, and titanium content (Snavely and MacLeod; 1974, Table 1). These rocks show a wide range in chemical composition and petrography; some dikes that cut the upper part of the sequence are of rhyodacitic composition.

Camptonitic marine lapilli tuff and pillow lavas of early(?) Oligocene age that crop out near the mouth of the Siletz River (Snavely and others, 1976a) are among the most unusual rocks in western Oregon. They are marked by low silica (as low as 39 percent) and high alkali, iron, titanium, and phosphorus content (Table 1, col. 5) and are strongly nepheline normative. Camptonite dikes and sills crop out over a broad area north and northwest of Euchre Mountain (fig. 1), and some show marked differentiation.

Nepheline syenite and phonolite (Table 1, col. 6) sills, dikes, and a small stock occur in the Tidewater and Waldport quadrangles (fig. 1). The largest intrusive body is the 80-meter-thick sill that caps Table Mountain (Snavely and others, 1976c). Cobbles of nepheline syenite are widely distributed in Pleistocene terrace deposits indicating that the nepheline syenite sills were formerly much more extensive. The camptonite and nepheline syenite intrusive rocks may be a late product of the period of igneous activity that produced the Yachats Basalt.

The Yachats Basalt overlies and grades laterally into thin-bedded tuffaceous siltstone of the Nestucca Formation (fig. 7) (Snavely and Vokes, 1949). Marine basaltic sandstone and conglomerate of latest Eocene age overlie the basalt sequences at Cape Perpetua and Cascade Head. These basaltic sands thin rapidly away from the volcanic centers from which they were derived and are absent throughout most of the map area. Massive to thick-bedded tuffaceous siltstone and very fine-grained sandstone of Oligocene age, referred to the Alsea Formation (fig. 8) (Snavely and others, 1975), overlie the upper Eocene volcanic and sedimentary rocks on the west flank of the Coast Range (fig. 1). The ubiquitous high ash content in the Oligocene marine siltstone was derived from explosive silicic volcanism in the ancestral Cascade Range. The ash was probably transported by rivers and streams to the former coast; some nearly pure tuff beds, however, may have resulted from ash fall directly into the marine environment.

Dikes, sills, and inclined sheets of iron-rich granophyric gabbro (Table 1, col. 7) of mid-Oligocene age (30 m.y.B.P.) crop out along the axial part of the Coast Range (Snavely and Wagner, 1961). The thickest sill, about 330 meters thick, underlies Marys Peak 20 km southwest of Corvallis (Roberts, 1953; Baldwin, 1956). Numerous other sills 100 to 200 meters thick, cap many of the higher peaks and upland surfaces in the Coast Range. Most of the sills show strong differentiation, with late development of ferrogranophyre and granophyre (MacLeod, 1970).

Sandstone and conglomerate with intercalated siltstone, tuff, and coal beds of late Oligocene and earliest Miocene age, assigned to the Yaquina Formation (fig. 9) (Schenck, 1928), overlie the siltstone of the Alsea Formation. These coarse-grained sedimentary rocks are interpreted as a deltaic deposit that developed at the mouth of a river that drained through the present site of the Coast Range (Snavely and Wagner, 1963; Goodwin, 1973). Andesitic and dacitic clasts in the conglomerate and crossbedded pumiceous sandstone of this unit were probably derived from an ancestral Cascade Range. The Yaquina Formation is restricted to the inner shelf as it was not penetrated in the Nautilus well (index map; fig. 6). Marine siltstone and very fine-grained sandstone of the Nye Mudstone (fig. 10) (Harrison and Eaton, 1920; Snavely and others, 1964) of early Miocene age and sandstone and siltstone of the Astoria Formation (fig. 11) (Packard and Kellogg, 1934; Snavely and others, 1964) of middle Miocene age overlie the Yaquina Formation. A few thick tuff beds (1 to 7 m) in the Astoria Formation attest to continued volcanism to the east in an ancestral Cascade Range.

Three periods of basaltic volcanism occurred in western Oregon and Washington in middle and late Miocene time (Snavely and others, 1973). The Miocene volcanic rocks and correlative intrusive rocks crop out in a narrow belt along the coast of northwestern Oregon and also crop out inland southeast and northeast of the mouth of the Columbia River in Oregon and Washington. Two of the Miocene basalt units are present in the field trip area. The oldest unit, the Depoe Bay Basalt (Table 1, col. 8) is the most voluminous and makes up many of the scenic headlands of the northwest coast, such as Cape Lookout and Cape Meares. Thick sills of Depoe Bay Basalt form Cape Falcon and Tillamook Head on the coast and also Mount Hebo and Mount Gauldy to the east in the Coast Range. This unit is exceptionally well exposed at its type locality at Depoe Bay, where it consists principally of pillow breccia. This flow unit extends as far west as the Standard-Union Nautilus well where it is about 15 m thick (cross section, fig. 6). North and east of Depoe Bay, Oligocene and Miocene sedimentary rocks are laced with a plexus of sills and dikes of basalt, breccia, and peperite that attest to the local origin of the extrusive sequence. The Depoe Bay Basalt is overlain by penecontemporaneously deformed massive arkosic sandstone and thin-bedded siltstone and sandstone informally referred to as the sandstone of Whale Cove.

The middle unit of the three Miocene basalt sequences, the Cape Foulweather Basalt (Snavely and others, 1973), overlies the sandstone of Whale Cove in several localities along the coast between Newport and the Columbia River, and dikes and sills related to this basalt are common near the coast. The most extensive exposure of this unit is at the type locality, Cape Foulweather (fig. 12), about 16 km north of Newport, where it consists chiefly of rudely jointed breccia, tuff breccia, and minor thin flows that are cut by related dikes, sills, volcanic necks, and irregular intrusive bodies. The basalt sequence at Cape Foulweather is largely of subaerial origin, but bedded lapilli tuffs and breccia that are exposed 3 to 7 km north of Cape Foulweather probably formed a broad fringing marine apron around the subaerial volcanic center. The Cape Foulweather volcanics are restricted to the inner shelf and do not extend as far west as the Nautilus well. They presumably grade laterally into strata equivalent to the sandstone of Whale Cove (fig. 2) before reaching the area of the well. Yaquina Head,3 km north of Newport, also is underlain by flows, breccia, dikes, and sills of Cape Foulweather Basalt. Dikes and sills of Cape Foulweather also occur farther south along the coast at Seal Rocks and cut Miocene and Oligocene marine sandstone and siltstone east of the coast between Cape Foulweather and Newport. The youngest of the three coastal Miocene basalt units is exposed only in the Coast Range of southwestern Washington (Snavely and others, 1973) where it is interbedded in sedimentary rocks of the lower part of the Montesano Formation of Weaver (1912).

The three Miocene basalt units are the same age as petrochemically, isotopically, and paleomagnetically identical units within the Yakima Subgroup of the Columbia River Basalt Group which was erupted from vents 500 km to the east on the Columbia Plateau (Snavely and others, 1973; McDougall, 1976).

A major episode of underthrusting is interpreted to have occurred in late middle Miocene time. A widespread unconformity at the base of the late Miocene in southwest Washington and on the Oregon and Washington continental shelves records regional uplift that probably occurred in response to this period of convergence. Middle Miocene and older strata were uplifted and folded on the inner shelf and later were truncated by erosion prior to downwarping and the deposition of upper Miocene and Pliocene marine strata. Acoustical profiles across the anticlinal structure tested by the Nautilus well clearly show the marked truncation of middle Miocene strata at the base of the late Miocene unconformity (cross section, fig. 6). Basalt flows that occur near the base of this unconformity in the Grays Harbor basin of southwestern Washington have a K/Ar age of about 9 m.y. (Snavely and others, 1973).

The axial part of the marginal basin shifted westward but remained the site of continued, but probably episodic, downwarping from late Miocene to Pleistocene time and more than 2000 meters of sand and silt were deposited on the continental shelf (fig. 2). The broad basin was essentially filled with Pliocene to middle(?) Pleistocene sediments, but by late Pleistocene time downwarping had generally ceased and upper Pleistocene and Holocene deposits extended across the basin and lapped onto older strata along both margins.

Underthrusting appears to have resumed in the late(?) Pleistocene and may still continue along some segments of the Oregon and Washington continental margin. This episode of compressional tectonics formed broad folds and imbricate thrusts that folded and uplifted the Pliocene and Pleistocene trench and abyssal plain deposits in the upper plate (cross section, fig. 6). About 12 km south of the cross section a study of Foraminifera in mudstone samples collected on the lower slope indicates that similar deposits there have been uplifted as much as 1100 m (Kulm and Fowler, 1974). At this time a wedge of inferred upper Oligocene to upper middle Miocene melange and broken formation between thrust faults C and B (fig. 6) was uplifted by an imbricate set of landward-dipping thrust faults as were the overlying abyssal Pliocene(?) deposits on the upper slope.

A complex zone of normal faults occurs on the inner continental shelf near the east end of the cross section (fig. 6). High-resolution profiles across this zone indicate that many of these steeply east-dipping normal faults offset Holocene(?) deposits. At least one of these faults reaches the sea floor. Several normal faults, which have an aggregate stratigraphic throw of about 1000 m (Braislin and others, 1971), are present in the nearshore area and north-trending normal faults that offset the Astoria Formation have been mapped near the coast in the Cape Foulweather and Yaquina quadrangles (Snavely and others, 1976a, 1976c). The inner-shelf zone of normal faulting, on the basis of linear aeromagnetic anomalies, can be extended about 35 km south of the cross section and more than 90 km north of it. Several earthquakes with intensities of III to IV were located near Newport (Berg and Baker, 1963); they may have been generated by movement on one or more of these normal faults. The zone of normal faulting is astride the "hinge line" between areas of post-late Miocene subsidence in the deep marginal basin and uplift in the Coast Range. These normal faults may result from extension and attenuation of the upper plate across the inner shelf due to the thickening and uplift of strata in the upper plate by imbricate thrust faulting on the outer continental shelf and slope.

In summary, the Tertiary and Quaternary sequences now present on the Oregon continental margin are interpreted as part of an upper plate above a low-angle east-dipping mega-thrust below which the Pacific plate has and may still be underthrusting the North American plate. As a result of this relative eastward motion, the Tertiary strata in the upper plate have been compressionally deformed across a 75-km belt that extends from the base of the slope landward to the western flank of the marginal basin (fig. 6).
The tectonic framework in the upper plate, as interpreted from our seismic profile, is consistent with a model of eastward dip-slip movement of an oceanic plate on a low-dipping underthrust. Major zones of vertical crustal movement in the upper plate appear to have a general pattern of (1) uplift along the continental slope and outer shelf by broad folds and by an imbricate set of landward dipping thrust faults (2) regional subsidence in the marginal basin on the inner shelf and (3) uplift in the Coast Range. These zones of vertical deformation appear to trend roughly parallel to the present locus of underthrusting at the base of the slope and indicate a generally eastward direction of underthrusting. A similar model of regional uplift and subsidence was documented by Plafker (1972) across the continental margin of Alaska following the 1964 earthquake.

References

Baldwin, E. M., 1956, Geologic map of the lower Siuslaw River area, Oregon: U.S. Geological Survey Oil and Gas Investigations Map OM-186.

_____ 1964, Geology of Oregon: Oregon University, Oregon Cooperative Bookstore, 2nd ed., 165 p.

_____ 1974, Eocene stratigraphy of southwestern Oregon: State of Oregon Bulletin 83, 40 p.

Baldwin, E. M., Brown, R. D., Jr., Gair, J. E., and Pease, M. H., Jr., 1955, Geology of the Sheridan and McMinnville quadrangles, Oregon: U.S. Geological Survey Oil and Gas Investigations Map OM-155.

Berg, J. W., Jr. and Baker, C. D., 1963, Oregon Earthquakes, 1841 through 1958: Bulletin of the Seismological Society of America, v. 53, no. 1, p. 95-108.

Berg, J. W., Jr., and others, 1966, Crustal refraction profile, Oregon Coast Range: Seismological Society of America Bulletin, v. 56, p. 1357-1362.

Braislin, D. B., Hastings, D. D., and Snavely, P. D., Jr., 1971, Petroleum potential of western Oregon and Washington, in Cram, I. A., ed., Possible future petroleum provinces of North America: Tulsa, Oklahoma, American Association of Petroleum Geologists Memoir 15, p. 229-238.

Brown, R. D., Jr., Gower, H. D., and Snavely, P. D., Jr., 1960, Geology of the Port Angeles-Lake Crescent area, Clallam County, Washington: U.S. Geological Survey Oil and Gas Investigations Map OM-203.

Cushman, J. A., Stewart, R. E., and Stewart, K. C., 1949, Upper Eocene Foraminifera from the Toledo Formation, Toledo, Lincoln County, Oregon: Oregon Department of Geology and Mineral Industries Bulletin 36, pt. 6, p. 126-145.

Durham, J. W., 1944, Megafaunal zones of the Oligocene of northwestern Washington: California University Publications, Department of Geological Sciences Bulletin, v. 27, no. 5, p. 101-211, pls. 13-18.

Goodwin, C. J., 1973, Stratigraphy and sedimentation of the Yaquina Formation, Lincoln County, Oregon: Oregon State University, Master's Thesis, 121 p.

Harrison and Eaton [firm], 1920, Report on investigations of oil and gas possibilities of western Oregon: Oregon Bureau of Mines and Geology, Mineral Resources of Oregon, v. 3, no. 1, p. 3-37.

Kulm, L. D., and Fowler, G. A., 1974, Oregon continental margin structure and stratigraphy: A test of the imbricate thrust model, in Burk, C. A., and Drake, C. L., eds., The Geology of Continental Margins: New York, Springer-Verlag, p. 261-283.

Lund, E. H., 1972, Coastal landforms between Florence and Yachats, Oregon: Ore Bin, v. 34, no. 5, p. 73-92.

MacLeod, N. S., 1970, Geology and igneous petrology of the Saddleback area, central part of the Oregon Coast Range: University of California, Santa Barbara doctoral dissertation, 205 p.

MacLeod, N. S., and Snavely, P. D., Jr., 1973, Volcanic and intrusive rocks of the central part of the Oregon Coast Range: Oregon Department of Geology and Mineral Industries Bulletin 77, p. 47-74.

McDougall, Ian, 1976, Geochemistry and origin of basalt of the Columbia River Group, Oregon and Washington: Geological Society of America Bulletin, v. 87, no. 5, p. 777-792.

Packard, E. L., and Kellogg, A. R., 1934, A new cetothere from the Miocene Astoria Formation of Newport, Oregon: Carnegie Institute Washington Publication 447, Contributions to Paleontology, p. 1-62.

Plafker, George, 1972, Alaskan earthquake of 1964 and Chilean earthquake of 1960--implications for arc tectonics: Journal of Geophysical Research, v. 77, no. 5, p. 901-925.

Rau, W. W., 1967, Geology of the Wynoochee Valley Quadrangle: State of Washington, Division of Mines and Geology Bulletin, no. 56, 51 p.

Roberts, A. E., 1953, A petrographic study of the intrusive at Marys Peak, Benton County, Oregon: Northwest Science, v. 27, no. 2, p. 43-60.

Schenck, H. G., 1928, Stratigraphic relations of western Oregon Oligocene formations: California University, Department of Geological Sciences Bulletin, v. 18, no. 1, 50 p.

Snavely, P. D., Jr., and Baldwin, E. M., 1948, Siletz River volcanic series, northwestern Oregon: American Association of Petroleum Geologists Bulletin, v. 32, p. 805-812.

Snavely, P. D., Jr., Brown, R. D., Jr., Roberts, A. E., and Rau, W. W., 1958, Geology and coal resources of the Centralia-Chehalis district, Washington: U.S. Geological Survey Bulletin 1053, 159 p.

Snavely, P. D., Jr., and MacLeod, N. S., 1971, Visitors' guide to the geology of the coastal area near Beverly Beach State Park, Oregon: Ore Bin, v. 33, p. 83-105.

_____ 1974, Yachats Basalt--an upper Eocene differentiated volcanic sequence in the Oregon Coast Range: U.S. Geological Survey Journal of Research, v. 2, no. 4, p. 395-403.

_____ 1977, Evolution of Eocene continental margin of western Oregon and Washington: Geological Society of America Abstracts with Programs, v. 9, no. 7, p. 1183.

Snavely, P. D., Jr., MacLeod, N. S., and Rau, W. W., 1969, Geology of the Newport area, Oregon: Ore Bin, v. 31, nos. 2 and 3, p. 25-71.

Snavely, P. D., Jr., MacLeod, N. S., Rau, W. W., Addicott, W. O., and Pearl, J. E., 1975, Alsea Formation--an Oligocene marine sedimentary sequence in the Oregon Coast Range: U.S. Geological Survey Bulletin 1395-F, 21 p.

Snavely, P. D., Jr., MacLeod, N. S., and Wagner, H. C., 1968, Tholeiitic and alkalic basalts of the Eocene Siletz River Volcanics, Oregon Coast Range: American Journal of Science, v. 266, p. 454-481.

_____ 1973, Miocene tholeiitic basalts of coastal Oregon and Washington and their relations to coeval basalts of the Columbia Plateau: Geological Society of America Bulletin, v. 84, p. 387-424.

Snavely, P. D., Jr., MacLeod, N. S., Wagner, H. C., and Rau, W. W., 1976a, Geology of the Cape Foulweather and Euchre Mountain quadrangles, Oregon: U.S. Geological Survey Miscellaneous Investigations Series Map I-868, scale 1:62,500.

_____ 1976b, Geology of the Waldport and Tidewater quadrangles, Oregon: U.S. Geological Survey Miscellaneous Investigations Series Map I-866, scale 1:62,500.

_____ 1976c, Geology of the Yaquina and Toledo quadrangles, Oregon: U.S. Geological Survey Miscellaneous Investigations Series Map I-867, scale 1:62,500.

Snavely, P. D., Jr., Niem, A. R., and Pearl, J. E., 1978, Twin River Group (upper Eocene to lower Miocene)--defined to include the Hoko River, Makah and Pysht Formations, Clallam County, Washington: U.S. Geological Survey Bulletin 1457-A, p. A111-A120.

Snavely, P. D., Jr., Pearl, J. E., and Lander, D. L., 1977, Interim report on petroleum resources potential and geologic hazards in the outer continental shelf-Oregon and Washington Tertiary Province: U.S. Geological Survey Open-File Report No. 77-282, 64 p.

Snavely, P. D., Jr., Rau, W. W., and Wagner, H. C., 1964, Miocene stratigraphy of the Yaquina Bay area, Newport, Oregon: Ore Bin, v. 26, no. 8, p. 133-151.

Snavely, P. D., Jr., and Vokes, H. E., 1949, Geology of the coastal area between Cape Kiwanda and Cape Foulweather, Oregon: U.S. Geological Survey Oil and Gas Investigations Preliminary Map 97, scale 1:62,500.

Snavely, P. D., Jr., and Wagner, H. C., 1961, Differentiated gabbroic sills and associated alkalic rocks in the central part of the Oregon Coast Range, Oregon, in Geological Survey research, 1961: U.S. Geological Survey Professional Paper 424-D, p. D156-D161.

_____ 1963, Tertiary geologic history of western Oregon and Washington: Washington Division of Mines and Geology Report of Investigations 22, 25 p.

Snavely, P. D., Jr., Wagner, H. C., and Lander, D. L., 1980, Interpretation of the Cenozoic geologic history, central Oregon continental margin: Geological Society of America Bulletin , v. 91.

Snavely, P. D., Jr., Wagner, H. C., and MacLeod, N. S., 1964, Rhythmic-bedded eugeosynclinal deposits of the Tyee Formation, Oregon Coast Range: Kansas Geological Survey Bulletin 169, v. 2, p. 461-480.

U.S. Geological Survey, 1970, Aeromagnetic survey composite map, Oregon Coast: U.S. Geological Survey Open-File Map, scale 1:500,000.

Vine, J. D., 1962, Stratigraphy of Eocene rocks in a part of King County, Washington: Washington Division of Mines and Geology Report of Investigations 21, 20 p.

Vokes, H. E., Myers, D. A., and Hoover, Linn, Jr., 1954, Geology of the west-central border area of the Willamette Valley, Oregon: U.S. Geological Survey Oil and Gas Investigations Map OM-150, scale 1:62,500.

Warren, W. C., Norbisrath, H., and Grivetti, R. M., 1945, Geology of northwestern Oregon, west of Willamette River and north of latitude 45°15': U.S. Geological Survey Oil and Gas Investigations Preliminary Map 42.

Weaver, C. E., 1912, A preliminary report on the Tertiary paleontology of western Washington: Washington Geological Survey Bulletin, v. 15, 80 p.

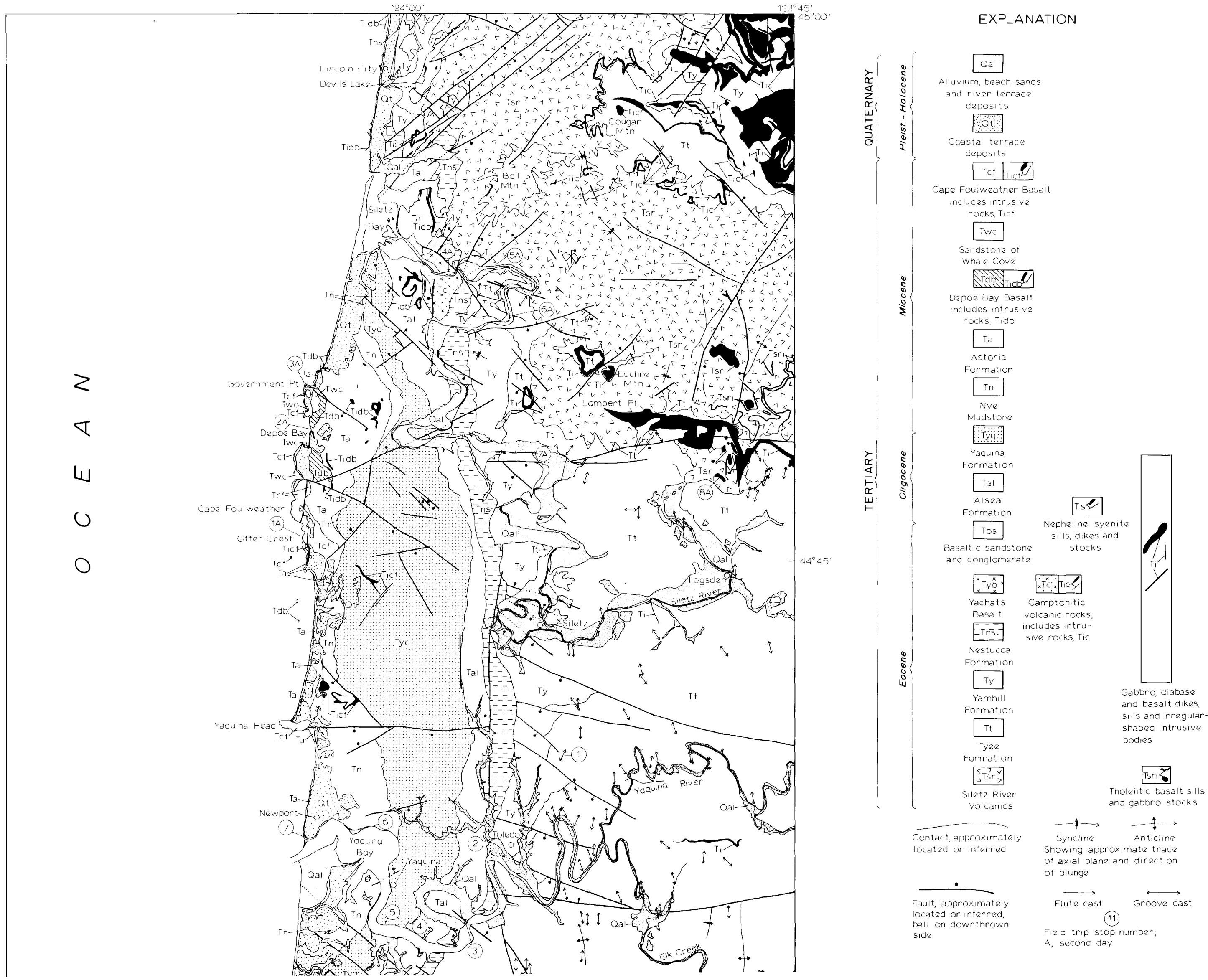
EXPLANATION
QUATERNARY
TERTIARY
Pleist - Holocene
Miocene
Oligocene
Eocene
Qal
Alluvium, beach sands and river terrace deposits
Qt
Coastal terrace deposits
Tcf Ticf
Cape Foulweather Basalt includes intrusive rocks, Ticf
Twc
Sandstone of Whale Cove
Tdb Tidb
Depoe Bay Basalt includes intrusive rocks, Tidb
Ta
Astoria Formation
Tn
Nye Mudstone
Tyq
Yaquina Formation
Tal
Alsea Formation
Tbs
Basaltic sandstone and conglomerate
Tis
Nepheline syenite sills, dikes and stocks
Tyb
Yachats Basalt
Tc Tic
Camptonitic volcanic rocks; includes intrusive rocks, Tic
Tns
Nestucca Formation
Ty
Yamhill Formation
Tt
Tyee Formation
Tsr
Siletz River Volcanics
Ti
Gabbro, diabase and basalt dikes, sills and irregular-shaped intrusive bodies
Tsri
Tholeiitic basalt sills and gabbro stocks
Contact approximately located or inferred
Syncline
Anticline
Showing approximate trace of axial plane and direction of plunge
Fault, approximately located or inferred, ball on downthrown side
Flute cast
Groove cast
11
Field trip stop number; A, second day
124°00′
123°45′
45°00′
44°45′
O C E A N
Lincoln City
Devils Lake
Cougar Mtn
Ball Mtn
Siletz Bay
Euchre Mtn
Lambert Pt
Government Pt
Depoe Bay
Cape Foulweather
Otter Crest
Siletz River
Siletz
Logsden
Yaquina Head
Yaquina River
Newport
Yaquina Bay
Toledo
Elk Creek

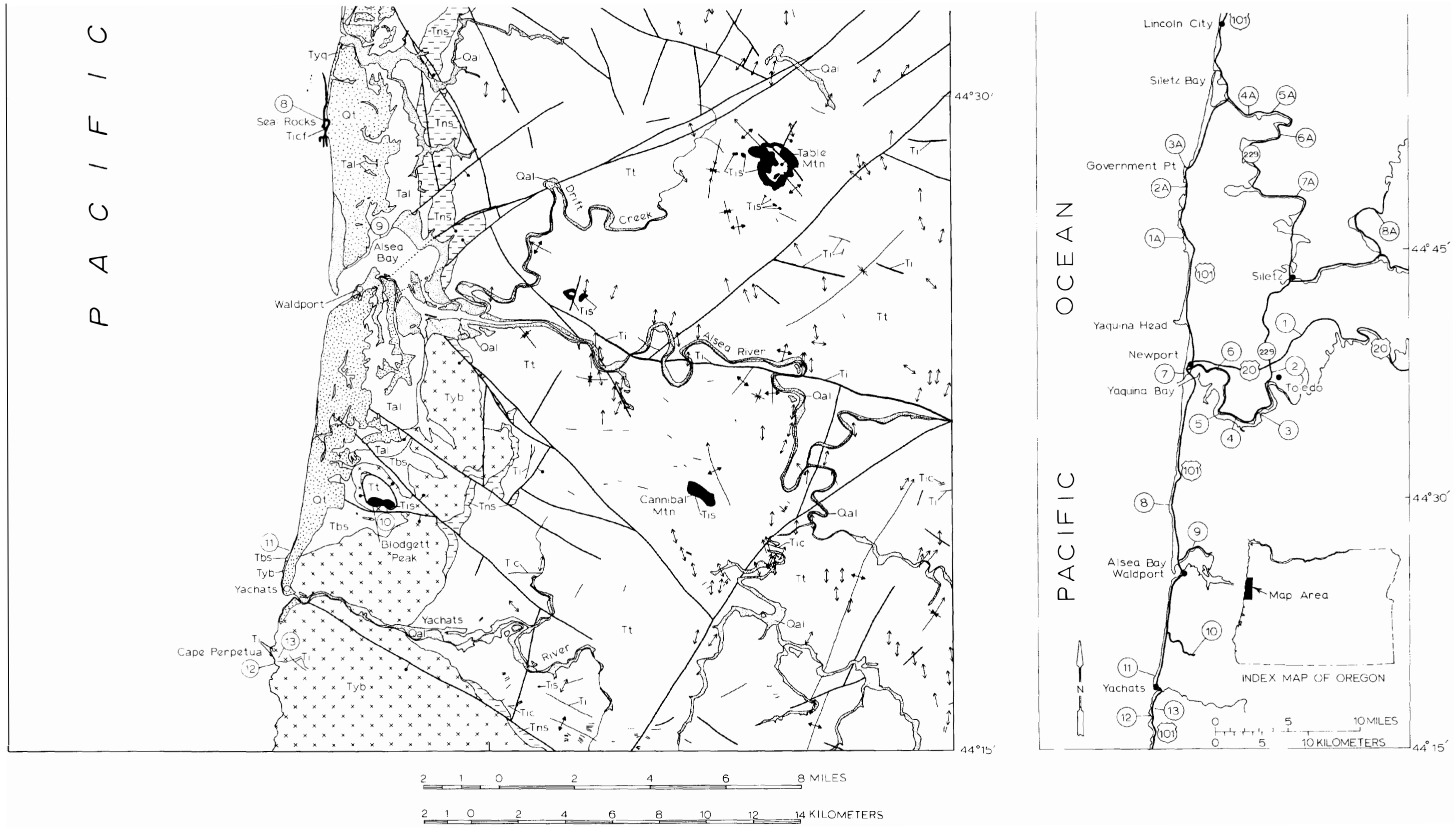

Figure 1. Generalized geologic map of the west-central part of the Oregon Coast Range (modified from Snavely and others, 1976a, b, c) and index map showing road network and locations of stops.

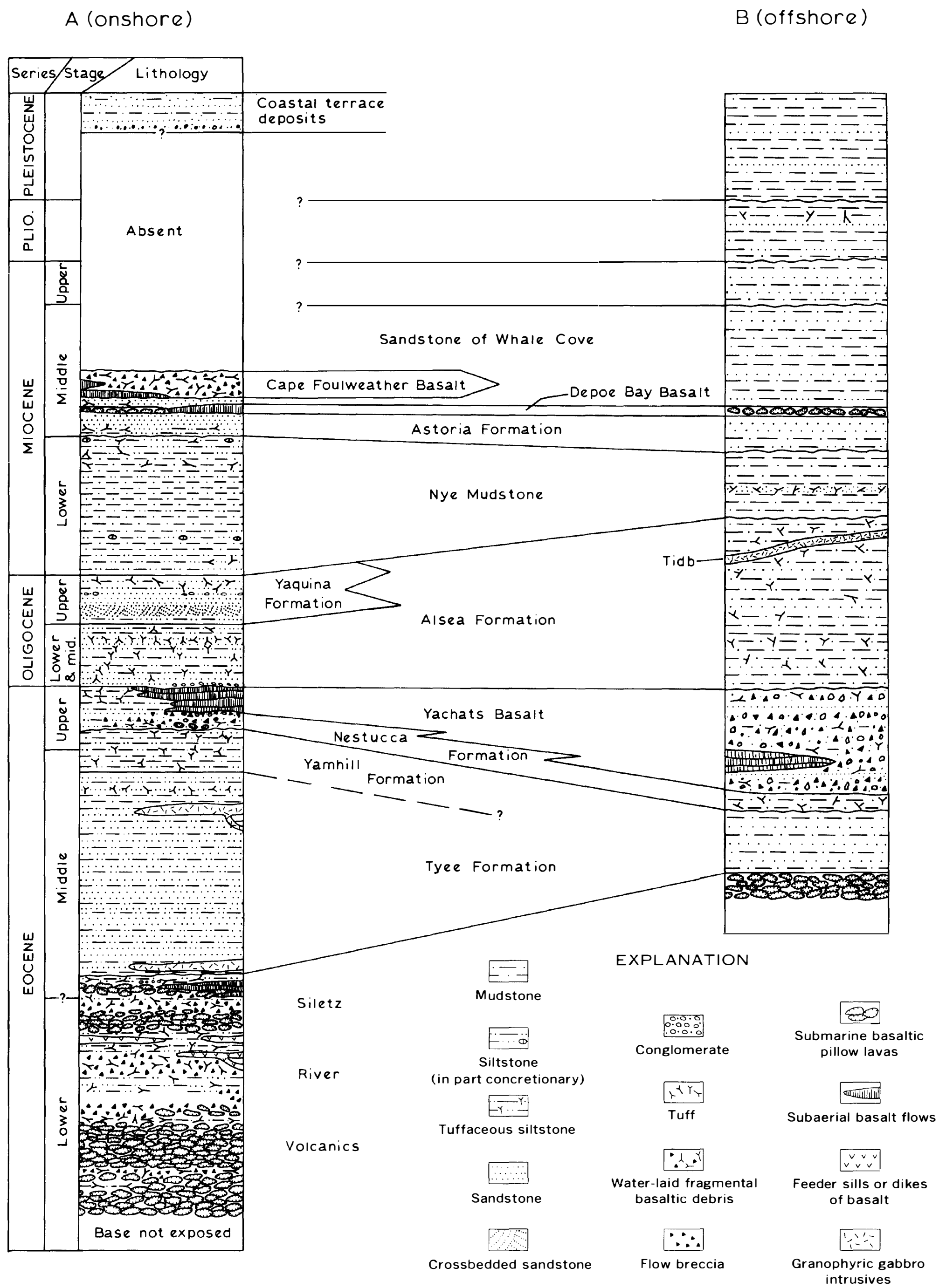

Figure 2. Generalized composite stratigraphic section, central Oregon continental margin. Column A, based on geologic mapping by Snavely and others, 1976a, b, c; column B based on units penetrated in Standard-Union Nautilus test well (Braislin and others, 1971) and interpretation of 24-channel seismic profile (Snavely and others, 1980). No vertical scale indicated.

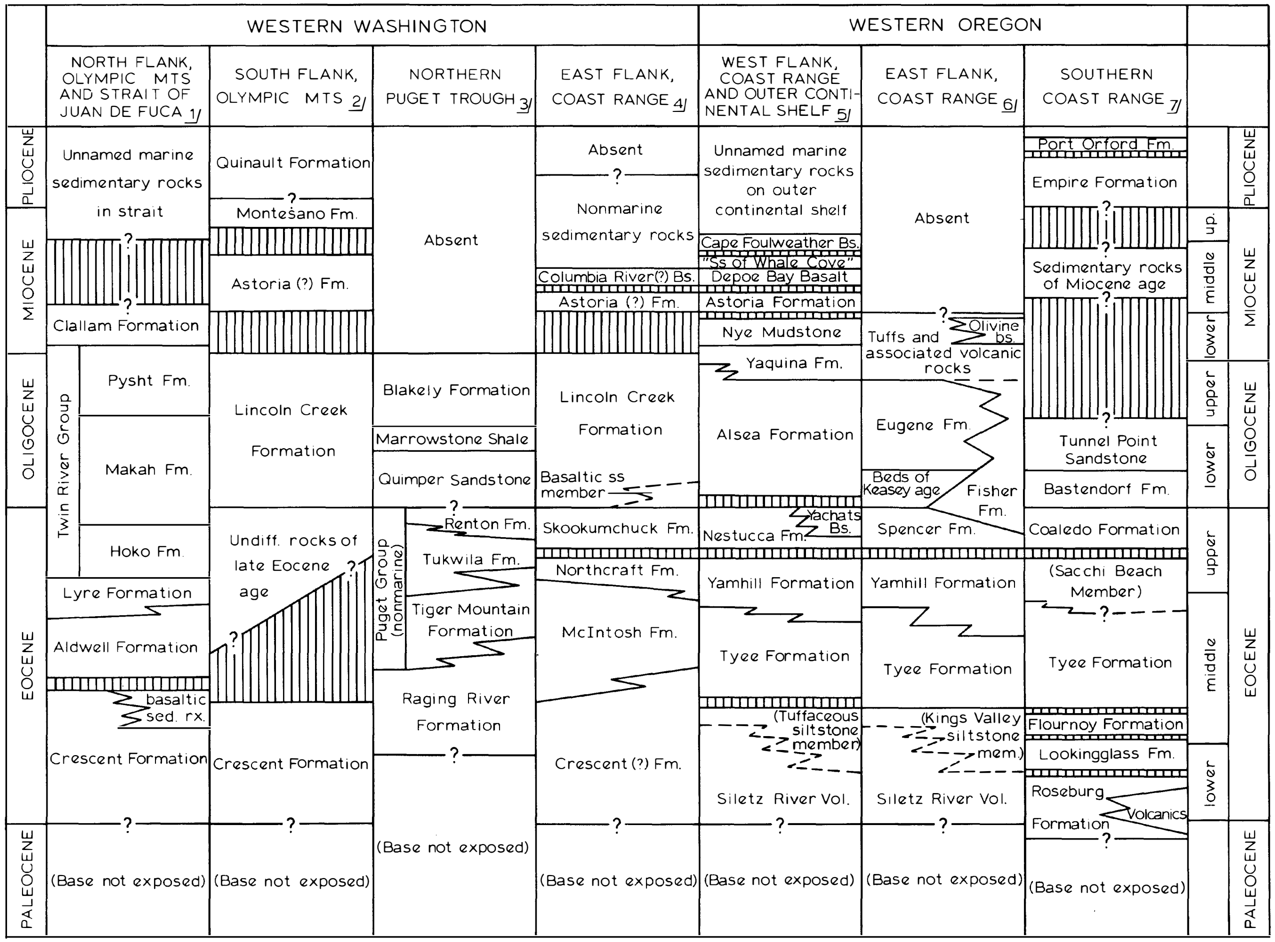

Figure 3. Chart showing the correlation between formations in western Washington and Oregon. Data adapted from (1) Brown and others (1960); Snavely and others (1978); (2) Rau (1967); (3) Durham (1944); Vine (1962); (4) Snavely and others (1958); (5) Snavely and others (1976a, b, c); Snavely, this report; (6) Vokes and others (1954); (7) Baldwin (1974).

Figure 4. Rhythmically bedded sandstone and siltstone of the Tyee Formation of middle Eocene age. Road-cut exposure along State Route 20, 4 miles east of Toledo, Oregon (Stop 1).

Figure 5. Tyee Formation showing graded units that range from medium-grained arkosic wacke in lower part to siltstone in upper part. Exposure along the Siletz River (near second day lunch stop) about 9 miles north of Siletz, Oregon.

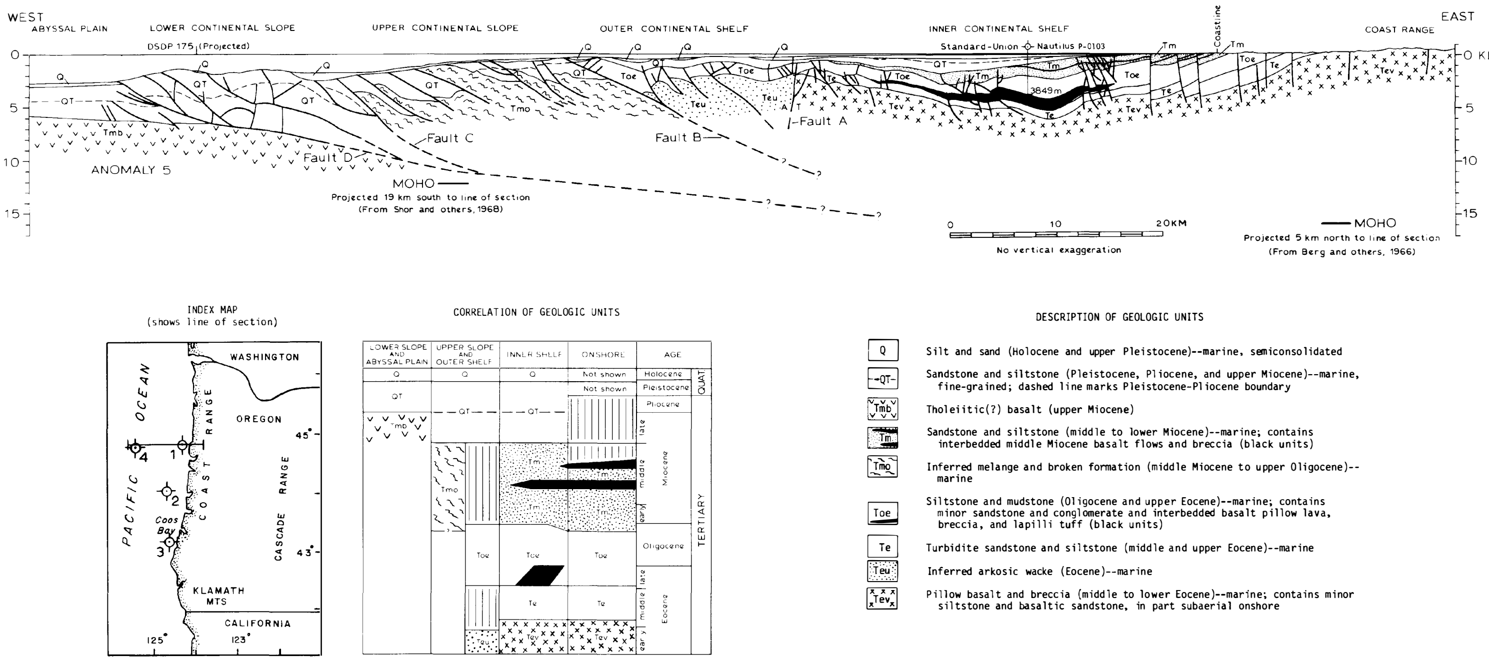

Figure 6. Generalized geologic cross section of the central Oregon continental margin (Snavely, Wagner, and Lander, 1980). Locations of exploratory test wells shown on index map include: (1) Standard-Union P-0103; (2) Union Oil Co. Fulmar P-0130; (3) Pan American Oil Co. P-0112; and (4) DSDP Site 175.

Figure 7. Thin-bedded tuffaceous siltstone with thin light-gray tuff beds; upper part of the late Eocene Nestucca Formation. Road-cut along Yaquina River three miles southwest of Toledo, Oregon (Stop 3).

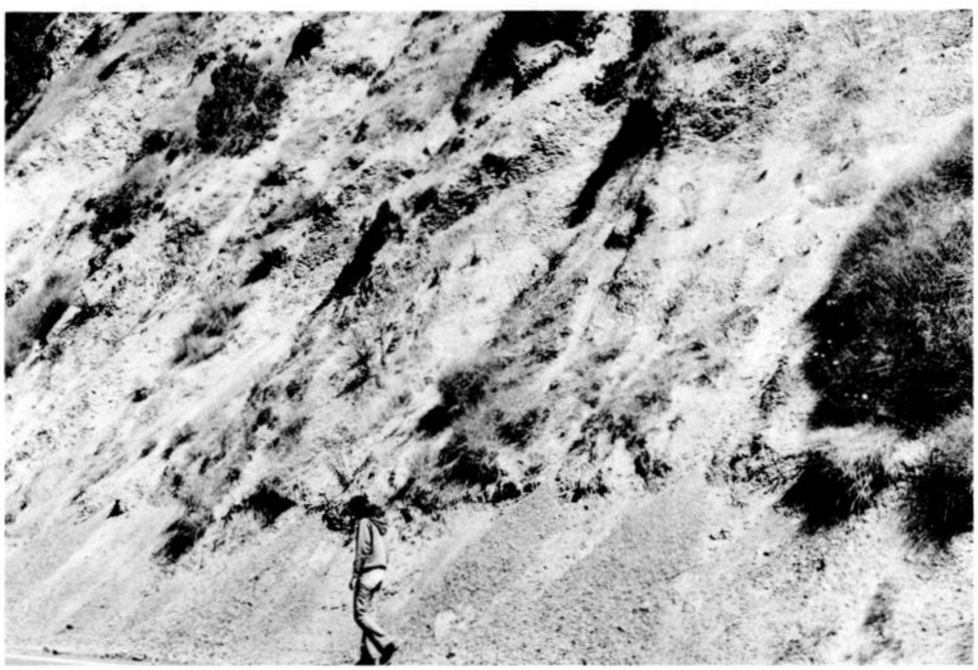

Figure 8. Massive concretionary tuffaceous siltstone and fine-grained sandstone of the Oligocene Alsea Formation. Road-cut along Yaquina River road 6.3 miles southwest of Toledo, Oregon (Stop 4).

Figure 9. Cross-bedded pebbly sandstone in the marine and nonmarine late Oligocene Yaquina Formation of deltaic origin. Thirty foot quarry face exposure on road along Yaquina River 1.4 miles south of the village of Yaquina (Stop 5).

Figure 10. Massive organic-rich Nye Mudstone of early Miocene age with ledge-forming beds and lenses of dolomite. Road-cut on north side of Yaquina Bay (Stop 6).

Figure 11. Unconformable contact between dark-gray Nye Mudstone and the overlying light-gray Astoria Formation at Jumpoff Joe, Newport, Oregon. These Miocene units are here overlain by Pleistocene deposits.

Figure 12. Cape Foulweather (Stop 1A) is a former eruptive center of basalt flows and breccias of middle Miocene age. The headland rises 500 feet above sea level and is capped by Pleistocene terrace deposits.

Table 1. Average chemical composition of selected volcanic and intrusive rocks of the central part of the Oregon Coast Range (averages recalculated water-free).

	Lower and middle Eocene		Lower(?) upper Eocene	Uppermost Eocene	Lower Oligocene		Mid-Oligocene	Middle Miocene	
	Siletz River Volcanics		Albitized Diabase	Yachats Basalt	Biotite Camptonite	Nepheline Syenite	Granophyric Gabbro	Depoe Bay Basalt	Cape Foulweather Basalt
	1	2	3	4	5	6	7	8	9
SiO_2	49.0	48.2	50.0	51.4	41.0	60.2	57.2	55.7	51.9
Al_2O_3	14.5	16.0	15.1	17.6	13.1	19.0	13.1	14.0	13.9
$FeO+Fe_2O_3$	11.6	12.0	12.3	10.9	16.5	6.0	14.3	12.3	14.5
MgO	8.3	6.1	5.2	3.6	7.6	0.22	1.3	3.6	4.1
CaO	12.2	7.4	10.0	8.7	10.0	1.2	5.3	7.1	7.9
Na_2O	2.3	4.3	3.6	3.6	3.6	8.6	3.7	3.3	3.0
K_2O	0.17	1.9	0.55	1.0	2.1	4.1	1.8	1.4	1.0
TiO_2	1.6	3.3	2.2	2.6	4.5	0.16	1.9	2.0	3.0
P_2O_5	0.15	0.71	0.35	0.59	1.4	0.23	0.77	0.38	0.69
MnO	0.19	0.20	0.22	0.16	0.21	0.23	0.28	0.21	0.22
Number of analyses	3	9	17	20	3	11	3	8	11

1. Tholeiitic basalt from lower part of Siletz River Volcanics (Snavely and others, 1968).
2. Alkalic basalt from upper part of Siletz River Volcanics (Snavely and others, 1968).
3. Albitized diabase sills and dikes, Euchre Mountain (Tsri, fig. 1), Valsetz, and Grande Ronde quadrangles.
4. Basalt from Waldport, Tidewater, and Mapleton quadrangles (Snavely and others, 1969).
5. Biotite camptonite dikes, Euchre Mountain quadrangle.
6. Nepheline syenite sills, dikes and stock, Tidewater and Waldport quadrangles.
7. Chilled margin basalt, Cedar Creek granophyric gabbro sill, Euchre Mountain quadrangle.
8. Depoe Bay Basalt, northwestern Oregon (Snavely and others, 1973).
9. Cape Foulweather Basalt, northwestern Oregon (Snavely and others, 1973).

TRIP 3. GEOLOGY OF THE WEST-CENTRAL PART OF THE OREGON COAST RANGE

ROAD LOG (First Day)

Mileage	
0	Start of trip on U.S. Route 20, 4 miles[1] NE of Toledo, Oregon.
Stop 1	Sandstone and siltstone of the middle Eocene Tyee Formation are exposed in road cut (fig. 4). Individual beds are graded from sandstone at the base to siltstone at the top; some siltstone interbeds were penecontemporaneously deformed. Siltstone ripups are abundant in the lower sandy parts of most beds, and carbonaceous material is generally scattered throughout. Fossils are absent except for Foraminifera in rare thin hemipelagic claystone laminae that occur at the tops of a few beds. The graded sandstone beds (fig. 5), sole markings, internal structures, and lack of fossils indicate that the sandstone and siltstone beds that constitute the Tyee Formation are turbidites. The northerly orientation of flute and groove casts (arrows, fig. 1) in the Tyee Formation over much of the Oregon Coast Range indicates that the source area was about 150 miles south of this locality in the ancestral Klamath Mountains. About 30 miles north of this locality the turbidites grade laterally into a predominantly siltstone sequence (lower part of the Yamhill Formation).
0.5	Contact between the Yamhill and the Tyee Formations.
1.6	Junction old U.S. Route 20. Turn left toward Toledo. Toledo is underlain by the Yamhill Formation, the light-brown weathered siltstone that crops out along the road. This rock is highly susceptible to landsliding.
2.6	The hills to the south of the road are held up by sandstone of the Tyee Formation.
3.7	The large integraded saw mill-paper plant to the right is operated by Georgia-Pacific Corp. The large cuts to the west beyond the mill are in tuffaceous siltstone of the Alsea Formation.
3.8	Junction Downtown Toledo. Proceed on old U.S. Route 20.
4.2 Stop 2	"Minnie's Sunset Cafe" locality of Cushman, Stewart, and Stewart (1949) (now Gordon's Cafe) of the Yamhill Formation. This formation underlies the town of Toledo and although poorly exposed is more than 2000 feet thick. Foraminifera at this location are assigned to the lower part of the Narizian (early late Eocene), whereas the lower part of the Yamhill is late Ulatisian (late middle Eocene). The Yamhill is an organic-rich siltstone and mudstone which contains abundant yellowish-gray calcareous concretions and thin arkosic sandstone beds. The Yamhill and older Eocene formations are more structurally complex than the Tertiary sequence above the late Eocene unconformity. In the area between Toledo and Siletz, many folds and faults mapped within the Yamhill and Tyee Formations do not extend above the unconformity at the base of the Nestucca Formation.
	Proceed west toward Newport on old U.S. Route 20.

[1]Metric system is not used in the road log sections of this field trip guide as odometers on most cars do not record kilometers.

4.3 Junction of Yaquina Bay Road and old U.S. Route 20. Turn left toward Newport.

4.4 Fault contact between the Yamhill Formation to the east and the lower and middle Oligocene Alsea Formation on the west. South of bridge across Depoe Creek are large cuts of massive tuffaceous siltstone with thin tuffaceous interbeds--the Alsea Formation.

4.8 Large exposure of the Alsea Formation siltstone which contains thin, light-colored volcanic ash beds. On the left is a good view of the G.P. mill.

5.7 Contact between the Alsea Formation and the underlying glauconitic sandstone in the upper part of the upper Eocene Nestucca Formation.

6.3 Uplifted estuarine deposits of laminated and thin-bedded silts.

6.7 Estuarine deposits overlying the Nestucca Formation.

7.5 Northeast end of Boone Island, a cut-off meander of the Yaquina River.

7.8 Stop 3 Thin-bedded tuffaceous siltstone of the upper Eocene Nestucca Formation which contains 1- to 4-inch thick light-brown ash beds and 1-foot-thick beds of tuffaceous glauconitic siltstone (fig. 7). The Nestucca grades upward into the overlying massive Alsea siltstone. Siltstone at this location contains a foraminiferal fauna assigned to the late Narizian Stage. The Nestucca in this area is only about 800 feet thick, whereas in the type area, 35 miles to the north in the Hebo quadrangle, it is more than 5000 feet thick. The small fault at the east end of the outcrop downdrops the overlying Alsea. Thin zones of penecontemporaneous deformation probably result from submarine slumping along some of the tuff interbeds.

Continue west along Yaquina Bay Road.

7.9 West drainage of Boone Island cut-off meander.

8.4 Unconformable contact of the Nestucca Formation and the underlying Tyee Formation. The unconformity at the base of the Nestucca Formation is the major unconformity in the Oregon Coast Range and on the adjacent continental shelf.

8.7 Medium- to thick-bedded sandstone of the Tyee Formation crops out on the right.

8.85 Tyee-Nestucca contact.

9.2 To the left is one of the oyster "factories" on Alsea Bay.

9.3 Contact between siltstone of the Alsea Formation and thin-bedded tuffaceous siltstone of the Nestucca Formation.

9.4 The basal part of the Alsea Formation is exposed in road cut. Foraminifera from this outcrop indicate an early Oligocene age (Refugian Stage).

10.1 Stop 4 Massive concretionary tuffaceous siltstone and fine-grained sandstone of the Alsea Formation which contains thin tuff beds (fig. 8). Mollusks from this part of the unit indicate a middle Oligocene age. A diverse assemblage referable to the "Lincoln Stage" (Refugian) occurs within 250 feet stratigraphically of the contact with the underlying Nestucca Formation, and mollusks referable to the lower part of the "Blakeley Stage" (Zemorrian) occur within 100 feet of the contact with the overlying Yaquina Formation. The abundant ash and pumice in the Oligocene strata in western Oregon and Washington were derived from pyroclastic volcanism in an ancestral Cascade Range.

10.4 Gradational contact between the Alsea Formation and the overlying Yaquina Formation.

10.9 Stop 5 Massive, cross-bedded, and thin-bedded sandstone and interbedded dark-gray marine siltstone of the Yaquina Formation are exposed in old quarry (fig. 9). The siltstone in this outcrop contains Foraminifera that are referred to the Zemorrian Stage. Sandstone forms the bulk of the Yaquina Formation and is typically cross-bedded, gritty, and contains abundant pumice fragments and carbonaceous material. Thick conglomerate beds, containing clasts of silicic volcanic and metamorphic rocks, and less common thin coal seams occur in the sandstone. Intercalated siltstone is indistinguishable in appearance from the underlying Alsea Formation, and occurs as thin beds and as interbeds more than 150 feet thick. Regionally, the Yaquina Formation has a crescent-shaped outcrop pattern, and to the north and south it strikes seaward onto the continental shelf. At Seal Rocks, its most southern onshore exposure, the Yaquina Formation is less than 500 feet thick. In the type section along the Yaquina River it is 1700 feet thick, and 10 to 15 miles to the north in the drainages of Spencer and Rocky Creeks it is well over 2000 feet thick. Near Kernville, 22 miles north of Stop 5, the Yaquina Formation again thins to about 500 feet. The sedimentological characteristics of the Yaquina Formation suggest that it is of deltaic origin (Snavely and Wagner, 1963; Goodwin, 1973). Continue west along Yaquina Bay Road.

11.5 Riverbend Moorage. Pleistocene terrace deposits overlie the Yaquina Formation on the right.

12.7 Fishing village of Yaquina. This was the end of the railroad line at the turn of the century. Massive fossiliferous concretionary Yaquina sandstone with some interbeds of glauconitic sandstone is exposed in the large cut on the right. The large blue dome at ten o'clock is a gas storage facility.

12.9 Contact between the Yaquina Formation and the Nye Mudstone.

13.0 Exposure of the concretionary Nye siltstone.

13.4 Contact between the Nye and Yaquina Formations. The contact here trends parallel to the road.

14.0 Massive very tuffaceous fine-grained sandstone, typical of the upper part of the Yaquina Formation.

14.4 Contact between the Nye Mudstone and Yaquina Formation is concealed in the small valley. The lower part of the Nye Mudstone becomes increasingly sandy toward its base and grades over a 50-foot interval into tuffaceous fine-grained sandstone of the upper part of the upper Oligocene Yaquina Formation. The contact is well exposed 2 miles south along the west bank of the Yaquina River.

15.3 Stop 6 The middle part of the Nye Mudstone, which here contains concretionary beds of dolomite, is exposed in the road cut (fig. 10). The Nye Mudstone consists predominantly of massive, organic-rich mudstone and siltstone. Brown fish scales and vertebrae are common. Although the rocks contain only a sparse molluscan fauna, Foraminifera, which are assigned to the Saucesian Stage are generally abundant. The Foraminifera, as well as oxygen isotope ratios, indicate a cold-water environment during deposition.

Proceed west along Bay Road.

16.0 The hills north of McClean Point are largely landslide material of the unstable Nye Mudstone.

16.2 The row of houses at twelve o'clock are on Pleistocene marine terrace deposits that overlie the Nye Mudstone.

16.8 On the north side of the road are lower Pleistocene sands that fill a large Pleistocene channel cut into the Nye Mudstone. This channel is overlain by light-brown weathered upper Pleistocene marine sand and gravel.

17.0 The old fishing community of Newport rests on the Nye Mudstone which is capped by Pleistocene marine terrace deposits.

17.4 The road leaves the bay and climbs up onto the marine terrace deposits.

17.5 U.S. Coast Guard, Yaquina Bay Station.

17.9 Proceed westward under bridge to Yaquina State Park.

Stop 7 Yaquina State Park, Newport, Lunch stop. Follow path to base of jetty, north side of Yaquina Bay. The unconformable contact between the basal concretionary arkosic sandstone of the middle Miocene Astoria Formation and the underlying lower Miocene Nye Mudstone is exposed in the sea cliff. The following foraminiferal species listed by Rau (Snavely and others, 1964) are among those that occur in the Astoria Formation but do not occur below this contact:

Buliminella elegantissima (d'Orbigny)

Robulus mayi Cushman and Parker

Uvigerinella californica ornata Cushman

Common species occurring in the Nye Mudstone up to the contact but not above it are:

Elphidium cf. *E. minutum* (Reuss)

Uvigerina auberiana d'Orbigny

Uvigerinella obesa impolita Cushman and Laiming

Although the unconformity between the Astoria and Nye Formations is not always apparent in single exposures, regional mapping has shown that the Astoria Formation overlaps the Nye Mudstone and rests on the upper Oligocene Yaquina Formation about 8-1/2 miles north of this stop (fig. 10). The Nye-Astoria contact is best exposed at Jumpoff Joe, 1-1/2 miles north of this stop (fig. 11). Marine Pleistocene terrace deposits overlie both Miocene units at this locality. North of the jetty in the sea cliffs along the beach, massive to well-bedded fossiliferous sandstone of the Astoria Formation contains interbedded siltstone, basaltic sandstone, and water-laid dacitic tuff beds up to 12 feet thick. The gabbro boulders on the beach near the base of the trail are granophyric gabbro from a middle Oligocene sill (30 m.y.B.P.) that crops out along Cedar Creek, 19 miles to the northeast. Most of the jetty is composed of this gabbro, but earlier nepheline syenite and Tyee sandstone were used for jetty rock.

0 — Start new mileage. Leave Yaquina Bay State Park, head east to join U.S. 101.

0.2 — Junction U.S. 101. Turn right, and proceed south across Yaquina Bay. This bridge was built in the early 1930's during the WPA days. To the east on the land-fill peninsula is Oregon State University's Marine Science Center. At eleven o'clock is Table Mountain which is capped by a 250-foot-thick sill of nepheline syenite.

1.2 to 7.2 — The highway passes through Pleistocene terrace deposits mantled by active and stabilized sand dunes that overlie the Nye Mudstone. The terrace deposits consist chiefly of aeolian and beach sands and wood- and plant-bearing silt and clay of fluvial and estuarine origin. Fossil wood from these terrace deposits, dated by C^{14} methods, is more than 38,000 years old. The base of the terrace is 30 to 40 feet above sea level near Newport and dips gently south toward Seal Rocks, where it lies near sea level.

3.1 — The Nye Mudstone is well exposed in the seacliff along the stretch of beach to the right.

7.2 — Contact between the Nye Mudstone and the Yaquina Formation.

7.8 — Beaver Creek.

9.6 — Seal Rock State Park.

10.1 Stop 8 — The basalt sills and dikes exposed at Seal Rocks (fig. 13) consist of Cape Foulweather Basalt, the younger of two sequences of Miocene basalt that crop out along the Oregon coast between here and Astoria. The Cape Foulweather Basalt is characterized by sparse but distinctive yellowish labradorite phenocrysts that distinguish it from the aphyric Depoe Bay Basalt, which is slightly older. The sills and dikes intrude cross-bedded tuffaceous sandstone of the Yaquina Formation of latest Oligocene age. This is the southernmost exposure of the Yaquina Formation and near the south end of the deltaic lens which is thickest just north of Newport. The sill at the headland is about 80 feet thick and is concordant with the sandstone beds it intrudes. Farther north, however, this intrusive becomes discordant and at its northernmost exposure it is a nearly vertical dike. The outer rocks are probably the Seal Rock sill that is repeated by a north-trending normal fault. On the continental shelf north-trending normal faults offset deposits as young as Holocene in age (fig. 6). The base of the terrace deposits here is near sea level and rises gently northward to 30 to 40 feet near Newport.

12.0 — Driftwood State Park.

13.9 — Turn right off U.S. 101. Follow along the north side of Alsea Bay on the road to Bayview. The deposits here are ancient dune sands.

15.0 Stop 9 — Road cut in the Alsea Formation (Snavely and others, 1975) within the type locality along the north side of Alsea Bay. The Alsea consists of tuffaceous siltstone and very fine-grained sandstone with interbeds of glauconitic sandstone, tuff and reworked lapilli-tuff. The formation contains abundant mollusks and foraminifers that indicate an early (upper Refugian - "Lincoln" Stage) to late (Zemorrian - lower "Blakeley" Stage) Oligocene age. Southeastward across the bay, Table Mountain is on the horizon. The hills to the south are held up by upper Eocene Yachats Basalt which does not extend north of Alsea Bay as it grades northward into Nestucca siltstone. Proceed eastward travelling through Alsea Formation.

15.4 Thin bedded fine-grained sandstone in the lower part of the Alsea Formation.

15.9 Turn around at red house. Return to U.S. 101.

17.9 Junction U.S. 101. Turn right, and proceed across bridge over Alsea Bay.

18.8 Waldport, Oregon.

19.1 In the south city limits of Waldport, the bluff on the right is in the upper part of the Alsea Formation of Zemorrian (Blakeley) age. A massive 15-foot-thick bed of mudflow breccia containing andesitic and dacitic clasts derived from Cascade Range is exposed in the upper part of the road cut. Between here and Yachats only Pleistocene deposits are exposed in low sea cliffs and road cuts.

22.1 Beachside State Park.

23.5 Turn east, (right) off U.S. 101 on Blodgett Road (Angells Job Corp Center sign). Follow main dirt road past center and sawmill to Blodgett Peak.

27.4 Stop 10 Quarry exposure of small porphyritic nepheline syenite stock that extends westward to Blodgett Peak (fig. 14). Anorthoclase phenocrysts in the nepheline syenite have been oriented by flowage. This flow banding generally parallels contacts with sedimentary and volcanic rocks. The nepheline syenite body was apparently injected forcibly and deformed the overlying sedimentary and volcanic rocks into a domal structure. The outcrop of nepheline syenite may be only the small surface exposure of a much larger body at depth. Other nepheline syenite bodies crop out to the east in the Tidewater quadrangle, where they intrude the Tyee Formation (fig. 1). The nepheline syenite is composed of anorthoclase, K-feldspar, nepheline, analcime arfvedsonite, aegirine, and opaque minerals. The strongly undersaturated nepheline syenite appears to represent a late continuation of the period of volcanism that produced the upper Eocene basalts. A close areal association of nepheline syenite with camptonite and shonkinite in the Tidewater quadrangle (fig. 1) suggests they may be comagmatic. The average chemical composition of nepheline syenite intrusives in the Tidewater and Waldport quadrangles is shown in Table 1, col. 6.

Return to U.S. 101 by same route.

31.3 Junction U.S. 101. Turn to right, south.

32.2 At twelve o'clock the hills are held up by upper Eocene Yachats Basalt.

34.3 Smelt Sands Beach. Turn right this side of the Chevron Station and proceed to beach.

34.6 Stop 11 Uppermost Eocene boulder and cobble conglomerate derived from the underlying Yachats Basalt is well exposed in the wave-cut platform at this stop (fig. 15). Several hundred feet of fossiliferous basaltic sandstone overlies the conglomerate farther to the north. The conglomerate, which contains boulders as much as 10 feet in diameter, was deposited on an irregular surface cut in basalt flows, breccia, and associated dikes of the Yachats Basalt. The top of individual flows commonly have red oxidized zones, and some aerodynamically shaped bombs occur in the breccia, indicating they are of subaerial origin. The Yachats Basalt (and the overlying conglomerate-sandstone unit) has been traced northward as far as Alsea Bay, but these units are present on the north side of the Bay. Similar basaltic conglomerate and sandstone units overlie many of the late Eocene volcanic sequences in western Oregon and Washington.

Proceed south on U.S. 101 toward Yachats.

35.6 The village of Yachats rests on a Pleistocene terrace cut on the Yachats Basalt.

35.9 Yachats River. Basalt flows cut by numerous feeder dikes that are well exposed along the coast and in road cuts are part of the upper Eocene Yachats Basalt. Talus breccia, terrace deposits, and dune sands locally mantle the volcanic rocks.

37.7 Cape Perpetua. This rugged headland is composed of 10- to 20-foot-thick subaerial flows of Yachats Basalt cut by feeder dikes. Irregularities in the coastline are due to differential erosion along numerous west-trending faults, joints, and dikes (fig. 16).

38.2 Turn right (west) into Devil's Churn parking lot and walk down trail to the coast (fig. 17).

Stop 12 The churn was produced by erosion along a fault in upper Eocene Yachats Basalt flows that are cut by dikes. Note that the dikes on either side of the fault-controlled churn do not match. Several small, irregularly jointed flows with aa tops are exposed on the wave-cut platform; oxidized zones are developed at the tops and bases of some flows. Some of the northwest-trending dikes that intrude the flows have sill-like apophyses into the flows; in other areas along the coast dikes are seen to feed flows. Many of the dikes are composite and show systematic variations in texture, phenocryst content, and chemical composition. The chemical composition of the volcanic rocks that form the upper Eocene Cape Perpetua - Heceta Head sequence varies considerably. The average chemical composition of 20 samples of Yachats Basalt is shown on Table 1, col. 4. Most flows contain 49 to 53 percent SiO_2 and are of basaltic composition, but a few are basaltic andesite. Dikes show an even greater variability in composition. They are predominantly basaltic, but several, particularly near Devils Churn, contain 60 to 68 percent SiO_2 and are of latitic and rhyodacitic chemical composition. All flows and intrusive rocks in this sequence are quartz normative and are characterized by relatively high contents of alumina (reflecting abundant plagioclase phenocrysts) and alkalies.

Depart Devils Churn; proceed south on U.S. 101.

38.4 Take first left (east) leading towards viewpoint. Proceed toward viewpoint. Exposures in road cuts are deeply weathered Yachats flows.

39.2 Take sharp left. Proceed up the hill.

40.2 Top of the hill, Cape Perpetua parking lot.

Stop 13 View south from Cape Perpetua is across the rugged seacoast which is held up by the Yachats Basalt (fig. 16). Heceta Head is the farthest headland. The view to the north is across a low-lying wave-cut platform on which the town of Yachats is located. Yaquina Head is in the near distance; Cape Foulweather in the middle distance, and Cascade Head in the far distance. Return to Newport. End of first day tour.

Figure 13. Sills and dikes of Cape Foulweather Basalt intrude cross-bedded sandstone of the Yaquina Formation at Seal Rocks (Stop 8).

Figure 14. Quarry in small stock of nepheline syenite at Blodgett Peak (Stop 10). Vertical jointing is along primary flow banding.

Figure 15. Basalt boulder and cobble conglomerate eroded from the underlying Yachats Basalt (Stop 11), Yachats, Oregon, hammer (circled) shows scale.

Figure 16. View looking south from Cape Perpetua (Stop 13) towards Heceta Head showing the coastal area that is underlain by upper Eocene Yachats Basalt. Ribs of basalt at edge of wave-cut terrace platform are bounded by small faults, shear zones, or joints along which the basalt erodes more rapidly.

Figure 17. Late Eocene Yachats Basalt cut by dikes at Devils Churn (Stop 12).

TRIP 3. GEOLOGY OF THE WEST-CENTRAL PART OF THE OREGON COAST RANGE

ROAD LOG (Second Day)

Mileage	
0	Start mileage at Yaquina Bay State Park; proceed east to U.S. 101 and turn north.
1.2	Junction U.S. Route 20 and U.S. 101.
3.8	West of the highway is Agate Beach. The agates found on the beach are reworked from the Pleistocene marine terrace deposits.
4.0	A middle Miocene volcanic center forms Yaquina Head, just north of Agate Beach. Between Yaquina Head and Cape Foulweather the highway traverses near the contact between the lower Miocene Nye Mudstone to the east and the middle Miocene Astoria Formation to the west. The seacliffs are all cut in the Astoria Formation. The Astoria contains many beds rich in mollusks and vertebrate-bearing concretions. The irregular surface of the highway is caused by landslides which are common in seaward-dipping rocks along coastal Oregon.
6.7	The large headland at twelve o'clock is Cape Foulweather (fig. 12, the type locality of the middle Miocene Cape Foulweather Basalt). The light-gray low headland in front of Cape Foulweather is composed of the Astoria Formation.
7.5	Beverly Beach State Park. The island immediately west of the park is Gull Island which is a flow of middle Miocene Depoe Bay Basalt. The larger island to the north is Otter Rock which is composed of water-lain lapilli tuff of Cape Foulweather Basalt.
8.5	Otter Rock turnoff.
9.8	To the right of the highway the bell-shaped feature with radiating columnar joints is a volcanic neck, one of the feeders to the Cape Foulweather Basalt.
10.1	Turn left and proceed to the Otter Crest viewpoint.
10.4 Stop 1A	Otter Crest, and much of the coastal area 5 miles to the north, is underlain by the Cape Foulweather Basalt. This unit is the younger of two middle Miocene volcanic sequences that are exposed along the northern part of the Oregon coast. Flow breccia, extrusive breccia, and intercalated massive flows constitute the bulk of the Cape Foulweather Basalt at Otter Crest whereas northward, farther from the vent area, water-laid lapilli tuff predominates. Numerous dikes, sills, and small plugs intrude the breccia near Otter Crest, indicating that this area was a former center of Miocene volcanism. Two ring dikes and several radial dikes are exposed at low tide on the wave-cut platform just south of Otter Crest (Frontispiece). The Cape Foulweather Basalt also crops out at Yaquina Head, about 5 miles south of Otter Crest, and on the large island (Otter Rock) immediately west of Otter Crest. The two smaller islands south of Otter Crest (Gull Rock and Whaleback), however, are composed of subaerial basalt flows of the Depoe Bay Basalt, which is older than the Cape Foulweather Basalt. Petrochemical studies

of the Cape Foulweather Basalt from its type locality and other areas along coastal northwestern Oregon show that it has a relatively uniform composition. The average chemical composition for 11 samples is shown in Table 1, col. 9. The Cape Foulweather Basalt can readily be distinguished from the Depoe Bay Basalt on the basis of petrochemistry, and it can be identified in the field on the basis of its sparse but ubiquitous labradorite phenocrysts, which do not occur in the Depoe Bay Basalt. The terrace at Otter Crest is about 500 feet above sea level and is one of the higher of several Pleistocene terraces developed along this coastline. Constructional marine terraces, about 50 feet above sea level, are developed on westward-dipping sandstone and siltstone beds of the Astoria Formation on the two nearby headlands to the south. Immediately north of the viewpoint, light-gray sandstone of the Astoria Formation is visible at sea level below flows of the Cape Foulweather Basalt.

Proceed northward on U.S. 101.

11.0 Cape Foulweather Basalt sills and dikes cutting breccia.

11.8 Rocky Creek.

12.2 Exposures at Rock Point State Park of interbedded breccia and flows of the Cape Foulweather Basalt.

12.4 Whale Cove on the left is eroded into middle Miocene massive sandstone referred to as the sandstone of Whale Cove. This sandstone unit separates the Cape Foulweather Basalt from the Depoe Bay Basalt.

14.2 Bridge at Depoe Bay.

14.4 Stop 2A Fisherman's Memorial Alcove, Depoe Bay. Isolated-pillow breccia of the Depoe Bay Basalt forms the east margin of the outer bay on which U.S. 101 is constructed (fig. 18). Excellent exposures of this unit can be seen directly below the rock wall bordering the west side of the highway. The Depoe Bay Basalt unconformably overlies the Astoria Formation, which is exposed in the inner bay. The basalt is overlain by the sandstone of Whale Cove that crops out along both the south and north ends of the outer bay. The Cape Foulweather Basalt, which forms the projecting headlands of the outer bay, unconformably overlies the sandstone of Whale Cove. The breccia matrix of the isolated-pillow breccia of Depoe Bay Basalt is composed of glassy or very fine grained basalt that is palagonitized on weathered surfaces. Some breccia fragments are broken pillow rims. The pillows have ropy rims, and some have multiple chilled margins and drained-out cores. Finely comminuted basaltic glass or calcareous sand and silt fill some of the drained pillows (fig. 19). Clusters of snakelike pillows and very elongate pillows are exposed in several places within the isolated-pillow breccia and appear to have resulted from more rapid extrusion of lava into the marine environment. Small quarries 1/2 mile south of Depoe Bay expose a thick, rudely jointed subaerial flow of Depoe Bay Basalt. Immediately north and south of these quarries, the lava apparently flowed into the Miocene sea and formed isolated-pillow breccia. The Depoe Bay Basalt extends seaward to (and beyond) the Standard-Union Nautilus well where a 50-foot flow of Depoe Bay Basalt was penetrated (fig. 6).

Numerous dikes, sills, and irregular bodies of Depoe Bay Basalt intrude sandstone and siltstone of the middle Miocene Astoria Formation immediately east of Depoe Bay and some probably were feeders to the extrusive basalt at Depoe Bay. The Depoe Bay Basalt is relatively uniform in composition (Table 1, col. 8). The basalt is characterized by a high content of SiO_2 and alkalies and is quartz-normative.

Continue north on U.S. 101.

15.4 Turn left at Boiler Bay State Park, Government Point.

15.6 Stop 3A The Cape Foulweather Basalt extends along the coast from Cape Foulweather to Government Point, but does not extend seaward as far as the Nautilus test well (fig. 6). At Cape Foulweather most of the extrusive tuff breccia is probably of subaerial origin. The water-laid, well-bedded lapilli tuff at Government Point apparently formed part of a fringing marine apron around the main vent at Cape Foulweather. Grading in many individual beds suggests that they were deposited by density currents; more massive units probably represent breccia transported by submarine landslides. Government Point is capped by sand and gravel of one of the lower Pleistocene marine terraces, but several nickpoints on the sea cliff indicate lower stands of sea level. On the north side of Boiler Bay, just north of Government Point, peperite and basalt dikes of the Depoe Bay Basalt intrude sandstone and siltstone of the Astoria Formation. Cascade Head, the prominent headland 15 miles to the north, is underlain by upper Eocene subaerial basalt flows that correlate with the Yachats Basalt. Cape Lookout, located about 35 miles north and visible on a clear day, is composed of a beautifully exposed sequence of pillow basalts and subaerial flows of the Depoe Bay Basalt.

Proceed north on U.S. 101.

16.4 Peperite dikes are exposed on the east side of the road.

16.7 Fogarty Creek State Park. Sandstone of the Astoria Formation and Miocene basalt breccia are well exposed along the sea cliffs in this area.

From Fogarty Creek to Salishan Lodge Pleistocene marine terrace deposits are exposed, but in places are overlain by sand dunes.

20.3 Salishan Lodge.

20.5 Siletz Bay.

20.8 Outcrop on the right is fossiliferous glauconitic sandstone and siltstone of the Yaquina Formation, which is underlain by the Alsea Formation just around the corner in cuts on a secondary road.

21.5 Siletz River bridge.

Turn right on State Route 229 and proceed toward Siletz.

22.1 Iron-stained channel sandstone in the Alsea Formation is exposed on the north side of the road. This sandstone is very similar to the Yaquina sandstone.

22.2 Outcrops of tuffaceous siltstone and tuff beds of the Alsea Formation are exposed in a small quarry on the north side of the highway.

22.6 The quarry at about twelve o'clock, south of the Siletz River, is in a sill of Depoe Bay Basalt.

23.0 Top of extrusive camptonite sequence of late Eocene age.

23.1 The "old" house across the Siletz River was constructed for the movie

"Sometimes a Great Notion," (Never Give an Inch) which was written by Ken Keasey and starred Paul Newman.

23.8 Stop 4A Camptonitic lapilli tuff and breccia exposed in small quarry on the south side of the road. Small camptonite dikes and sills are exposed in this quarry and along the river bank. Most of the fragmental material was originally camptonitic glass clouded with microlites, but the glass is now largely altered. Biotite and hornblende phenocrysts and microphenocrysts are sparsely distributed through the tuff and breccia. Thin and distorted siltstone interbeds in camptonitic tuff breccia contain latest Eocene foraminiferal faunas. The camptonitic extrusive sequence is approximately equivalent in age to the Yachats Basalt flows of latest Eocene age that form Cascade Head and Cape Perpetua. The internal structure of the camptonitic extrusive sequence is complex; mapping along the poorly exposed northern part of the sequence (see Snavely, MacLeod, Wagner, and Rau, 1976a) suggests that the breccia and tuff were extruded along a west-trending fault whose scarp restricted the northern extent of these volcanic rocks.

Continue east on State Route 229.

24.8 New hillside cuts in tuff-breccia of the lower to middle Eocene Siletz River Volcanics.

25.2 Tyee sandstone is exposed in the road cut on the left.

25.4 Fault contact between the Tyee Formation and the Siletz River Volcanics.

25.6 Turn left on small road to Kauffman quarry (private property).

25.7 Stop 5A Filled feeder-tube composed of columnar-jointed alkalic basalt is exposed at the base of the quarry (fig. 20). The filled tube is surrounded by a carapace of elongate basalt pillows. The pillows and filled feeder-tube rest on fine-grained basaltic sandstone. Alkalic basalt, such as that exposed in the quarry, is common in the upper part of the Siletz River Volcanics. A small, filled feeder-tube on the east side of the quarry (formerly well exposed but now partly removed by quarrying) contains aphyric alkalic basalt at the base that grades upward into porphyritic augite basalt in the center. Feeder-tubes such as these exposed at Kauffman quarry are common in the upper part of the Siletz River Volcanics. Lava flowed through these tubes below a self-formed protective cover of pillow lava.

Continue east on Siletz River road, State Route 229.

26.8 To the right are natural levees of the Siletz River.

The Siletz River Volcanics are exposed throughout this stretch of the road.

27.3 A waterfall that drops across massive tuff-breccia of the Siletz River Volcanics.

28.1 Road to Euchre Mountain.

28.8 On the right, across the river, is Medicine rock which is composed of massive breccia of the Siletz River Volcanics capped by the Tyee Formation. A west-trending fault that runs along the river makes the contact of the Tyee Formation to the south and the Siletz River Volcanics to the north.

29.7 Stop 6A — Small quarry in a dike of biotite camptonite is located on the right side of the road. Camptonite dikes, sills and inclined sheets crop out in a large area in the northeastern part of the Euchre Mountain quadrangle (Snavely and Vokes, 1949; Snavely, MacLeod, Wagner, and Rau, 1976a) and extend east and northeast into the Valsetz and Grande Ronde quadrangles (MacLeod, 1970). Camptonitic rocks are particularly well exposed in the vicinity of Cougar Mountain (fig. 1). These alkaline mafic intrusive rocks range from aphyric rocks rich in augite, aegerine-augite, or titaniferous augite to rocks that contain abundant large equant crystals of barkevikitic hornblende or titaniferous biotite set in a matrix containing alkali-feldspar, sodic plagioclase, analcime, feldspathoids, apatite, and opaque minerals. Some of the sills and dikes are differentiated and contain small pegmatitic camptonite bodies and phonolite veinlets. The biotite camptonite dike at this stop and several other camptonite dikes that have been mapped immediately to the west were apparently feeder dikes to the extrusive sequence at Stop 4A. The camptonite intrusive rocks and the correlative extrusive rocks are strongly undersaturated with respect to silica (nepheline normative) and are characterized by high contents of Fe, Ti, K, and P. The camptonite is approximately equivalent in age to the uppermost Eocene basalt flows that form Cascade Head, 30 miles north of Newport. Although the camptonite and some of the Cascade Head basalts have many chemical similarities, the camptonite contains considerably lower silica and more alkalies (Table 1, col. 5). A K/Ar date of 33 m.y.B.P. was obtained for the biotite camptonite at this stop.

31.4 — Unconformable contact between the Nestucca and Tyee Formations.

32.0 — Exposure of Nestucca siltstone.

33.1 — Marine basaltic breccia interbed in the Nestucca Formation.

36.4 to 36.5 — Siltstone of the Nestucca Formation cut by sandstone dikes and sills.

37.0 — Contact of the Yamhill and Nestucca Formations is exposed in the banks of the Siletz River.

37.5 — Cedar Creek; head of tidewater on the Siletz River. Two miles up Cedar Creek a quarry in granophyric gabbro supplied the rock for the Newport jetty. Chemical analysis of the chilled border facies of the Cedar Creek granophyric sill is shown in Table 1, col. 7.

Seismic refraction work from a large shot in this quarry indicate the depth to the Moho is 15.8 km (Berg and others, 1966).

37.7 — Contact of the Tyee and Yamhill Formations is exposed in the river banks.

39.6 Stop 7A — Lunch stop. Lincoln County A. W. "Jack" Morgan Memorial Park.

40.1 — Excellent exposure of turbidites of the Tyee Formation (fig. 5).

41.4 — Bridge over Euchre Creek.

42.1 — The logged, conical-shaped, hill on the horizon to the north is Euchre Mountain which is capped by a differentiated granophyric gabbro sill.

42.6 — Bridge over the Siletz River.

45.0 — Bridge over the Siletz River. The road follows near the upper contact of the Tyee and Yamhill Formations; the contact is well exposed in the river banks.

45.7 Town of Siletz. Turn east toward Logsden (E. Buford Street).

0 Start new mileage at Siletz.

0.8 Gravel pits in terrace deposits of the Siletz River.

2.7 Excellent exposures of the Tyee Formation composed of 1- to 3-foot-thick graded sandstone and siltstone turbidite beds.

4.8 Old covered bridge over the Siletz River on Sams Creek Road.

7.6 Bridge over the Siletz River at Logsden. Take the first left, heading north (up river) on the Upper Farm Road.

7.9 Outcrop of the Tyee Formation.

10.6 At twelve o'clock a view of a granophyric gabbro sill of mid-Oligocene age caps the west-trending ridge.

11.3 Road junction, stay on paved road turning to the left.

11.6 Moonshine Park. Loop around park to see excellent exposures of the Tyee Formation.

Head back to main road.

12.2 Junction of Siletz River Road and Moonshine Park Road.

Turn left onto gravel road.

12.7 Contact between the Tyee Formation and the underlying Siletz River Volcanics is well exposed in the river bed. About 100 feet of indurated siltstone occurs above the highest tuff and lapilli tuff in the Siletz River Volcanics and below the lowest sandstone beds of the Tyee Formation along the river.

14.1 Stop 8A An inclined sheet of granophyric gabbro is exposed in the gorge of the Siletz River. This large intrusive extends from Green Mountain in the Valsetz quadrangle east of the Siletz River gorge to Lambert Point west of the river (fig. 1). Near the Siletz River gorge the granophyric gabbro dike "rolls-over" within a few hundred feet to form a south-dipping inclined sheet that is discordant to the Siletz River Volcanics but is generally concordant with the overlying Tyee Formation. This intrusive may have extended northward 8 miles as a sill to Stott Mountain, which is capped by a 500-foot-thick sill. Other sills, or inclined sheets, cap many of the higher peaks, ridges, and upland surfaces in the Coast Range between latitudes 43°45' and 45°N; these include Fanno Ridge, Prairie Peak, Marys Peak, and Roman Nose Mountain. They are typically 300 to 500 feet thick, although the sill at Marys Peak is about 1000 feet thick. Three K/Ar dates of mineral separates from these intrusives indicate an absolute age of about 30 m.y.B.P. The granophyric gabbro is composed of plagioclase, ferroaugite, intergrown quartz and alkali feldspar, apatite, opaque minerals, and iron-rich clay minerals. Fayalitic olivine is a constituent of most granophyric gabbro but is absent in a few. Most of the sills are differentiated, and bodies of pegmatitic gabbro, ferrogranophyre, and granophyre are commonly developed within them. These more silicic rocks contain the same minerals as the gabbro but in different proportions, and the mafic minerals are more Fe-rich and the feldspars more Na- and K-rich. At this stop, the upper contact of the inclined sheet is exposed in the small quarry where the gabbro intrudes basaltic siltstone, tuff breccia, and pillow lavas of the Siletz

River Volcanics. Granophyric gabbro and ferrogranophyre in the upper part of the body are well exposed along the steep walls of the river. The faint layering shown by the granophyric gabbro and ferrogranophyre has been noted in the upper parts of several of the sills. The lower two-thirds of most sills shows no visible layering, but petrographic and chemical studies show that they have a systematic upward variation in modal proportions, mineral compositions, and rock compositions (MacLeod, 1970). Continue upstream along the Siletz River road.

15.0 Top of granophyric gabbro sill is exposed in the west bank and in the river bed.

15.1 Baked basaltic tuff of the Siletz River Volcanics overlies a gabbro sill. A small north-trending fault offsets the upper contact along the river. Proceed northward through the granophyric gabbro sill.

15.2 The Lambert Point sill is exposed on both sides of the gorge.

15.5 The columnar-jointed sill is well exposed on the south side of the river from here to the bridge.

16.1 The base of the sill.

16.3 Bridge over the Siletz River gorge near Camp Gorge.

End of field trip. Turn around and head back on the same road to Logsden. Proceed east from Logsden to U.S. Route 20 and return to and return to Corvallis. End of field trip.

Figure 18. View north across Depoe Bay, Oregon, type locality of the Depoe Bay Basalt (Stop 2A). The Depoe Bay Basalt is well exposed along the east side of the bay (adjacent to U.S. Highway 101) and is overlain by sandstone of Whale Cove. The Cape Foulweather Basalt overlies the sandstone and forms the jagged coastline.

Figure 19. Isolated-pillow breccia of the Depoe Bay Basalt at Depoe Bay, Oregon. Note the discontinuous chilled zone developed inward from the chilled margin of the pillow in foreground and the sandstone-filled tension cracks and sandstone-filled core of the originally hollow pillow in center (under hammer).

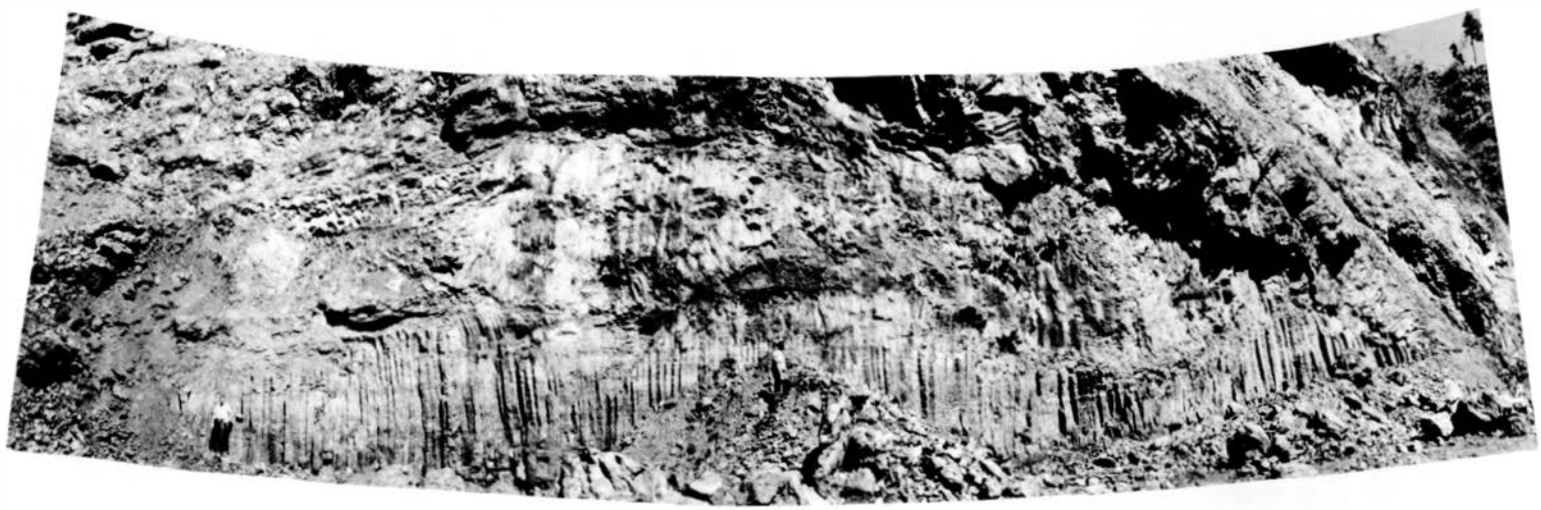

Figure 20. Filled feeder-tube in the Siletz River Volcanics at Kauffman quarry (Stop 5A). Columnar-jointed alkalic basalt in the central part of tube is surrounded by a carapace of pillow basalt.

FIELD TRIP NO. 4

GEOLOGIC SUMMARY FOR A FIELD GUIDE THROUGH THE NORTH-CENTRAL KLAMATH MOUNTAINS

BY

M. A. Kays, University of Oregon, and
M. L. Ferns, Oregon Department of Geology and Mineral Industries

NOTE
This guide is published separately in OREGON GEOLOGY

GEOLOGIC FIELD TRIP GUIDE FOR THE CENOZOIC STRATIGRAPHY AND LATE EOCENE PALEOECOLOGY OF SOUTHWESTERN WASHINGTON[1/]

John M. Armentrout, Kristin McDougall, and Paula T. Jefferis
U.S. Geological Survey
Menlo Park, California 94025
and
Elizabeth Nesbitt
University of California
Berkeley, California 94720

INTRODUCTION

A field trip guide for the Cenozoic stratigraphy of southwestern Washington describes 15 rock units and four measured sections. The field trip consists of 15 stops along a 157-mile route from Portland, Oreg., to Olympia, Wash. A road log gives directions to localities where 11 of these rock units can be observed. Of particular note are stops at two of Washington State's best known and most productive late Eocene macro- and microfossil localities: the Big Bend of the Cowlitz River-Cowlitz Formation, an early late Eocene shelf deposit; and the Porter Bluff sequence-Lincoln Creek Formation, a late Eocene mid-bathyal slope deposit.

Text figures 1-3 present the geologic framework and stratigraphic nomenclature used in this report. Figure 4 is an index map of the trip route. The remaining figures 5-25 are arranged within the road log to be most accessible for use on the field trip.

ACKNOWLEDGMENTS

The senior author is indebted to those Pacific Northwest geologists who guided him through their field areas, in particular: Parke Snavely and Norm MacLeod, U.S. Geological Survey; Weldon Rau, Washington (State) Department of Natural Resources; Robert Van Atta, Portland State University; Alan Niem, Oregon State University; Ewart Baldwin, University of Oregon; V. S. Mallory, University of Washington; and Paul Vandeveer and Roger Paul, Washington Irrigation and Development Inc. The field trip guide has benefited from review by Les Magoon and John Barron, U.S. Geological Survey, and Weldon Rau.

STRATIGRAPHY

Cenozoic rocks in southwestern Washington measure from 10,000 to 23,000 feet or more and include these rock units: Crescent Formation, Cowlitz Formation, McIntosh Formation, Northcraft Formation, Skookumchuck Formation, Goble Volcanics, Lincoln Creek Formation, Astoria(?) Formation, Columbia River Basalt, Montesano Formation, Troutdale Formation, Logan Hill Formation, Terrace Deposits, Vashon Drift, and Alluvium. These units crop out in several structural depressions separated by early to middle Eocene volcanics. These structural depressions formed in Cenozoic time along the tectonically

---

[1/]This report is preliminary and has not been edited or reviewed for conformity with Geological Survey standards and nomenclature.

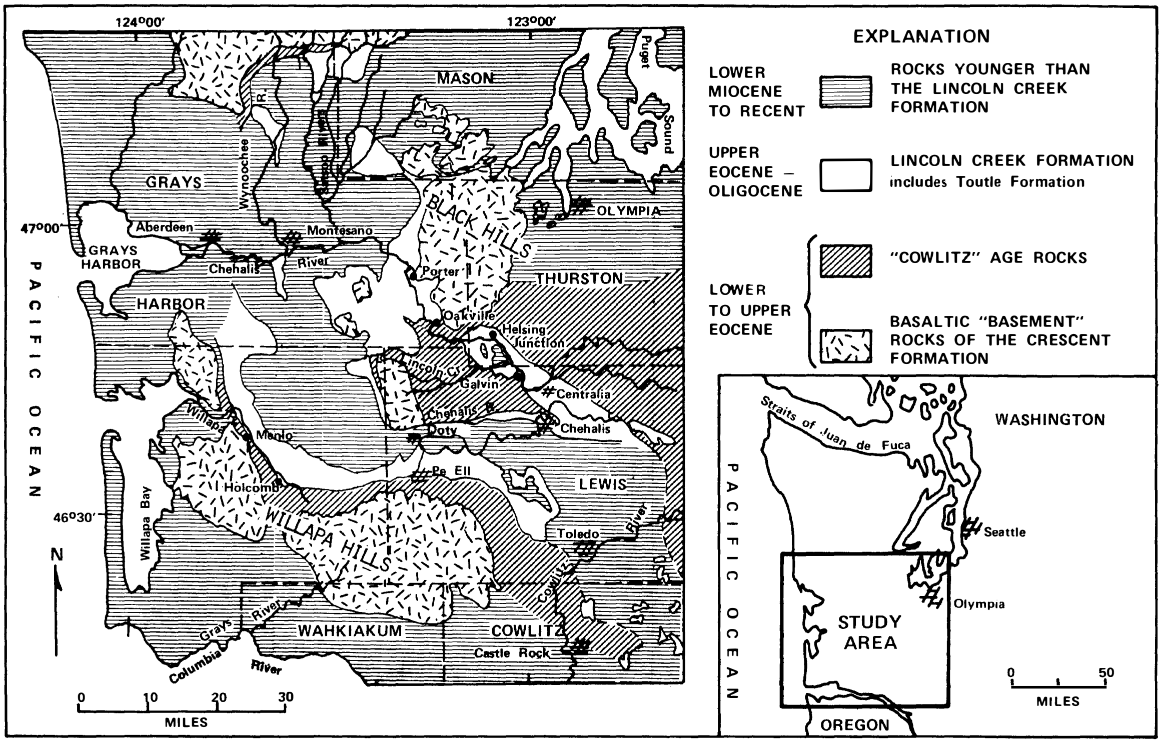

Figure 1. Generalized geologic map, southwest Washington. Geology from Pease and Hoover (1957), Snavely, Brown, Roberts, and Rau (1958), Huntting, Bennett, Livingston, and Moen (1961), Gower and Pease (1965), and Wagner (1967). Figure modified from Beikman, Rau, and Wagner (1967); reproduced from Armentrout (1975).

active Pacific Margin of the North American Plate. The strata are marine sedimentary rocks with interbedded volcanics that grade eastward to nonmarine sedimentary and volcanic rocks.

The age relationships of the foraminiferal and molluscan faunas for the Eocene through Miocene follows Armentrout (1973, 1975) (fig. 3). Fossil localities shown on figures are from Armentrout (1973).

Crescent Formation

The oldest rocks within the field trip area are assigned to the Crescent Formation of early to middle Eocene age (Field trip stops 8-9, 14-15). Crescent Formation rocks are typically aphanitic to porphyritic augite-rich basalts with lesser amounts of interbedded marine sandstones and siltstones. The type area for the formation is Crescent Bay along the northern shore of the Olympic Peninsula (Arnold, 1906). Crescent Formation basalts underlie the higher hills of the Willapa Hills and Black Hills of southwestern Washington (fig. 1). The basalts are commonly zeolitized (Snavely and others, 1958).

The Crescent Formation basalts are part of a major, early to middle Eocene volcanic sequence which extends from Vancouver Island on the north to the flanks of the Klamath Mountains in southern Oregon. This sequence includes at least 60,000 cubic miles of flood basalts which erupted onto the sea floor from fissures and vents, either as flows or extrusive breccia (Snavely and Wagner, 1963). Local volcanic centers appear to have become subaerial toward the end of middle Eocene time. Volcanic rocks that correlate with the Crescent Formation include the Crescent(?) Formation of Pease and Hoover (1957) and Snavely and others (1958), the Metchosin Volcanics of Vancouver Island (Clapp, 1917), and the Siletz River Volcanic Series (Snavely and Baldwin, 1948), Tillamook Volcanics (Warren and others, 1945), and the Roseburg Formation volcanics of Oregon (Baldwin, 1974).

The early to middle Eocene age of the Crescent Formation has been determined from fossils recovered from interbedded sedimentary rocks. Foraminifera indicate a Ulatisian age assignment (Rau, 1964, 1966).

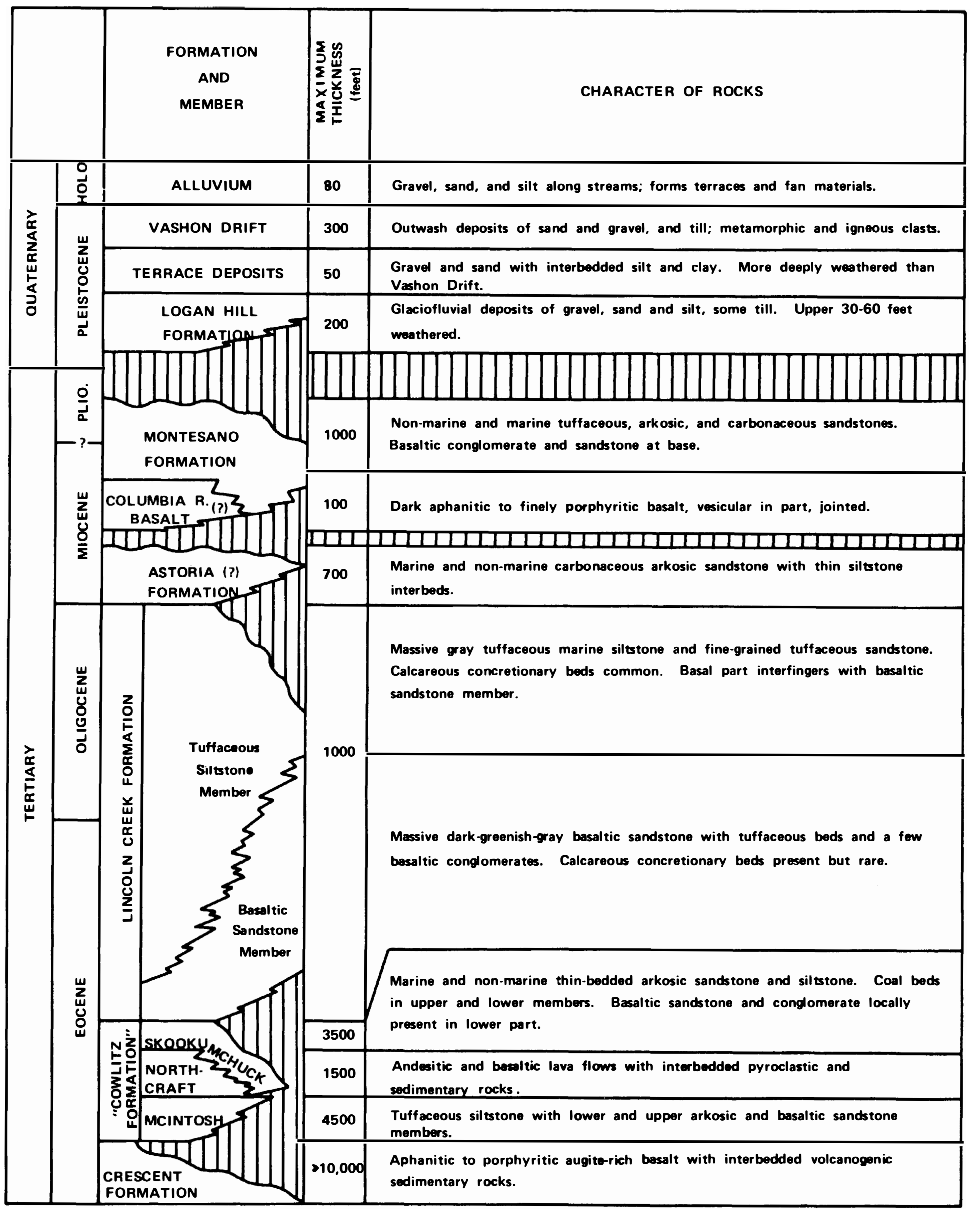

Figure 2. Stratigraphic column for field trip. Modified from Snavely, Brown, Roberts, and Rau (1958). The Goble Volcanics and Troutdale Formation are not on this figure as they crop out to the south in a separate structural basin.

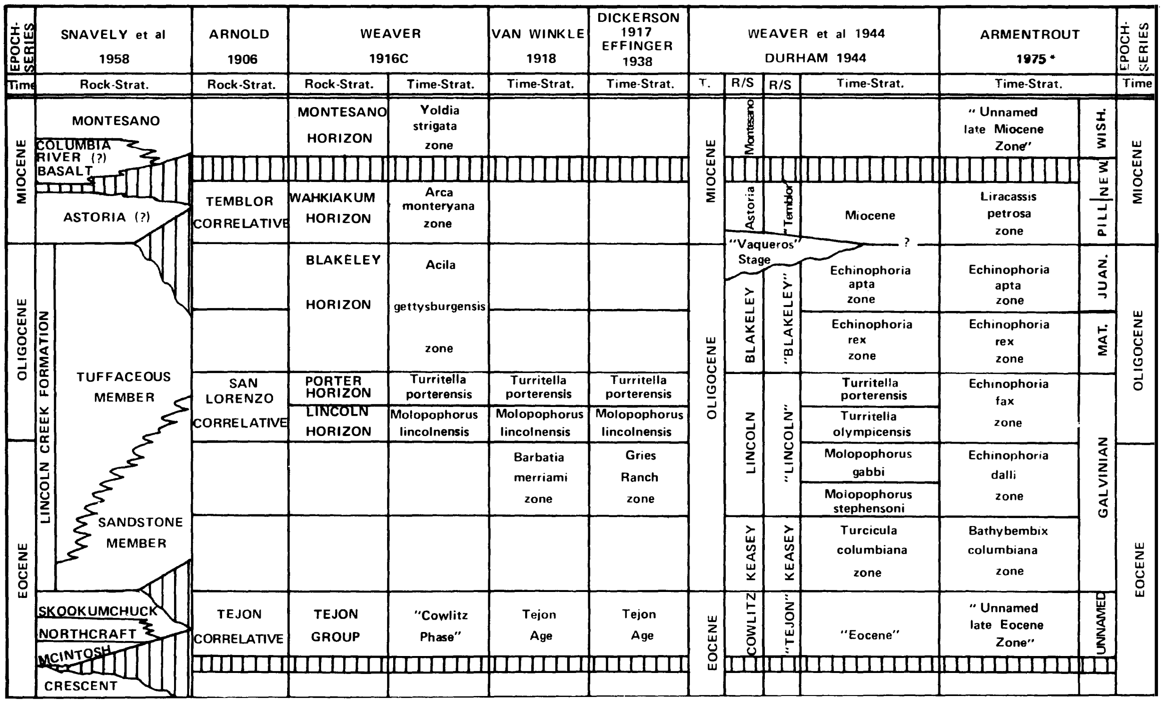

Figure 3. Selected rock-stratigraphic and time-stratigraphic nomenclature applied to Eocene and Miocene units in southwestern Washington. Stage sequence (Galvinian, Matlockian, Juanian, Pillarian, Newportian, Wishkahan) from Armentrout (1975, 1978) and Addicott (1976).

Cowlitz Formation

Arnold (1906) referred a molluscan fauna from the area around Vader, Washington (fig. 5, locality UW-1, figs. 5-9), to the Eocene and, using California nomenclature, called it a "Tejon Correlative" (fig. 3). The strata containing that fauna were subsequently named Cowlitz Formation by Weaver (1912). Locally, these rocks unconformably overlie the Crescent Formation. The type area of the Cowlitz Formation is along Olequa and Stillwater Creeks, and the Cowlitz River (fig. 5, Field trip stops 3 and 4). The maximum thickness of the Cowlitz Formation is approximately 9,500 feet (fig. 2). The unit is predominantly siltstone with sandstone locally well developed. Both marine and nonmarine rocks occur in the type area (Henriksen, 1956). Molluscan fossils from the type section of the Cowlitz Formation have been studied by Weaver (1912) and Van Winkle (1918), and Foraminifera have been studied by Beck (1943) and Rau (1958). Both faunas indicate a late Eocene (Narizian Stage) age.

The Cowlitz Formation, as used by Weaver (1912, 1916b, 1937), includes several distinct formations of present usage: the McIntosh and Skookumchuck Formations of the Centralia-Chehalis area (Snavely, Rau, and others, 1951; Snavely, Roberts, and others, 1951; Snavely and others, 1958); the "Sedimentary rocks of Late Eocene Age" in the Satsop River area (Rau, 1966, 1967); and the McIntosh Formation as mapped along the Willapa River (Wagner, 1967). These late Eocene units represent deltaic environments to the east (Skookumchuck) and open marine to the north and west (McIntosh). The sedimentology of "Cowlitz" [Formation] units is discussed by Buckovic (1979).

The following discussion of the McIntosh, Northcraft, and Skookumchuck Formations, which are not visited on the trip, is to provide a perspective to the lithofacies recognized within southwestern Washington that are correlative with the Cowlitz Formation of Weaver (1912, 1916b, 1937).

McIntosh Formation

The McIntosh Formation is a lower upper Eocene sequence of tuffaceous marine sedimentary rocks and local centers of porphyritic basalt flows. The formation was named and described by Snavely, Rau, and others (1951) from road cuts along the south shore of McIntosh Lake. The type area is the axial part of the Crawford Mountain anticline east of Tenino, Wash. Maximum measured thicknesses of the McIntosh Formation are 5,000 feet (fig. 2). The middle McIntosh siltstones and claystone are foraminiferally rich and indicate a late Eocene (Narizian Stage) age (Rau, 1956). The lower and upper McIntosh Formation include nearshore sequences of basaltic and arkosic sandstones.

Regional relationships suggest that the McIntosh Formation overlies Crescent Formation basalts with local unconformity and is locally interbedded with upper Crescent Formation lava flows and sediments. The formation is gradationally overlain by or locally interbedded with the Northcraft and Skookumchuck Formations. The McIntosh Formation is correlative to parts of the Aldwell, Lyre, and lower Twin River Formations of the Olympic Peninsula (Rau, 1964), and to late Eocene units both in the Satsop River area (Rau, 1966) and along the Willapa River (Rau, 1951; Wagner, 1967). In Oregon, the Tyee and Yamhill Formations are correlative with the McIntosh Formation (Snavely and others, 1977).

Northcraft Formation

The Northcraft Formation lavas and associated volcanically derived sediments are typed in the vicinity of Northcraft Mountain on the southwest flank of Crawford Mountain anticline (Snavely, Roberts, and others, 1951). The Northcraft Formation gradationally overlies or is interbedded with the McIntosh Formation and is overlain by the Skookumchuck Formation with an apparent local angular unconformity. Those aspects of the Northcraft Formation interbedded with fossiliferous sediments of the McIntosh Formation permit assignment of an early late Eocene (Narizian Stage) age.

The Northcraft Formation consists chiefly of ferromagnesian lavas and flow breccias, with pyroclastic rocks in the upper part and basaltic conglomerates, sandstone, and pyroclastic material in the lower part. In the vicinity of Northcraft Mountain the formation is nearly 1,500 feet thick and is predominantly lavas. To the west and south of Northcraft Mountain, this formation thins and is mostly fine-grained pyroclastic rocks (Snavely and others, 1958).

The Northcraft Formation is correlated by superposition and rock type with the Yachats Volcanics of northwest Oregon (Snavely and others, 1977).

Skookumchuck Formation

The Skookumchuck Formation is typified by interbedded shallow marine and continental facies. The formation was defined by Snavely, Roberts, and others (1951) and the type section is along the Skookumchuck River. The Skookumchuck Formation may be as much as 3,500 feet thick in the Centralia-Chehalis area. Lower and upper basaltic and arkosic sandstone members are separated by carbonaceous siltstones which thicken westward. Tuffaceous coals are abundant in the lower and upper members. The coals rank from lignite to subbituminous B. Most of the coal is subbituminous C.

The Skookumchuck Formation overlies the Northcraft Formation with local angularity. To the west, the underlying McIntosh Formation siltstones grade upward into Skookumchuck siltstones. The Skookumchuck Formation is conformably overlain by the Lincoln Creek Formation within structural lows, and unconformably overlain by the Lincoln Creek Formation over late Eocene structural highs. The maximum measured thickness for the Skookumchuck Formation is up to 3,500 feet (Snavely and others, 1958).

Molluscan and foraminiferal fossils of the Skookumchuck Formation indicate a late Eocene age (Snavely and others, 1958). Correlative rock units include the upper part of the type section of the Cowlitz Formation of Weaver (1912); the lower Twin River Formation of the Olympic Peninsula (Rau, 1964); the "Sedimentary Rocks of Late Eocene age" of Rau (1966) in Washington; and the "Cowlitz" Formation of northwestern Oregon (Niem and Van Atta, 1973).

Goble Volcanics

The thick sequence of basaltic flows and pyroclastic rocks that crop out on both sides of the Columbia River in southwestern Washington and northwestern Oregon are mapped as Goble Volcanics (Warren and others, 1945; Livingston, 1966) (Field trip stops

1-2). The type area is the vicinity of Goble, Oregon, where a thickness of more than 5,000 feet was mapped by Wilkinson and others (1946). Only 1,000 feet of Goble Volcanics occur in southwestern Washington. Both upper and lower contacts of the Goble Volcanics are transitional, interfingering with the Eocene sedimentary rocks of the Cowlitz Formation below and latest Eocene to Oligocene rocks of the Lincoln Creek and Toutle Formations above (Livingston, 1966; Armentrout, 1975). Whole rock K/Ar ages from Goble outcrop samples in southwest Washington range from 45.0 ± 1.4 to $32.2 \pm 0.3 \times 10^6$ years (Beck and Burr, 1979), which spans middle Eocene to early Oligocene.

Recent paleomagnetic studies of Goble Volcanics indicate that the mean direction of remanent magnetism points about 25° east of the expected mid-Tertiary geomagnetic field direction for the area (Beck and Burr, 1979). Beck and Burr suggest that the Goble Volcanics are part of a block that has been rotated about a pivot located somewhere nearby, either as part of the Coast Range or as an independent microcontinental block.

Lincoln Creek Formation

From 2,000 to 9,000 feet of sedimentary beds are assigned to the "Lincoln Formation" of Weaver (1912, 1916c, 1937). The type section (Weaver, 1912) was established along the Chehalis River near Lincoln Creek just northwest of Galvin, Washington, and was considered to be of middle Oligocene age (fig. 15). Subsequently, the formation has been redefined (Weaver and others, 1944) to include a composite of many sections along the Chehalis River between Centralia and Porter, Washington (Field trip stops 5-7 and 10-12). This formation was further redefined by Beikman and others (1967) as the Lincoln Creek Formation.

Four rock types express four different depositional environments within the Lincoln Creek Formation. Along the easternmost margin of the exposures of the formation are strandline and continental deposits of the Lincoln Creek Formation of Snavely and others (1958), and correlative sedimentary beds of the Toutle Formation (Roberts, 1958). These rocks grade westward into marine glauconitic basaltic sandstones that are 1,500 feet thick just east of Centralia (Snavely and others, 1958). Further westward, these sandstones become thinner but persist in all sections studied. Higher in the formation, the basaltic sandstones grade upward to highly fossiliferous marine fine-grained tuffaceous sandstones and siltstones. This gradation appears to be indicative of a deepening depositional environment, probably to shelf and to mid-bathyal slope conditions. The more tuffaceous deeper marine facies are best expressed in the Satsop River area, along the Willapa River, and at Porter Bluff and PeEll-Doty.

The greatest thickness of the Lincoln Creek Formation occurs toward the western margin of the outcrop area. The formation thins locally and onlaps highs of older rocks that now form the Doty and Black Hills, and Minot Peak (Pease and Hoover, 1957). The Lincoln Creek Formation molluscan (Armentrout, 1973, 1975) and foraminiferal faunas (Rau, 1958, 1966) both indicate an age range from late Eocene to latest Oligocene, encompassing the Refugian and Zemorrian Stages of benthic foraminiferal chronology and the molluscan Galvinian, Matlockian, and Juanian Stages (Armentrout, 1975, 1978; Addicott, 1976) (fig. 3). The Lincoln Creek strata correlate with the Blakeley Formation of the Seattle and Bainbridge Island areas (Tegland, 1933; Weaver, 1937; Durham, 1944; Fulmer, 1975), with parts of the Twin River Formation (Brown and Gower, 1958; Rau, 1964), and with the Makah Formation (Snavely and others, 1979) to the north on the Olympic Peninsula. Correlatives in northwest Oregon include the Keasey, Pittsburg Bluff, and Scappoose Formations (Baldwin, 1964; McDougall, 1979); in the central Oregon Coast Range the uppermost Nestucca, Alsea, and Yaquina Formations (Snavely and others, 1969, 1973); in the Willamette Valley the Eugene Formation (Hickman, 1969); and in the southern Oregon Coast Range the Tunnel Point Formation (Baldwin and Beaulieu, 1973).

Astoria(?) Formation

The Lincoln Creek Formation is overlain by the Astoria(?) Formation, a dark medium-gray micaceous and carbonaceous fine-grained sandstone that generally has a glauconitic sandstone bed(s) at its base. Snavely and others (1958) describe the Astoria(?) Formation as including those strata referred to as: "basaltic conglomerate" of Miocene(?) age along the North Fork of the Newaukum River mapped by Snavely, Roberts, and others (1951); lower Astoria Formation of Pease and Hoover (1957) in the Doty-Minot Peak area; and the Astoria Formation of Etherington (1931) in Grays Harbor and Thurston Counties.

In the Centralia-Chehalis area, where a series of late Oligocene structural highs developed, the Astoria(?) Formation unconformably overlies the Lincoln Creek Formation (Snavely and others, 1958). Farther west, away from the structural highs, the Astoria(?) Formation conformably overlies the Lincoln Creek Formation. The Astoria(?) Formation is unconformably overlain by any of several younger units. Because of these unconformable relationships, the thickness of the Astoria(?) Formation is locally variable measuring only about 700 feet thick in the field trip area. The maximum measured thickness of the formation approaches 3,500 feet in the Wynoochee River area (Rau, 1967).

The foraminiferal faunas of the Astoria(?) Formation have been studied by Rau (1948b, 1951, 1958, 1966, 1967), and the molluscan faunas have been studied by Etherington (1931), Moore (1963), Strong (1967), Armentrout (1973), and Addicott (1976). All faunas suggest early to middle Miocene age assignments.

Correlative units of the Astoria(?) Formation of southwestern Washington are the Clallam Formation of northwest Washington, and the Astoria and Nye Formations and Coos Bay and Cape Blanco "Miocene Beds" of Oregon (Moore, 1963; Armentrout, 1973, 1975; Addicott, 1976).

Columbia River Basalt

In the southwestern areas of the Centralia-Chehalis district, a gray aphanitic basalt rests unconformably upon sedimentary rocks of the Astoria(?) and Lincoln Creek Formations, and is overlain by beds ranging in age from late Miocene to Holocene. This single basalt flow averages 70-80 feet in thickness. The basalt has been dated at 15.7±0.8 m.y. (K/Ar) by Turner (1970), and is correlated with the Yakima Basalt of the Columbia River Group of middle Miocene age (Snavely and others, 1973).

Montesano Formation

A sequence of interbedded fluvial, lacustrine, brackish-water, and shallow-marine deposits overlap the Astoria(?) Formation and Columbia River Group basalt to rest with angular unconformity upon beds of the Lincoln Creek Formation (fig. 17). The continental deposits are unnamed (Snavely and others, 1958; Roberts, 1958) whereas the marine units are mapped either as Montesano Formation (Weaver, 1912, 1937; Etherington, 1931) or as upper Astoria(?) Formation (Pease and Hoover, 1957). The Montesano Formation is locally variable in thickness, but approaches a maximum thickness of 3,000 feet in the Wynoochee River area (Rau, 1967).

The marine deposits of the Montesano Formation have been dated with mollusks as late Miocene (Weaver, 1912, 1937; Weaver and others, 1944; Addicott, 1976), and with foraminifers as late middle and late Miocene Mohnian-Delmontian Stages (Fowler, 1965; Rau, 1966, 1967, 1970; Bergen and Bird, 1972). In Oregon, rock units that correlate with the Montesano Formation include the Empire Formation of Coos Bay (Baldwin and Beaulieu, 1973), and unnamed sedimentary rocks along the Columbia River near Clifton (Baldwin, 1974).

Troutdale Formation

The name Troutdale was first used by Hodge in 1933 and was formally proposed by him in 1938 to describe conglomerate and sandstone beds that crop out near Troutdale, Oregon. Semiconsolidated gravels and sands correlative with the Troutdale Formation occur in restricted areas along the lower Columbia River in the Longview and Cathlamet areas of Washington (Livingston, 1966) (Field trip stop 2). In this area the Troutdale Formation unconformably overlies the Goble Volcanics. The interbedded well-rounded cobbles, lens-shaped gravels, and friable sandstone and mudstone indicate a fluvial origin for this formation. Composition of the pebbles suggests derivation from a quartzite and metamorphic, acidic volcanic terrain such as occurs in northwestern Washington or eastern Oregon and Idaho, as well as basaltic andesites of the Cascades and basalts of the Coast Ranges. The restricted occurrence of Troutdale Formation deposits along the Columbia River and the clast types suggest that these fluvial deposits were probably associated with an ancestral Columbia River system.

Leaves from the Troutdale Formation (Trimble, 1963) indicate an early Pliocene age (Livingston, 1966).

Logan Hill Formation

The Logan Hill Formation is composed mainly of reddish- to yellowish-brown, iron-stained gravel and minor amounts of interbedded sand and silty clay up to 200 feet thick. The formation was named by Snavely, Roberts, and others (1951) in the Centralia-Chehalis area where the deposits form flat-topped upland surfaces. The Logan Hill Formation is interpreted as glaciofluvial in origin with the primary sediment source coming from alpine glaciation to the east. The initial surface of the Logan Hill Formation has an elevation of approximately 1,000 feet in the eastern outcrop area and decreases uniformly westward to an altitude of about 350 to 400 feet just east of Galvin (Snavely and others, 1958).

The Logan Hill Formation is considered to be early Quaternary in age, coeval with the maximum extent of the alpine valley glaciers of the western Cascade Mountains (Snavely and others, 1958).

Terrace Deposits

Unconsolidated gravel and sand of glaciofluvial origin form terraces along many of the river and stream valleys of southwestern Washington (Field trip stop 13). The terraces are highly dissected and often are difficult to map separately from the alluvium (Snavely and others, 1958). The pebbles and cobbles of the terrace deposits are principally porphyritic andesite and basalt derived from the Northcraft Formation, some cobbles of middle Eocene sedimentary rocks, Cascade andesite(?), and weathered rocks reworked from the Logan Hill Formation. The terrace deposits are assigned to the Pleistocene (Snavely and others, 1958).

Vashon Drift

The Tenino Prairie, between Olympia and Centralia, is a terrace surface on which the Vashon Drift was deposited. The Vashon Drift is a glacial deposit of morainal and outwash silts, sands and gravels laid down by the Puget Lobe of the Cordilleran Ice Sheet (fig. 14). The Puget Lobe moved southward through the Puget Sound area at least four times during the late Quaternary. The maximum advance of the Puget Lobe, between 15,000 and 13,500 years ago, reached an area just north of Centralia (Easterbrook, 1969, 1979). The glacier rode up to a maximum altitude of about 1,100 feet along the volcanic highlands extending from Tenino eastward.

The Vashon Drift is generally less than 50 feet thick (Snavely and others, 1958). Vashon till is light bluish gray with a matrix of well-compacted silt and clay holding subangular to rounded cobbles and boulders up to 8-10 feet in diameter. Outwash sand and gravel are composed of only slightly weathered igneous and metamorphic rocks. Outwash deposits are massive to well bedded. Crossbedding and foreset bedding are common. The gravels have three sources: exotic igneous and metamorphic rocks from terrains well to the north, carried in by the Puget Lobe; locally derived igneous rocks; and igneous rocks from the Cascade Mountains carried westward into the Puget Lowland by alpine glaciation. Locally, the Vashon Drift has been reworked by streams and rivers into a series of terraces. Older terrace gravels of glaciofluvial origin have been highly dissected and are difficult to map. They may be distinguished from Vashon Drift terraces by the deeper weathering or iron-stained rind on the clasts. Clast types of the older terrace gravels do not include the exotic igneous or metamorphic rock types characteristic of Puget Lobe-Vashon Drift sediments (Snavely and others, 1958).

Alluvium

Alluvium, as used in this paper, includes a variety of Holocene sands and gravels associated with river and stream and valley fills. The maps of Pease and Hoover (1957) and Snavely and others (1958) detail these deposits.

STRATIGRAPHIC SECTIONS

Four stratigraphic sections will be visited on the accompanying field trip. The following review of work on these sections provides some insight into southwestern Washington stratigraphic nomenclature (fig. 3), and presents new paleoecologic data of two particularly significant fossil localities.

Olequa Creek section

Weaver's (1916b) section of the late Eocene Cowlitz Formation occurs along Olequa Creek from Vader toward Winlock, Washington (fig. 5). Although the field trip does not visit this section it is important as the paleoecology study locality at the Big Bend of the Cowlitz River is correlated into the Olequa Creek section. Occurrences of "Cowlitz" fossils are sporadic along the Olequa Creek section and only one occurrence of "Lincoln" fossils from the overlying Lincoln Creek Formation is known (University of Washington locality 291). Between the two closest outcrops of subjacent Cowlitz and superjacent Lincoln Creek strata is an interval of 400 feet (horizontal) without exposure. Regional structural patterns would suggest an unconformable relationship within this interval.

Previously listed Lincoln Creek Formation fossils from the vicinity of Winlock are those of Van Winkle (1918) [probably Weaver's (1916b) locality 291]. That locality has been recollected by V. S. Mallory and students (University of Washington localities A102 and A103). Taxa of both collections are listed in Table 2 of Armentrout (1973).

Faunal studies of the Olequa Creek section and correlative units nearby are Beck (1943) and Rau (1958) for Foraminifera, and Weaver (1916b), Van Winkle (1918), and Armentrout (1973) for Mollusca. All faunas are late Eocene in age.

Big Bend of the Cowlitz River locality

Molluscan Paleoecology

The most fossiliferous locality of the Cowlitz Formation is at the "Big Bend" of the Cowlitz River (fig. 5, Stop 4, locality UW-1; fig. 8). This locality consists of nearly sixty feet of fossiliferous poorly consolidated tuffaceous sandstones and siltstones. There is a general decrease in grain size and in molluscan fossil density and diversity upsection. The section is divided into three units (A, C, and E), separated by two prominent thin calcareous marker beds (B and D) (figs. 8 and 9). Bulk samples were taken at measured intervals through the section and preliminary studies suggest the following paleoecological interpretations.

The diverse tropical molluscan fauna appears very similar to those from the Jackson Group, Gulf Coast, and the Bartonian formations of the Paris Basin. All three faunas have numerous genera in common and are characterized as Tethyan faunas.

The lowermost unit, A, consists of brown and gray sandstones and silty sandstones with a high proportion of fossil material. Bedding and current structures are absent. Most of the fossils are well preserved, although some are abraded and many of the clams are disarticulated. Figure 10 lists the common species from University of California, Museum of Paleontology localities D-8031 to D-8035 and D-8043. Several of these species are illustrated in figure 11. A random measurement of turritellid gastropods in the outcrop revealed no preferred orientation. All the common taxa are represented by a wide range in size classes, and there is generally an equal number of left and right bivalve shells. For these reasons the fauna is interpreted to be an in-place, disturbed, time-averaged assemblage. Bioturbation could account for some of the disturbance.

The fauna is dominated by the infaunal suspension feeding turritellids, scaphopods, *Venericardia*, *Tivelina*, and *Pitar*. There are many carnivorous gastropods reflecting a high diversity of prey species, including many soft-bodied taxa. Washed sediment samples picked for micromollusks yielded numerous juvenile turritellids, *Crepidula* n. sp., turrids, and pyramidellids. *Turritella* shells are encrusted with bryozoan, annelid and bivalve epibionts. The dominance of slow-burrowing infaunal filter feeders, and the high density of fossil material in the sediment, suggests a low sedimentation rate. The absence of herbivores and the general species content of the fauna indicates an inner neritic environment, well below the wave base.

Unit E consists of blue-gray glauconitic siltstone with a lower fossil density and a different species assemblage than unit A. A list of the common species from University of California, Museum of Paleontology localities D-8040 to D-8042 is on figure 10 (see also figure 11). The most prominent elements are the neogastropods. Turritella is rare and the bivalve fauna consists of minute deposit-feeding protobranchs, which are widely scattered. There are isolated "nests" of the brachiopod Rynchonella. These features, as well as the high-spired morphology of the Conus species, and the presence of Fulgurofusus and Scaphander indicate a relatively deeper water environment than for unit A. The density of the fossils and the paucity of infaunal suspension feeders suggests a high rate of sedimentation.

Unit C appears to be a transition zone with elements from both assemblages. However, the large number of infaunal suspension feeders is not present. The high silt content and low fossil density indicates an increasing rate of sedimentation. This unit encompasses University of California, Museum of Paleontology localities D-8036 through D-8039 (fig. 9).

Henriksen (1956) described the type section of the Cowlitz Formation as fluctuating normal marine and brackish water facies. Buckovic (1979) described the coeval Puget Group of central Washington as deposits from an extensive Eocene deltaic system that developed from an eastern highland to a marine embayment in the west. The increased sedimentation rate, the abundant plant fragments and the changing faunal content upsection in the Cowlitz River bend locality corresponds with a shifting deltaic environment.

Foraminiferal Paleoecology

Foraminifers and associated microfossils were examined from six samples from the Cowlitz Formation collected at the Big Bend of the Cowlitz River, Washington (fig. 9). The stratigraphically oldest samples, Mf5622 and Mf5621, are barren of foraminifers. Analysis of the other samples, Mf5618 through Mf5620, confirm the earlier paleoecologic interpretations--outer neritic warm subtropical waters--of Beck (1943) from the same section and identifies the stage and zone assignments which were described subsequent to Beck's work (Mallory, 1959).

The Cowlitz microfaunal assemblages indicate outer neritic water depths (300-600 ft) with a slight increase in water depth in the youngest sample, Mf5617. Abundant species, particularly of the outer neritic superfamilies Nodosariacea and Orbitoidacea, are present (fig. 13). Most of the specimens are Cibicides natlandi Beck and Cibicides baileyi Beck, previously identified as characteristic of the outer neritic facies (McDougall, 1979). The slight increase in water depth is suggested by the increase in abundance of Bolivina hunneri Beck, Globocassidulina globosa (Hantken), Epistominella parva (Cushman and Laiming), and Lenticulina welchi (Church). These species are all more characteristic of bathyal or deeper portions of the outer neritic zone (McDougall, 1979).

Benthic foraminifers present in the Cowlitz samples suggest the late Narizian, Amphimorphina jenkinsi Zone of Mallory (1959) and the Bulimina schencki-Plectofrondicularia cf. P. jenkinsi Zone of Rau (1958, 1966) as modified by McDougall (1979). The assemblages are characteristic of the upper part of the stage and zones because many of the Cibicides natlandi species have become more convex and begun to resemble the Refugian species, Cibicides haydoni. Several foraminifers characteristic of the Big Bend of the Cowlitz River faunas are illustrated in figure 12.

Galvin section - type Lincoln Creek Formation

Approximately 1,200 feet of gray tuffaceous siltstone and fine-grained sandstone crop out along the Union-Pacific Railroad tracks paralleling the Chehalis River between Galvin and Independence, Washington (fig. 15). This section is the original type "Lincoln Formation" of Weaver (1912, 1937). The strata are poorly exposed except for two fossiliferous areas which Weaver (1916a) called the "Molopophorus lincolnensis Zone."

Two thousand five hundred feet of strata are estimated to be present in the type area; the lowermost 400 feet were recovered in cores and cuttings of a nearby test hole (Snavely and others, 1958). The Lincoln Creek strata are composed predominantly of tuffaceous siltstone and sandy siltstone. They conformably overlie the Skookumchuck Formation. Northwesterly, the uppermost Lincoln Creek Formation strata are overlain disconformably by the Astoria(?) Formation. Mollusks within the Galvin section have been described by Weaver (1916a, 1916c, 1942), Van Winkle (1918), Etherington (1931), Durham (1944), Snavely and others (1958), and Armentrout (1973, 1975). Foraminifers have been described by Frizzell (1937), Cushman and Frizzell (1940, 1943), and Rau (1958).

Oakville section

Arnold and Hannibal (1913) noted the occurrence of "San Lorenzo Formation" fossils just east of Oakville, Washington. Strata of the Lincoln Creek Formation occur in this area and are bounded by faults obscuring superpositional relationships (fig. 16). Van Winkle (1918) studied two molluscan faunas from the section (localities UW161 and UW367) between Oakville and the southern end of the Porter Bluff section to the north. Weaver (1942) lists additional species from the Oakville Quarry (= locality UW 161). Outcrops are few and all are deeply weathered. Mapping by Pease and Hoover (1957) suggests as much as 1,700 feet of rock occur in the Oakville section between the unconformable contact with underlying Crescent(?) Formation basalts and the faulted top where Lincoln Creek Formation rocks are in contact with upfaulted Crescent(?) Formation (fig. 16). The rocks of this section are very similar to the lower sandstones and middle tuffaceous siltstones of the Porter Bluff section.

The lower sandstone fossil locality of Van Winkle (1918) at the Oakville Quarry has been removed by renewed quarrying, and Van Winkle's upper locality along Gibson Creek was not productive of fossils. Weaver's quarry locality and the road cut locality east of the sandstone/basalt contact along the highway have also been removed.

Van Winkle (1918) considered the basaltic sandstone fauna coeval with the fauna collected near the old dam on Porter Creek (fig. 17, loc. PB-2) and used both to define her "*Barbatia merriami* Zone."

Pease and Hoover (1957) indicated the occurrence of molluscan fossils in NW¼NE¼ sec. 24, T. 16 N., R. 4 W. This locality (fig. 16, PH-M) was visited and found to be a three-foot high outcrop of silty sandstone beneath fallen logs along a small creek. The author found only poorly preserved molds in friable sandstone (Armentrout, 1973).

Van Winkle's (1918) Oakville section faunas are late Eocene in age (Armentrout, 1973, 1975).

Porter Bluff section

Approximately 3,000 feet of predominantly fine- to medium-grained, tuffaceous, silty sandstone, with interbedded medium- to coarse-grained sandstones and concretionary layers, is exposed along the highway north and south of Porter, Washington (figs. 17 to 23). The lowermost 100 feet are a conglomeratic, coarse-grained, basaltic sandstone unconformably overlying Crescent(?) Formation basalts. This sandstone grades upward into progressively finer grained rocks. The Lincoln Creek strata are probably overlain unconformably by the Astoria(?) Formation (Pease and Hoover, 1957).

The Porter Bluff section was first mentioned by Arnold (1906) who described three new molluscan species and referred the "Porter Shales" to the Oligocene. A correlation was subsequently made with the San Lorenzo Formation of California (Arnold, 1909). Weaver (1912) considered the "Porter Shales" to be stratigraphically higher, but gradational with, his type "Lincoln Formation" section near Galvin. He listed the fossils from the "Porter Shales" and described several new species and correlated the fauna in part with the lower portion of the Blakeley Formation of Bainbridge Island. Arnold and Hannibal (1913) summarized the Tertiary of the North Pacific Coast of America and divided the Oligocene of Washington into three formations, of which the "Porter Shales" were used as the type for Arnold and Hannibal's lower unit, the "San Lorenzo Formation." Weaver (1916a) listed numerous species from the Porter Bluff section, and defined the "*Turritella porterensis* zone." This "zone" was considered to occur in strata referred to as the "Porter Horizon," a time-stratigraphic term which Weaver (1916c) considered preferable to the "misapplied San Lorenzo Formation" of Arnold and Hannibal (1913).

Van Winkle (1918) studied the Porter Bluff and Oakville (fig. 16) sections and reported on their fauna comparing it to the type Lincoln Formation and the "Gries Ranch Fauna" of Dickerson (1917). She erected the "*Barbatia merriami* Zone" based upon the fossils of the basal Lincoln Creek Formation sandstone and considered this "zone" older than either the "*Molopophorus lincolnensis* Zone" of Weaver (1916a) or the "Gries Ranch Fauna" of Dickerson (1917).

Bruce Clark (1929, 1930) described Oligocene megafossil "horizons" for the West Coast of North America based upon fossil data from Washington. He considered the lower horizon to be that of the Gries Ranch strata, the middle the "Lincoln Horizon" of Porter Bluff, and the upper the "Restoration Point (Blakeley) Horizon" of Bainbridge Island, Kitsap County, Washington. He did not accept Arnold's usage of "San Lorenzo Formation" in Washington.

More recent studies of Porter faunas are Rau (1948a) and Mumby (1959) on Foraminifera and Durham (1944) and Armentrout (1973, 1975) on Mollusca. All faunal elements of the type "Porter Shales" are latest Eocene to Oligocene in age in the current provincial nomenclature (Armentrout, 1975). Molluscan faunas from the uppermost units of the Porter Section near Malone (see fig. 17, localities PB 28-30) are early Oligocene in age (Armentrout, 1973, 1975).

Molluscan Paleoecology

The Porter Bluff section of the Lincoln Creek Formation is highly fossiliferous. Thirty faunal localities were sampled (figs. 17, 19, and 20). Characteristic molluscan fossils are listed in figure 20 and several are illustrated in figure 21.

The basic unit of paleoecological analysis used in the study of the Porter Bluff mollusks is the zonule. The definition of zonule follows Fenton and Fenton (1928), and constitutes those rocks bearing a faunule, the faunule being "***a cluster of fossils, the autochthonous elements of which at least could be ascertained to be a fossilized community" (Berry, 1966, p. 1492). Dominant genera present in each zonule give them their name. Five zonules are described for the Porter Bluff section. The following references are the major sources of depth and temperature data used for paleoecologic interpretation: Natland (1957), Keen (1963, 1971), Durham (1950), Kleinpell and Weaver (1963), Moore (1963), Addicott (1967, 1970, 1973), McCormick and Moore (1969), and Hickman (1974).

PB-I: *Acesta*-*Ostrea* Zonule

A faunule occurring within a silty sandstone immediately above the basal unconformable contact of the Lincoln Creek Formation with Crescent(?) Formation basalts (loc. PB 1), is dominated by the occurrence of molds of the epifaunal bivalves *Acesta* and *Ostrea*. The fossils occur in dense layers indicating the probability of post-mortem transport. *Acesta* and *Ostrea* suggest shallow depths, 60 to 120 feet at most, with warm-temperate conditions.

PB-II: *Barbatia*-*Mytilus* Zonule

Well up Porter Creek, near the site of an old dam, Van Winkle (1918) collected a faunule from basal sandstones of the Lincoln Creek Formation (loc. PB 2). This faunule, of the *Barbatia*-*Mytilus* Zonule, occurs in a coarse-grained sandstone and is characterized by the occurrences of epifaunal bivalves, principally *Barbatia* and *Mytilus*. Other genera well represented in the faunule are the gastropods *Acmaea*, *Gyrineum*, and *Bruclarkia*. *Mytilus* and *Barbatia* are restricted to the intertidal region whereas *Acmaea* and *Barbatia* range from there down to depths of 200 feet. Ornamentation on the specimens of *Barbatia* and *Bruclarkia* is extremely well preserved suggesting that although the environment was high energy, burial occurred rapidly with little if any abrasion. *Barbatia* is today restricted to tropical seas while *Mytilus* and *Acmaea* are found in temperate waters. The faunule thus suggests warm waters of subtropical to warm-temperate climates, with depths of probably less than 200 feet.

PB-III: *Turritella*-*Priscofusus* Zonule

The middle 1,800 feet of section along Porter Bluffs (locs. PB 3 to PB 26) is claystone grading upward to tuffaceous siltstone with minor fine-grained sandstone. The faunule is rather uniform throughout. Gastropods far outnumber pelecypods which are only locally abundant. Specimens of *Turritella* and *Priscofusus* dominate while such genera as *Exilia*, *Natica*, *Turricula*, *Dentalium*, and crabs are common.

The structureless bioturbated fine-grained sediments, and distribution of the modern counterparts of the genera present, suggest bathyal water depths with a warm-temperate to temperate watermass. Earlier paleoecological interpretations (Durham, 1950) suggested affinities of several genera present in the Turritella-Priscofusus Zonule as being more tropical in character. Those genera are known today to be more tolerant, occurring in cool-temperate waters (Addicott, 1970). The abundance of large numbers of epifaunal and shallow infaunal carnivorous mollusks also suggests upper bathyal depths (Hickman, 1974).

PB-IV: Solena-Priscofusus Zonule

The sandstone of the upper part of the Porter section is porous and weathers deeply. Fossils recovered are casts and molds along bedding surfaces (PB 25-27). Occasionally entire leaves and pieces of wood occur together with such mollusks as Solena, Lucinoma, and Priscofusus, along with rare echinoids of the genus Brisaster. It is suggested that this faunule was transported from shallower depths into an upper bathyal environment. This interpretation is based upon the transported nature of the fossils occurring in coarser sediments within a dominantly bathyal fine-grained sequence.

PB-V: Solemya-Thyasira Zonule

Locality PB 30 was collected in 1958 by students of V. S. Mallory at the University of Washington. The collecting locality has weathered so deeply since the original excavation that considerable digging failed to recover fossils. Genera listed as occurring in siltstones at this locality include Solemya, Thyasira, and Lucinoma. This faunule is one that recurs throughout western Washington in strata of latest Eocene to early Miocene age. The community is suggestive of low-energy, lower neritic or bathyal depths of cool-water temperature, an environment in which these three genera co-occur today.

Above this zonule the strata of the upper Lincoln Creek Formation crop out discontinuously and are so deeply weathered as to prevent sampling.

Foraminiferal Paleoecology

Benthic foraminifers from seven localities in the Porter Bluffs section (PB 6, 8, 10, 12, 17, 20, and 22), southwestern Washington, are the basis for the paleoenvironmental interpretation and reexamination of the age presented here (figs. 19 and 20). Foraminifers present in the Porter Bluffs section (fig. 24) indicate an upper to middle bathyal (600-1,800 ft) water depth and an age assignment of late Eocene, late Refugian Stage. Several important species are illustrated in figure 22.

Paleobathymetric interpretation is based on the diversity (average 18 species per sample), the suborder specimen percentages (agglutinated 8 percent, porcelaneous 10 percent, hyaline 82 percent), and analysis of the hyaline superfamilies. Middle bathyal depths are indicated by the dominance of hyaline species in Cassidulinacea, a bathyal superfamily (Sliter and Baker, 1972) and further corroborated by the minor representation of the Orbitoidacea (average 15 percent) and Robertinacea (average 2.5 percent), typical neritic superfamilies, and Buliminacea (average less than 1 percent). The middle bathyal form of Cibicides elmaensis (smooth, more biconvex) is more abundant than the outer neritic zone form (lobate, planoconvex) (McDougall, 1979). Downslope transport is responsible for the abundance of porcelaneous specimens in the stratigraphically highest samples (loc. PB 20 and PB 22).

Rau (1948a) considered the Porter Bluffs section to be not older than late Eocene and not younger than middle Oligocene. Reexamination indicates a late Refugian age. Characteristic foraminifers include Anomalina californiensis, Cibicides elmaensis, Gaudryina alazaensis, Hoeglundina eocenica, and Cassidulina galvinensis. This age assignment is equivalent to the California Uvigerina vicksburgensis Zone (Donnelly, 1976) and the Washington Cassidulina galvinensis Zone (Rau, 1958, 1966) as modified by McDougall (1979).

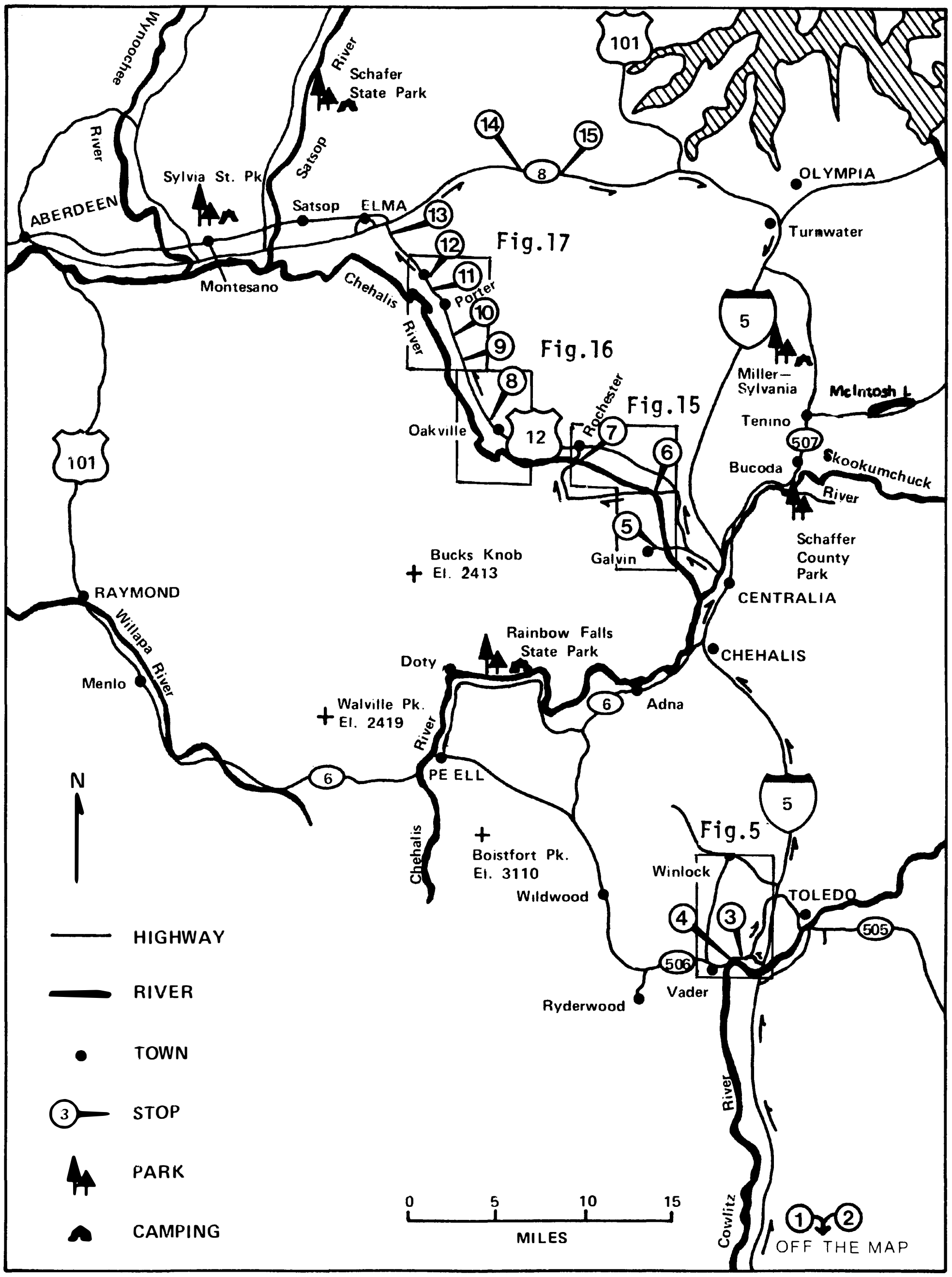

Figure 4. Index map for field trip route. Note that stops 1-2 are to the south of this map on Interstate Highway 5.

FIELD TRIP ROAD LOG

The purpose of this field trip is to examine type and/or reference sections of the principal Cenozoic formations of southwestern Washington. The field trip consists of 15 stops along highway Interstate 5 between Portland, Oregon, and Olympia, Washington (fig. 4). Specific information is provided concerning access to each locality, particularly those on private land. Formations discussed include: Alluvium, Vashon Drift, Terrace Deposits, Logan Hill Formation, Montesano Formation, Columbia River Group, Astoria(?) Formation, Lincoln Creek Formation, Cowlitz Formation, Skookumchuck Formation, Goble Volcanics, Northcraft Formation, McIntosh Formation, Crescent Formation.

NOTE: All potassium/argon radiometric age dates reported in this guide have been recalculated as suggested by Dalrymple (1979) using the new decay and abundance constants proposed by the IGUS Subcommission on Geochronology (Steiger and Jager, 1977).

MILEAGE DESCRIPTION

Cumulative (Interval)

THE FIELD TRIP ORIGINATES IN PORTLAND, OREGON.

0.0 Start mileage at north end of Interstate 5 bridge across Columbia River. Stay in left two lanes passing north through Vancouver, Washington, on Interstate 5 toward Seattle.

(6.3)

6.3 Salmon Creek. Holocene flood plain terraces occur along both sides of Salmon Creek valley. A meander cutbank exposes the lower terrace sequence of gravels along Salmon Creek east of the highway.

(2.2)

8.5 Interstate 5 climbs from one floodplain terrace upward to a higher terrace.

(5.3)

13.8 Junction of Hwys I-5 and Washington 501. Stay on I-5. The hills directly ahead are underlain by Goble Volcanics of late Eocene-Oligocene age.

(4.2)

18.0 East Fork of Lewis River. Goble Volcanics crop out along hills to the right of I-5.

(1.7)

19.7 North Fork of Lewis River.

(2.9)

22.6 Goble Volcanics form cliffs along I-5 for the next several miles. Subaerial lava flows, agglomerates, and oxidized soil horizons are typical features of the cliff exposures.

(2.6)

25.2 View of Columbia River on the left.

(4.1)

29.3 View of Trojan Nuclear Reactor Power Plant ahead on left across the Columbia River.

(1.4)

30.7 Quarry to the right exposes flood plain terrace sediments.

(0.6)

31.3 The isolated hill to the right of I-5 is formed of Goble Volcanics.

(0.2)

31.5 Kalama River.

(0.2)
31.7 Exit I-5 onto Kalama River Road and make an immediate right turn onto frontage road (Meeker Drive). Drive back south, parallel to I-5, to the south end of the frontage road and Kalama River bridge.

(0.5)
32.2 STOP 1: GOBLE VOLCANICS. Park on the left side of the frontage road next to the side road entrance.

The outcrop along the frontage road exposes several basalt flows and oxidized soil horizons of the late Eocene-early Oligocene Goble Volcanics. The basalt is generally fresh, fine grained, and has masses of iddingsite scattered throughout along with microphenocrysts of plagioclase and pyroxene. Unpublished K/Ar whole rock data on the lowest basalt flow in this outcrop yield an age of $37.4 \pm 0.7 \times 10^{6}$ years (Mobil Oil Corporation-Field Research Laboratory Sample #4338: Armentrout, 1979, unpub. data). The sample was treated for removal of the diagenetic minerals and the date obtained is considered a minimum although probably close to the time of crystallization.

(0.5)
32.7 Return to Kalama River Road and re-enter Interstate 5 heading north.

(0.1)
32.8 Major road cut to left of Hwy. I-5 exposes numerous lava flows, volcaniclastic deposits, and dikes of the Goble Volcanics.

(0.8)
33.6 The cliffs on the right of I-5 here and for the next two miles are Goble Volcanics.

(1.1)
34.7 Leave Interstate 5 at Corrolis-Longview exit.

(0.3)
35.0 Stop sign: Longview to the left--Kelso to the right. Turn right toward the bluff and then bear north on the road toward Kelso Drive paralleling I-5. Park on the large pull-off at the north end of the bluff outcrops.

(0.2)
35.2 STOP 2: GOBLE VOLCANICS. A variety of rock types are exposed in this outcrop. They are mostly in fault contact with each other and represent the predominantly volcanic facies of the Goble Volcanics and predominantly sedimentary marine to nonmarine facies of the late Eocene Cowlitz Formation. Goble Volcanics rock types include pillow, columnar or hackly jointed, massive or vesicular basalt flows and dikes. Sandstone and carbonaceous shale represent the Cowlitz Formation.

At the top of the bedrock outcrop in this road cut is a remnant of the Troutdale Formation. The conglomerates and sandstones of the Pliocene Troutdale Formation are flood plain deposits of the Columbia River (Livingston, 1966).

Retrace route to Interstate 5 entrance heading north.

(0.2)
35.4 Enter I-5 heading north.

(0.2)
35.6 On the right are exposures of volcaniclastic rock of the Goble Volcanics, overlying a light-tan friable sandstone of the Cowlitz Formation. The contact between the Cowlitz and the Goble is typified by an interfingering relation where the sandstone beds of the Cowlitz gradually decrease in number upsection and give way to volcanic rocks of the Goble.

(0.5)
36.1 In the road cut on the right are tuffaceous basaltic sandstones underlain by light-tan sandstones of the Cowlitz Formation. From here northward to the city of Castle Rock (about 9 miles) the road cuts are primarily in Cowlitz Formation sandstone. The sandstones are generally deeply weathered and friable.

The highway runs along the flood plain of the Columbia, Coweman, and Cowlitz Rivers for the next several miles. Extensive levee systems have been constructed to prevent flooding in the area.

(1.3)
37.4 Coweman River.
(8.2)
45.6 Community of Castle Rock.
(1.4)
47.0 Major road cut through Goble Volcanics.
(0.7)
47.7 Toutle River.
(1.5)
49.2 Goble Volcanics on left of Hwy. I-5.
(1.0)
50.2 Highway Rest Stop.
(2.2)
52.4 Cowlitz River.
(0.2)
52.6 Vader-Ryderwood Jct. - LEAVE I-5 and follow signs toward Washington Hwy 506, turning right and driving back south under the I-5 Cowlitz River Bridge.
(0.7)
53.3 Stop sign at entrance to Washington Hwy. 506. Turn left toward Vader.
(0.6)
53.9 Hwy. 506 traverses Cowlitz River flood plain terrace.
(1.0)
54.9 STOP 3: COWLITZ FORMATION. Outcrops along the high road cuts on the right reveal sandstone channels cutting into the siltstones of the Cowlitz Formation (figs. 5-7). Abundant siltstone rip-ups occur in some channels. Note that moss grows on the permeable sandstone beds.

Continue west on Hwy. 506.
(0.2)
55.1 Lacamas Creek.
(0.7)
55.8 STOP 4: COWLITZ FORMATION. Pull-off to the left onto shoulder. A farm gate just east of the turn-out provides access via a farm road to Cowlitz Formation outcrops along the "Big Bend" of the Cowlitz River (fig. 5). The outcrops are 1/4 mile down this road at the river's edge. This is private land and permission for access should be obtained for large groups. The farm road makes a sharp right turn at the river's edge. Outcrops of the Cowlitz Formation are upstream along the river below this turn.

These outcrops are the type locality of the Cowlitz Formation molluscan fauna (figs. 5, 8, and 9). Abundant pelecypods, gastropods, and foraminifera are found in the claystones and calcareous siltstones (figs. 10-13). This stratigraphic interval is in the upper Cowlitz Formation and is late Eocene in age. Additional strata of the Cowlitz Formation are accessible along Olequa Creek (fig. 5). The fossil locality is at river level and is best visited during late summer, low river flow. The river bottom is nearly flat and shallow at the locality, but swift currents occur during high river level. A discussion of the molluscan and foraminiferal paleoecology of this locality appears earlier in this report with the description of the Olequa Creek section.

Return to vehicles at the farm gate. Retrace route eastward to Interstate 5.
(2.5)
58.3 Entrance to I-5. Bear left continuing north on Washington Hwy. 506 parallel to I-5.
(1.1)
59.4 Outcrops across I-5 to the east expose Quaternary terrace gravels of Cowlitz River flood plain.
(0.6)
60.1 Intersection of Hwy. 506 and I-5. Turn left onto I-5 heading north toward Centralia and Olympia.
(4.0)

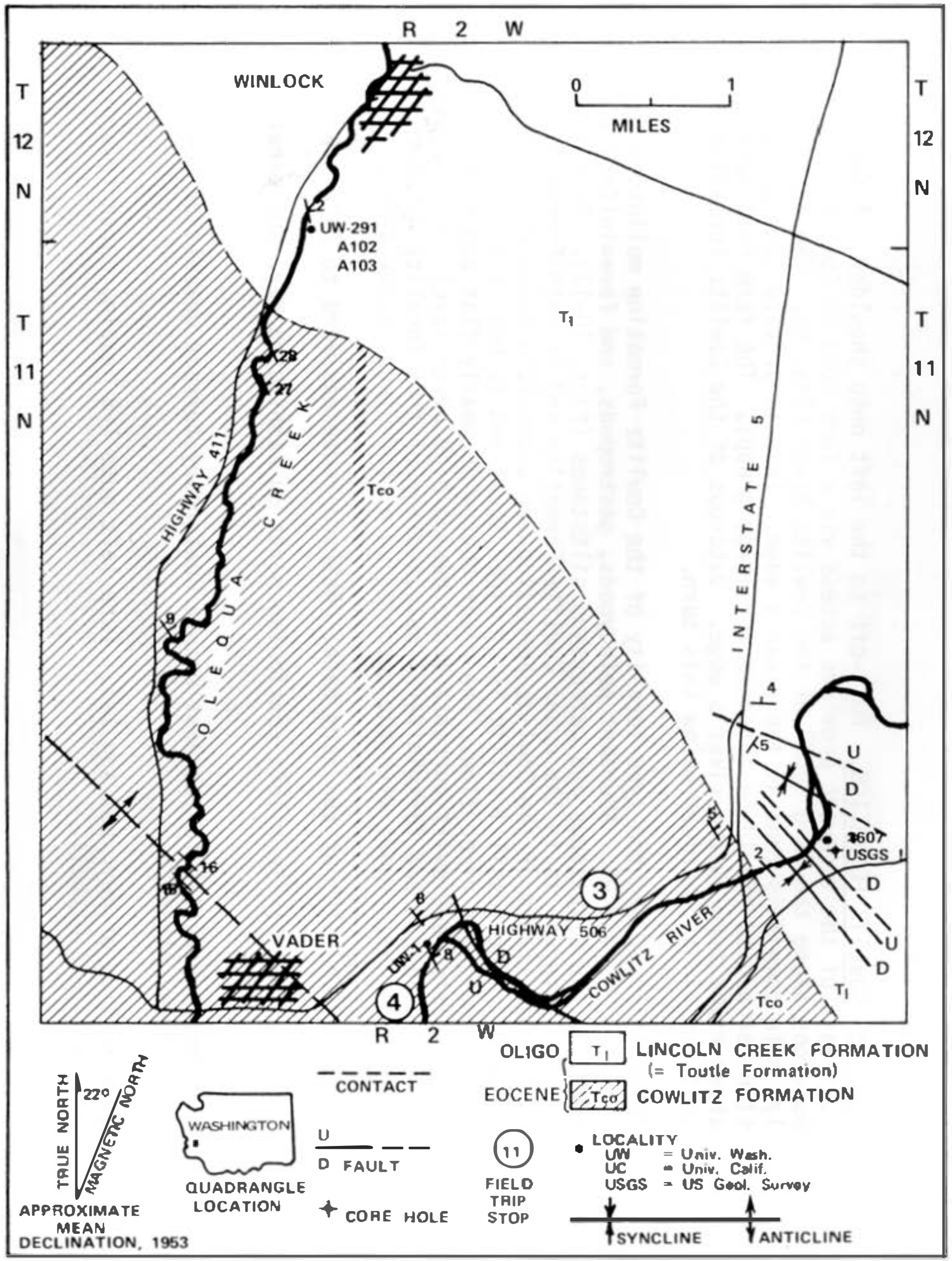

Figure 6.
Cowlitz Formation:
Stop 3.
Light-colored tuffaceous siltstones are cut by a channel. The channel is filled with darker (wet) sandstones and shale rip-ups (see also fig. 7).

Figure 5. Geology of Vader-Teledo area [after Henricksen (1956) and Roberts (1958): all Quaternary removed].

Figure 7. Cowlitz Formation: Stop 3.
Close-up of shale rip-ups in the channel of fig. 6.

Figure 8. Big Bend of the Cowlitz River: Stop 4.
Upper Eocene siltstones at this stop are the type locality for the Cowlitz Formation faunas.

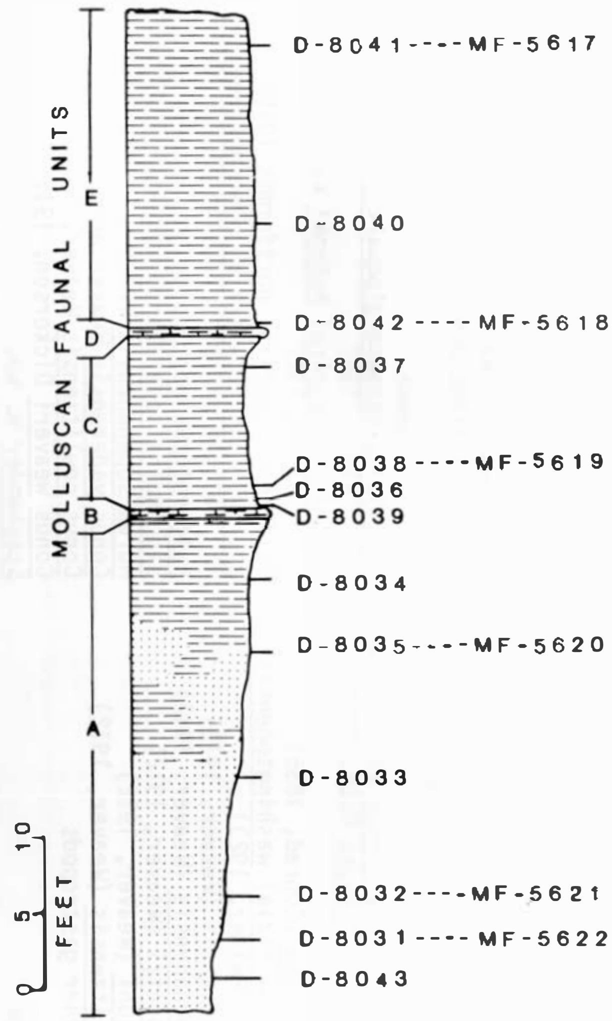

Figure 9. Measured stratigraphic column of the Cowlitz Formation locality at the Big Bend of the Cowlitz River.

Biofacies Interval A; lower sand; UCMP localities D-8031 through D-8035 and D-8043.

Gastropoda

Turritella uvasana olequahensis Weaver and Palmer, 1922
Turritella vaderensis Weaver and Palmer, 1922
Polinices (Euspira) hotsoni Weaver and Palmer, 1922
Polinices (Euspira) nuciformis (Gabb, 1864)
Neverita (Neverita) globosa Gabb, 1869
Crepidula n. sp.
Calyptraea diegoana (Conrad, 1855)
Ectinochilus (Cowlitzia) washingtonensis (Clark and Palmer, 1923)
Ficopsis cowlitzensis (Weaver, 1912)
Siphonalia sopenahensis (Weaver, 1912)
Molopophorus bretzi (Weaver, 1912)
Exilia dickersoni (Weaver, 1912)
Turricula cowlitzensis (Weaver, 1912)
and 27 other gastropods

Pelecypoda

Glycymeris sagittata (Gabb, 1864)
Venericardia hornii clarki Weaver and Palmer, 1922
Schedocardia brewerii (Gabb, 1864)
Pitar (Lamelliconcha) eocenica (Weaver and Palmer, 1922)
Tivelina vaderensis (Dickerson, 1915)
and 10 other bivalves

Scaphopoda

Dentalium stramineum Gabb, 1864
Cadulus gabbi Sharp and Pilsbry, 1898
and fragments of crab, barnacle, shark's teeth, and teleost otoliths

Biofacies Interval E; upper silt; UCMP localities D-8040 through D-8042.

Gastropoda

Turritella uvasana olequahensis Weaver and Palmer, 1922
Polinices (Euspira) hotsoni Weaver and Palmer, 1922
Polinices (Euspira) nuciformis (Gabb, 1864)
Ectinochilus (Cowlitzia) washingtonensis (Clark and Pilsbry, 1923)
Fulgurofusus washingtoniana (Weaver, 1912)
Siphonalia sopenahensis (Weaver, 1912)
Murex sopenahensis Weaver, 1912
Conus vaderensis Weaver and Palmer, 1922
Conus cowlitzensis Weaver, 1912
Conus weaveri Dickerson, 1915
Scaphander n. sp.
and 8 other gastropods

Pelecypoda

Nuculaniidae species

Scaphopoda

Cadulus gabbi Sharp and Pilsbry, 1898
and 1 other species

Figure 10. Species list of fossil mollusks characteristic of each biofacies unit of the Cowlitz Formation locality at the Big Bend of the Cowlitz River.

Figure 11. Late Eocene mollusks from the Cowlitz Formation locality at the Big Bend of the Cowlitz River.

1. Venericardia hornii clarki Weaver and Palmer. UCMP 14696, loc. D-8031. Length 12.4 mm.
2. Glycymeris sagittata (Gabb). UCMP 14694, loc. D-8032. Length 9.4 mm.
3. Neverita (Neverita) globosa Gabb. UCMP 14701, loc. D-8043. Length 8.7 mm.
4. Polinices (Euspira) hotsoni Weaver and Palmer. UCMP 14699, loc. D-8044. Length 9.7 mm.
5. Polinices (Euspira) nuciformis (Gabb). UCMP 14700, loc. D-8040. Length 14.8 mm.
6. Tivelina vaderensis (Dickerson). UCMP 14695, loc. D-8032. Length 11.8 mm.
7. Molopophorus bretzi (Weaver). UCMP 14702, loc. D-8031. Length 10.5 mm.
8. Conus vaderensis Weaver and Palmer. UCMP 14706, loc. D-8041. Length 14.3 mm.
9. Fulgurofusus washingtoniana (Weaver). UCMP 14705, loc. D-8040. Length 23.5 mm.
10. Ectinochilus (Cowlitzia) washingtonensis Clark and Pilsbry. UCMP 14704, loc. D-8032. Length 21.2 mm.
11. Exilia dickersoni (Weaver). UCMP 14707, loc. D-8043. Length 34.2 mm.
12. Turritella vaderensis Weaver and Palmer. UCMP 14698, loc. D-8032. Length 26.7 mm.
13. Turritella uvasana olequahensis Weaver and Palmer. UCMP 14697, loc. D-8032. Length 30.0 mm.
14. Ficopsis cowlitzensis (Weaver). UCMP 14703, loc. D-8044. Length 42.9 mm.
15. Siphonalia sopenahensis (Weaver). UCMP 14708, loc. D-8038. Length 24.0 mm.
16. Aturia sp. UCMP 16065, loc. D-8046. Height 122.7 mm (incomplete), depth 52.2 mm.

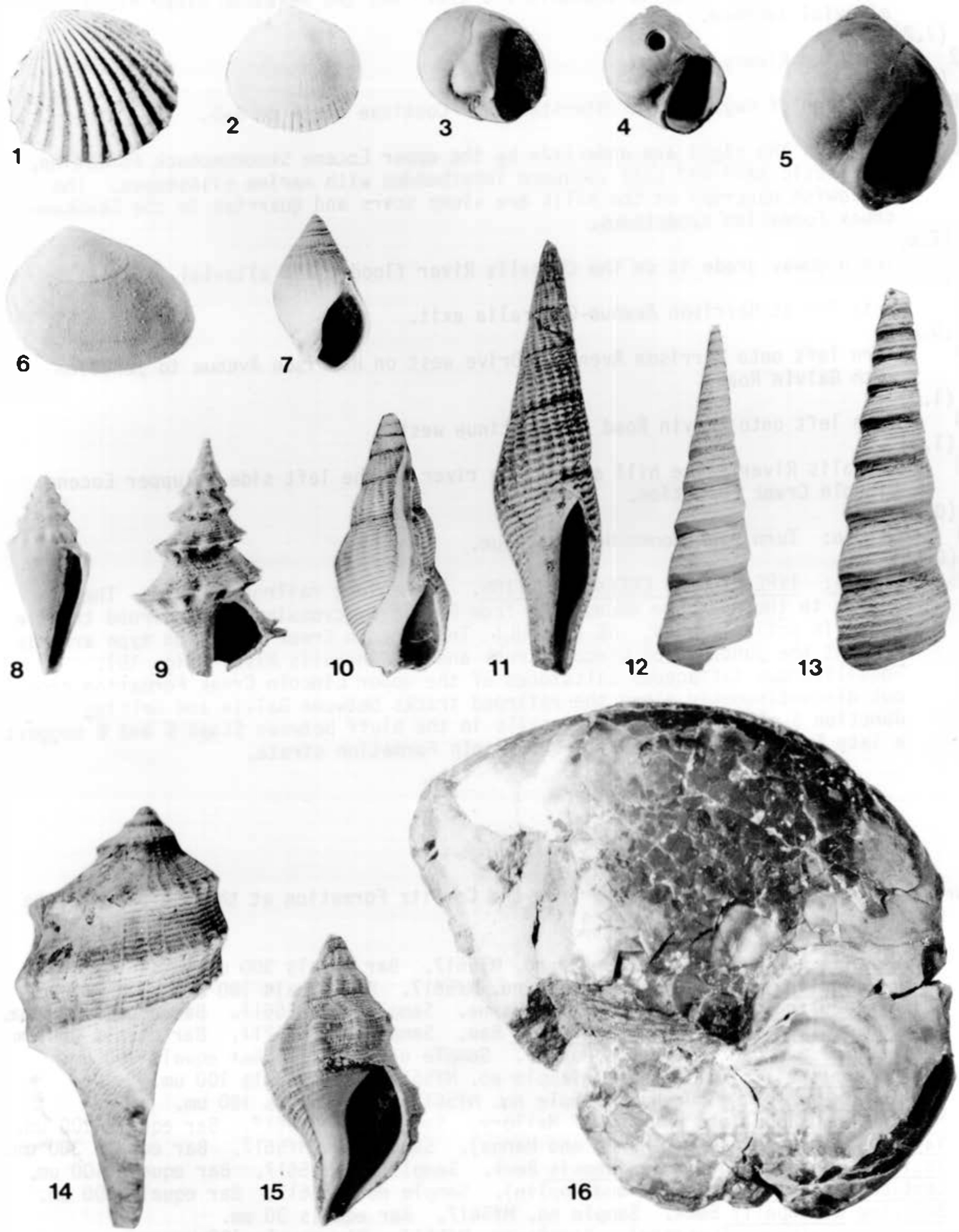

Figure 11. Late Eocene mollusks from the Cowlitz Formation locality at the Big Bend of the Cowlitz River.

64.0 From this area north to Chehalis I-5 traverses the Newaukum River flood plain alluvial terrace.

(7.2)

71.2 Newaukum River.

(5.6)

76.8 Junction of Hwy. 6 with Interstate 5. Continue north on I-5.

(1.2)

78.0 Hills to the right are underlain by the upper Eocene Skookumchuck Formation, an arkosic sand and coal sequence interbedded with marine siltstones. The yellowish outcrops on the hills are slump scars and quarries in the Skookumchuck Formation sandstones.

(2.0)

80.0 The highway grade is on the Chehalis River flood plain alluvial terrace.

(2.7)

82.7 Exit I-5 at Harrison Avenue-Centralia exit.

(0.2)

82.9 Turn left onto Harrison Avenue. Drive west on Harrison Avenue to junction with Galvin Road.

(1.0)

83.9 Turn left onto Galvin Road and continue west.

(1.7)

85.6 Chehalis River: The hill across the river on the left side is upper Eocene Lincoln Creek Formation.

(0.4)

86.0 Galvin: Turn right onto Union Avenue.

(0.05)

86.05 STOP 5: TYPE LINCOLN CREEK FORMATION. Park along railroad tracks. The bluffs to the west are accessible from Galvin by crossing the railroad trestle which is actively used. BE CAREFUL! The Lincoln Creek Formation type area is here at the juncture of Lincoln Creek and the Chehalis River (fig. 15). Fossiliferous tuffaceous siltstones of the upper Lincoln Creek Formation crop out discontinuously along the railroad tracks between Galvin and Helsing Junction 5 miles northwest. Fossils in the bluff between Stops 5 and 6 suggest a late Eocene age assignment for Lincoln Formation strata.

Figure 12. Late Eocene Foraminifera from the Cowlitz Formation at the Big Bend of the Cowlitz River.

1. *Karreriella contorta* Beck. Sample no. MF5617. Bar equals 300 um.
2. *Quinqueloculina minuta* Beck. Sample no. Mf5617. Bar equals 100 um.
3. *Quinqueloculina goodspeedi* Hanna and Hanna. Sample no. MF5617. Bar equals 100 um.
4. *Quinqueloculina imperialis porterensis* Rau. Sample no. Mf5717. Bar equals 300 um.
5. *Triloculina globosa* (Hanna and Hanna). Sample no. Mf5617. Bar equals 100 um.
6. *Lagena semistriata* Williamson. Sample no. Mf5617. Bar equals 100 um.
7. *Lenticulina welchi* (Church). Sample no. Mf5617. Bar equals 100 um.
8. *Marginulina subbullata* Hantken of Mallory. Sample no. Mf5617. Bar equals 100 um.
9. *Vaginulinopsis saundersi* (Hanna and Hanna). Sample no. Mf5617. Bar equals 300 um.
10. *Vaginulinopsis saundersi lewisensis* Beck. Sample no. Mf5617. Bar equals 100 um.
11. *Lenticulina texana* (Cushman and Applin). Sample no. Mf5617. Bar equals 100 um.
12. *Bolivina kleinpelli* Beck. Sample no. Mf5617. Bar equals 30 um.
13. *Eponides mexicanus* (Cushman). Sample no. Mf5617. Bar equals 100 um.
14. *Cibicides natlandi* Beck. Sample no. Mf5617. Bar equals 100 um.
15. *Caucasina schencki* (Beck). Sample no. Mf5617. Bar equals 30 um.
16. *Globocassidulina globosa* (Hantken). Sample no. Mf5617. Bar equals 100 um.
17. *Nonion halkyardi* Cushman. Sample no. Mf5617. Bar equals 100 um.
18. *Boldia hodgei* (Cushman and Schenck). Sample no. Mf5617. Bar equals 100 um.
19. *Boldia hodgei* (Cushman and Schenck). Sample no. Mf5617. Bar equals 100 um.

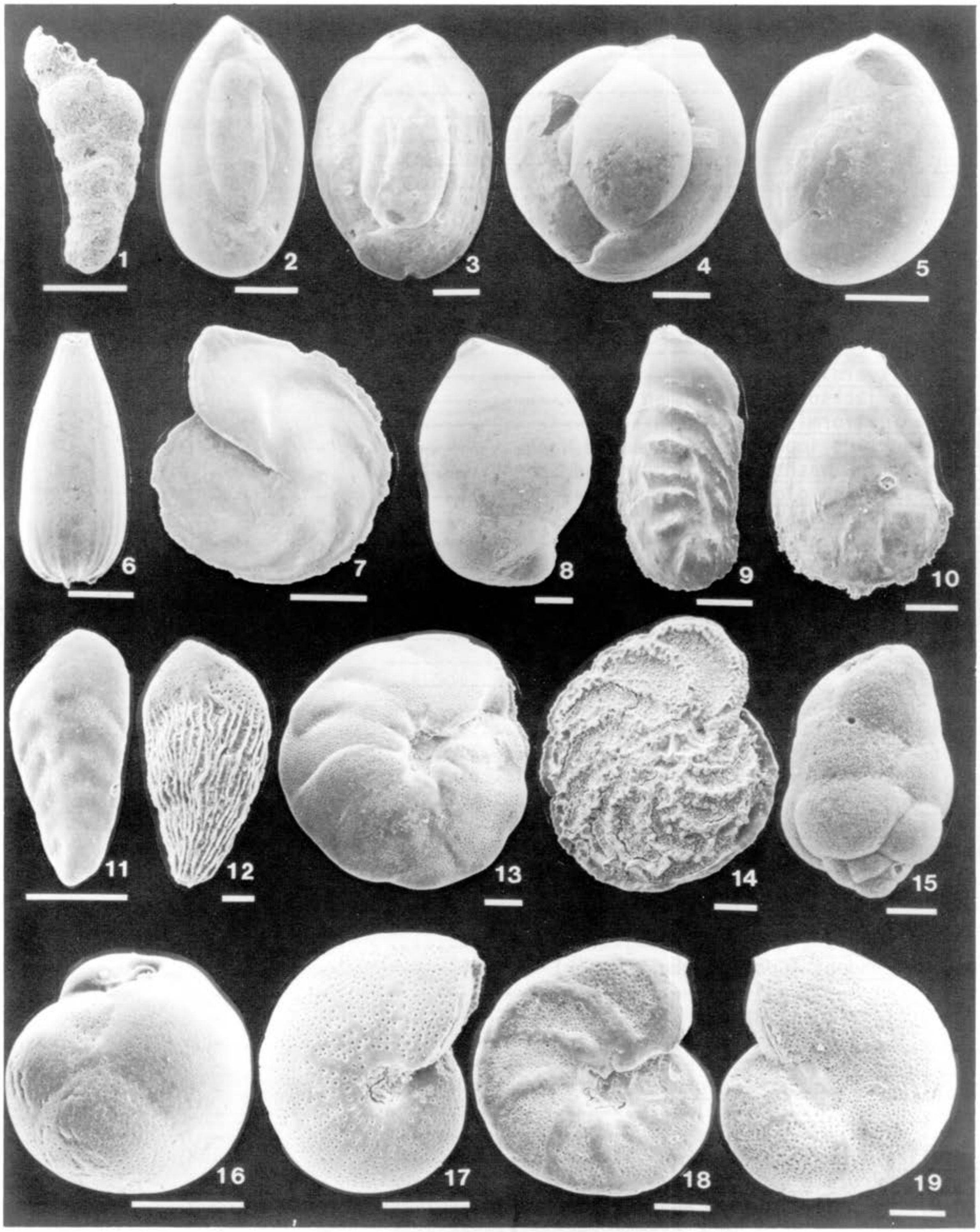

Figure 12 Late Eocene Foraminifera from the Cowlitz Formation at the Big Bend of the Cowlitz River.

SPECIES / LOCATION	Mf5620	Mf5619	Mf5618	Mf5617
Cibicides natlandi Beck	25	25	42	47
Globobulimina pacifica Beck	50	2	-	X
Lenticulina inornata (d'Orbigny)	25	11	24	X
Biloculinella cowlitzensis Beck	-	X	-	-
Bolivina hunneri Howe	-	X	1	8
Bolivina kleinpelli Beck	-	1	-	4
Cibicides baileyi Beck	-	37	X	1
Cyclammina pacifica Beck	-	1	-	-
Dentalina communis (d'Orbigny)	-	2	2	-
Eponides mexicanus (Cushman)	-	5	12	2
Gyroidina soldanii d'Orbigny	-	1	-	-
Marginulina adunca (Costa)	-	X	-	-
Nonion halkyardi Cushman	-	7	-	3
Nonionella jacksonensis Cushman	-	1	-	-
Pyrulina fusiformis (Roemer)	-	2	-	-
Quinqueloculina imperialis Hanna and Hanna	-	1	9	2
Ceratobulimina washburnei Cushman and Schenck	-	-	1	-
Globocassidulina globosa (Hantken)	-	–	X	4
Globulina landesi (Hanna and Hanna)	-	-	X	X
Karreriella contorta Beck	-	-	1	4
Lenticulina crassa (d'Orbigny)	-	-	X	X
Lenticulina texana (Cushman and Applin)	-	-	1	X
Quinqueloculina goodspeedi Hanna and Hanna	-	-	2	X
Quinqueloculina imperialis porterensis Rau	-	-	2	X
Trifarina hannai Beck	-	-	X	-
Vaginulinopsis saundersi (Hanna and Hanna)	-	-	2	3
Boldia hodgei (Cushman and Schenck)	-	-	-	X
Caucasina schencki (Beck)	-	-	-	3
Cibicides lobatulus (Walker and Jacob)	-	-	-	X
Cibicides mcmastersi Beck	-	-	-	4
Dentalina dusenburyi Beck	-	-	-	X
Dentalina jacksonensis Cushman and Applin	-	-	-	X
Dyocibicides perforata Cushman and Valentine	-	-	-	X
Epistominella parva (Cushman and Laiming)	-	-	-	6
Gaudryina alazaensis Cushman	-	-	-	X
Guttulina irregularis (d'Orbigny)	-	-	-	X
Guttulina problema d'Orbigny	-	-	-	X
Gyroidina condoni (Cushman and Schenck)	-	-	-	1
Lagena becki Sullivan	-	-	–	X
Lagena costata (Williamson)	-	-	-	X
Lagena semistriata Williamson	-	-	-	X
Lagena vulgaris Williamson	-	-	-	X
Lenticulina cf. L. pseudorotulata (Asano)	-	-	-	X
Lenticulina welchi (Church)	-	-	-	X
Marginulina exima Neugeboren	-	-	-	X
Marginulina subbullata Hantken	-	-	-	X
Nodosaria pyrula d'Orbigny	-	-	-	1
Nonionellina applini (Howe and Wallace)	-	-	-	X
Quinqueloculina minuta Beck	-	-	-	X
Triloculina globosa (Hanna and Hanna)	-	-	-	X
Vaginulinopsis saundersi lewisensis Beck	-	-	-	X
Planktic Foraminifers	-	-	-	2
Total number of specimens	4	299	339	320

Figure 13. Cowlitz Formation foraminiferal faunal list. Numbers represent percent of total foraminiferal fauna and the X represents rare species not found in first 300 specimens. Samples Mf5621 and Mf5622 are barren of foraminifers.

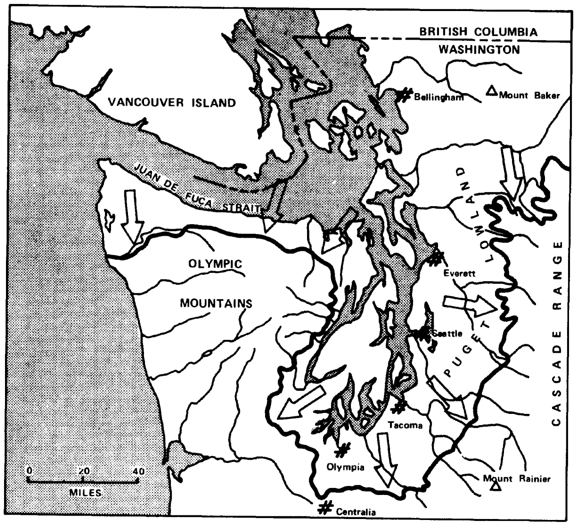

Figure 14. Maximum southern extent of Puget Lobe during the last glacial period is shown by the heavy line (15,000-13,500 year B.P.). Arrows show direction of ice flow. (Modified from Easterbrook, 1969.)

(0.05)
86.1 Return to Galvin and turn left, back onto Galvin Road toward Centralia.
(0.5)
86.6 On a clear day Mt. Rainier (14,408 ft) and Mt. St. Helens (9,677 ft), south of Mt. Rainier, can be seen straight ahead.
(1.6)
88.2 Back at the intersection of Galvin Road and Harrison Avenue; turn left toward Rochester. Harrison Avenue is Old Hwy. 99.
(2.8)
91.0 Turn left off Old 99 onto Prather Road.
(0.8)
91.8 The bluffs off to the left, across the Chehalis River, are part of the Galvin Section. These bluffs are on the northeast flank of the Centralia Syncline.
(0.6)
92.4 Chehalis River.
(0.1)
92.5 STOP 6: LINCOLN CREEK FORMATION. Park along Prather Road near the railroad tracks. Outcrops of late Eocene Lincoln Creek Formation are accessible about 0.3 mile east along the railroad tracks (fig. 15). The fossiliferous siltstones are similar to those of STOP 5. Calcareous concretionary beds are common.

Return to vehicles and continue west on Prather Road.
(1.0)
93.5 Weathered outcrops on the right are Lincoln Creek Formation siltstones.
(0.9)
94.4 The upland surface of these hills is underlain by Pleistocene Logan Hill Formation sands and gravels. The Logan Hill Formation unconformably overlies Tertiary rocks of the Lincoln Creek Formation.
(1.2)
95.6 Junction of Prather Road and Michigan Hill Road; turn right.
(1.1)
96.7 The Michigan Hill Road drops down an alluvial floored stream valley.
(0.7)
97.4 Road cut on the right exposes weathered Lincoln Creek Formation rocks.
(0.8)
98.2 STOP 7: LINCOLN CREEK FORMATION. Helsing R.R. Junction (fig. 15). Junction of Michigan Hill Road and Ludeen Road. Park beside the road and walk east along the road and railroad tracks for 0.5 mile.

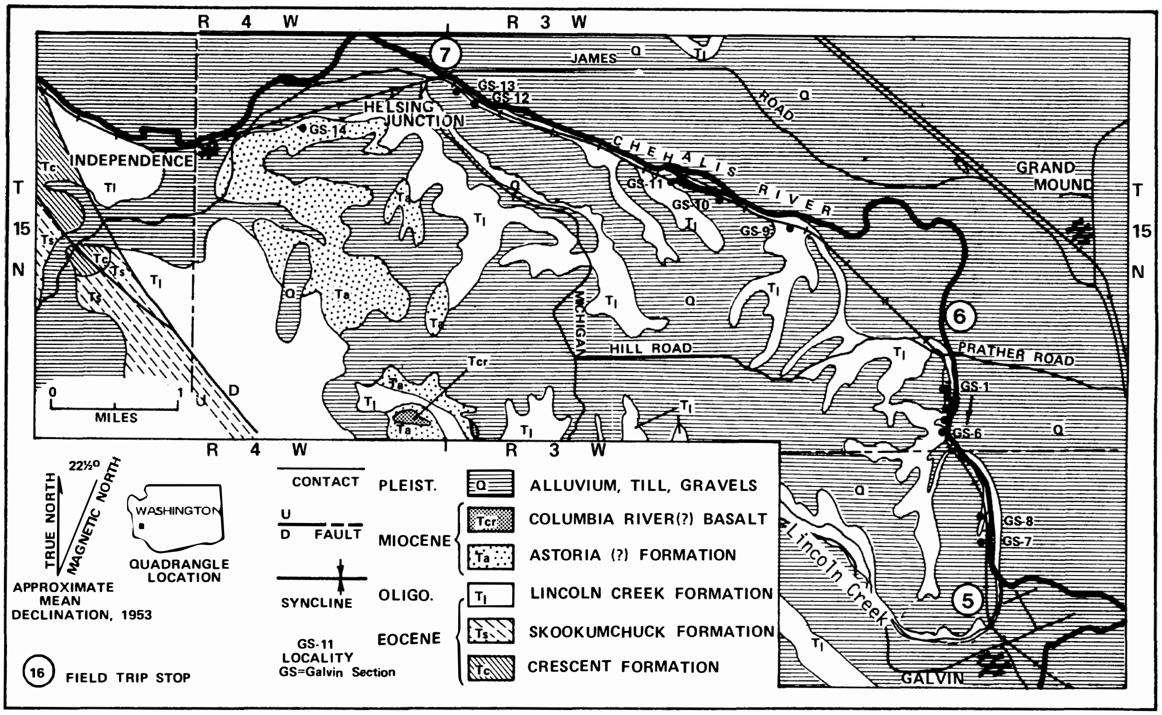

Figure 15. Geology of the Galvin-Helsing Junction area (after Snavely, Brown, Roberts, and Rau, 1958).

Outcrops of Oligocene upper Lincoln Creek Formation siltstones occur in the high banks off to the right of the railroad tracks. These outcrops are the stratigraphically highest Lincoln Creek Formation strata examined on this field trip. About one mile further west along the railroad tracks the Lincoln Creek Formation is overlain with apparent unconformity by the Miocene Astoria(?) Formation. Outcrops along that traverse are restricted to landslide scarps and are poorly exposed.

Return to vehicles.

(0.1)

98.3 Proceed under the railroad trestle to junction of Michigan Hill and Independence Roads. (Trestle has low clearance--buses and trucks should proceed with a visual check.) Turn right and bear left cross the Chehalis River following James Road.

(1.8)

100.1 Bear right at Triangle Store junction staying on James Road.

(0.4)

100.5 Sharp left turn off James Road onto Albany Road. This area is called Ground Mound Prairie and is underlain by Vashon Drift. Uncultivated areas exhibit Mima Mounds.

(0.3)

100.8 The hill off to the right is cored by Lincoln Creek Formation and mantled by Logan Hill Formation.

(0.7)

101.5 Junction of Albany Road and Hwy. 12 in Rochester. Turn left toward Oakville-Elma.

(1.0)

102.5 The forested hills to the right are the Black Hills. They are underlain by Crescent Formation volcanics.

(3.4)

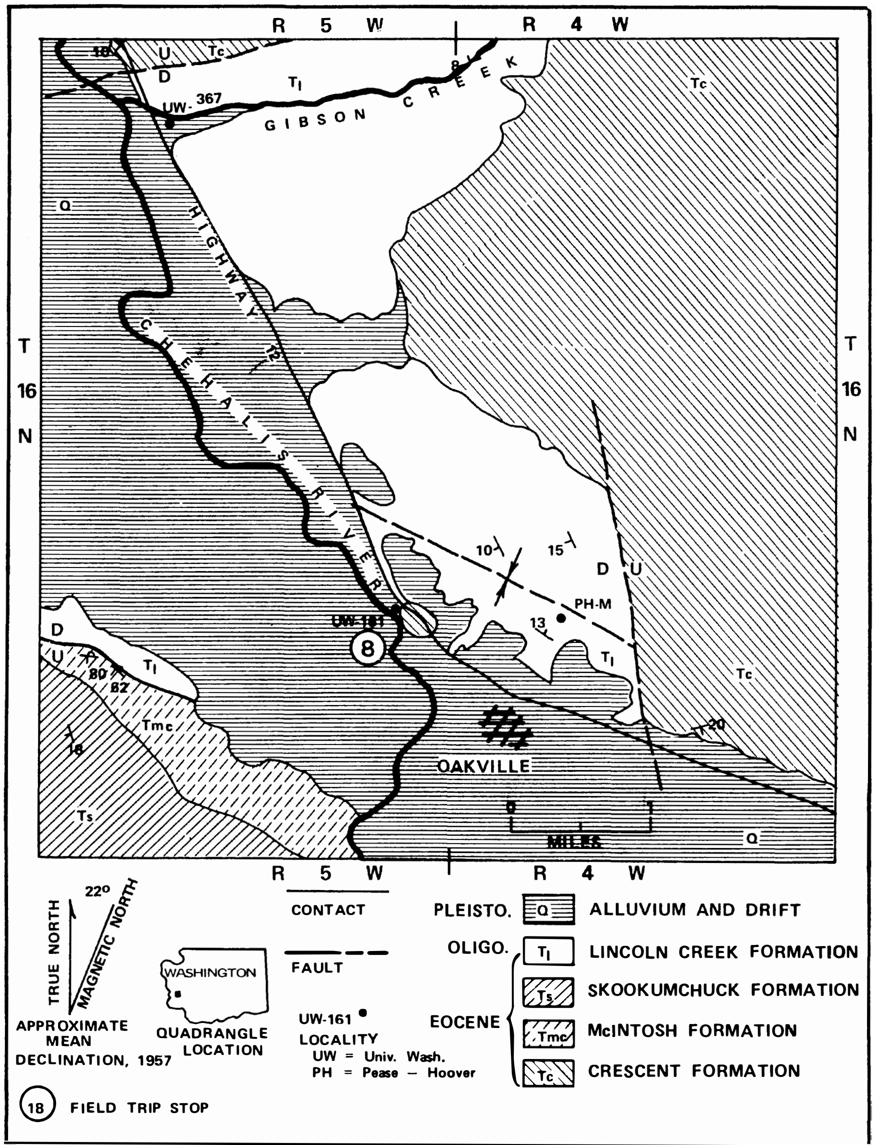

Figure 16. Geology of Oakville section (after Pease and Hoover, 1957).

105.9 Black River.
(2.1)
108.0 Oakville; continue northwest on Hwy. 12.
(1.3)
109.3 STOP 8: CRESCENT FORMATION. Pull off to left on road shoulder. The small side road provides access to a quarry in Crescent Formation basalts (fig. 16). Recent quarry activity (1978) has exposed relatively fresh columnar basalts. Fossil mollusks of late Eocene age have been found in conglomeratic sandstones of the Lincoln Creek Formation overlying the basalts but quarrying has destroyed the locality.

(0.1)
109.4 Continuing north on Hwy. 12, the road passes between outcrops of Crescent basalts, stratigraphically equivalent to those in the quarry at STOP 8. These basalts are the basal unit of the Oakville Section (fig. 16).

(0.2)
109.6 Hwy. 12 is underlain by Pleistocene Vashon Drift which forms the upper terrace surface along the margins of the Chehalis River Valley. The river valley is floored with Recent alluvium.

(4.9)
114.5 STOP 9: CRESCENT FORMATION. Pull off to the right along side road. Base of Porter Section (fig. 17). The basalt outcrop along Hwy. 12 is mapped as Crescent Formation. The basalts are in fault contact with Lincoln Creek Formation siltstones to the south. Fossiliferous late Eocene sandstones of the Lincoln Creek Formation overlie the basalts in the quarry on the northeast side of this outcrop (PB-1 *Acmaea-Ostrea* Mollusk Zonule of the paleoecologic discussion). The sandstones are basaltic and deeply weathered. Unpublished K/Ar whole rock data on this outcrop yield an age of $38.9 \pm 1.2 \times 10^6$ years (Mobil Oil Corporation-Field Research Laboratory Sample #4334: Armentrout, 1979, unpub. data). The basalt is altered with minor amounts of sericite and chlorite present. Although the sample was treated for removal of these components, the date should be considered a minimum for the time of crystallization.

(0.3)
114.8 Road cuts expose deeply weathered tuffaceous siltstones of the Lincoln Creek Formation.

(0.3)
115.1 Outcrops on the right are Lincoln Creek Formation siltstones: note distinct tuff bed.

(0.4)
115.5 STOP 10: LINCOLN CREEK FORMATION. Park on highway shoulder near Lytle Logging Road. Outcrops along the next mile toward Porter are the type "Porter Shales", now included in the Lincoln Creek Formation (fig. 18). The tuffaceous siltstones are of late Eocene age. Calcareous concretionary beds serve as marker horizons for fault control and fossil localities (fig. 19). The "Porter Shales" are stratigraphically equivalent to the lower Galvin section. The lower part of the traverse from Lytle Logging Road to Porter is along a very fossiliferous shale sequence susceptible to slumping (figs. 20-22). As the rocks become increasingly silty and tuffaceous the bluffs become more stable. The Porter Bluff traverse is posted "No Trespassing" by the Washington State Highway Department. Some of the most fossiliferous shales near the Lytle Logging Road are not posted.

(0.1)
115.6 Fossiliferous shales of Lincoln Creek Formation.

(0.3)
115.9 Fossiliferous siltstones of "Porter Shale" Lincoln Creek Formation (figs. 17-19).

(0.7)
116.6 Porter Creek.

(0.1)
116.7 Porter: junction of Hwy. 12 and Capitol Forest Road.

(0.1)
116.8 Lower units of upper "Porter Shale" Lincoln Creek Formation.

(0.2)
117.0 STOP 11: LINCOLN CREEK FORMATION. Park on shoulder of highway. From this point the upper "Porter Shale" Lincoln Creek Formation siltstones are accessible. Small faults occur at the south end of the outcrops north of the parking area (figs. 17 and 19). Fossils indicate a late Eocene age for these strata (upper PB-III: *Turritella-Priscofusus* Mollusk Zonule of paleoecologic discussion).

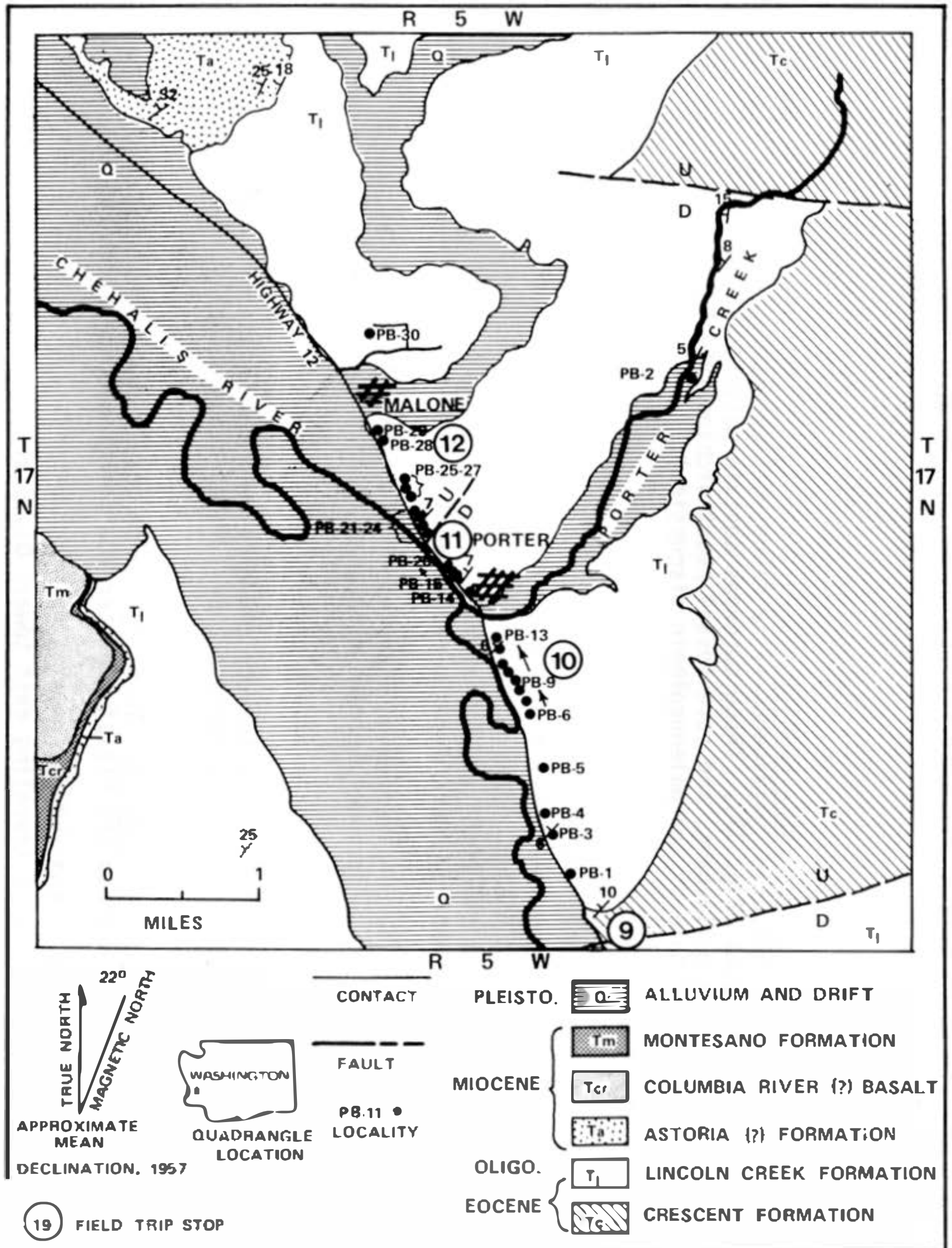

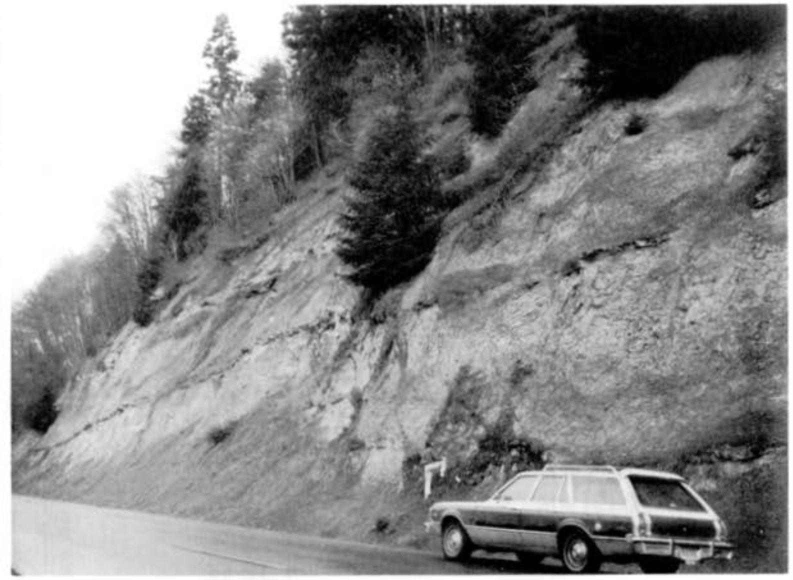

Figure 18.
Porter Bluffs:
Stop 10.
These siltstone bluffs are the type section of the "Porter Shales," of the Lincoln Creek Formation.

Figure 17. Geology of Porter Bluffs section (after Pease and Hoover, 1957).

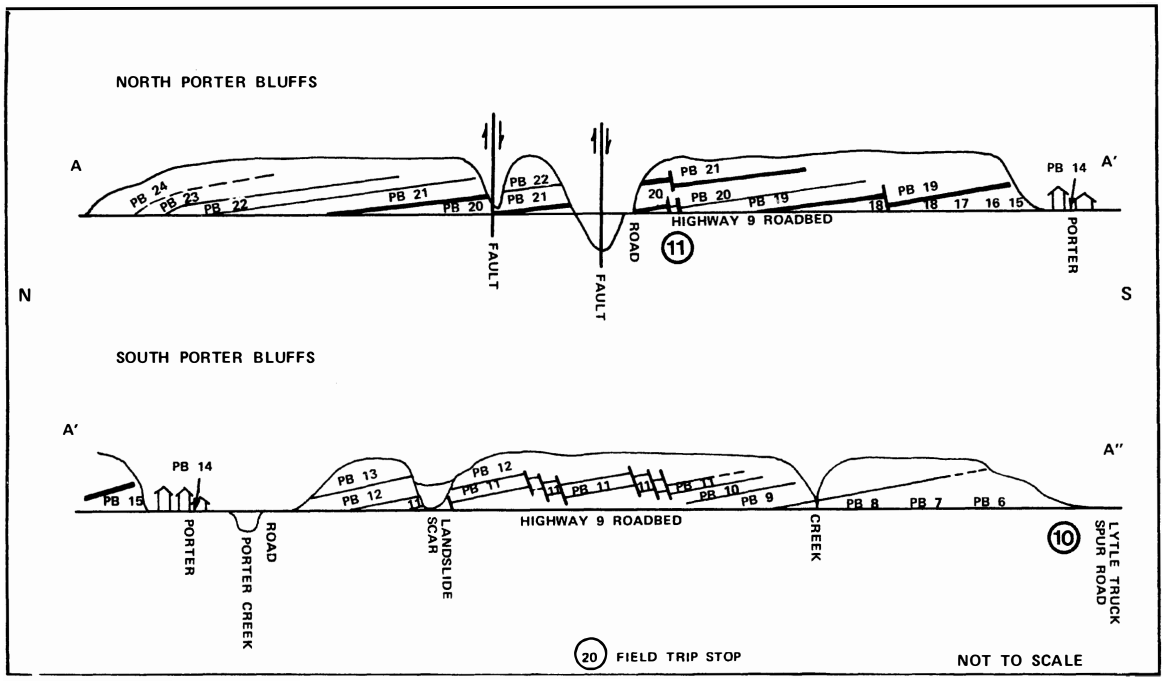

Figure 19. Porter Bluffs: Stops 10 and 11. Sketch-section for Porter Bluffs fossil localities. Localities are separated by calcareous concretionary beds offset by faults.

(0.8)

117.8 STOP 12: LINCOLN CREEK FORMATION. Park on right shoulder by private road. Upper Lincoln Creek tuffaceous silty sandstones crop out 0.1 mile north of the parking area (fig. 17). These outcrops contain molds and casts of early Oligocene molluscans, and rare fossil heart urchins (PB-IV: Solena-Priscofusus Mollusk Zonule of the paleoecologic discussion).

(0.5)

118.3 Malone.

(0.3)

118.6 Road cuts along the highway are deeply weathered upper Lincoln Creek Formation shales. Fresh outcrops yield a late Oligocene fossil assemblage (fig. 17; PB-V: Solemya-Thyasira Mollusk Zonule of the paleoecologic discussion).

(1.9)

120.5 The hills to the right are underlain by lower Miocene Astoria(?) Formation marine sedimentary rocks unconformably overlying the Lincoln Creek Formation.

(0.1)

120.6 The roadbed is constructed on a terrace surface underlain by Pleistocene Vashon Drift. The lower terrace along the river is Holocene alluvium.

(1.1)

121.7 Road cuts along this area expose gravels of the Vashon Drift.

(0.6)

122.3 An outcrop of Pleistocene terrace gravel is exposed in the bluff behind the small shingle mill. This terrace gravel is stratigraphically above the Vashon Drift.

(0.1)

122.4 STOP 13: TERRACE GRAVELS. Turn right onto gravel road. This short deadend provides access to the Pleistocene terrace gravel outcrop at the shingle mill.

(0.2)

122.6 Return to Hwy. 507 and continue north. Junction of Hwy. 12 with Hwy. 8; turn right onto Hwy. 8 traveling east toward Olympia.

(0.7)
123.3 Excellent exposures of Quaternary terrace gravels crop out on the right side of the highway.
(1.9)
125.2 Highway Rest Stop.
(2.0)
127.2 Terrace gravels.
(2.5)
129.7 Junction of Hwys. 8 and 108 at McCleary-Shelton exit.
(1.3)
131.0 Hwy. 8 traverses the Black Hills between Elma and Olympia. These hills are cored by lower to middle Eocene Crescent Formation basalts which crop out along the highway from McCleary to Olympia.
(1.2)
132.2 STOP 14: CRESCENT FORMATION. Pillow basalts are exposed in the road cut on the left across the west bound lane of Hwy. 8 (fig. 23). Parking along this area is limited to the highway shoulder and is restricted to emergency parking only.
(0.2)
132.4 STOP 15: CRESCENT FORMATION. Basalt flows of the Crescent Formation are well exposed across Hwy. 8 to the left (fig. 25). Fractured flows show the typical pattern of collonade below and hacky entablature above. Again only emergency parking is allowed along the highway shoulder.

Unpublished K/Ar whole rock data on the main outcrop flow at this locality yield an age of $47.5 \pm 1.7 \times 10^6$ years (Mobil Oil Corporation-Field Research Laboratory Sample #4337: Armentrout, 1979, unpub. data). The rock is highly altered and the age should be considered a minimum for the time of crystallization.

Continue east toward Olympia.
(18.4)
150.8 Mt. Rainier is "occasionally" visible to the east.
(0.4)
151.2 The bay on the left is part of the southern terminus of Puget Sound.
(4.0)
155.2 Terrace deposits of Quaternary fluvial and glaciofluvial origin crop out in excavations to the left.
(1.7)
156.9 Off to the left is another branch of Puget Sound. The Washington State Capitol Building is on the terrace surface above this bay.
(0.1)
157.0 Junction of Hwy. 8 and I-5.

END OF FIELD TRIP.

NOTE: The *Aturia* sp. illustrated on Figure 11 is from an unknown locality within the Cowlitz Formation, D-8046. This genus has been reported from the Big Bend locality.

NUMBER OF SPECIMENS
X RARE (1)
0 FEW (2-4)
● COMMON (5-10)
■ ABUNDANT (11-20)
* DOMINANT (> 20)
? QUESTIONABLE

FORMATION	LINCOLN CREEK																													
ZONULE	I	II	PB III																								PB IV		PB V
ZONE	E. dalli		E. fax																								E. rex		
LOCALITY	PB-1	PB-2	PB-3	PB-4	PB-5	PB-6	PB-7	PB-8	PB-9	PB-10	PB-11	PB-12	PB-13	PB-14	PB-15	PB-16	PB-17	PB-18	PB-19	PB-20	PB-21	PB-22	PB-23	PB-24	PB-25	PB-26	PB-27	PB-28	PB-29	PB-30
GASTROPODA																														
Acmaea oakvillensis	-	X	-	-	-	-	-	-	-	-	-	-	-	-	-	-	-	-	-	-	-	-	-	-	-	-	-	-	-	-
Aforia campbelli	-	-	-	-	-	X	0	-	-	0	X	-	-	-	-	-	-	-	-	-	-	-	-	X	-	-	-	-	-	-
Aforia packardi	-	-	-	-	-	X	-	-	0	●	0	0	-	-	-	X	-	-	-	-	-	-	-	-	X	-	-	-	-	-
Bruclarkia columbianum	-	X	-	-	-	-	-	-	-	-	-	-	-	-	-	-	-	-	-	-	-	-	-	-	-	-	-	-	-	-
Exilia lincolnensis	-	-	-	-	-	■	●	-	■	■	■	●	●	-	X	X	0	0	-	0	X	-	■	●	-	-	-	-	-	-
Gyrineum jeffersonensis	-	0	-	-	-	-	-	-	-	-	-	-	-	-	-	-	-	-	-	-	-	-	-	-	-	-	-	-	-	-
Natica (Cryptonatica) weaveri	-	-	-	-	-	-	-	-	-	-	X	-	-	-	-	0	-	-	-	X	-	X	0	-	-	-	-	-	-	-
Olequahia lincolnensis	-	-	-	-	-	-	-	-	-	-	X	-	-	-	-	-	-	-	-	-	-	-	X	-	-	-	-	-		-
Perse lincolnensis	-	-	-	-	-	X	X	-	-	X	-	-	X	-	-	0	X	X	-	X	-	-	●	-	-	-	-	-	-	-
Polinices (Euspira) washingtonensis	-	-	-	-	-	-	-	-	0	0	-	0	0	-	X	-	0	X	-	0	0	0	■	-	-	-	-	X	-	-
Priscofusus chehalisensis	-	-	X	-	-	-	X	-	●	●	●	●	X	-	0	●	0	0	X	0	0	0	■	0	-	-	-	-	-	-
Priscofusus foxi	-	-	-	-	-	-	-	-	-	-	-	-	-	-	-	-	-	-	-	-	-	-	-	-	-	-	-	●	-	-
Scaphander washingtonensis	-	-	-	-	-	-	-	-	-	-	-	-	-	-	-	-	X	-	-	-	X	0	0	-	-	-	-	-	-	-
Siphonalia washingtonensis	-	-	-	-	-	-	-	-	-	-	-	-	-	-	-	-	-	-	-	-	-	-	X	-	-	-	-	-	-	-
Spirotropis dickersoni	-	-	-	-	-	-	X	-	-	-	-	-	X	-	-	-	-	-	-	-	-	-	-	-	-	-	-	-	-	-
Spirotropis kincaidi	-	-	-	-	-	-	-	-	-	X	0	X	-	-	X	-	-	-	-	-	-	-	0	-	-	-	-	-	X	-
Suavodrillia thurstonensis	-	-	-	-	-	-	-	-	-	-	-	-	-	-	-	0	-	-	-	-	-	X	-	-	-	-	-	-	-	-
Suavodrillia worchesteri	-	-	-	-	-	-	X	-	X	0	X	X	-	-	-	-	-	-	-	-	X	-	-	-	-	-	-	-	-	-
Turricula washingtonensis	-	-	-	-	-	X	■	-	■	■	*	■	0	-	-	X	0	X	-	0	X	-	●	X	-	-	-	-	-	-
Turritella porterensis	-	-	-	-	-	X	X	-	●	●	■	0	0	-	0	*	●	■	●	■	●	0	*	X	-	-	-	-	-	-
PELECYPODA																														
Barbatia (Acar) reinharti	-	0	-	-	-	-	-	-	-	-	-	-	-	-	-	-	-	-	-	-	-	-	-	-	-	-	-	-	-	-
Callista pillsburyensis	-	-	-	-	-	-	-	-	-	-	-	-	-	-	-	-	-	-	-	X	X	0	X	-	-	-	-	-	-	-
Crassatella (Crassatella) washingtoniana	-	-	-	-	-	-	-	-	-	-	-	-	-	-	-	-	-	-	-	X	-	-	●	-	-	-	-	-	-	-
Lima oregonensis	●	X	-	-	-	-	-	-	-	-	-	-	-	-	-	-	-	-	-	-	-	-	-	-	-	-	-	-	-	-
Lucinoma hannibali	-	-	-	-	-	-	-	-	-	-	-	-	-	-	X	●	X	-	X	0	-	-	X	-	-	-	-	0	-	?
Nemocardium (Keenaea) lorenzanum	-	-	-	-	X	-	-	-	X	-	-	0	-	-	X	0	X	-	-	-	X	-	●	-	-	-	-	-	-	-
Nuculana washingtonensis	-	-	-	-	-	-	-	-	X	-	-	-	-	-	X	0	X	X	-	-	-	-	●	-	-	-	-	X	-	-
Ostrea lincolnensis	*	-	-	-	-	-	-	-	-	-	-	-	-	-	-	-	-	-	-	-	-	-	-	-	-	-	-	-	-	-
Pitar (Pitar) dalli	-	-	-	-	-	-	-	-	-	-	-	-	-	-	0	0	-	-	0	-	-	X	0	-	-	-	-	-	-	-
Pododesmus (Pododesmus) newcombei	-	X	-	-	-	-	-	-	-	-	-	-	-	-	-	-	-	-	-	-	-	-	-	-	-	-	-	-	-	-
Solemya dalli	-	-	-	-	-	-	-	-	-	-	-	-	-	-	-	-	-	-	-	-	-	-	-	-	-	-	-	-	-	?
Solena lincolnensis	-	-	-	-	-	-	-	-	-	-	-	X	-	-	-	X	-	-	-	-	-	-	X	-	-	-	-	X	-	-
Thyrasira (Conchocele) bisecta	-	-	-	-	-	-	-	-	-	-	-	-	-	-	-	-	-	-	-	-	-	-	-	-	-	-	-	-	-	?
SCAPHOPODA																														
Dentalium porterensis	-	-	-	-	-	●	●	X	■	*	■	■	-	-	-	0	X	-	-	X	X	-	●	-	●	0	-	0	0	-

Figure 20. Species checklist of common molluscan fossils from the Porter Bluff section of the Lincoln Creek Formation.

Figure 21. Late Eocene mollusks from the Lincoln Creek Formation at Porter Bluffs.

1, 2. Scaphander washingtonensis Weaver. Syntype, CAS 475b, loc. UW 256. Height 12.9 mm, diameter 7.4 mm (incomplete).

3, 4. Olequahia lincolnensis (Weaver). Syntype, CAS 466A, loc. UW 256. Height 36.2 mm, diameter 25.0 mm.

5. Bruclarkia columbianum (Anderson and Martin). Holotype, CAS 155. Height 57.0 mm, diameter 37.5 mm.

6, 7. Exilia lincolnensis Weaver. Syntype, CAS 468a. Height 29.5 mm (incomplete), diameter 6.7 mm.

8, 9. Turricula washingtonensis (Weaver). Holotype, CAS 560, loc. UW 352. Height 25.7 mm (incomplete), diameter 10.4 mm.

10. Dentalium porterensis Weaver. Holotype, CAS 7517, loc. UW 90. Length 39.3 mm (incomplete), diameter 8.6 mm.

11, 12. Turritella porterensis Weaver. Syntype, CAS 506a, loc. UW 160. Height 31.5 mm, diameter 11.2 mm.

13, 14. Perse lincolnensis (Van Winkle). Holotype, CAS 7564, loc. UW 352. Height 31.6 mm, diameter 17.6 mm.

15, 16. Priscofusus chehalisensis (Weaver). Syntype, CAS 507b. Height 62.6 mm, diameter 22.8 mm.

17, 18. Pitar dalli (Weaver). Syntype, CAS 460a. Length 59.1 mm, height 49.4 mm (incomplete), depth 17.5 mm (single valve).

19, 20. Crassatella (Crassatella) washingtoniana (Weaver). Syntype, CAS 480A, loc. US 352. Length 36.3 mm, height 28.8 mm, depth 10.3 mm (single valve).

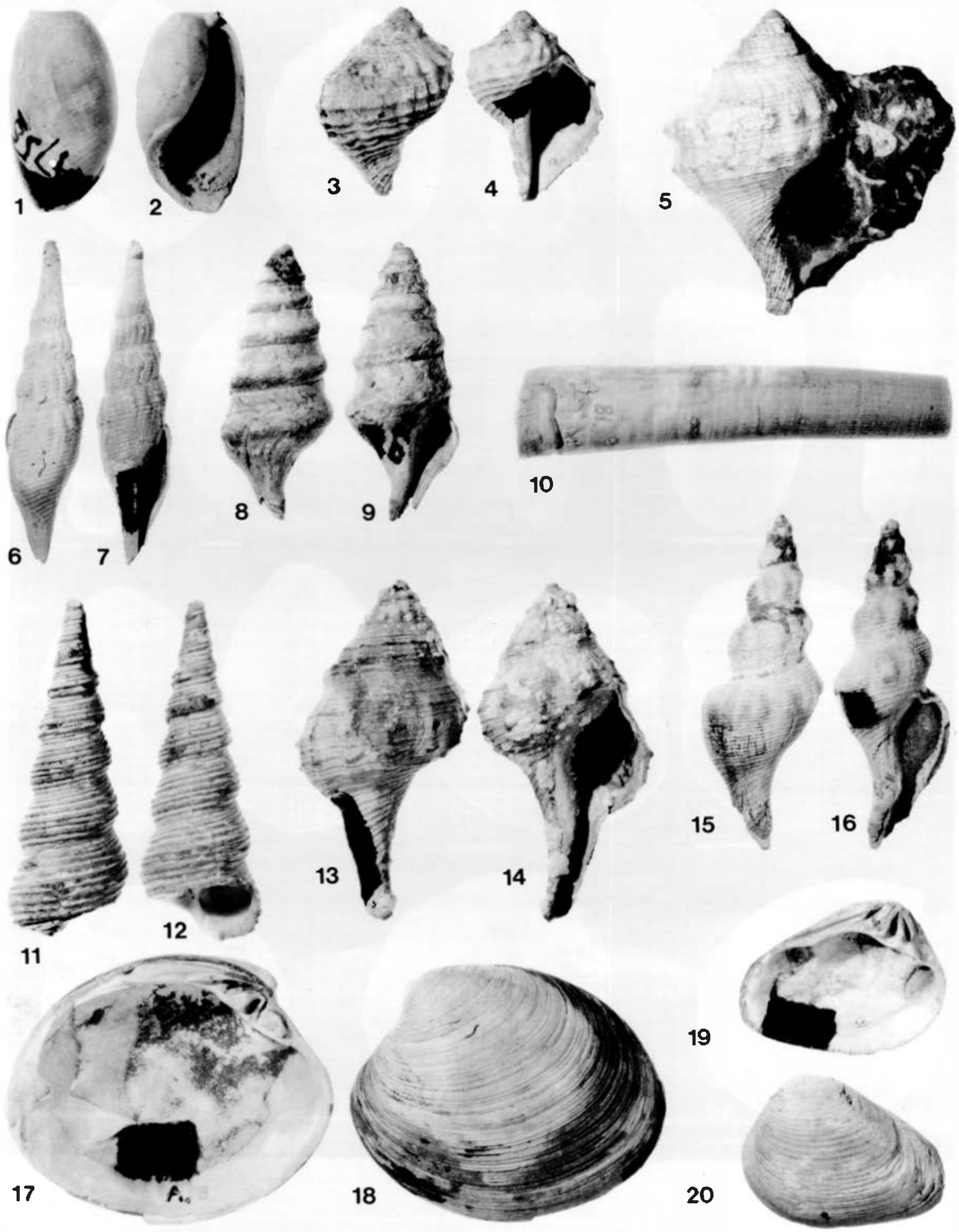

Figure 21. Late Eocene mollusks from the Lincoln Creek Formation at Porter Bluffs.

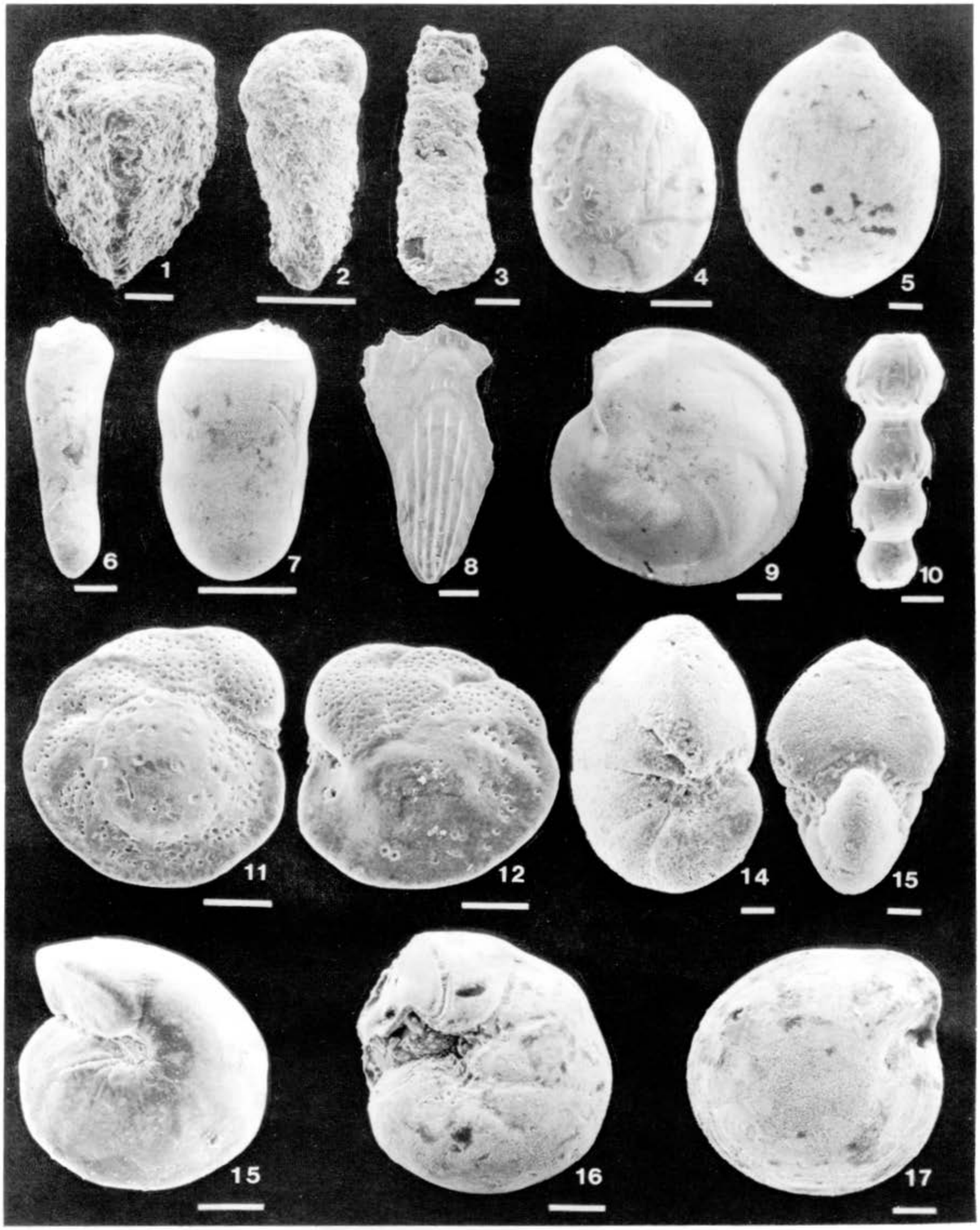

Figure 22. Late Eocene Foraminifera from the Lincoln Creek Formation at Porter Bluffs.

Figure 22. Late Eocene Foraminifera from the Lincoln Creek Formation at Porter Bluffs.

1. Gaudryina alazaensis Cushman, sample no. 10. Bar equals 100 um.
2. Gaudryina alazaensis Cushman, sample no. 10. Bar equals 300 um.
3. Martinottiella communis (d'Orbigny), sample no. 6. Bar equals 100 um.
4. Quinqueloculina weaveri Rau, sample no. 10. Bar equals 100 um.
5. Pseudonodosaria inflata (Costa), sample no. 20. Bar equals 100 um.
6. Marginulina exima Neugeboren, sample no. 10. Bar equals 100 um.
7. Marginulina alazaensis Nuttall, sample no. 17. Bar equals 300 um.
8. Plectofrondicularia gracilis Smith, sample no. 10. Bar equals 100 um.
9. Lenticulina lincolnensis (Rau), sample no. 20. Bar equals 300 um.
10. Stilostomella advena (Cushman and Laiming), sample no. 10. Bar equals 100 um.
11. Cibicides elmaensis Rau, sample no. 10. Bar equals 100 um.
12. Cibicides elmaensis Rau, sample no. 10. Bar equals 100 um.
13. Nonionellina applini (Howe and Wallace), sample no. 10. Bar equals 30 um.
14. Nonionellina applini (Howe and Wallace), sample no. 12. Bar equals 30 um.
15. Gyroidina orbicularis planata Cushman, sample no. 6. Bar equals 100 um.
16. Ceratobulimina washburnei Cushman and Schenck, sample no. 20. Bar equals 100 um.
17. Hoeglundina eocenica (Cushman and Hanna), sample no. 6. Bar equals 100 um.

Figure 23. Crescent Formation: Stop 14. Close inspection of the road cut at this stop reveals pillow basalts of early and middle Eocene age.

Taxon Localities	PB 6	PB 10	PB 12	PB 17	PB 20	PB 22
Allomorphina trigona Reuss	.5	-	-	-	-	-
Anomalina californiensis Cushman and Hobson	.5	4	2	-	-	-
Cassidulina galvinensis Cushman and Frizzell	.2	32	21	1	.6	-
Cassidulina globosa Hantken	.2	-	-	-	-	-
Cibicides elmaensis Rau	33	27	45	29	40	33
Cyclamina pacifica Beck	.2	-	-	-	.6	-
Dentalina dusenburyi Beck	.2	.3	-	-	-	-
D. jacksonensis Cushman and Applin	2	-	.3	-	-	-
D. sp.	.5	-	.3	-	-	-
D. spinosa d'Orbigny	.2	-	-	-	-	-
Eponides sp.	.2	-	-	-	-	-
Gaudryina alazaensis Cushman	2.6	2.6	1.6	13	2	17
Gyroidina orbicularis planata Cushman	8	10	19.5	40.5	9.9	33
Hoeglundina eocenica (Cushman and Hanna)	32	-	-	-	-	-
Lenticulina crassa (d'Orbigny)	.5	-	-	-	-	-
L. sp. A	.5	-	-	-	3.5	-
L. weaveri (Beck)	.2	-	-	-	-	-
Marginulina exima Neugeboren	.2	.3	-	-	-	-
Martinottiella communis (d'Orbigny)	7	.7	.3	-	-	-
Melonis sp.	.5	.3	-	-	-	-
Nodosaria sp.	.8	.3	.3	.5	1.0	-
Oridorsalis umbonatus (Reuss)	2	-	-	-	-	-
Quinqueloculina imperialis Hanna and Hanna	1.0	-	-	4.5	21	7
Fissurina marginata (Montagu)	-	.3	-	-	-	-
Lagena costata (Williamson)	-	.3	-	-	-	-
L. vulgaris Williamson	-	.3	-	.5	-	-
Lenticulina limbosa hockleyensis (Cushman and Applin)	-	.3	-	-	-	-
L. cf. *L. pseudorotulata* (Asano)	-	.3	-	1.5	5.8	-
L. sp.	-	1.0	.3	-	-	-
Nodosaria longiscata d'Orbigny	-	5.5	2	-	.6	-
Plectofrondicularia gracilis Smith	-	.3	-	-	-	-
Pseudonodosaria inflata (Costa)	-	2	-	-	1.0	-
Stilostomella adolphina (d'Orbigny)	-	.7	-	-	-	-
S. advena (Cushman and Laiming)	-	2.6	.7	-	-	-
Quinqueloculina weaveri Rau	-	1.6	-	3	7.6	-
Guttulina sp.	-	-	.3	-	-	-
Nonionellina applini (Howe and Wallace)	-	-	.7	-	-	-
Cyclogyra byramensis (Cushman)	-	-	-	.5	.6	-
Eponides mexicanus (Cushman)	-	-	-	1.0	-	-
Lagena becki Sullivan	-	-	-	.5	-	-
Lenticulina inornata (d'Orbigny)	-	-	-	.5	-	-
Marginulina alazaensis Nuttall	-	-	-	.5	-	-
Ceratobulimina washburnei Cushman and Schenck	-	-	-	-	2.9	-
Dentalina consobrina d'Orbigny	-	-	-	-	.6	-
Lenticulina lincolnensis (Rau)	-	-	-	-	.6	4
Biloculina cowlitzensis Beck	-	-	-	-	-	2
Foraminiferal fragments	6	7	5.4	3.5	1.7	4
Planktic Foraminifera	-	.3	.3	-	-	-
Total number of specimens	342	296	307	200	171	46

Figure 24. Species checklist of fossil Foraminifera from the Porter Bluffs section of the Lincoln Creek Formation. Numbers represent percent of total foraminiferal fauna. Sample number PB 8 is barren of foraminifers.

Figure 25.
Crescent Formation:
Stop 15.
Fractured flows show the typical pattern of collonade below and hacky entablature above.

REFERENCES CITED

Addicott, W. O., 1967, Zoogeographic evidence for late Tertiary lateral slip on the San Andreas fault, California: U.S. Geological Survey Professional Paper 593-D, p. D1-D12.

_____1970, Latitudinal gradients in Tertiary molluscan faunas of the Pacific Coast: Palaeogeography, Palaeoclimatology, Palaeoecology, v. 8, no. 4, p. 287-312.

_____1973, Oligocene molluscan biostratigraphy and paleontology of the lower part of the type Temblor Formation, California: U.S. Geological Survey Professional Paper 791, 48 p., 9 pls.

_____1976, Neogene molluscan stages of Oregon and Washington, in Neogene Symposium: Society of Economic Paleontologists and Mineralogists, Pacific Section, San Francisco, Calif., April 1976, p. 95-115.

Armentrout, J. M., 1973, Molluscan paleontology and biostratigraphy of the Lincoln Creek Formation (late Eocene-Oligocene), southwestern Washington: University of Washington (Seattle), unpub. Doctoral Dissertation, 479 p.

_____1975, Molluscan biostratigraphy of the Lincoln Creek Formation, southwest Washington, in Weaver, D. W., and others, eds., Paleogene Symposium and Selected Technical Papers: American Association of Petroleum Geologists-Society of Economic Paleontologists and Mineralogists-Society of Economic Geologists, Pacific Sections, 1975 Annual Meeting, Long Beach, Calif., p. 14-18.

_____1978, Progress report on Cenozoic correlations, West Coast North America: Geological Society of America, Abstracts with Programs, v. 10, no. 7, p. 360.

Arnold, Ralph, 1906, The Tertiary and Quaternary pectens of California: U.S. Geological Survey Professional Paper 47, 264 p.

_____1909, Environment of the Tertiary faunas of the Pacific Coast of the United States: Journal of Geology, v. 17, p. 509-533.

Arnold, Ralph, and Hannibal, Harold, 1913, The marine Tertiary stratigraphy of the north Pacific Coast of America: American Philosophical Society Proceedings, v. 52, no. 212, p. 559-605.

Baldwin, E. M., 1964, Geology of Oregon: Ann Arbor, Michigan, Edwards Brothers, 165 p.

Baldwin, E. M., 1974, Eocene stratigraphy of southwestern Oregon: Oregon Department of Geology and Mineral Industries Bulletin 83, 40 p.

Baldwin, E. M., and Beaulieu, J. D., 1973, Geology and mineral resources of Coos County, Oregon: Oregon Department of Geology and Mineral Industries Bulletin 80, 82 p.

Beaulieu, J. D., 1973, Geologic field trips in northern Oregon and southern Washington: Oregon Department of Geology and Mineral Industries Bulletin 77, 206 p.

Beck, M. E., Jr., and Burr, C. D., 1979, Paleomagnetism and tectonic significance of the Goble Volcanic Series, southwestern Washington: Geology, v. 7, p. 175-179.
Beck, R. W., 1943, Eocene Foraminifera from Cowlitz River, Lewis County, Washington: Journal of Paleontology, v. 17, no. 6, p. 584-614.
Beikman, H. M., Rau, W. W., and Wagner, H. C., 1967, The Lincoln Creek Formation, Grays Harbor Basin, southwestern Washington: U.S. Geological Survey Bulletin 1244-I, p. I1-I14.
Bergen, F. W., and Bird, K. J., 1972, The biostratigraphy of the Ocean City area, Washington, _in_ Symposium on Miocene Biostratigraphy of California: Society of Economic Paleontologists and Mineralogists, Pacific Section, Bakersfield, Calif., March 1972, p. 173-198.
Berry, W. B. N., 1966, Zones and zones - with exemplification from the Ordovician: American Association of Petroleum Geologists Bulletin, v. 50, p. 1487-1500.
Brown, R. D., Jr., and Gower, H. D., 1958, Twin River Formation (redefinition), northern Olympic Peninsula, Washington: American Association of Petroleum Geologists Bulletin, v. 42, no. 10, p. 2492-2512.
Buckovic, W. A., 1979, The Eocene deltaic system of west central Washington, _in_ Armentrout, John M., Cole, Mark R., and TerBest, Harry, Jr., eds., Cenozoic Paleogeography of the Western United States, Pacific Coast Paleogeography Symposium 3: Society of Economic Paleontologists and Mineralogists, Pacific Section, March 1979, Anaheim, Calif., p. 147-163.
Clapp, C. H., 1917, Sooke and Duncan map areas, Vancouver Island: Canada Geological Survey Memoir 96, 445 p.
Clark, B. L., 1929, Stratigraphy and faunal horizons of the Coast Ranges of California: Ann Arbor, Michigan, University Microfilms, Inc., 30 p.
_____1930, Tectonics of the Coast Ranges of Middle California: Geological Society of America Bulletin, v. 41, p. 747-828.
Cushman, J. A., and Frizzell, D. L., 1940, Two new species of Foraminifera from the Oligocene, Lincoln Formation, of Washington: Cushman Laboratory of Foraminiferal Research Contributions, v. 16, pt. 2, p. 42-43.
_____1943, Foraminifera from the type area of the Lincoln Creek Formation (Oligocene) of Washington State: Cushman Laboratory of Foraminiferal Research Contributions, v. 19, pt. 4, p. 79-89.
Dalrymple, G. B., 1979, Critical table for conversion of K-Ar ages from old constants to new constants: Geological Society of America, Geology, in press.
Dickerson, R. E., 1917, Climate and its influence upon the Oligocene faunas of the Pacific Coast, with descriptions of some new species from the _Molopophorus lincolnensis_ Zone: California Academy of Sciences Proceedings, ser. 4, v. 7, no. 6, p. 157-192.
Donnelly, A. T., 1976, The Refugian Stage of the California Tertiary: Foraminifera zonation, geologic history, and correlations with the Pacific Northwest: University of California, Ph.D. dissert., p. 151.
Durham, J. W., 1944, Megafaunal zones of the Oligocene of northwestern Washington: University of California Publications, Department of Geological Sciences Bulletin, v. 27, no. 5, p. 84-104.
_____1950, Cenozoic marine climates of the Pacific Coast: Geological Society of America Bulletin, v. 61, no. 11, p. 243-1264.
Easterbrook, D. J., 1969, Pleistocene chronology of the Puget Lowland and San Juan Islands, Washington: Geological Society of America Bulletin, v. 80, p. 2273-2286.
_____1979, The last glaciation of northwest Washington, _in_ Armentrout, John M., Cole, Mark R., and TerBest, Harry, Jr., eds., Cenozoic Paleogeography of the Western United States, Pacific Coast Paleogeography Symposium 3: Society of Economic Paleontologists and Mineralogists, Pacific Section, March 1979, Anaheim, Calif., p. 177-189.
Effinger, W. L., 1938, The Gries Ranch Fauna (Oligocene) of western Washington: Journal of Paleontology, v. 12, no. 4, p. 355-390.
Etherington, T. J., 1931, Stratigraphy and fauna of the Astoria Miocene of southwest Washington: University of California Publications, Department of Geological Sciences Bulletin, v. 20, no. 5, p. 31-142.
Fenton, C. L., and Fenton, M. A., 1928, Ecologic interpretations of some biostratigraphic terms: American Midland Naturalist, v. 11, p. 20-22.

Frizzell, D. L., 1937, Foraminifera of the type area of the Lincoln Formation of Washington (Abs.): Geological Society of America Proceedings, p. 383.
Fowler, G. A., 1965, The stratigraphy, Foraminifera, and paleoecology of the Montesano Formation, Grays Harbor County, Washington: University of Southern California, Unpublished Doctoral Dissertation, 355 p.
Fulmer, C. V., 1975, Stratigraphy and paleontology of the type Blakeley and Blakeley Harbor Formations (Washington), in Weaver, D. W., and others, eds., Paleogene Symposium and Selected Technical Papers: American Association of Petroleum Geologists-Society of Economic Paleontologists and Mineralogists-Society of Economic Geologists, Pacific Sections, 1975 Annual Meeting, Long Beach, Calif., p. 210-271.
Gower, H. D., and Pease, M. H., Jr., 1965, Geology of the Montesano quadrangle, Washington: U.S. Geological Survey Geologic Quadrangle Map GQ-374.
Henriksen, D. A., 1956, Eocene stratigraphy of the lower Cowlitz River-Eastern Willapa Hills area, southwestern Washington: Washington Division of Mines and Geology Bulletin 43, 122 p.
Hickman, C. S., 1969, The Oligocene marine molluscan fauna of the Eugene Formation, Oregon: University of Oregon Museum of Natural History Bulletin no. 16, 112 p.
_____1974, Characteristics of bathyal mollusk faunas in the Pacific Coast Tertiary: Western Society of Malacologists Annual Report, v. 7, p. 41-50.
Hodge, E. T., 1933, Age of Columbia River and lower canyon [abs.]: Geological Society of America Bulletin, v. 44, pt. 1, p. 156-157.
_____1938, Geology of the lower Columbia River: Geological Society of America Bulletin, v. 49, p. 831-929.
Huntting, M. T., Bennett, W. A. G., Livingston, V. E., Jr., and Moen, W. S., compilers, 1961, Geologic map of Washington: Washington Division of Mines and Geology, scale 1:500,000.
Keen, A. M., 1963, Marine molluscan genera of western North America - An illustrated key: Stanford, Calif., Stanford University Press, 126 p.
_____1971, Sea shells of tropical West America, marine mollusks from Baja California to Peru: Stanford, Calif., Stanford University Press, 1,064 p.
Kleinpell, R. M., and Weaver, D. W., 1963, Oligocene biostratigraphy of the Santa Barbara embayment, California: University of California Publications in Geological Science, v. 43, 3 pts., 250 p.
Livingston, V. E., Jr., 1966, Geology and mineral resources of the Kelso-Cathlamet area, Cowlitz and Wahkiakum Counties, Washington: Washington Division of Mines and Geology Bulletin 54, 110 p.
Mallory, V. S., 1959, Lower Tertiary biostratigraphy of the California Coast Ranges: Tulsa, Okla., American Association of Petroleum Geologists, 416 p.
McCormick, Lavon, and Moore, R. C., 1969, Outline of classification (of Bivalvia), in Part N, Volume 1, Mollusca 6, of Moore, R. C., ed., Treatise on invertebrate paleontology: New York and Lawrence, Kansas, Geological Society of America and Kansas University Press, p. N218-N222.
McDougall, Kristin, 1979, Paleoecological evaluation of late Eocene biostratigraphy of the west coast: U.S. Geological Survey Open-File Report 79-934, 206 p.
McKee, B., 1972, Cascadia, the Geologic Evolution of the Pacific Northwest: New York, McGraw-Hill Book Co., 394 p.
Moore, E. J., 1963, Miocene mollusks from the Astoria Formation in Oregon: U.S. Geological Survey Professional Paper 419, 109 p. [1964].
Mumby, J. I., 1959, Oligocene stratigraphy and Foraminifera of the Porter Bluffs area, Washington: University of Washington (Seattle), Unpublished Masters Thesis, 137 p.
Natland, M. L., 1957, Paleoecology of West Coast Tertiary sediments, chapter 19 of Treatise on marine ecology and paleoecology, v. 2, Paleoecology: Geological Society of America Memoir 67, p. 543-571.
Niem, A. R., and Van Atta, R. O., 1973, Cenozoic stratigraphy of northwestern Oregon and adjacent southwestern Washington, in Beaulieu, J. D., ed., Geologic Field Trips in northern Oregon and southern Washington: Oregon Department of Geology and Mineral Industries Bulletin 77, p. 75-132.
Pease, M. H., and Hoover, Linn, 1957, Geology of the Doty-Minot Peak area, Washington: U.S. Geological Survey Oil and Gas Investigations Map OM-188.
Rau, W. W., 1948a, Foraminifera from the Porter Shale (Lincoln Formation), Grays Harbor County, Washington: Journal of Paleontology, v. 22, no. 2, p. 152-174.
1948b, Foraminifera from the Miocene Astoria Formation in southwestern Washington:

Journal of Paleontology, v. 22, no. 6, p. 774-782.
Rau, W. W., 1951, Tertiary Foraminifera from the Willapa River valley of southwest Washington: Journal of Paleontology, v. 25, no. 4, p. 417-453.
_____1956, Foraminifera from the McIntosh Formation (Eocene) at McIntosh Lake, Washington: Cushman Foundation for Foraminiferal Research Contributions, v. 7, pt. 3, p. 69-78.
_____1958, Stratigraphy and foraminiferal zonation in some of the Tertiary rocks of southwestern Washington: U.S. Geological Survey Oil and Gas Investigations Chart OC-57, 2 sheets.
_____1964, Foraminifera from the northern Olympic Peninsula, Washington: U.S. Geological Survey Professional Paper 374-G, p. G1-G33.
_____1966, Stratigraphy and Foraminifera of the Satsop River area, southern Olympic Peninsula, Washington: Washington Division of Mines and Geology Bulletin 53, 66 p.
_____1967, Geology of the Wynoochee Valley quadrangle, Grays Harbor County, Washington: Washington Division of Mines and Geology Bulletin 56, 51 p.
_____1970, Foraminifera, stratigraphy, and paleoecology of the Quinault Formation, Point Grenville-Raft River Coastal Area, Washington: Washington Division of Mines and Geology Bulletin 62, 41 p.
Roberts, A. E., 1958, Geology and coal resources of the Toledo-Castle Rock district, Cowlitz and Lewis Counties, Washington: U.S. Geological Survey Bulletin 1062, 71 p.
Schenck, H. G., 1927, Marine Oligocene of Oregon: University of California Publications, Department of Geological Sciences Bulletin, v. 16, no. 12, p. 449-460.
Sliter, W. V., and Baker, R. A., 1972, Cretaceous bathymetric distribution of benthic foraminifers: Journal of Foraminiferal Research, v. 2, no. 4, p. 167-183.
Snavely, P. D., Jr., and Baldwin, E. M., 1948, Siletz River volcanic series, northwestern Oregon: American Association of Petroleum Geologists Bulletin, v. 32, no. 5, p. 805-812.
Snavely, P. D., Jr., Brown, R. D., Jr., Roberts, A. E., and Rau, W. W., 1958, Geology and coal resources of the Centralia-Chehalis district, Washington: U.S. Geological Survey Bulletin 1053, 159 p.
Snavely, P. D., Jr., MacLeod, N. S., and Rau, W. W., 1969, Geology of the Newport area, Oregon, Part 1: The Ore Bin, v. 31, no. 2, p. 25-48.
Snavely, P. D., Jr., MacLeod, N. S., and Wagner, H. C., 1973, Miocene tholeiitic basalts of coastal Oregon and Washington and their relations to coeval basalts of the Columbia Plateau: Geological Society of America Bulletin, v. 84, no. 2, p. 387-424.
Snavely, P. D., Jr., Niem, A. R., MacLeod, N. S., Pearl, J. E., and Rau, W. W., 1979, Makah Formation--A deep marginal basin sedimentary sequence of late Eocene and Oligocene age in the northwestern Olympic Peninsula, Washington: U.S. Geological Survey Open-File Report 79-581, 75 p.
Snavely, P. D., Jr., Pearl, J. D., and Lander, D. L., 1977, Interim report on petroleum resources potential and geologic hazards in the outer continental shelf--Oregon and Washington Tertiary province: U.S. Geological Survey Open-File Report 77-282, 68 p.
Snavely, P. D., Jr., Rau, W. W., Hoover, Linn, Jr., and Roberts, A. E., 1951, McIntosh Formation, Centralia-Chehalis coal district, Washington: American Association of Petroleum Geologists Bulletin, v. 35, p. 1052-1061.
Snavely, P. D., Jr., Roberts, A. E., Hoover, Linn, Jr., and Pease, M. H., Jr., 1951, Geology of the eastern part of the Centralia-Chehalis coal district, Lewis and Thurston Counties, Washington: U.S. Geological Survey Coal Investigations Map C-8, 2 sheets.
Snavely, P. D., Jr., and Wagner, H. C., 1963, Tertiary geologic history of western Oregon and Washington: Washington Division of Mines and Geology Report of Investigations 22, 25 p.
Steiger, R. H., and Jager, E., 1977, Subcommission on geochronology: convention on the use of decay constants in geo- and cosmochronology: Earth and Planetary Science Letters, v. 36, p. 359-362.
Strong, C. P., Jr., 1967, Geology and paleontology of the Pe Ell-Doty area, Washington: University of Washington (Seattle), unpublished Masters thesis, 110 p.

Tegland, N. N., 1933, The fauna of the type Blakeley upper Oligocene of Washington: University of California Publications, Department of Geological Sciences Bulletin, v. 23, no. 3, p. 81-174.
Trimble, D. E., 1963, Geology of Portland, Oregon, and adjacent areas: U.S. Geological Survey Bulletin 1119, 119 p.
Turner, D. L., 1970, Potassium-Argon dating of Pacific coast Miocene foraminiferal stages, in Bandy, O. L., ed., Radiometric dating and paleontological zonation: Geological Society of America Special Paper 124, p. 91-129.
Van Winkle, K. E., 1918, Paleontology of the Chehalis Valley, Washington: University of Washington (Seattle) Publications in Geology, v. 1, no. 2, p. 69-97.
Wagner, H. C., 1967, Geology of the Raymond quadrangle, Washington: U.S. Geological Survey Open-File Report, preliminary map.
Warren, W. C., Norbisrath, H., and Grivetti, R. M., 1945, Geology of northwestern Oregon, west of Willamette River and north of latitude 45°15': U.S. Geological Survey Oil and Gas Investigations Preliminary Map 42.
Weaver, C. E., 1912, A preliminary report on the Tertiary paleontology of western Washington: Washington Geological Survey Bulletin 15, 80 p.
_____1916a, Tertiary faunal horizons of western Washington: University of Washington (Seattle) Publications in Geology, v. 1, no. 1, p. 1-67.
_____1916b, Eocene of the lower Cowlitz Valley, Washington: California Academy of Sciences Proceedings, ser. 4, v. 6, no. 1, p. 1-17.
_____1916c, The post-Eocene formations of western Washington: California Academy of Sciences Proceedings, ser. 4, v. 6, no. 2, p. 19-40.
_____1937, Tertiary stratigraphy of western Washington and northwestern Oregon: University of Washington (Seattle) Publications in Geology, v. 4, 266 p.
_____1942, Paleontology of the marine Tertiary formations of Oregon and Washington: University of Washington (Seattle) Publications in Geology, v. 5, 790 p.
Weaver, C. E., and others, 1944, Correlation of the marine Cenozoic formations of western North America: Geological Society of America Bulletin, v. 55, p. 569-598.
Wilkinson, W. D., Lowry, W. D., and Baldwin, E. M., 1946, Geology of the St. Helens quadrangle, Oregon: Oregon Department of Geology and Mineral Industries Bulletin 31, 39 p.

MARYS PEAK FIELD TRIP: STRUCTURE OF THE EASTERN FLANK OF THE CENTRAL COAST RANGE, OREGON

Robert D. Lawrence, Charles L. Rosenfeld, & William Ruddiman, III
Oregon State University, Corvallis, OR 97331

INTRODUCTION

Marys Peak (4097 feet, figure 1) is the highest elevation in the Oregon Coast Range. The peak is topped by an erosion resistant sill which intrudes bedded sandstones of the middle Eocene Flournoy Formation which in turn overlie the early Eocene Siletz River Volcanics. The Corvallis fault trends northeast past the eastern base of the peak and is the most significant structure of the area. The Kings Valley fault which passes through the top of the peak is a minor structure. The main bulk of the peak is composed of northwest dipping rocks of the Siletz River Volcanics. This field trip guides you through a southeast to northwest traverse across the strucutral grain of the area to illustrate the structure and stratigraphy.

Figure 1. Aerial oblique photo of Marys Peak from the southeast.

STRATIGRAPHY

The rock units of the area are representative of the Eocene units and younger intrusions that make up the bulk of the exposures of the Coast Range.

The oldest exposed unit is the early to early middle Eocene Siletz River Volcanics. It is composed of submarine pillow and massive basalt flows, basalt breccias and tuffs, and associated thin basaltic-sedimentary rocks (Snavely and others, 1968). The base of the unit is not exposed, but geophysical data (Dehlinger and others, 1968) suggest lower density materials (sediments?) beneath it. The lower part of the unit is similar to oceanic curstal basalts and is thought to be oceanic crust which accreted to the continental margin. Rocks of more varied composition accumulated locally in the upper part of the unit as seamounts (MacLeod and Snavely, 1973). The unit is estimated at over 10,000 feet thick and one of the best sections is exposed on Marys Peak (Baldwin, 1955).

The upper part of the Siletz River volcanics is a separate member, the Kings Valley Siltstone Member. This is 3000 feet thick in Kings Valley to the northeast (Vokes and other, 1954), but only about 500 feet on Marys Peak. It is a unit mainly of tuffaceous siltstones and minor tuffaceous sandstones of basaltic derivation. Locally white ash beds are present.

The Flournoy Formation overlies the Kings Valley siltstone with little or no unconformity. It was formerly mapped as the Tyee Formation (Baldwin, 1955), and Snavely and others, 1964), but recent work (Baldwin, 1974) found that the Tyee is restricted to the southern Coast Range of Oregon, while the Flournoy is more widespread. The Flournoy Formation is a thick sequence of rhythically bedded marine sandstones and siltstones of middle Eocene age derived from the Klamath Mountains (Snavely and others, 1964). At the latitude of Marys Peak it is mostly fine-grained sandstone and siltstone which accumulated in graded beds six inches to three feet thick. The sandstone is arkosic and micaeous, well compaced, and greenish gray or bluish gray in color. Sedimentary structures indicative of turbidite deposition are common. The unit is 6000 feet thick west of Marys Peak and thins rapidly to the east.

The Flournoy Formation is overlain unconformably by the late Eocene Spencer Formation east of the Corvallis fault and the area of this field trip. The unconformity is marked adjacent to the fault suggesting that the Spencer, a series of thick-bedded basaltic, arkosic, and micaceous marine sandstones was deposited off the block west of the Corvallis fault during and after the early motion on the fault.

The Marys Peak sill is intruded between beds of the Flournoy Formation. It formed from a basaltic magma and developed a typical basalt differentiation sequence (Roberts, 1953). The entire sill is about 1000 feet thick. It has chilled margins. Between these it ranges from a pyroxene-rich base of granophyric gabbro to a granophyric diorite cut by aplitic dikes near the top. A radiometric date of 29.9 m.y. by Park Snavely (reported in Simpson and Cox, 1977) gives an Oligocene age for the sill. Similar intrusions are common in the Coast Range.

STRUCTURE

The major structure of the area is the Corvallis fault (figure 2) which trends N50E for about 35 miles from within the Coast Range to north of Corvallis, significantly oblique to the north-south trend of the Coast Range. Demonstrable motion on this fault is up on the west with at least 5000 feet of vertical stratigraphic separation best estimate is about 7500 feet) southeast of Marys Peak. The fault is steeply dipping, but the actual attitude has never been determined. The fault itself is a zone of steep shears up to 500 feet wide including blocks of sandstone and basalt. Blocks with overturned attitudes can be found within the zone. No evidence regarding lateral movement is available. We consider the fault most likely to be an east dipping normal fault, possible with some component of strike slip motion associated with tectonic rotation of the Coast Range Block (see below). The fault was probably first active during the late Eocene to provide the sediment source for the Spencer formation and must have been reactivated after the Oligocene intrusive episode as it may displace some of these.

East of the Corvallis fault near Marys Peak the Flournoy Formation dips toward the fault along the west limb of an anticline of about two miles wavelength (Vokes and others, 1954). This anticiline limb is reversely oriented for a drag feature and is probably younger than the fault. However, steep dips are only found near the fault and the fold train dies out rapidly to the east. Possibly the damped fold train formed under compression from the stronger, poorly layered block of Siletz River volcanics are exposed to near the top of Marys Peak. Dips range from 12^{o} to 39^{o} (including primary dips of flows). Generally dips are steeper near the Corvallis fault and decrease to the northwest becoming almost horizontal at Marys Peak. At Marys Peak the N30E-trending Kings Valley fault is crossed. This is a steeply west-dipping normal fault with 700 ± 100 feet of vertical separation at Marys Peak. It dies out to the south-west and increases in displacement to the northeast. Motion on the fault post-dates emplacement of the Marys Peak still 29.9 m.y. ago. West of the Kings Valley fault the Flournoy Formation covers the main bulk of the Coast Range. Folds are gentle with dips greater than 15^{o} uncommon. Thus the structure is primarily a northwest tilted block west of the Corvallis fault.

Paleomagnetic studies indicate very substantial tectonic rotation of the Oregon Coast Range between 20 and 50 m.y. ago. Simpson and Cox (1977) have determined a clockwise rotation of 65 to $75^{o}+12^{o}$ for various flows of the Siletz River volcanics and of $64^{o}+16^{o}$ for the Flournoy Formation. Clark (1969) determined a clockwise rotation of $28^{o} \pm 12^{o}$ for the Marys Peak sill. These rotations probably explain the oblique structural grain of the Coast Range. The northwest trend of the Corvallis and Kings Valley faults reflects clockwise rotation of these features since they were formed. The 20^{o} difference in general trend reflects the greater age of teh Corvallis fault and therefore its greater rotation. Studies of joint and fault patterns recorded as lineaments on U-2 high flight false-color infrared photography and SLAR imagery (figures 2 and 3) reveal major NE and NW sets of features. Thus study of these structural features offers an additional means of investigating the history of tectonic rotation of this area. The current north-south trending mountain range is a young, post-Miocene feature developed across an older structural grain.

Dehlinger and others (1968) presented a geophysical cross-section through the Oregon Coast Ranges that passes through Marys Peak. This section shows a density and velocity inversion under much of the Coast Range that suggests that the Siletz River volcanics are underlain by lower density sediments. Thus it is possible that the entire exposed section is an allochthonous sheet of oceanic crust thrust on some sedimentary material (melange?) probably at the tiem of emplacement of the Siletz River Volcanics and perhaps also during the rotation. Thus the rotated block may not be very thick.

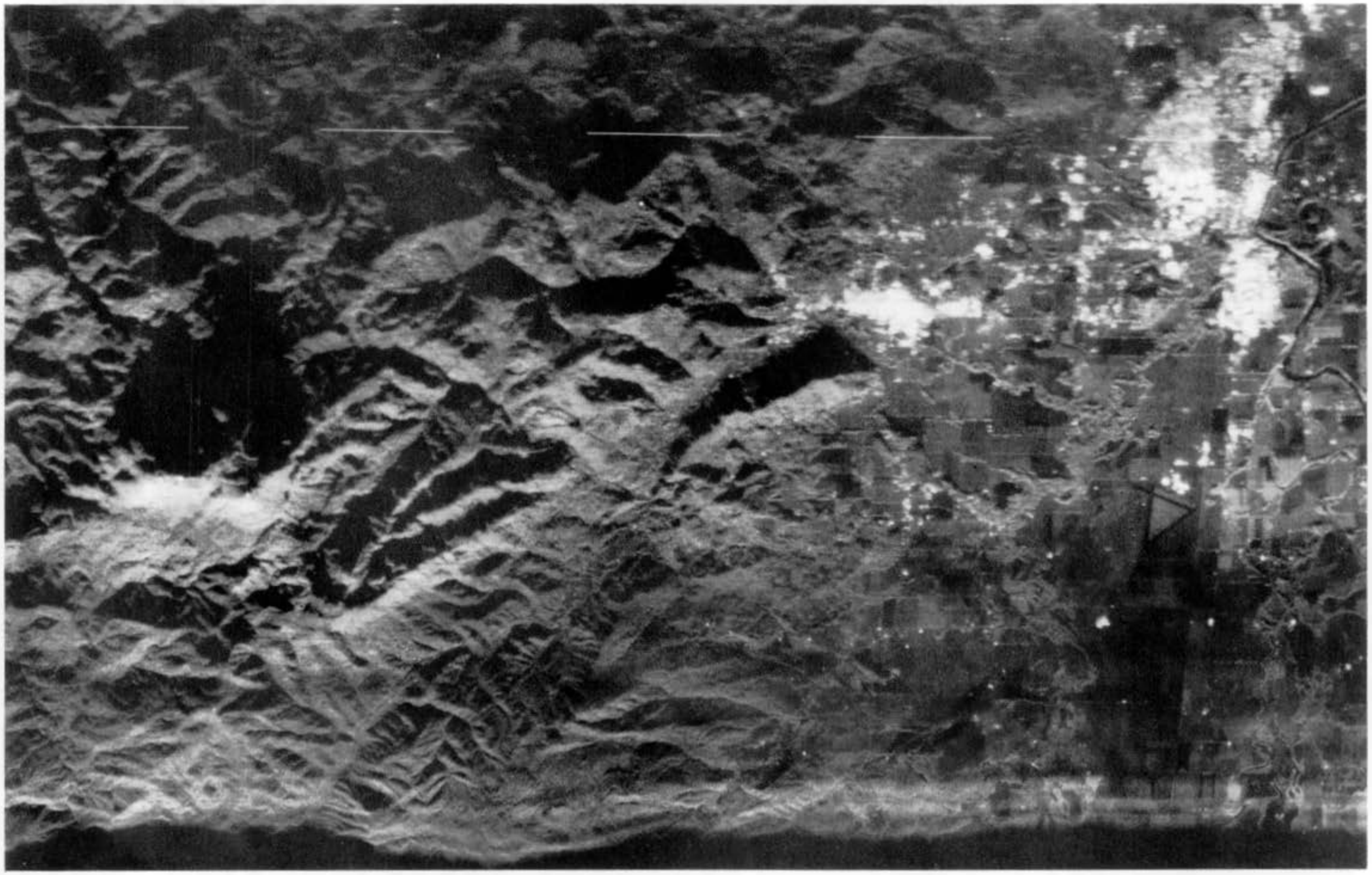

Figure 2. Side-looking airborne radar image of the Corvallis-Marys Peak area, Oregon. Compare to figure 3.

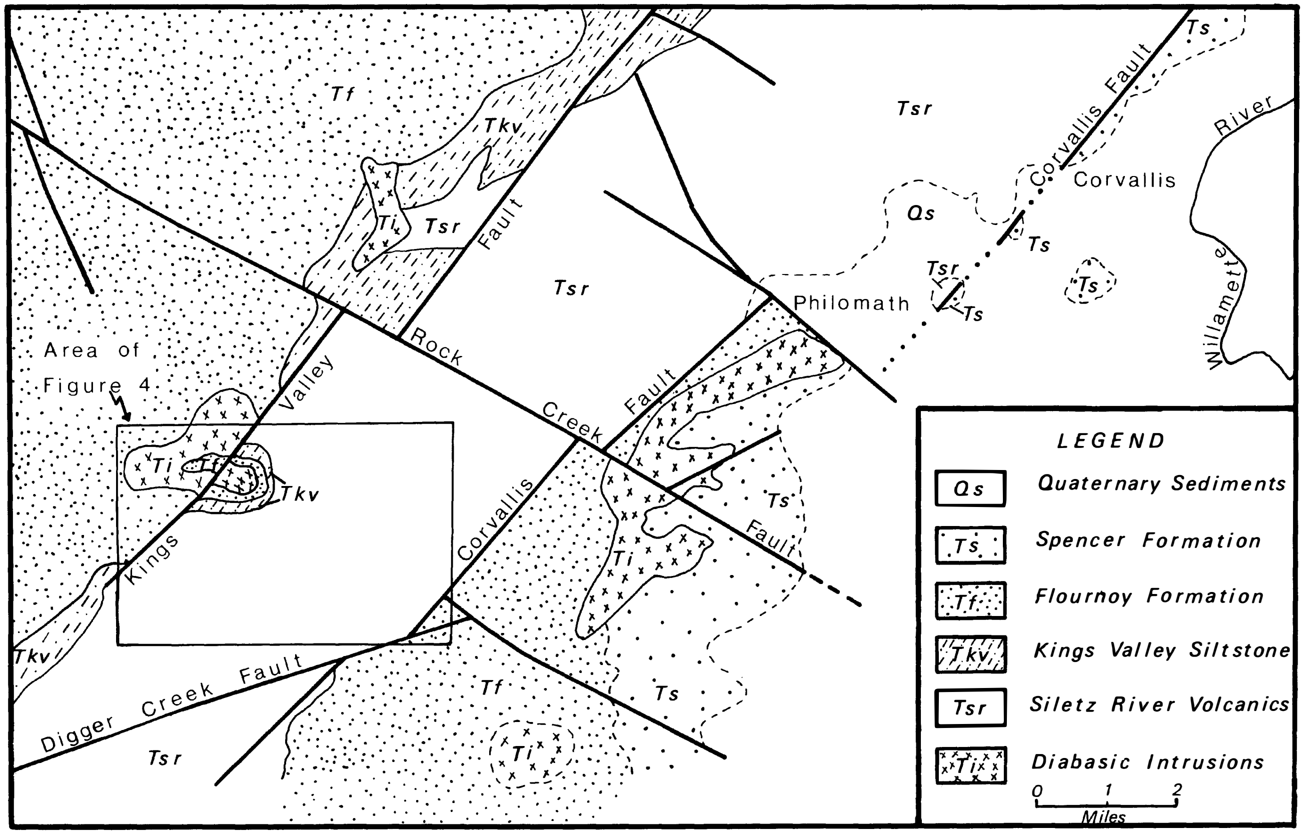

Figure 3. Sketch map of geology and structure of the area shown on SLAR in figure 2. Structural interpretation is that of the authors and shows the Corvallis fault displaced by younger structures. Inset rectangle shows the location of the detailed map of the field trip route (see figure 4).

ROAD LOG

Follow road log on figure 4.

Mileage: Cummulative	Mileage: Interval	
		To begin drive west from Corvallis on highways 20 and 34 combined, through Philomath, to the intersection where the two highways separate. About 6 miles.
0	7.6	TURN left on highway 34 at the junction of highways 20 and 34.
7.6	1.0	STOP 1. Flournoy sandstone outcrop immediately east of the Corvallis fault. Note steep dips toward the fault. Most of the outcrop is a fine-grained, miceaceous, arkosic sandstone. Bed grade upwards into siltstones. Grading best distinguished by looking for the sharp breaks at the bottoms of beds. Parting lineation is visible.
8.6	0.4	STOP 2. Flournoy sandstone within the Corvallis fault zone. Fault zone is about 500 feet wide here. Blocks of Flournoy sandstone are variously oriented, including overturned, in this area.
9.0	0.1	Landslide in deeply weathered pyroclastic rocks of the Siletz River volcanics.
9.1	0.6	TURN RIGHT on Marys Peak road. Altered Siletz River volcanics in this area.
9.7	1.1	Thick regolith of altered pyroclastics of the Siletz River volcanics. Much of the rock texture and several minor faults can be distinguished on close inspection of the outcrop. Similar material is exposed for about ½ mile.
10.8	0.5	Pillow basalts of the Siletz River Volcanics. Greater resistance to weathering results in a thin regolith over these rocks.
11.3	0.5	STOP 3. A relatively fresh outcrop of Siletz River Volcanics showing the contact between pyroclastics on the east and a columnar jointed flow on the west. Relatively steep northwest dip. A small low angle fault cuts the outcrop. Much zeolite and calcite secondary mineralization is present filling voids and interstitial spaces in the rocks.
11.8	1.2	STOP 4. Weather permitting this overlook allows a view southwest along the Corvallis fault and east across the Willamette Valley. Southeast across the Corvallis fault Flat Moutain and Green Peak are supported by sill similar to that on Marys Peak. Massive, jointed flows of Siletz River basalt in outcrop across road.

13.0 STOP 5. Excellent outcrop of Siletz River pillow basalts passing upward into massive basalt. This is topped by a thin bed of basaltic glass tuff over which there is another pillow basalt unit. Several small faults are present. The pillows are well preserved (some as large as 3 feet across). Most are surrounded by a glassy rind and show a well developed radial joint. Calcite and zeolites occur between pillows. The basalt is composed of labradorite, augite, titaniferous magnetite, and glass is
1.6 commonly intensely latered.

14.6 TURN RIGHT on road to Harlan.
0.9
15.5 STOP 6. Kings Valley siltstone outcrop. Mainly basaltic siltstone with some coarse grained sandstone beds. White beds are air fall ash layers. Early Eocene pelecypods and gastropods were collected by Baldwin (1955)
0.5 just uphill.
16.0 Cross Kings Valley fault.
0.1
16.1 TURN AROUND at Parker Creek. Outcrop of Flournoy sandstone about 150 feet below the base of the Marys Peak sill. Here we are west of the Kings Valley fault in the down dropped block. From turn return to
1.5 Marys Peak road.

17.6 TURN LEFT back onto the Marys Peak road.
0.1
17.7 Side road (mud) leads left from here to an overlook of the Willamette Valley that can sometimes be used if the top of Marys Peak is in the
0.3 clouds. See discussion at 21.7 miles.

18.0 Large landslide of Flournoy sandstone and Marys Peak sill blocks sliding
0.6 over the Kings Valley siltstone.

18.6 STOP 7. Good fresh exposures of Flournoy Formation on the east side of the Kings Valley fault. The unit is a bluish gray, rhythically bedded micaceous and arkosic sandstone and sandy siltstone. Most beds are graded and sedimentary structures indicating turbidite deposition include bottom marks, intraformational mud chip conglomerates, and others.
0.2 Plant fragments are abundant. A few large concretions are present.

18.8 Base of Marys Peak sill is poorly exposed here.
0.1
18.9 Approximate location of Kings Valley fault.
0.1
19.0 STOP 8. Middle of Marys Peak sill (figure 5) at Parker Creek waterfall. The rock is a dark gray, coarse-/to medium-grained granophyric gabbro (Roberts, 1953). Mineralogy is labradorite, titaniferous augite, olivine, titanomaghetite, apatite, and quartz or micropegmatite. Olivine occurs rimmed by pyroxene or magnetite which prevented further reaction with the late fluid residuum from which the quartz and micropegmatite crystallized. Pyroxene forms about 25 to 30 percent of the rock here and increase to 30 to 35% toward the base. Olivine, titanomagnetite, and anorthite content of plagioclase also increase toward the base. The rock
1.0 transitionally into a granophyric diorite upwards.

20.0 STOP 9. Overlook to the west across the Coast Range. On a clear day the bridge across the Yaquina estuary can be seen. By walking up the dirt road to the east of the parking lot it is possible to see some of the differentiated upper part of the sill and intruding late stage
0.8 aplite dikes. These must be dug out of the bank above the road.

20.8 Flournoy Formation contact metamorphosed to epidote-amphibolite hornfels.
0.6 Much small scale faulting.

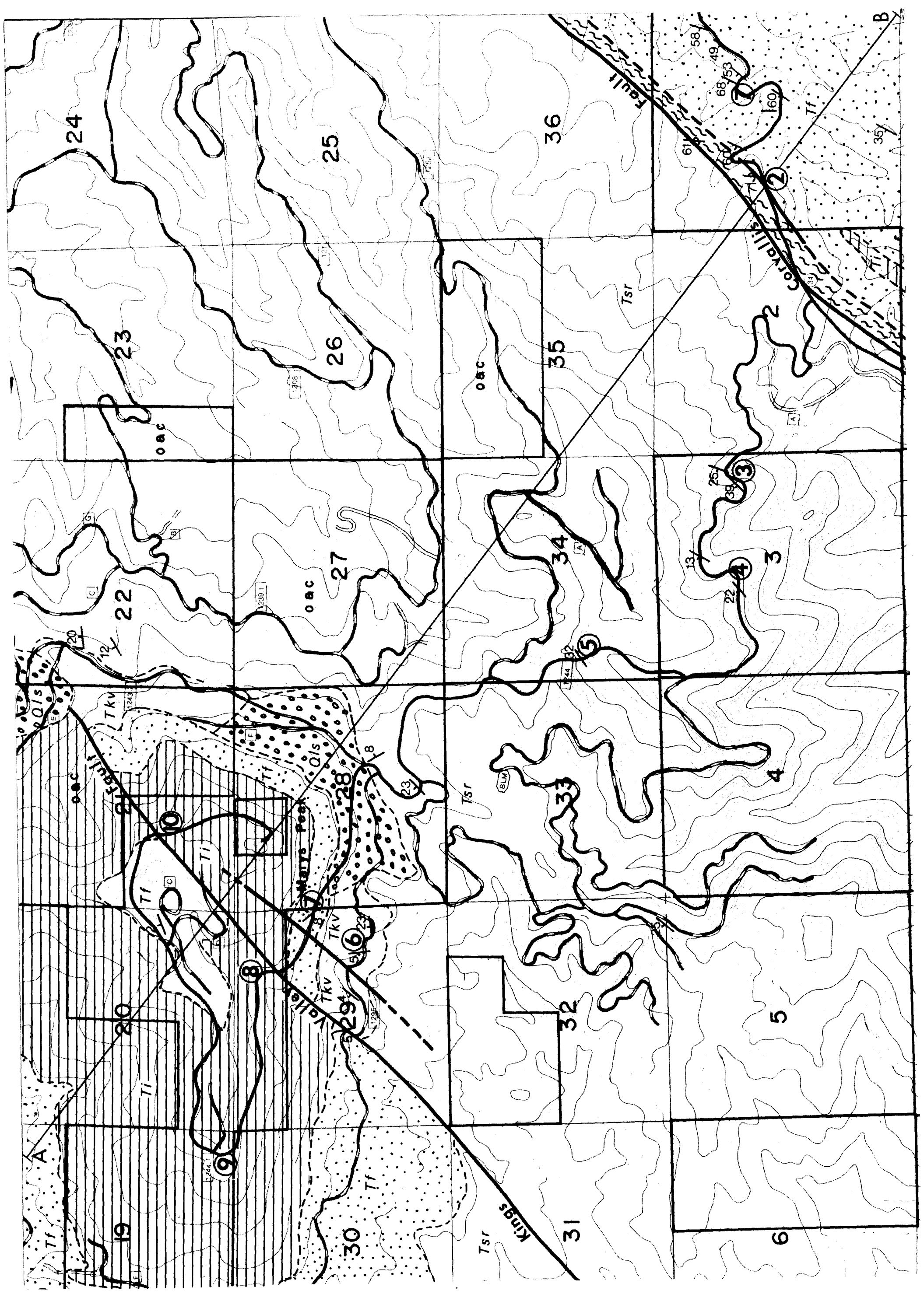
A
B
Kings
Valley
Fault
Corvallis
Fault
Marys Peak
Tsr
Tf
Ti
Tkv
Qls
oac

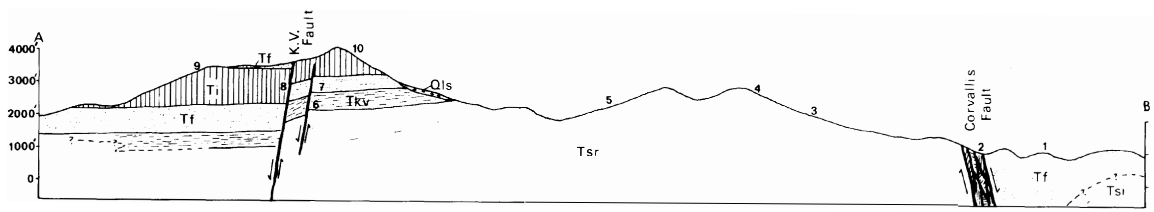

Figure 4. Geologic map and cross section of the field trip area. Units are: Qls = Landslides (small circle pattern), Tf = Flournoy Formation (dot pattern), Tkv = Kings Valley siltstone (no pattern), Tsr = Siletz River Volcanics (no pattern), Ti = mafic intrusions (lined pattern), and fault zone = (squiggle pattern). Field trip stops located by circled numbers.

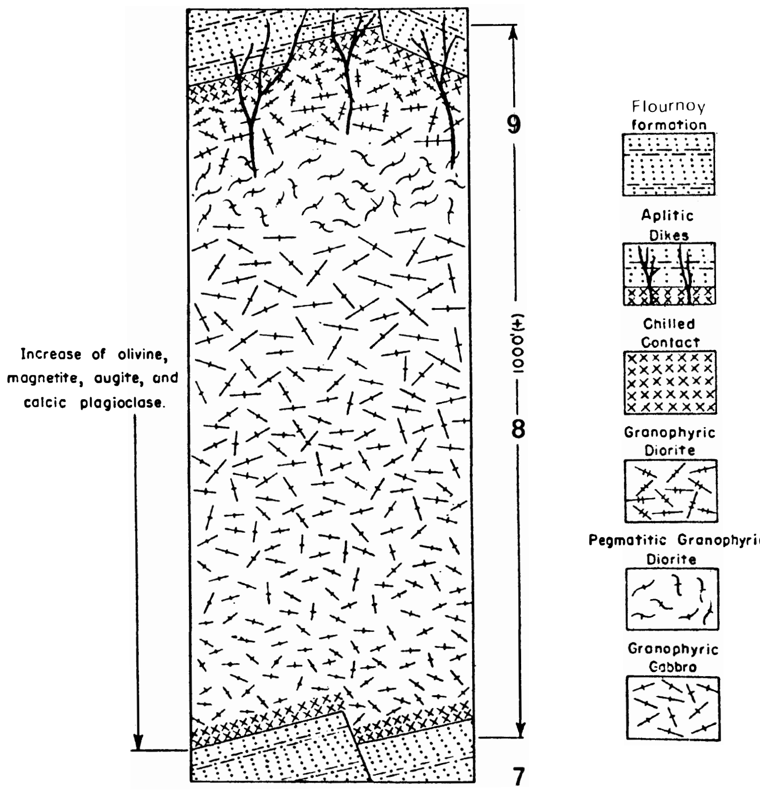

Figure 5. Marys Peak sill section after Roberts (1953) showing the pattern of deformation. Numbers indicate the approximate positions of the field trip stops.

21.4 Cross the Kings Valley fault again.

0.3

21.7 STOP 10. Rest area near top of Marys Peak. A short walk will take you to the top of the peak for a spectacular view (weather permitting). To the east you look across the Willamette Valley structural depression to the Cascade Range with its volcanoes. In the foreground is the trace of the Corvallis fault east of the ridge (Vinyard Mountain) that trends northeast on the west side of Corvallis and Philomath. The Kings Valley fault extends northeast through Kings Valley itself. Vinyard Mountain is a horst of Siletz River Volcanics. To the southeast prominent peaks include Flat Mountain and Green Peak supported by sills. The Corvallis fault continues southwest in the hills just west of the North Fork of the Alsea River and Crooked Creek. To the west you look across the Coast Range to the Pacific Ocean.

End of field trip. Return to Corvallis.

REFERENCES

Baldwin, E. M., 1955, Geology of the Marys Peak and Alsea quadrangles, Oregon: U.S. Geol. Survey Oil and Gas Inv. Map OM-162, scale 1:62:500.

_____, 1974, Eocene stratigraphy of southwestern Oregon: Oregon Dept. Geol. and Mineral Indus. Bull. 83, 40 p.

Dehlinger, P., Couch, R. W., and Gemperle, M., 1968, Continental and oceanic structure from the Oregon coast westward across the Juan de Fuca Ridge: Can. Jour. Earth Sci., v. 5, p. 1079-1090.

Johnson, A.M., 1970, Physical Processes in Geology, Freeman, Cooper & Company, 577 p.

MacLeod, N.S., and Snavely, P.D., Jr., 1973, Volcanic and intrusive rocks of the central part of the Oregon Coast Range, in Geologic field trips in northern Oregon and southern Washington: Oregon Dept. Geol. and Mineral Indus. Bull. 77, p. 49-74.

Roberts, A.E., 1953, A petrographic study of the intrusive at Marys Peak, Benton County, Oregon: Northwest Sci., v. 27, p. 43-60.

Simpson, R.W., and Cox A., 1977, Paleomagnetic evidence for tectonic rotation of the Oregon Coast Range: Geology, v. 5, p. 585-589.

Snavely, P.D., Jr., Macleod, N.S., and Wagner, H.C., 1968, Tholeiitic and alkalic basalts of the Eocene Siletz River Volcanics, Oregon Coast Range: Am. Jour. Sci., v. 266, p. 454-481.

_____, Wagner, H.C., and Macleod, N.S., 1964, Rhythic-bedded eugeosynclinal deposits of the Tyee Formation, Oregon Coast Range: Kansas Geol. Survey Bull. 169, v. 2, p. 461-480.

Vokes, H.E., Myers, D.A., Hoover, L., 1954, Geology of the west-central border area of the Willamette Valley, Oregon: U.S. Geol. Survey Oil and Gas Inv. Map OM-150, scale 1:62,500.

GUIDE TO THE GEOLOGY OF THE UPPER CLACKAMAS AND NORTH SANTIAM RIVERS AREA, NORTHERN OREGON CASCADE RANGE

P.E. Hammond, J.L. Anderson, and K.J. Manning

INTRODUCTION

This report is a guide to the geology of the upper Clackamas and North Santiam Rivers in the northwestern Oregon Cascade Range. The area covered by this guide lies within six 15-minute USGS topographic quadrangles: Battle Ax, Breitenbush Hot Springs, Fish Creek Mtn., High Rock, Mt. Jefferson, and Detroit. Current road maps are available through the U.S. Forest Service for the Clackamas River area in the Mt. Hood National Forest and for the North Santiam River area in the Willamette National Forest. Information on accessibility can be acquired at Estacada Ranger Station in Estacada and Ripplebrook Ranger Station, 26 mi southeast of Estacada, for the Clackamas River and at the Detroit Ranger Station, 1.4 mi west of Detroit, for the North Santiam River.

This guide has been assembled in a format which enables the traveler to visit parts of the area as separate trips according to weather conditions and available time. In total there are 54 stops: numbers 1-25 in the North Santiam area, and 26-54 in the upper Clackamas area. At least two full days are necessary to complete the tour.

Physiography

The area covers about 2600 sq km (1000 sq mi). Elevation ranges from 213 m (700 ft) to 1759 m (5771 ft), making the relief steep locally. The area is densely forested up to an elevation of about 1370 m (4500 ft). Extensive logging has provided a network of secondary roads, many of which are paved.

Drainage patterns displayed by the Clackamas and North Santiam Rivers are typical and atypical for major streams draining the western flank of the Oregon Cascade Range. The westward flow of the North Santiam River is typical of most Cascade streams. However, a northward direction is exhibited by headwaters of the North Santiam and Clackamas Rivers, and the lower portion of the Clackamas River has a northwestward course. The atypical drainage patterns are influenced primarily by well-developed northwestward and north-south fault systems.

Access

The main access into the North Santiam area is along State Highway 22, which exits Interstate Highway I-5 south of Salem (Fig. 1). Stops 1-3, 20-25 are on State Highway 22 between Detroit Reservoir and Marion Forks (Fig. 2). The remaining stops are along U.S. Forest Service Highway 46 and secondary roads.

Main access into the Clackamas River area is through Estacada, which can be reached via State Highway 211 from Salem or via State Highway 224 from the Portland area (Fig. 1). Stops 26-35 are along U.S. Forest Service Highway 46 between Estacada and the Ripplebrook Ranger Station (Fig. 3). The remaining stops are scattered in the upper part of the drainage along major and secondary roads.

Exposure

The bedrock geology is exposed chiefly in roadcuts, stream beds, and ridge crests. Pervasive faulting of thick stratigraphic sections of tuffs, breccias, lavas, and volcanically derived sediments has contributed to landsliding that encompasses up to about 25 percent of the area. This part of the Cascade Range is exceedingly difficult to synthesize geologically because of the extensive surficial cover of landslide debris and till, the complex volcanic stratigraphy, and the extensive faulting. Five years have been spent in field investigations. Studies of the petrography, geochemistry, and correlation of the volcanic units,other than the flows of the Columbia River Basalt Group, are just beginning. Accordingly this guide is preliminary.

Acknowledgments

Anderson is primarily responsible for the stratigraphy and structures in the Columbia River Basalt Group. Manning contributed a major part to the structural geology of the Clackamas-Collawash River drainage. Hammond is responsible for the structural interpretation of the North Santiam River area and the regional stratigraphy. We have also drawn on the information gathered in unpublished reports and theses by Clayton (1976), Dyhrman (1975), Jackson (1980), Olson (1978), Pungrassami (1969), Portwood (1979), Rollins (1976), and Sutton (1974). R.L. Armstrong and Joe Harakal of the University of British Columbia and the Mobil Research and Development Corporation provided the K-Ar age dates summarized in Table 3. We are gratefully indebted to R.W. McKay, cartographer, and to Paula Greer, typist, both of Portland State University, for working under an extremely tight schedule.

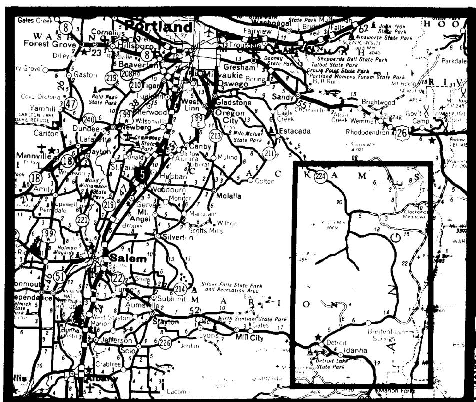

Figure 1. Index map showing highway routes into the upper Clackamas-North Santiam Rivers area (outlined).

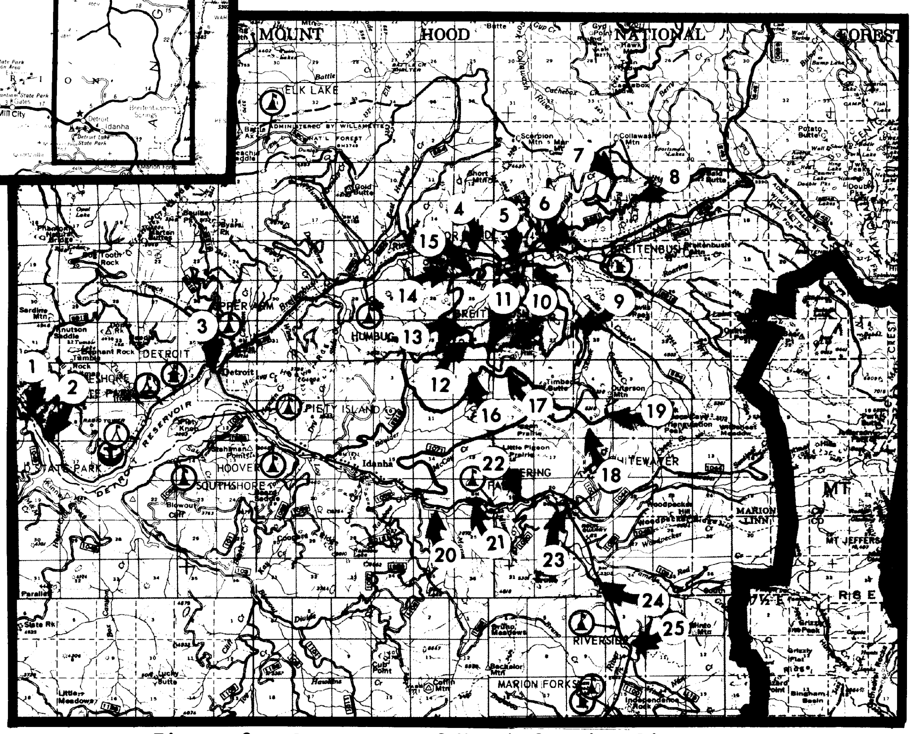

Figure 2. Route map of North Santiam River area within Willamette National Forest, showing road numbers and stops 1

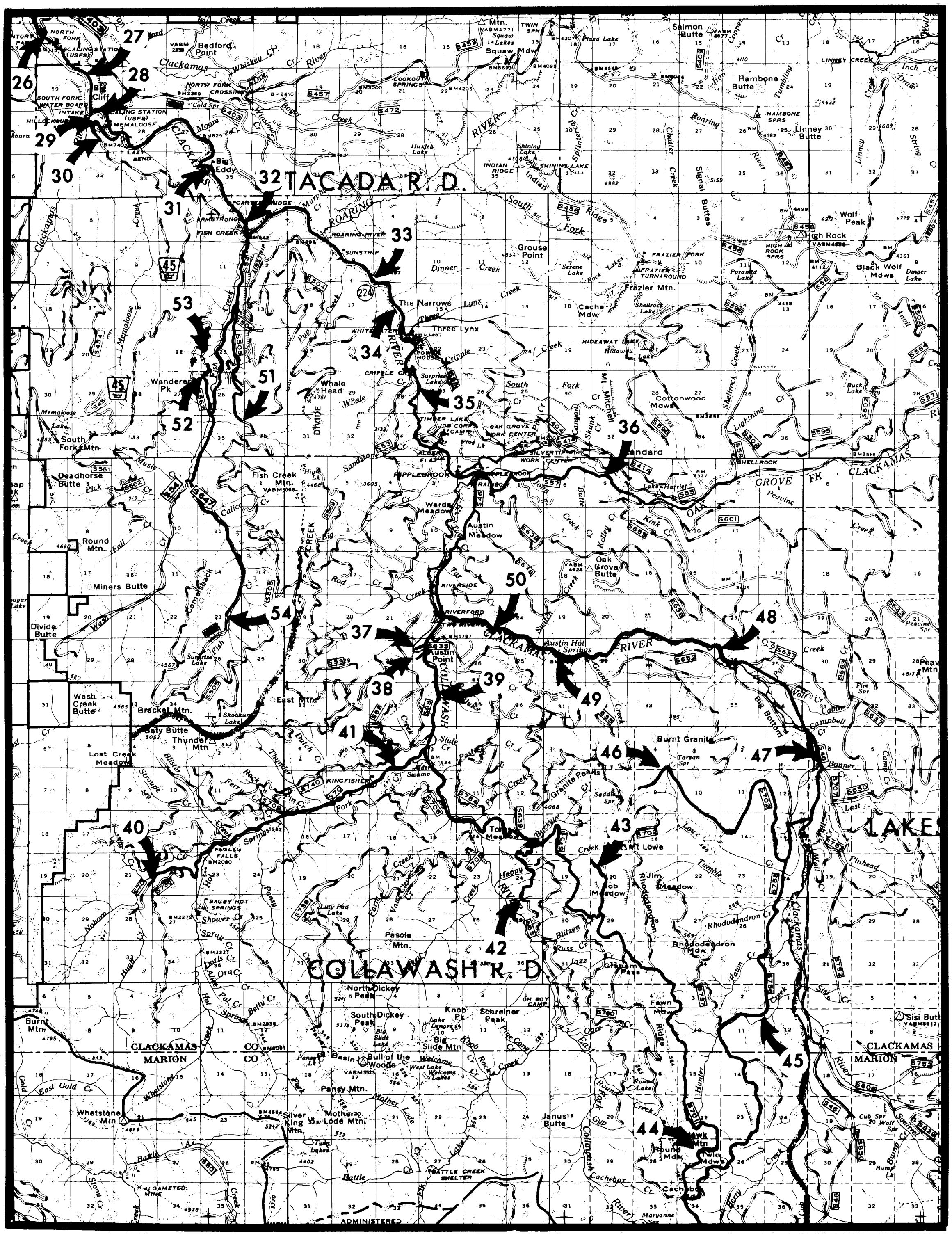

Figure 3. Route map of upper Clackamas River area within Mt. Hood National Forest, showing road numbers and stops 31

GENERAL GEOLOGY

The upper Clackamas and North Santiam Rivers area is underlain by over 8000 m of volcanic strata. The older strata, ranging in age from about 30 Ma to 5 Ma, are irregularly warped but dip generally homoclinally eastward. They are intruded by many dikes, sills, and small plutons, ranging from basalt to granodiorite, and have been altered hydrothermally. The younger lavas form a plateau capping the range and supporting Mount Jefferson stratovolcano. The strata have been cut by sets of strike-slip northwest-trending and normal north-trending faults. The area has been uplifted possibly 500 m during the late Cenozoic and deeply dissected by stream and glacial erosion.

Stratigraphy

The geologic units are separated stratigraphically into an older Western Cascade Group and younger High Cascade Group (Peck and others, 1964; Walker and others, 1966; Hammond, 1979; Table 1). The Western Cascade Group underlies the western slope of the range, consists chiefly of dark-colored andesitic lava flows and light-colored pyroclastic flow and volcaniclastic deposits, and is over 6825 m thick. The group has been structurally deformed, intricately intruded by plutons of diverse composition, and altered hydrothermally. The High Cascade Group forms a plateau across the crest of the range, largely covers the eastern slope, and consists predominantly of gray basalt and basaltic andesite lava flows and minor andesitic and dacitic High Cascade stratocones. Maximum thickness of the High Cascade Group is about 1150 m. The contact between the groups is placed at the lowest stratigraphic occurrence of the gray basaltic lava flows. In most occurrences this contact is unconformable.

Western Cascade Group

The Western Cascade Group is subdivided into a lower, middle, and upper part (Table 1). The Breitenbush Formation, which lies at the base of the middle part, is the most diagnostic unit of the Western Cascade Group. All strata underlying the Breitenbush are assigned to the lower part, the "Sardine" Formation. The middle part consists of the Breitenbush Formation, Nohorn Andesite, and beds of Bull Creek, in ascending order. The Columbia River Basalt Group, derived from sources well beyond the Cascade volcanic province, separates the middle and upper parts in the Clackamas River area. However, the basalt lava flows are interstratified with the beds of Bull Creek and the Rhododendron Formation. The upper part of the Western Cascade Group consists of the Rhododendron Formation in the Clackamas River area and of the Outerson Basalt in the North Santiam River area. Where applicable, the geologic units of Thayer (1936, 1937, 1939) have been adopted in preference to the large lithologic units of Peck and others (1964).

Most formational units of the Western Cascade Group can be recognized by their lithologies. However, because of commonly interfingering relationships and extensive faulting throughout the area, some contacts are approximate, and thicknesses of the units are estimated.

Lower part of Western Cascade Group: The "Sardine" Formation (Ts) represents the lower part of the Western Cascade Group in the area. It consists chiefly of volcaniclastic sandstones and lithic-rich mudflow deposits and is extensively exposed along the Breitenbush and North Santiam Rivers east of Detroit Reservoir (stops 3 and 4) and in the Collawash River drainage of the Clackamas River (Figs. 2-4). To the west, the strata contain an increasing proportion of lava flows. Because these strata trend beneath Sardine Mountain north of Detroit Reservoir, they are considered as part of the Sardine Series of Thayer (1939). Radiometric age dates from the upper part of the formation indicate that the strata are 23 Ma and older (Table 2).

Middle part of Western Cascade Group: The Breitenbush Formation (Tb) consists chiefly of pale-green to gray dacitic to rhyolitic tuff, representing pyroclastic flow

Table 1. Main geologic units in upper Clackamas-North Santiam Rivers area, northern Oregon Cascade Range

Symbol	Unit	Max. exposed thickness, ft/m	Age	Description
Qls	Landslide deposits	100/30	Quaternary	Unsorted deposits of clay, to boulder size debris, incorporating some glacial deposits, talus, colluvium, and most bedrock units; some coherent masses over 100m in length. Temporarily stable to active.
				HIGH CASCADE GROUP
Qj	Volcanic deposits of Mount Jefferson	300/90	<100,000(?) B.P. <690,000 B.P.	Includes lava flows, avalanche and mudflow deposits of chiefly basaltic andesite and minor amounts of silicic andesite and dacite.
				unconformity
Qb	Younger High Cascade basalt	1800/550	< 690,000(?) B.P. < 1,000,000 B.P.	Consist of shield forming and intracanyon lava flows and tephra cone deposits of chiefly basalt and minor amounts of basaltic andesite.
				unconformity
QTb	Older High Cascade basalt	2000/610	Pliocene to early Pleistocene	Similar to above but generally dipping eastward beneath younger basalt. Deeply dissected, commonly capping ridges.
				Generally unconformable, conformable locally with Outerson Basalt. Approximate thickness of High Cascade Group 1150 m
QTi, Ti	Quaternary and Tertiary intrusions		Pliocene-Quaternary; Late Oligocene to late Miocene	Dikes, sills, and plugs of basalt, pyroxene and/or hornblende andesite porphyry, dacite, pyroxene diorite, and quartz diorite, and larger plutons of medium-grained pyroxene and/or hornblende quartz diorite and granodiorite.
				WESTERN CASCADE GROUP
Upper part:				
To	Outerson Basalt	2200/670	Approximately middle Miocene to earliest Pliocene	Dark-colored olivine basalt lava flows, scoria, and interbeds of basaltic volcaniclastic deposits.
				unconformity
Tr	Rhododendron Formation	3000/915	Approximately middle to possibly late Miocene	Chiefly gray to brown olivine and/or pyroxene andesite porphyry lava flows, scoria, and breccia, interbedded light-colored mudflow, salic pyroclastic flow, and tephra deposits, and minor basaltic lava flows and scoria.
				Partly contemporaneous with Outerson Basalt and Columbia River Basalt Group. Unconformable with older units
Tcr	Columbia River Basalt Group Yakima Basalt Subgroup Wanapum Basalt Grande Ronde Basalt	1800/550	Early to middle Miocene	Dark-colored aphyric to plagioclase phyric basalt lava flows, pillow lava, hyaloclastite beds, and thin interbeds of volcaniclastic deposits
				Partly contemporaneous with the beds of Bull Creek and Rhododendron Formation. Unconformable with other units.
Middle part:				
Tbc	Beds of Bull Creek (Eagle Creek Formation)	1200/375	Approximately late Oligocene to middle Miocene	Consists chiefly of varied-colored mudflow and coarse volcaniclastic deposits and minor platy andesite and basalt lava flows.
				Partly contemporaneous in its upper part with Columbia River Basalt Group (Grande Ronde Basalt) and in its lower part with Nohorn Andesite
Tn	Nohorn Andesite	1000/300	Approximately late Oligocene to middle Miocene	Chiefly brown, platy jointed pyroxene andesite porphyry lava flows and breccia, minor red silicic lava flows, and thin interbeds of volcaniclastic deposits.
				Partly contemporaneous with Breitenbush Formation
Tb	Breitenbush Formation Members: Vitrophyric andesite lava flow of Boulder and Hoover Ridges Gray tuff of Boulder Ridge Green tuff of Cleator Bend	3000/915	Approximately late Oligocene to middle Miocene	Chiefly light-colored salic pyroclastic flow deposits and minor interbedded volcaniclastic deposits and andesite lava flows of Nohorn Andesite.
				unconformity
Lower part:				
Ts	"Sardine" Formation (Beds at Detroit)	>10,000/3000	Late Oligocene and older	Well-stratified brown to gray-green beds, consisting chiefly of volcaniclastic sandstone, mudflow deposits, lithic and vitric tuff, and minor andesite and basalt lava flows.
	Approximate thickness of Western Cascade Group: 6875m			Base of formation not exposed.

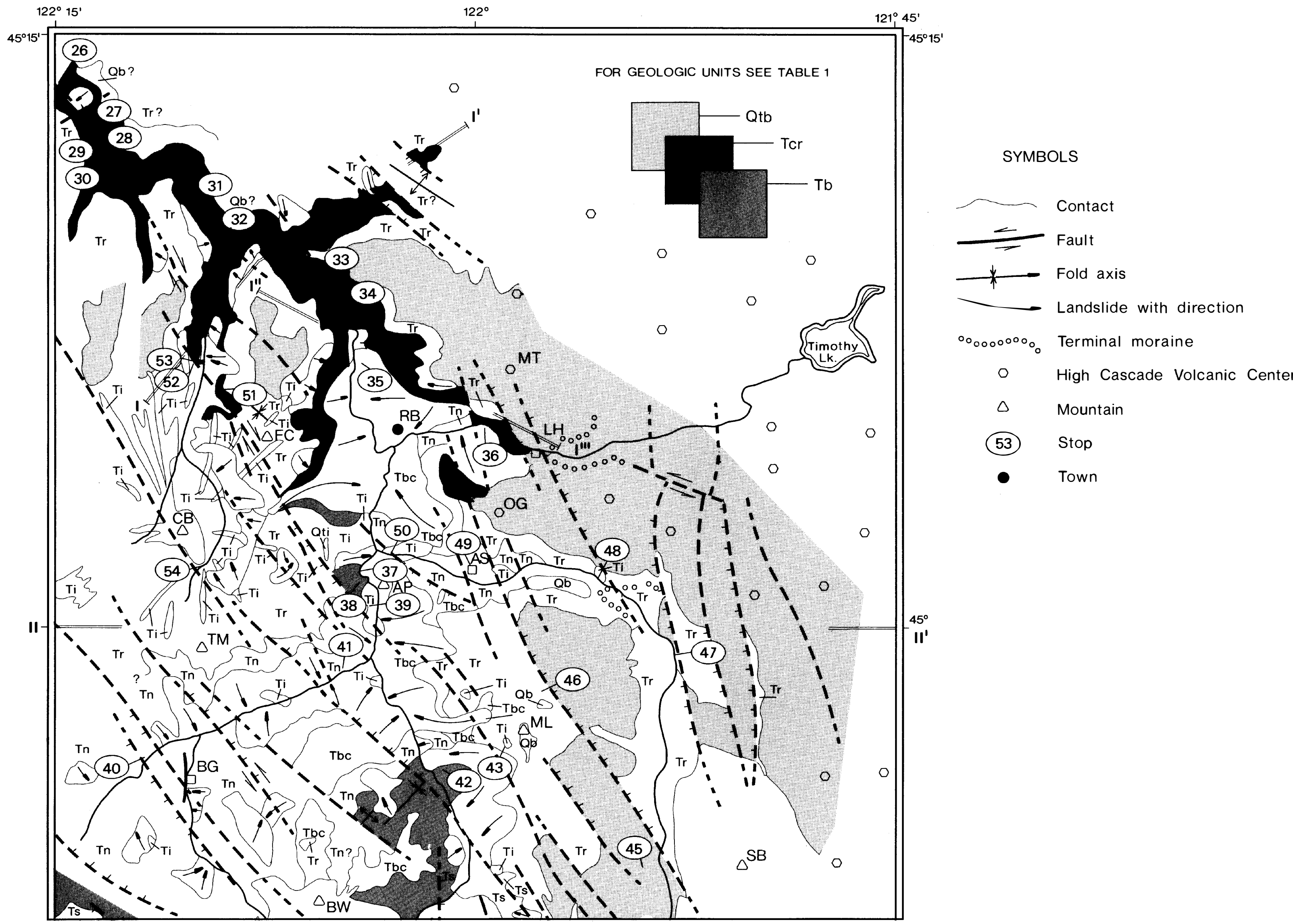

122° 15'
122°
121° 45'
45°15'
45°15'
45°
II
II'
I'
I''
I'''
FOR GEOLOGIC UNITS SEE TABLE 1
Qtb
Tcr
Tb
SYMBOLS
Contact
Fault
Fold axis
Landslide with direction
Terminal moraine
High Cascade Volcanic Center
Mountain
53
Stop
Town
Timothy Lk.
MT
LH
RB
OG
FC
CB
AS
AP
TM
ML
BG
BW
SB
Tr
Tr?
Qb?
Qb
Ti
Qti
Tn
Tn?
Tbc
Ts
26
27
28
29
30
31
32
33
34
35
36
37
38
39
40
41
42
43
45
46
47
48
49
50
51
52
53
54

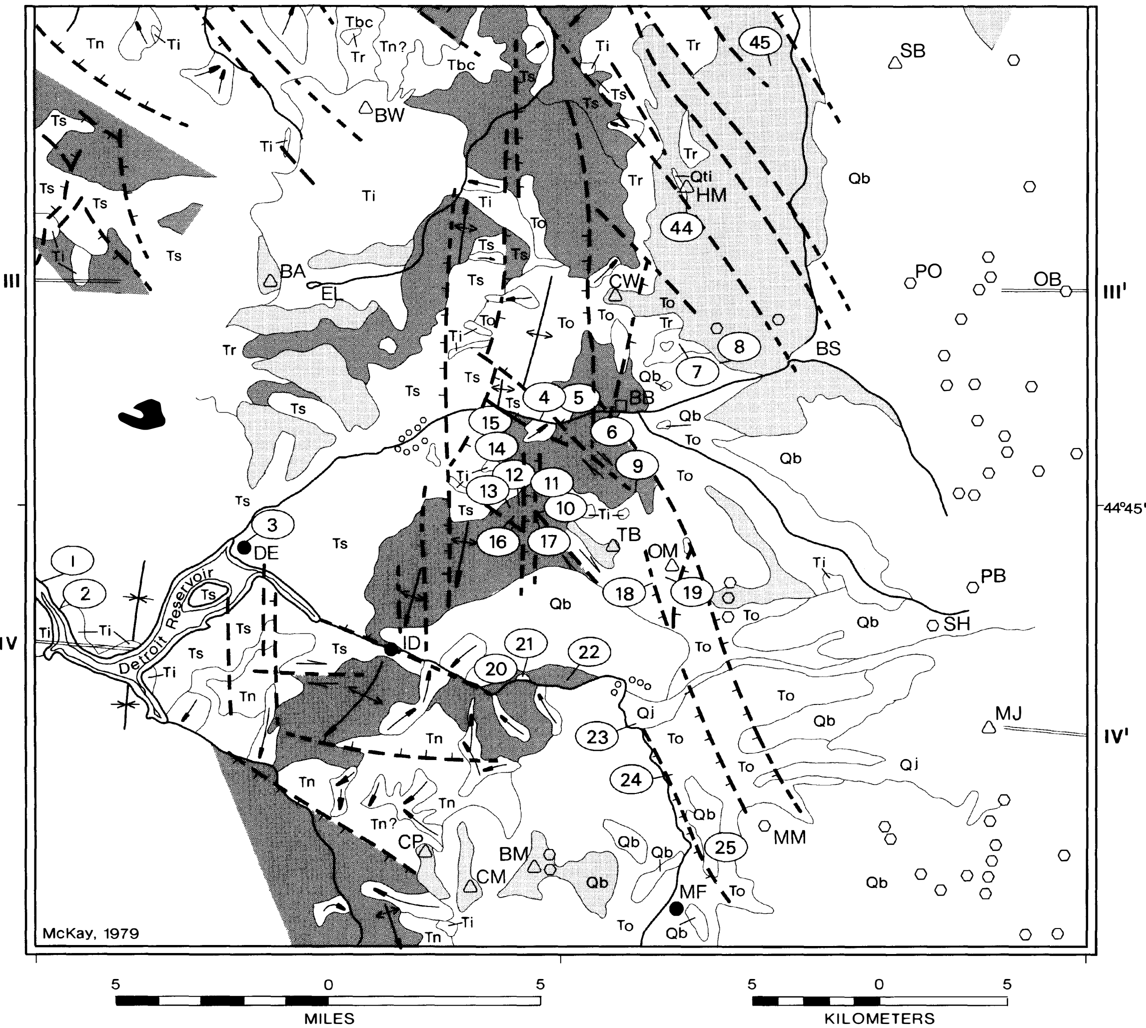

LANDMARKS

AP	Austin Point
BA	Battle Ax
BM	Bachelor Mountain
BS	Breitenbush Saddle
BW	Bull-of-the-Woods
CB	Camelsback
CM	Coffin Mountain
CP	Cub Point
CW	Collawash Mountain
DE	Detroit
EL	Elk Lake
FC	Fish Creek Mountain
HM	Hawk Mountain
ID	Idanha
LH	Lake Harriet
MF	Marion Forks
MJ	Mt. Jefferson
ML	Mt. Lowe
MM	Minto Mountain
MT	Mt. Mitchell
OG	Oak Grove Butte
OB	Olallie Butte
OM	Outerson Mountain
PB	Park Butte
PO	Potato Butte
RB	Ripplebrook
SB	Sisi Butte
SH	Sentinel Hills
TB	Timber Butte
TL	Three Lynx
TM	Thunder Mountain

HOT SPRINGS

AS	Austin
BG	Bagby
BB	Breitenbush

Figure 4. Preliminary reconnaissance geologic map of upper Clackamas - North Santiam Rivers, Oregon Cascade Range

ELEVATIONS ABOVE SEA LEVEL ARE SHOWN IN FEET

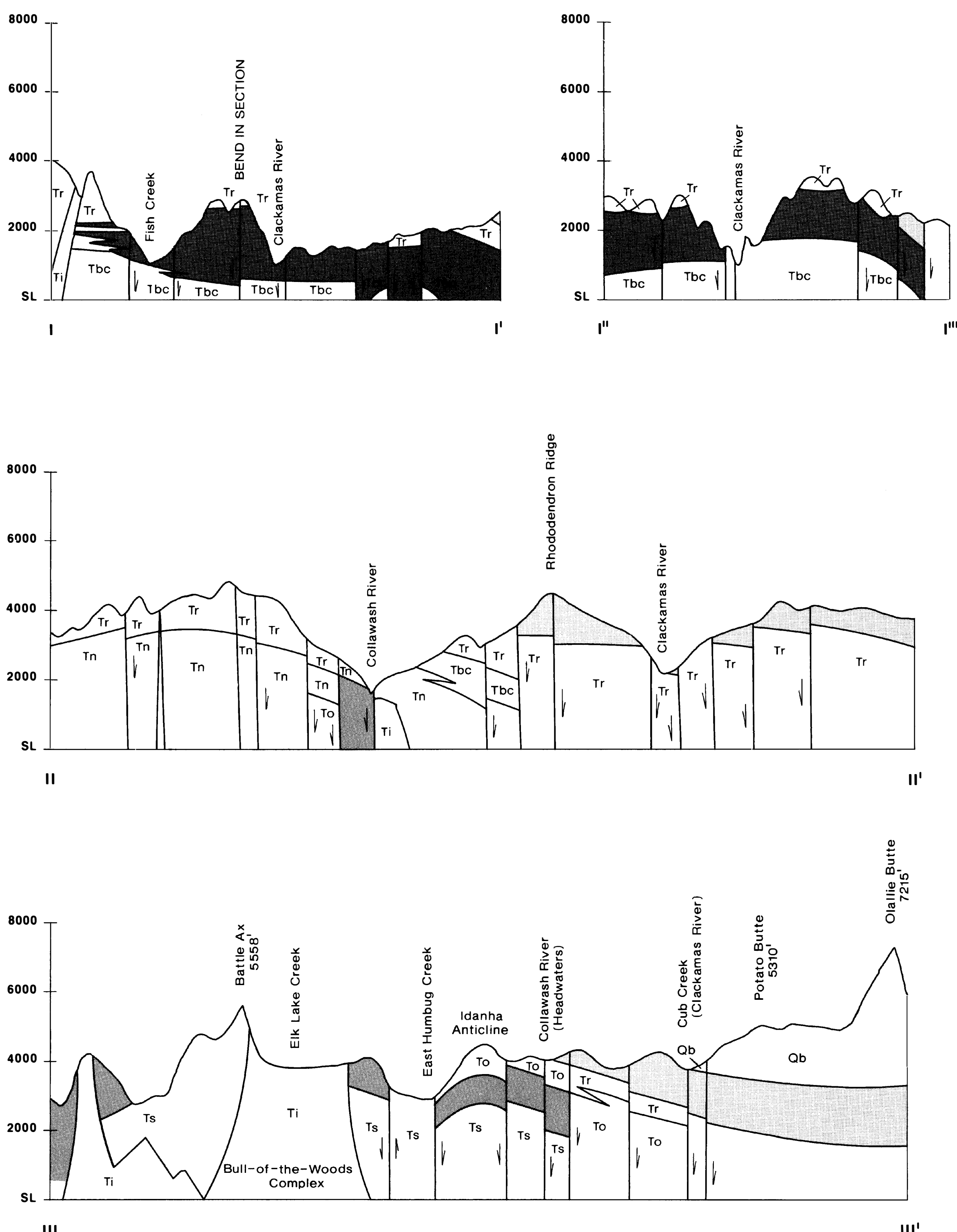

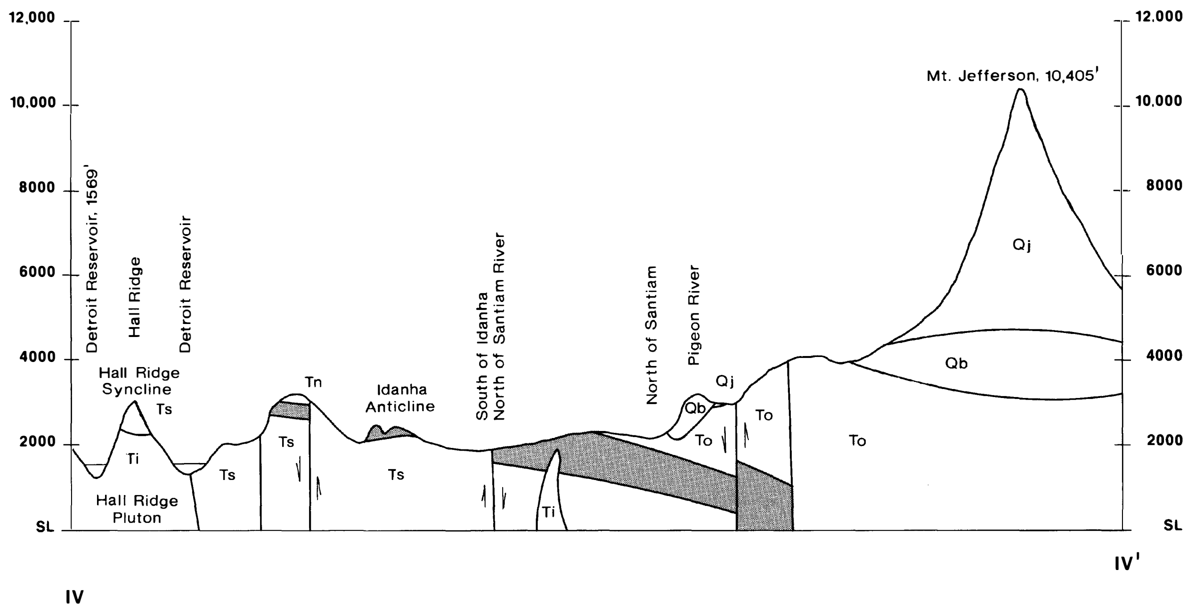

Horizontal Scale ——— Same as Figure 4
Vertical Scale ——— Exaggerated 5X
Legend ——— See Figure 4 and Table 1

Figure 5. Generalized geologic cross-sections of upper Clackamas-North Santiam Rivers, Oregon Cascade Range

Table 2. Radiometric age dates of geologic units in upper Clackamas-North Santiam Rivers area

No.	Date, m.y.[1]	Geologic unit	Symbol	Reference
		HIGH CASCADE GROUP		
1	0.25±0.03	Basaltic lava flow of Battle Ax	QTb	Sutter, 1978, no. 3
2	0.26±0.02	Basaltic lava flow west of Outerson Mountain	QTb	Sutter, 1978, no. 5
3	0.44±0.19	Basaltic lava flow west of Outerson Mountain	QTb	Sutter, 1978, no. 4
4	1.24±0.53 1.41±0.60	Basaltic lava flow of Battle Ax	QTb	Sutter, 1978, no. 1
5	1.88±0.50 1.27±0.41	Basaltic lava flow of Battle Ax	QTb	Sutter, 1978, no. 2
6	2.80±0.18	Basaltic lava flow east of Outerson Mountain	QTb	Sutter, 1978, no. 13
7	3.60±0.05	Basaltic lava flow north of Outerson Mountain	QTb	Sutter, 1978, no. 7
8	4.20±0.30	Tephra interbed at base of High Cascade basalt	QTb	See Table 3, no. 1
		WESTERN CASCADE GROUP		
9	4.55±0.07	Outerson Basalt	To	Sutter, 1978, no. 9
10	4.72±0.19	Outerson Basalt	To	Sutter, 1978, no. 8
11	5.60±0.10	Outerson Basalt	To	Sutter, 1978, no. 6
12	9.68±0.18	Diorite of Detroit (Hall Ridge) pluton	Ti	Sutter, 1978, no. 53
13	10.40±1.20	Rhododendron Formation atop Boulder Ridge	Tr	See Table 3, no. 2
14	10.96±0.75	Rhododendron (?) Fm or Nohorn Andesite(?) near Battle Ax	Tr or Tn	Sutter, 1978, no. 17
15	11.02±0.35	"Sardine" Formation (intrusion?)	Ts	Sutter, 1978, no. 24
16	11.23±0.17	Outerson Basalt	To	Sutter, 1978, no. 18
17	11.50±0.30 11.90±0.30	Near base of Rhododendron Formation	Tr	See Table 3, no. 3
18	12.00±0.40 12.50±0.40	Near base of Rhododendron Formation	Tr	See Table 3, no. 4
19	12.20±0.60 13.00±0.60	Breitenbush Formation: Gray tuff of Boulder Ridge member	Tb	Laursen and Hammond, 1978
20	12.30±0.20 12.60±0.20	Tuff of Rhododendron Formation	Tr	See Table 3, no. 5
21	12.30±0.80 12.70±0.80	Breitenbush Formation: Gray tuff of Boulder Ridge member	Tb	Laursen and Hammond, 1978
22	13.10±0.50 13.10±0.60	Breitenbush Formation: Gray tuff of Boulder Ridge member	Tb	Laursen and Hammond, 1978
23	13.00±0.70 13.30±1.60 13.50±0.50 16.50±1.00	Nohorn Andesite	Tn	Laursen and Hammond, 1978
24	14.50±0.20 15.40±1.00	Breitenbush Formation: Vitrophyric andesite flow of Boulder Ridge member	Tb	See Table 3, no. 6
25	15.50±0.20	"Sardine(?)" Formation atop Hall Ridge	Ts	Sutter, 1978, no. 26
26	15.94±0.21	Andesite dike intruding "Sardine(?)" Formation of Hall Ridge	Ti	Sutter, 1978, no. 25
27	16.72±0.20	Andesite vent rock in "Sardine(?)" Formation of Hall Ridge	Ti	Sutter, 1978, no. 27
28	17.24±0.32 17.18±0.20	Breitenbush Formation: Vitrophyric andesite flow of Boulder Ridge member See no. 24 above	Tb	Sutter, 1978, no. 35
29	18(fission track)	Breitenbush Formation: Gray tuff of Boulder Ridge member See no. 21 above	Tb	See Table 3, no. 7
30	19.74±0.24	Breitenbush Formation: Green tuff of Cleator Bend member	Tb	Sutter, 1978, no. 51
31	23 (zircon: Pb-alpha)	Hornblende diorite stock 8 mi above Detroit Dam	Ti	Laursen and Hammond, 1974
32	23.20±0.80 24.30±1.10	Upper part of "Sardine" Formation	Ts	See Table 3, no. 8
33	24.22±0.27	Upper part of "Sardine" Formation	Ts	Sutter, 1978, no. 52
34	25±10 (zircon: Pb-alpha)	Granodiorite from stock along highway 22 near Detroit Dam	Ti	Laursen and Hammond, 1978

[1] Unless specified, all dates are K-Ar determined.

Table 3. Data on new K-Ar and fission-track radiometric dates

1. R.L. Armstrong (written commun. 1979). Sample no. PH 1 D. Salic tephra interbed near base of High Cascade Group. (44°48.04'N, 121°55.81'W; NW¼NW¼NW¼S14,T9S,R7E; 3600 ft elev.; at end of Spur road 220, off USFS road 4688 (S981); east of Mink Cr; Breitenbush Hot Springs 15' quad., Marion Co., OR). See stop 8. Collector: P.E. Hammond. Analyzer: Joe Harakal, Univ. of British Columbia. Analytical data: %K: $\bar{x}$ = 0.325±0.005±1.5%(2)[1]; Ar^{*40}[2]/Total Ar^{40}=12.1%; Ar^{*40}(10^{-5}cc STP/g)=5.388x10^{-3}; Ar^{*40}/K^{40}=2.431x10^{-4}. Constants: a,b,c. <u>(plagioclase) 4.2±0.3m.y.</u>

2. R.L. Armstrong (written commun.1979). Sample no. PH 40A. Salic tephra bed of Rhododendron Formation interstratified with Outerson Basalt (44°44.91'N, 122°0.55'W; NE¼NE¼SE¼S36,T9S,R6E; 4040 ft elev., along USFS road 2231; (S916), atop Boulder Ridge, Detroit 15' quad., Marion Co., OR). See stop 11. Collector: P.E. Hammond. Analyzer: Joe Harakal, Univ. British Columbia. Analytical data: %K: $\bar{x}$=0.444± 0.008±1.8%(2)[1]; Ar^{*40}[2]/Total Ar^{40}=6.5%; Ar^{*40}(10^{-5}cc STP/g)= 1.839x10^{-2}; Ar^{*40}/K^{40}=6.075x10^{-4}. Constants: a,b,c. <u>(plagioclase) 10.4±1.2m.y.</u>

3. M.C. Parsons (written commun. 1978). Sample no. PEH-77-6 (FRL#4821) Salic tephra bed near base of Rhododendron Formation. (44°59.79'N, 122°8.87'W; NE¼NE¼NW¼S1T7S,R5E;4240 ft elev. along USFS road 53 (S53) east of Thunder Mtn. Battle Ax 15' quad., Clackamas Co., OR). Collector: P.E. Hammond. Analyzer: R.E. Denison, Mobil Research and Development Corporation. <u>(plagioclase) 11.5±0.3m.y.</u>; <u>(plagioclase) 11.9±0.3m.y</u>.

4. M.C. Parsons (written commun. 1978). Sample no. PEH-77-7 (FRL #4822). Welded pyroclastic flow deposit near base of Rhododendron Formation. (44°53.35'N, 122°13.20'W;SE¼SW¼SE¼S8,T8S,R5E; 3600 ft elev. along USFS road 730 (S741) near head of Hugh Cr., Battle Ax 15' quad., Clackamas Co., OR). Collector: P.E. Hammond. Analyzer: R.E. Denison, Mobil Research and Development Corporation. <u>(plagioclase) 12.0±0.4m.y.</u>; <u>(plagioclase) 12.5±0.4m.y.</u>

5. M.C. Parsons (written commun. 1978). Sample no. PEH-77-10 (FRL #4825). Pyroclastic flow deposit of Rhododendron Formation. (44'48.35'N, 121°56.32'W; NW¼NW¼SW¼S10,T9S,R7E; 4100 ft elev. along USFS road 4688 (S981); south of Collawash Mtn., Breitenbush Hot Springs 15' quad., Marion Co., OR). Collector: P.E. Hammond. Analyzer: R.E. Denison, Mobil Research and Development Corporation. <u>(plagioclase) 12.3±0.2m.y.</u>; <u>(plagioclase) 12.6±0.2m.y.</u>

6. M.C. Parsons (written commun. 1978). Sample no. PEH-77-9 (FRL #4824). Vitrophyric andesite lava flow member of Breitenbush Formation. (44°45.05'N, 122°1.18'W; SE¼NE¼NW¼S36,T9S,R6E; 3920 ft elev. along USFS road 2231 (S916), north slope of Boulder Ridge, Detroit 15' quad., Marion Co., OR). See stop 12. Collector: P.E. Hammond. Analyzer: R.E. Denison, Mobil Research and Development Corporation. <u>(whole rock) 14.5±0.2m.y.</u>; <u>(whole rock) 14.7±0.2m.y.</u>; <u>(plagioclase) 14.8±0.9m.y.</u>; <u>(plagioclase) 15.4±1.0m.y</u>.

7. J.A. Vance (personal commun. 1979). Pyroclastic flow deposit, gray tuff of Boulder Ridge Member of Breitenbush Formation. (44°41.46'N, 121°59.76'W; SW¼SW¼NE¼S19,T10S,R7E; 2060 ft elev. along highway 22, 5.0 mi east of Idanha, Mt. Jefferson 15' quad., Marion Co., OR). See stop 22. Collector: P.E. Hammond. Analyzer: J.A. Vance, Univ. Washington. Note: Sample site is part of same roadcut riported in Laursen and Hammond (1978); (zircon, fission-track) <u>18m.y.</u>

8. M.C. Parsons (written commun. 1978). Sample no. PEH-77-8 (FRL #4823). Pyroclastic flow deposit in upper part of "Sardine" Formation. (44°46.88'N, 122°1.01'W; NW¼SW¼NE¼S24,T9SR6E; 2120 ft elev. along USFS highway 46 7.7 mi east of Detroit, Breitenbush Hot Springs 15' quad., Marion Co., OR). See stop 4. Collector: P.E. Hammond. Analyzer: R.E. Denison, Mobil Research and Development Corporation. <u>(plagioclase) 23.2±0.8m.y.</u>; <u>(plagioclase) 24.3±1.1m.y.</u>

Footnotes:

1 Number in parenthesis refers to number of K analyses.

2 Ar^{*40} refers to radiogenic Ar^{40}

Constants:

a λ_{ε}=0.585x10^{-10}yr^{-1}

b λ_{β}=4.72x10^{-10}yr^{-1}

c K^{40}/K=1.19x10^{-4}

Table 4. Hot springs in upper Clackamas-North Santiam Rivers area

Symbol[1]	Name	Location[2]	Elevation[3]	T°C	Volume[4]	Host Rock	Associated Structure	Notes	References
A	Austin (Carey)	SE¼NW¼ 30-6S-7E Fish Cr. Mtn. 15-min. SE Stop 49.	1670/509	86-91	950-1170	Interstratified lava flows, tuffs, and volcaniclastic rocks of the Nohorn Andesite	Major NW-trending fault zone	Issues from several orifices along a 100-m stretch of Clackamas River	Mariner and others (1974); Bowen and others (1978).
B	Bagby	E½NW¼ 26-7S-5E Battle Ax 15-min. NW.	2270/707	58	100	Lava flows of the Nohorn Andesite	Intersection of N- and NW-trending fault zones	Issues from several small orifices on east bench above Hot Springs Creek	Bowen and others (1978).
BB	Breitenbush	NE¼ 20-9S-7E Breitenbush Hot Springs 15-min. SW. Stop 6.	2200/671	92	3400	Tuff of Breitenbush Fm and basalt dikes of probable Outerson Basalt.	Within a zone of several NW- and N-trending faults and basalt dikes.	Issues from about 40 springs along a 400-m stretch of the Breitenbush River.	Mariner and others (1974); Bowen and others (1978).

1 Map symbol (Fig. 4) 2 Sec., Twp., Rge. 3 ft/m 4 liters/min.

deposits. They range in thickness from 30 to 135 m and are separated by fluvial volcaniclastic beds. The tuff contains abundant lithic and pumice fragments and variable amounts of quartz, plagioclase, and pyroxene. Most tuffs are extensively altered and locally colored red to purple. At least three members can be delineated in the Breitenbush area: a lower, pale-green Cleater Bend member (stops 5, 20); a middle, gray Boulder Ridge member with black pumice (stops 16, 22), distinguished locally by eroded pillars (stop 13); and the upper, vitrophyric andesite lava flow member, 95 m thick, atop Boulder and Hoover Ridges (Fig. 2; stop 12). The lower two members each contain two to three flow units. At least nine flow units are recognized in the Happy-Blitzen Creeks section above the Collawash River (stop 42), but none are similar to the Breitenbush section. Two tuff beds are interbedded in the basal Nohorn Formation along the Hot Springs Fork of the Collawash River (Fig. 3; stop 40). Radiometric age dates of the Breitenbush Formation range from 19.7 to 12 Ma (Table 2).

The formation was formerly mapped as part of the Breitenbush Tuff by Thayer (1939) and the Little Butte Series by Peck and others (1964).

The Nohorn Andesite (Tn), a newly recognized unit, contains chiefly lava flows, averaging 30 to 40 m thick, with fluvial volcaniclastic interbeds up to 6 m thick. The lava flows occur in two areas, indicating the possibility that they were erupted from separated centers. The formation is exposed extensively along the Hot Springs Fork of the Collawash River (Figs. 3 and 4; stop 40), where the lava flows are interstratisfied with thin, pyroclastic-flow deposits similar to the tuffs of the Breitenbush Formation. To the east, the lava flows are interstratified with beds of Bull Creek (Fig. 5). The formation is not present in the Breitenbush River drainage, but farther south, in the Blowout Creek drainage southeast of Detroit Reservoir (Fig. 2), similar lava flows are interstratified with pyroclastic-flow deposits of the Breitenbush Formation. The Hugh Creek lava flow, located southwest of stop 40, yielded a radiometric age of 13 to 16.5 Ma (Table 2).

The Nohorn Andesite was formerly mapped as part of the Sardine Formation by Peck and others (1964), McBirney and others (1974), and Sutter (1978).

The beds of Bull Creek (Tbc), occurring in the upper Clackamas River drainage, were informally named by Barnes and Butler (1930) (Table 1). Bull Creek sinks into the large landslide complex just north of the Ripplebrook Ranger Station (Figs. 3 and 4). The strata were included in the Little Butte Volcanic Series by Peck and others (1964). The beds are probably equivalent to the Eagle Creek Formation of the Columbia River Gorge (Wolfe, 1954; Hammond, 1980). They are interstratified to the north with the Grande Ronde Basalt (stops 33 and 34) and to the south with the Nohorn Andesite. No radiometric age determinations of the beds have been made.

Columbia River Basalt Group (Tcr): Tholeiitic flood basalts equivalent to the Yakima Basalt Subgroup of the Columbia Plateau have a thickness of 550 m along the Clackamas River (Beeson and others, 1976a, b; Anderson, 1978). These lava flows thin abruptly to the south over a distance of 10 km and interfinger with strata of the Rhododendron Formation and beds of Bull Creek (Figs. 4 and 5). Two formations of the Yakima Basalt Subgroup are present in the Clackamas River area: the Grande Ronde Basalt and overlying Wanapum Basalt (Frenchman Springs Member) (Anderson, 1978; Fig. 6). Radiometric age dates for these units in the Columbia Plateau range from about 13.5 to 16 Ma (Swanson and others, 1979).

The Grande Ronde Basalt is the most voluminous and laterally extensive formation of the Columbia River Basalt Group within the Clackamas River section. The formation contains 11 lava flows totaling 370 m in thickness. Most Grande Ronde Basalt, exclusive of units Tgn_2h and Tpv (Fig. 6), consists of very fine-grained aphyric flows having well-developed hackly entablatures and less prominent colonnades. Individual flows average 60 m, but locally exceed 90 m, in thickness. Upper, middle, and lower stratigraphic units, consisting respectively of normally (Tgn_2h and Tgn_2l), reversely (Tpv and Tgr_2), and normally (Tgn_1) polarized lava flow sequences (Fig. 6), are equivalent to the "N_2", "R_2", and "N_1" paleomagnetic intervals of the Columbia Plateau (Swanson and others, 1979). The upper N_2 unit is capped by a two-flow sequence, 45-50 m thick, of coarser grained, diktytaxitic, microphyric basalt with blocky to columnar jointing (stop 29) and higher

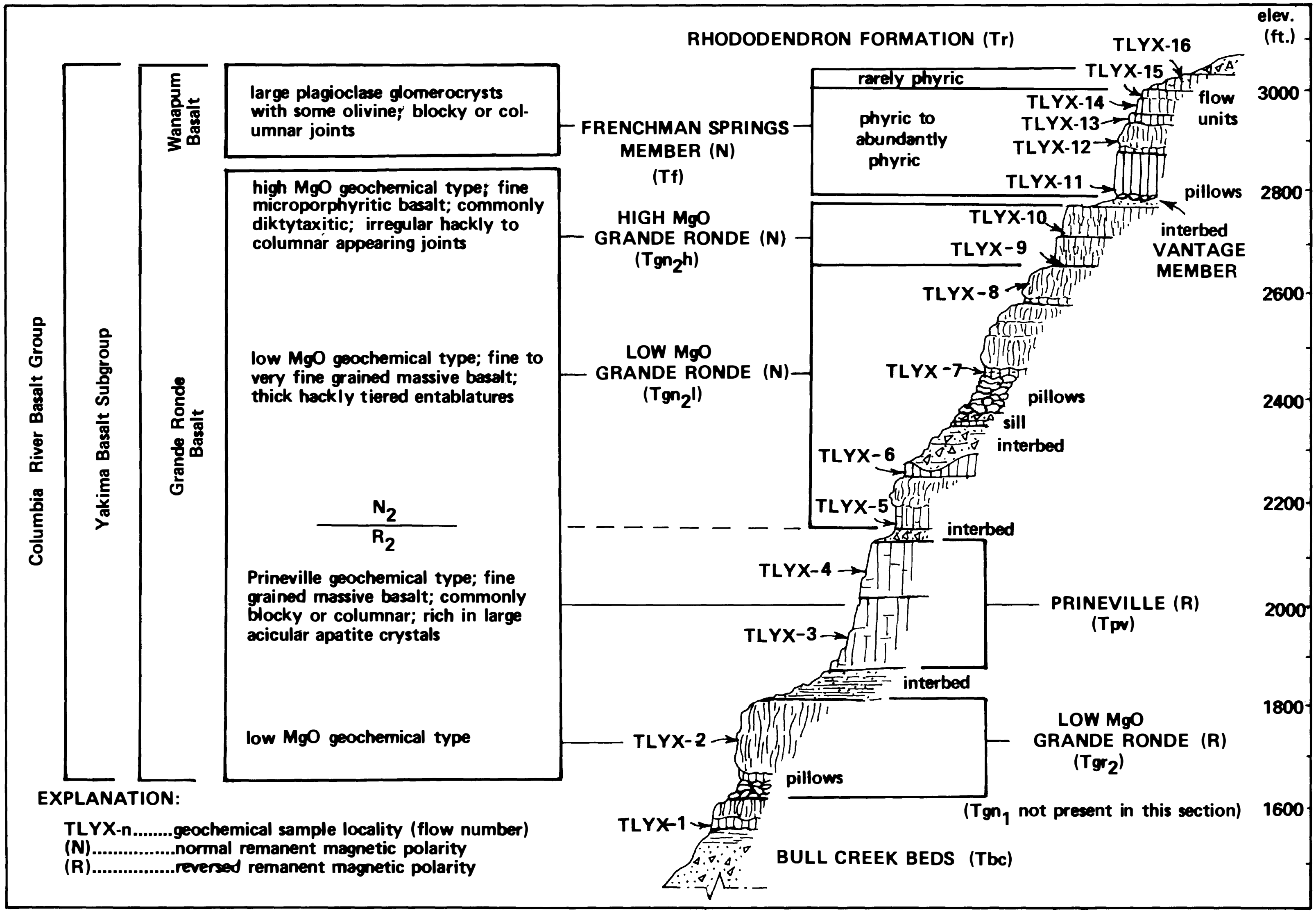

Figure 6. Stratigraphic section of the Columbia River Basalt Group southeast of Three Lynx.

concentrations of MgO than underlying basalt. Similar "high magnesium" flows at the top of the Grande Ronde Basalt have been found elsewhere in northwestern Oregon (Beeson and Moran, 1979) and in the western Columbia Plateau (Wright and others, 1973; Nathan and Fruchter, 1974). The middle R_2 unit is capped by a two-flow sequence, 85-90 m thick, of predominantly columnar-jointed basalt equivalent to the chemically distinctive "Prineville" basalt (Tpv) of Uppuluri (1974). The "Prineville" basalt (stops 28 and 31) resembles the post-Wanapum Saddle Mountains Basalt of the Columbia Plateau but intertongues with Grande Ronde Basalt (Brock and Grolier, 1973; Wright and others, 1973; Swanson and others, 1979).

The Frenchman Springs Member (Tf) of the Wanapum Basalt, up to 110 m in thickness, has plagioclase glomerocrysts ranging in size from 0.5 to 3.5 cm and is therefore distinguishable from Grande Ronde Basalt (stop 30). These flows are characterized by blocky columns, up to 3 m in width, with local zones of platy jointing. The Frenchman Springs flows are generally coarser grained than Grande Ronde Basalt and are distinguishable locally flow by flow by their differing abundance and distribution of phenocrysts. These flows are poorly exposed in the area and commonly form rounded hills behind a broad bench at the top of the Grande Ronde Basalt.

Upper part of the Western Cascade Group: Individual aa and block lava flows and breccia deposits of the Rhododendron Formation (Tr) are 6 to 45 m thick; tephra and pyroclastic flow deposits range from 3 to 180 m thick. The gray pyroxene andesite porphyry lava flows and light-colored pyroclastic deposits form the lower part of the formation in the upper Clackamas River area (stops 43 and 46). A few lava flows are interstratified with the Outerson Basalt along the drainage divide separating the Breitenbush River area (Figs. 4 and 5). Thin pyroclastic deposits extend well southward and are interstratified with the Outerson (stops 11, 19, and 25). The upper, dark-colored lava flows of chiefly olivine-pyroxene andesite porphyry overlie the Columbia River Basalt Group along the Clackamas River and extend northwestward to at least Estacada. The strata were probably derived from eruptive centers in the upper Clackamas River drainage in the area west of the map (Fig. 4).

The formation is continuous with similar volcanic strata mapped west of Mount Hood (Barnes and Butler, 1930; Wise, 1969). It includes most strata mapped as Sardine Formation by Peck and others (1964).

Radiometric age determinations of the rocks range from about 11 to 12.6 Ma (Table 2).

The Outerson Basalt (To), formerly called the Outerson Volcanics by Thayer (1937, 1939), consists predominantly of dark-colored, blocky jointed aa lava flows of phyric olivine basalt (stops 9 and 24). Platy jointed aphyric lava flows are minor (stop 11). Lava flows are 4 to 15 m thick; intervening scoria and breccia beds are 1 to 25 m thick. A lens of palagonitic hyaloclastite and pillow lava occurs on the southern slope of Timber Butte west of Outerson Mountain (Figs. 2 and 4). The strata are intruded by many dikes and plugs of similar basalt.

The formation probably forms the remnant of a large shield volcano complex centered north of Outerson Mountain. It filled a broad valley and blocked drainage, resulting in formation of a lower sequence of palagonitized fluvial and lacustrine volcaniclastic deposits along the northwestern side of the volcano complex (stop 10). These deposits are about 300 m thick and are called the beds of Leone Lake (Clayton, 1976). The basalt lava flows extend well southward along the North Santiam River (stops 24 and 25) as the Grizzly Creek lavas of Rollins (1976), indicating the possibility of additional source areas. The upper part of the Outerson Basalt includes a 245-m section of chiefly volcaniclastic beds called the Cheat Creek beds and the Nan Creek volcanics by Rollins (1976). These beds contain basaltic boulder mudflow and fluvial deposits and several pyroclastic flow deposits of the Rhododendron Formation (stops 18 and 19).

The Outerson Basalt conformably underlies the lighter colored basaltic lava flows of the older High Cascade Group and may therefore be a transitional formation between the Western and High Cascade Groups.

Radiometric ages of the basalt range from about 4.5 to 11 Ma (Table 2).

Intrusions: Of the abundant intrusions (QTi, Ti) in the area (Table 1), some olivine basalt dikes are feeders to the High Cascade basalt (stops 8 and 44). Other dark-colored basalt dikes and plugs are feeders to the Outerson Basalt (stops 9 and 17). Other intrusions (stops 21 and 43) are probable feeders to the Rhododendron Formation including the Camelsback intrusion and its radial dikes (stop 54). Some of the larger dioritic plutons may have been sources of the lava flows and tuffs of the middle Western Cascade Group. The Austin Point intrusion, forming the inner canyon of the Collawash River (stops 38, 39, and 50), is a complex of microdiorite sills. A plug of vitrophyric dacite (?) lies just northwest of the Austin Point intrusion (Fig.4). The large intrusions and their associated dikes form a northeast-trending intrusive zone (Fig. 4). They include the Hall Ridge diorite porphyry of Thayer (1939) and Pungrassami (1969), commonly called the Detroit pluton (stop 2); the intrusions of the North Santiam Mining District (Olson, 1978; Fig. 2); and the Bull-of-the-Woods complex (Jackson, 1980).

The country rock surrounding the Detroit pluton (stop 1) is strongly depleted in ^{18}O at distances up to 3 km from the intrusive contact, indicating that a large meteoric-hydrothermal convection system was associated with the cooling intrusion (Taylor, 1971). The abundant dikes and small plugs and width of alteration suggest that the pluton is the exposed top of a larger intrusion with irregular, outward-dipping contacts. (Fig. 5)

Radiometric ages of the intrusions range from about 9 to 25 Ma (Table 2).

High Cascade Group

In the upper Clackamas-North Santiam Rivers area, the High Cascade Group is separated into three parts: an older High Cascade basalt, a younger High Cascade basalt, and the volcanic deposits of Mount Jefferson (Table 1).

Older High Cascade Basalt: The older High Cascade Basalt (QTb) consists chiefly of gray, blocky to platy-jointed olivine basalt and lesser amount of basaltic andesite aa lava flows, 5 to 30 m thick, separated by interbeds of light-colored conglomeratic volcaniclastic deposits and whitish salic tephra beds, 0.5 to 2 m thick (stops 44, 45, and 47). All strata dip eastward, generally 5 to 10°, but as much as 25° on the eastern slope of Rhododendron Ridge south of Mount Lowe and Collawash Mountain (Figs. 2-5). The lava flows are deeply dissected and generally cap ridge crests, and most eruptive centers have been obliterated by erosion.

The margin of this basalt lies about 10 km west of the younger High Cascade basalt, indicating that High Cascade basaltic volcanism either began in the west and migrated eastward or initiated as a much broader belt, narrowing in time to the crest of the range. A zone of older basaltic eruptive centers extending northwestward from Mount Jefferson through Outerson Mountain to Battle Ax (Fig. 4) was influenced possibly by an underlying zone of shear or extension faulting. The shield volcano of Outerson Basalt lies on this same northwest-trending zone, and its position may also have been structurally controlled.

Most radiometric ages of older High Cascade basaltic rocks range between 4 and 1 Ma (Table 2).

Younger High Cascade Basalt: The younger High Cascade basalt (Qb) also consists chiefly of basalt and lesser basaltic andesite, with interbeds of scoria and fluvial volcaniclastic and tephra deposits similar to the older basalt. The lava flows are medium to light gray, generally containing phenocrysts of plagioclase, olivine, and pyroxene, in decreasing order of abundance (Greene, 1968; Sutton, 1974; Rollins, 1976). Thin interbeds of salic tephra, derived probably from High Cascade stratocone eruptions, occur sporadically yet suggest two styles of volcanism ongoing in this part of the Cascade Range. The younger lava flows, in contrast to the older basalt, are generally flat-lying and form low shield volcanoes and intracanyon lava flows. The latter have commonly well-developed columnar jointing.

Most younger basalt lava flows have normal RMP and are probably younger than 0.69 Ma. Most intracanyon lava flows are overlain by weathered glacial deposits that are older than 10,000 y. Therefore, the younger High Cascade basalt is tentatively considered to be no older than about 1 Ma. Post-glacial (less than about 10,000 B.P.) basaltic volcanism in the area is possibly at the cinder cone southeast of Triangulation Peak (Rollins, 1976) and in the area about Olallie Butte (Fig. 2).

Volcanic deposits of Mount Jefferson: The lava flows of the volcanic deposits of Mount Jefferson (Qj) are aa to block flows, 3 to 5 m thick, separated by scoria and breccia. They are composed chiefly of gray basaltic andesite, bearing abundant plagioclase and lesser pyroxene phenocrysts, and a minor amount of silicic hornblende and dacite (Greene, 1968; Sutton, 1974). Avalanche and mudflow deposits are as equally abundant as lava flows. They consist of light-gray, poorly sorted deposits, 3 to 10 m thick, of angular andesite clasts in pebble to boulder size, in a silty to coarse sand matrix. One post-glacial deposit blocked Hunts Creek to form Pamelia Lake. Another descended Whitewater Creek to its confluence with the North Santiam River (Fig. 4; stop 23). The deposits have normal RMP. Most were deposited pre-glacially, more than about 20,000 B.P., and may be younger than 100,000 B.P.

Structure

The major structures in the area consist of two fault sets: earlier developed, northwest-trending faults of chiefly right-lateral movement and younger, north-south normal faults (Fig. 4). Folding is less well defined. Northwest-trending folds parallel right-lateral faulting in the northern part. Folds trend northeastward in the central part and north-south in the southern part of the area (Fig. 4).

Faulting: The northwest-trending fault set is the most strongly developed structure. The faults are irregularly spaced but well distributed. Few faults, however, are clearly exposed in outcrop. Most faults are shear zones, tens to hundreds of meters wide, containing parallel shear planes. Stops 4, 20, 22, 31, 32, 36, and 39 are among better exposures. Some shear surfaces reveal horizontal right-lateral slickensides; a few have vertical slickensides. The amount of vertical displacement ranges from 60 to 300 m within the Columbia River Basalt Group. The amount of lateral displacement remains uncertain without stratigraphic control but is probably comparable.

Intense right-lateral shearing along the northwest faults is concentrated within a zone about 10 km wide which extends northwestward from southern Rhododendron Ridge, through the Collawash River, and probably southwest of the Clackamas River. The zone is the possible extension of the Sisters fault zone (Lawrence, 1976) and ties with the probable Portland Hills fault to the northwest.

Some plutons were emplaced along northwest-trending faults and subsequently cut by later movement. Among these plutons are the Austin Point intrusion (stops 39 and 50) and the Camelsback intrusion, whose dikes are concentrated along the northwest trend (stop 54) (Fig. 4). Other dikes serving as probable feeders to the older High Cascade basalt lie along northwest faults (stop 44).

The younger north-south normal faults occur principally in two areas: the North Santiam River area and the northeastern part of the upper Clackamas River area (Fig. 4). Generally, the east side of the fault is down-dropped. Displacement ranges from 150 to 300 m. Most younger High Cascade eruptive centers appear to be aligned on these faults.

Northeast-trending faults are widely distributed. They show normal as well as strike-slip movement. Measureable normal displacement ranges from a few meters to more than 150 m (stops 3 and 27).

The relationship of the faults is not clear. The north-south set generally offsets or terminates the northwest set. The northwest set of faults originated probably as early as 12 Ma, whereas the north-south set developed with outpouring of the High Cascade basalt, about 5 Ma. However, movement has continued on some northwest faults, especially those at Rhododendron Ridge. Perhaps some displacement may have been transferred from northwest right-lateral separation to east-west extension on the north-south faults, indicating a possible shift in the regional stress pattern.

Folding: The folds rarely extend any distance. They are open and upright, with the strata dipping generally less than 25° except along fault zones. The folds are terminated or offset by faulting. Possibly the divergent fold directions will be a measure of the amount of displacement along these faults.

Alteration

Several types of alteration affecting rocks of the Western Cascade Group occur in the area: zeolitic, propylitic, phyllic, potassic, and argillic alteration (Peck and others, 1974; Pungrassami, 1969; Taylor, 1971; and Olson, 1978).

Zeolitic alteration is widespread, pervading all volcanic rocks of the lower and middle parts of the Western Cascade Group. Fragmental volcanic rocks are more completely altered than lava flows. The altered rocks vary from well to poorly indurated; the latter are deeply weathered and susceptible to landsliding. Glass and fine crystals and clasts are replaced by aggregates of zeolite--chiefly mordenite and clinoptilolite (Peck and others, 1964), silica, smectite (montmorillonite, celadonite), and carbonate minerals, imparting a greenish color to the rock. Amygdules consist commonly of zeolites--thompsonite, laumontite, stilbite, heulandite, and chabazite--and carbonate minerals, chalcedonic quartz, and various clay minerals.

Hydrothermal propylitic and argillic alteration is local, occurring peripherally and within intrusive rocks. These alterations occur chiefly within the northeast-trending intrusive belt between Detroit Reservoir and Bull-of-the-Woods and are associated with sparse precious and base metal mineralization (Olson, 1978). The propylitically altered rocks are greenish gray and well indurated. Feldspar is partly replaced by albite, and epidote and carbonate minerals; ferromagnesian minerals by chlorite, and epidote and carbonate minerals. Glassy matrix of some rocks is replaced by aggregates of similar minerals. Sericite, celadonite, chalcedonic quartz, and pyrite occur sporadically.

An irregular zone of phyllic alteration, about 7.8 sq km (3 sq mi) in area, that encloses a small core area of less than 0.65 sq km (0.25 sq mi) of potassic alteration, occurs within the northeast-trending propylite zone along the Little North Santiam River (Olson, 1978). Aggregates of quartz, sericite, and kaolinite occur most abundantly in wall rocks of thin mineralized veins within northwest-trending shear and fracture zones. Potassic alteration is characterized by concentration of biotite and lesser potassium feldspar associated with quartz, sericite, and kaolinite.

Alteration tentatively identified as argillic alteration occurs within the vitrophyric andesite lava flow of the Breitenbush Formation atop Hoover Ridge south of Idanha (Figs. 2 and 4). Here about 2.5 sq km (1 sq mi) area of the lava flow is altered to a soft, light-colored mass streaked by various hues of iron oxide. An argillically altered pyroxene andesite intrusion is well exposed along the Clackamas River (stop 48). Argillic alteration at these locations is possibly caused by hydrothermal processes, at least within the limited area of the vitrophyric lava flow. The intrusion may be altered deuterically.

Hot Springs

The locations and characteristics of Austin (Carey), Babgy, and Breitenbush Hot Springs within the upper Clackamas-North Santiam Rivers area (Fig. 4) are summarized in Table 4. The hot springs lie within the north-trending hot spring zone of the western slope of the Cascade Range. These springs contain chiefly sodium chloride waters of largely meteoric origin and are typical of hot-water dominated thermal systems (Mariner and others, 1974).

Glaciation

At least two extensive alpine glaciations are recognized in the area. The older glaciation covered ridge crests, leaving high morainal deposits, and extended far down the valleys. Terminal moraines of this glaciation have not been recognized. Some definitely lie beyond the area of the map (Fig. 4), corresponding to either the Mill City or Detroit moraines of Thayer (1939) in the North Santiam River drainage. Older glaciers of the Clackamas River drainage probably did not extend beyond the map area; their terminal moraines may have been obliterated by the extensive landsliding. The ridge top morainal deposits are up to about 20 m thick and oxidized to depths of 2 m or more. A brown soil, part of which appears to be loessial in origin, mantles much of this deposit, especially on the upland surfaces, for example, east of Oak Grove Butte and the northeastern slope of Rhododendron Ridge. These morainal deposits are probably correlative with the Hayden Creek Drift of Salmon Springs Glaciation of the southern Washington Cascade Range (Crandall and Miller, 1974) and the Jack Creek formation on the eastern slope of the Oregon Cascade Range (Scott, 1977). Its age may be more than 100,000 B.P., based on studies in Washington by Porter (1976) and Waitt (1977).

The younger glaciation was of lesser extent. Its deposits mantle the lower valley slopes and bottoms. They consist of gray morainal till and outwash gravels, locally as much as 20 m thick, with an upper oxidized zone up to 1.5 m thick. Terminal moraines of this glaciation are plotted on the map (Fig. 4), and outwash terraces extend discontinuously downstream from them. These deposits resemble those of Evans Creek Glaciation, between 12,500 and 20,000 B.P., of the Washington Cascade Range (Crandall and Miller, 1974) and are possibly correlative. The deposits are also probably correlative with the Suttle Lake member of the Cabot Creek formation recognized on the eastern slope of the Oregon Cascade Range by Scott (1977).

Landslides

Landslides occur in several forms, ranging from small debris flows to large, creeping earth flows, some covering several square kilometers (stop 39). They are generally associated with either specific geologic units, fault zones, or dike concentrations. In the North Santiam River area, slides occur commonly on the Breitenbush Formation. In the upper Clackamas River area, landslides occur on beds of Bull Creek, the Nohorn Andesite, and Vantage interbed of the Columbia River Basalt Group. In both areas, a few landslides occur on glacial till deposited in steep valleys.

STOPS

Overview of the North Santiam River Area

From its intersection with Interstate Highway I-5 (Exit 253), State Highway 22 ascends a gentle dipslope atop the Columbia River Basalt Group. Before reaching the turnoff to Stayton (11.5 mi from the junction of I-5 and 22), the highway breaks over the ridge crest of the basalt and descends into the broad, gravel-covered valley of the North Santiam River. From Stayton, the highway proceeds eastward and downsection (Table 1), crossing strata of the Rhododendron Formation and the Columbia River Basalt Group and penetrating strata of the middle and lower parts of the Western Cascade Group. Dark-colored lava flows exposed near Mill City (16 mi from the Stayton junction) are part of either the "Sardine" Formation or Nohorn Andesite. As the highway approaches Detroit Reservoir, the valley narrows in response to resistance of the "Sardine" Formation, which was contact metamorphosed by the Hall Ridge or Detroit pluton (Fig. 4). Stop 1 is in hornfels at Detroit Dam; stop 2 is in the pluton (0.7 mi east). The north-trending Hall Ridge syncline is crossed at the eastern margin of the pluton (Fig. 4). Eastward, the route penetrates a thick, west-dipping homoclinal sequence of the "Sardine" Formation, a part of which is examined at stop 3 at Detroit. From Detroit, the tour explores the Breitenbush and North Santiam River valleys and the intervening Boulder Ridge (Fig. 2). The axis of the Idanha anticline and several faults lie between Humbug Creek and Breitenbush Hot Springs along the Breitenbush River (Figs. 2 and 4), which is paralleled by U.S. Forest Service Highway 46 (224). Battle Ax lavas of the basaltic High Cascade Group cap the ridges to the north. The terminal moraine of the last major glaciation lies west of Humbug Creek. Stops 4 and 5 are in tuffs of the "Sardine" and Breitenbush Formations, respectively, east of the fold axis. Breitenbush Hot Springs (stop 6) lies within the widened valley, where erosion, principally glaciation and landsliding, have removed a large part of the fault-disrupted Breitenbush Formation. Stops 7 and 8 to the northeast of the hot springs examine part of the Rhododendron Formation and unconformably overlying High Cascade basalt (Table 1). Stops 9 through 19 cover the stratigraphy and structures exposed in Boulder Ridge. Here, as in all adjacent ridge crests, the older High Cascade basalt dips eastward beneath the crest of the range. Stops 20 through 25 are located along the North Santiam River valley between Idanha and Marion Forks, 4.5 and 14.5 mi east, respectively, of Detroit along Highway 22 (Figs. 2 and 4).

Stops in the North Santiam River Area

Stops are listed numerically 1 through 25 (Figs. 2 and 4). Each is titled and briefly described. Location is given by ¼¼¼ section, township, range; 15-minute quadrangle quarter; latitude, longitude; and elevation, in this order. Access to each stop is given via road number, old U.S. Forest Service road number in parentheses, and distance from nearest main road junction.

North Santiam River Area

1. Contact metamorphosed "Sardine" Formation, by Detroit pluton at Detroit Dam. Location: SE NW NW 7-10S-5E; Detroit NW; 44°43.41'N, 122°14.86'W; 483 m (1585 ft) elev. Along north side of Highway 22, 13.0 mi east of Mill City and 8.1 mi west of Detroit. Parking at dam, south side of highway. High cut of irregularly fractured, probable mudflow breccia, with abundant dark-colored coarse lithic fragments. Contact metamorphosed to albite-epidote hornfels facies. Bedding indistinct. Several northwest-trending shear fractures cut rock.

2. West margin of Detroit pluton along Highway 22. Location: NW SW SE 7-10S-5E; Detroit NW; 44°42.91'N, 122°14.43'W; 506 m (1660 ft) elev. Along north side of Highway 22, 0.7 mi

east of Detroit Dam (stop 1). Parking on south side of highway. Cut exposes two facies of Detroit pluton: contact facies of massive, bluish-gray hornblende granodiorite porphyry with medium-grained phenocrysts of andesine and hornblende in a fine-grained, equigranular groundmass of equal parts orthoclase and quartz; intruded by core facies of massive, light-gray hornblende granodiorite porphyry with medium-grained matrix. Both facies partly altered to clay minerals, epidote, chlorite, and calcite (Thayer, 1939; Pungrassami, 1969).

3. "Sardine" Formation at Detroit. Location: NE SE SE 2-10S-5E; Detroit NW; 44°44.33'N, 122°9.14'W; 488 m (1600 ft) elev. Along southwest side of Highway 22, 0.1 mi northwest of Detroit and junction with Highway 46. Parking on both sides of highway near junction. Westward-dipping interstratified thin- to medium-bedded volcaniclastic sandstone and tuff beds overlain by eutaxitically layered welded tuff unit over 100 m thick. Bedding is displaced in cut and along Breitenbush River by 2-3 northeast-trending normal faults of small magnitude.

4. "Sardine" Formation along Breitenbush River near Scorpion Creek. Location: NW SW NE 24-9S-6E; Battle Ax SE; 44°46.88'N, 122°1.01'W; 646 m (2120 ft) elev. Along north side of USFS Highway 46 (224) 7.7 mi east of junction with Highway 22. Parking along southern shoulder of highway or in quarry just to east. Over 10 m of brown tuff and 2 m of volcaniclastic beds, dipping 15° NE, are exposed on the west. Green crystal (pyroxene-plagioclase)-vitric tuff over 20 m thick, with indistinct bedding, is exposed on the east. It is stratigraphically near the top of the formation and is dated at 23-24 Ma (Table 3, no. 8). The brown and green tuffs are not exposed in contact but are very likely separated by faulting. Several near-vertical north-trending faults showing normal and strike-slip displacement, as shown by slickensides, cut the rocks.

5. Green tuff at Cleator Bend member of Breitenbush Formation. Location: SE SW NE 19-9S-7E; Breitenbush Hot Springs SW; 44°46.72'N, 121°59.76'W; 652 m (2140 ft) elev. Along north side of USFS Highway 46 at junction of roads 2231 (S916) and 4693 (S921), 8.9 mi east of Detroit and 1.0 mi west of Breitenbush Hot Springs store. Parking on south side of highway to east of junction. Walk west 0.2 mi to observe probable Outerson Basalt dike cutting tuff along a fault as well as observing the adjacent cut. Over 135 m of pumice crystal(quartz-plagioclase)-vitric tuff, dipping about 35°SE, forms the lower member of the Breitenbush Formation. Tuff is dated by K-Ar at 19.7 Ma (Table 2).

6. Breitenbush Hot Springs (Table 4). Location: NE 20-9S-7E; Breitenbush Hot Springs SW; 44°46.87'N, 121°58.71'W; 671 m (2200 ft) elev. Store, bungalows, and private baths are located on south side of USFS Road 4600/050, 0.5 mi east of turnoff from Highway 46 (224), 1.0 mi east of junction of road 2231 and Highway 46, and 9.9 mi east of Detroit. Walk, or drive if permitted, to footbridge crossing to bath house on south bank of Breitenbush River. Springs issue from fractures, or faults, and contacts of basalt dikes cutting Breitenbush tuff. Most springs in area are piped. Open hot springs occur along river about 0.25 mi upstream on private land.

7. Rhododendron Formation and older High Cascade basalt between Rapidan and Mansfield Creeks, south of Collawash Mtn. Location: NW NW SW 10-9S-7E; Breitenbush Hot Springs SW; 44°48.35'N, 121°56.32'W; 1250 m (4100 ft) elev. Along west side of USFS road 4688 (S981), after climbing 4.1 mi from junction with Highway 46 (224). This junction lies 1.0 mi east of western end and 0.5 mi west of eastern end, respectively, of Breitenbush Hot Springs road 4600/050. Parking along east shoulder of road or to north at road junction. Light-gray crystal (plagioclase)-vitric tuff, 45 m thick, forms the upper part of a 180-m section of interstratified light-colored fluvial volcaniclastic beds, air-fall tephra, and thin pyroxene andesite porphyry lava flows of Rhododendron Formation. Gray tuff is dated at 12 Ma (Table 3, no. 5). It is cut by a 2.5-m wide dike, trending N30°W, of probable High Cascade basalt. Base of older High Cascade basalt is exposed to the south and north. Good view east to Olallie Butte and southeast to Mt. Jefferson.

8. Older High Cascade basalt south of Collawash Mtn. Location: NW NW NW 14-9S-6E; Breitenbush Hot Springs SW; 44°48.64'N, 121°55.81'W; 1097 m (3600 ft) elev. At end of USFS spur road 4688/220, 1.4 mi from junction with 4688 and 2.1 mi from junction of 4688 and 46 (224). Last 0.2 mi is generally boulder strewn. Parking and turn-around space

lies at first exposed dikes. About 190-m exposed section of interstratified gray olivine basalt aa lava flows, scoria, palagonitized tephra beds, and a salic tephra layer, about 70 cm thick at the top, all dipping 10°E. Section is cut by northwest-trending strike-slip faults and several dikes, 2-4 m wide, of similar phyric basalt. Salic tephra layer yielded date of 4.2 Ma (Table 3, no. 1).

9. Outerson Basalt at ridge end above Skunk Creek, southeast of Breitenbush Hot Springs. Location: SW NW NW 33-9S-7E; Breitenbush Hot Springs SW; 44°45.24'N, 121°57.97'W; 1097 m (3600 ft) elev. Road cuts along south side of USFS road 2230 (1071), the Skunk Creek road, 0.5 mi southeast of junction of roads 2230 and 2231 (S916F). This junction lies 3.3 mi south of junction of road 2231 with Highway 46 (224), 4.4 mi east of junction of road 2231 with 840 (S916), and 5.1 mi east of junction of road 2231 with road 4693 (S921). Parking and turn-around space on outside of bend, north shoulder of road. Base of section of Outerson Basalt. Road cut here exposes parts of two dark-gray phyric plagioclase-olivine basalt aa lava flows, 6-10 m thick, separated by 3-7 m of red to purple scoriaceous breccia. Two north-trending basaltic dikes are emplaced along a fault zone. The beds of Leone Lake (see stop 10) underlie the road. The section is continuous along the road for about 1 km. It is easily examined on foot or by vehicle, although the road is frequently closed by landslides or washouts.

10. Leone Lake beds at base of Outerson Basalt. Location: NE NE SW 31-9S-7E; Mt. Jefferson NW; 44°44.98'N, 121°59.88'W; 1219 m (4000 ft) elev. Roadcut along south side of USFS road 2231 (S916F), 5.2 mi south of junction of road 2231 with Highway 46 (224), and 2.5 mi east of junction of road 2231 and road 840 (S916), and 3.2 mi east of junction of road 2231 with road 4693 (S921). Parking along north shoulder of road. Road cut exposes about 12 m of well-stratified volcaniclastic beds, including laminated fine- to coarse-grained sandstone, claystone, and palagonitic lapilli-breccia. Bedding dips 15° NW. Sandstones show compaction and slump structures. Bedding is disrupted by adjacent landsliding. North-south faulting occurs in valley to west. Additional good exposures lie 0.3 mi east along road.

11. Outerson Basalt intracanyon lava flow amid tuff beds of Rhododendron Formation. Location: NE NE SE 36-9S-6E; Detroit NE; 44°44.91'N, 122°0.55'W; 1231 m (4040 ft) elev. Roadcut along south side of USFS road 2231 (S916F), 1.5 mi east of junction with road 840 (S916) and 2.2 mi east of junction with road 4693 (S921). Parking along north shoulder of road on outside of bend. A 6-m thick, dark-gray phyric olivine basalt aa lava flow fills about a 20-m wide valley cut into about 25 m of interstratified soft light-colored pumice crystal (plagioclase)-vitric tuff beds of different origins. Tuff west of lava flow gave a K-Ar age date of 10.4 Ma (Table 3, no. 2).

12. Vitrophyric andesite lava flow member of Breitenbush Formation atop Boulder Ridge. Location: SE SE NW 36-9S-6E; Battle Ax SE; 44°45.05'N, 122°1.18'W; 1195 m (3920 ft) elev. Roadcut along west side of USFS road 2231 (S916F), 0.6 mi east of junction with road 840 (S916) and 1.3 mi east of junction with road 4693 (S921). Parking along both shoulders of road. Typical poor exposure of vitrophyric andesite. Rock is K-Ar age dated at 14.5-15.5 Ma (Table 3, no. 6) and 17 Ma (Table 2, no. 28).

13. Gray tuff of Boulder Ridge member of Breitenbush Formation. Location: NW SE NW 36-9S-6E; Battle Ax SE; 44°45.15'N, 122°1.33'W; 1177 m (3860 ft) elev. Roadcut along south side of USFS road 2231 (S916F), 0.3 mi east of junction with road 840 (S916) and 0.8 mi east of junction with road 4693 (S921). Parking on north shoulder of road. Roadcut exposes upper oxidized zone of lower pyroclastic flow unit of member, chiefly a lithic-pumice crystal (plagioclase)-vitric tuff. This unit is approximately 200 m thick. The upper unit is similar but about 100 m thick. It is intensely welded, has black pumice (observable in boulder float to west), and weathers to form columns resembling stone statues which can be seen on the slopes to the west.

14. Fault block of "Sardine" Formation tuff east of Eagle Rock. Location: SW SW SW 24-9S-6E; Battle Ax SE; 44°46.33'N, 122°1.67'W; 1049 m (3440 ft) elev. Roadcut along west side of USFS raod 4693 (S921), 2.2 mi north of junction with road 2231 (S916F) and 3.2 mi south of junction with Highway 46 (224). Parking on east shoulder of road. Light-colored tuff containing sparse lithic fragments lies between parallel faults trend-

ing N70-75°W. Volcaniclastic sandstone is poorly exposed on the west. To the east lies a 75-m thick brown silicified lithic breccia of probably mudflow origin. It dips about 20° SE and is cut by several northwest-trending faults.

15. Basalt sill atop conglomerate of "Sardine" Formation, east of Eagle Rock. Location: NE SE SW 24-9S-6E; Battle Ax SE; 44°46.47'N, 122°1.21'W; 927 m (3040 ft) elev. Roadcut along south side of USFS road 4693 (S921), 2.3 mi southwest of junction with Highway 46 (224), and 3.1 mi north of junction with road 2231 (S916F). Parking along north shoulder of road. Roadcut exposes more than 3 m of silicified layered conglomerate, probably part of lithic breccia exposed at stop 14, overlain sharply by a blocky jointed sill, over 7 m thick, of fine-grained basalt. Similar basalt intrusions are abundant locally, one forming Eagle Rock, and are probably part of the Outerson Basalt. Units are cut by a northwest-trending fault, showing about 3 m of normal displacement. Excellent view of Breitenbush Valley from road bend to west.

16. Black pumice-bearing gray tuff of Boulder Ridge member of Breitenbush Formation. Location: NE NE NW 1-10S-6E; Detroit NE; 44°44.45'N, 122°1.20'W; 1128 m (3680 ft) elev. Roadcut on north side of USFS road 810 (S916E), 0.9 mi north of junction with road 515 (1071A), and 2.8 mi east of junction with the Boulder Ridge road 2231 (S916). This junction lies 2.4 mi south of junction of roads 2231 (S916) and 4693 (S921). It also lies about 3.5 mi north of State Highway 22, about 1 mi west of Idanha. Parking along the south shoulder of the road. Road cut exposes about 18 m of gray eutaxitically layered highly welded lithic-pumice crystal(plagioclase)-vitric tuff. Glassy pumice contains plagioclase phenocrysts. This tuff is the uppermost flow unit of the member and weathers to form the stone statues standing above stop 13. It is overlain just to the east (at the road bend) by the vitrophyric andesite lava flow. Here the tuff is cut by northwest-trending shear zone. Paralleling faults are abundant in this area.

17. Outerson Basalt dikes cutting gray tuff member of Breitenbush Formation south of Gale Hill. Location: SW NE NW 6-10S-7E; Detroit NE; 44°45'N, 122°0.12'W; 1274 m (4180 ft) elev. Roadcut on west side of USFS road 810 (S916E), 4.3 mi east of junction with Boulder Ridge road 2231 (S916). See stop 16. Parking along east shoulder of road. Six basalt dikes, 1-4 m thick, intrude this tuff. Remnant of breccia cone, to which these dikes were feeders, lies upslope. Northwest-trending right-lateral fault cuts tuff. Immediately north, older High Cascade basalt lies in contact with Breitenbush Formation along unexposed northwest-trending fault.

18. Cheat Creek beds west of Outerson Mtn. (Rollins, 1976). Location: SE NE SW 9-10S-7E; Mt. Jefferson NW; 44°43.15'N, 121°57.39'W; 1414 m (4640 ft) elev. Roadcut along north side of USFS road 2233/650 (1071M), 0.8 mi east of junction with McCoy Creek road 2233 (1071). This junction lies 7.7 mi north via Mc Coy Creek road from junction with State Highway 22, about 1.5 mi east of Idanha. Parking along south shoulder of road. Stop is at base of well-exposed section, about 200 m thick, of light-colored interstratified fluvial volcaniclastic, tephra, and pyroclastic flow deposits of interfingering Outerson and Rhododendron formations. Several northwest-trending faults cut and repeat the section.

19. Gray pumice tuff of Outerson Mountain. Location: NW SE NE 9-10S-7E; Mt. Jefferson NW; 44°43.42'N, 121°57.01'W; 1463 m (4800 ft) elev. Eastern slope of Outerson Mountain along west side of USFS road 2233/650 (1071M), 1.4 mi east of junction with road 2233 (1071). See stop 18. Parking along east side of road just to north. Well-exposed, gray pumice vitric tuff, about 60 m thick, caps section of Cheat Creek beds. Tuff is of pyroclastic flow origin and shows excellent zonation, from a thin base surge layer, through a 6-m thick shear flowage zone, 6-m thick lithic-rich zone of mostly angular phyric olivine basalt, into the upper massive part. Tuff is unwelded. It is overlain by red lithic breccia of basalt, over 15 m thick. This breccia is in turn overlain by older High Cascade basalt lava flows. The tuff is considered tentatively as part of the Rhododendron Formation, is interstratified with volcaniclastic Outerson Basalt, and is conformably overlain by High Cascade Basalt. Several northwest and north-south faults cut these units.

20. Faulted green tuff of Cleator Bend member of Breitenbush Formation east of Idanha.

Location: SW NW SE 23-10S-6E; Detroit NE; 44°41.31'N, 122°2.22'W; 579 m (1900 ft) elev. Along north side of State Highway 22, 1.9 mi east of Idanha. Parking along south side overlooking North Santiam River. Long roadcut exposes pervasively faulted green tuff and brown-weathering fine-grained basalt dike. Flat-lying faults with north-south movement are exposed at eastern end of cut.

21. Intrusion near Whispering Falls campground. Location: NW NW SE 24-10S-6E; Detroit NE; 44°41.47'N, 122°0.96'W; 591 m (1940 ft) elev. High roadcut along north side of State Highway 22, 1.1 mi east of Idanha. Parking along both sides of highway west of cut. Cut exposes brown-weathering and zeolitized microdiorite. Inclined columnar jointing suggests that intrusion is a sill. It resembles the Austin Point intrusion (stop 50).

22. Gray tuff of Boulder Ridge member of Breitenbush Formation, between Whispering Falls campground and Whitewater Creek. Location: SW SW NE 19-10S-7E; Mt. Jefferson NW; 44° 41.46'N, 121°59.76'W; 628 m (2060 ft) elev. Long roadcut along north side of State Highway 22, 2.7 mi east of Idanha, 0.8 mi east of Whispering Falls campground, and 1.4 mi west of Whitewater Creek. Parking along south side of highway at east end of cut. Roadcut exposes pervasively faulted crystal (plagioclase)-vitric tuff, chemically analyzed as dacite (Peck and others, 1964, Table 7, no.18). Tuff has been radiometrically dated at 12 and 18 Ma (Table 2, nos. 21 and 29, respectively). It is probably the lower flow unit of the member. See stops 13 and 16. Columnar-jointed intracanyon basalt of Pigeon Prairie (younger High Cascade basalt) overlies the tuff.

23. Whitewater Creek mudflow deposit from Mt. Jefferson. Location: NE SE SE 20-10S-7E; Mt. Jefferson NW; 44°41.15'N, 121°58.13'W; 671 m (2200 ft) elev. Cut along east side of State Highway 22, 0.2 mi south of bridge over Whitewater Creek and 5.3 mi north of Marion Forks. Parking on west shoulder of highway just south of cut. Low cut exposes about 2 m of friable gray sand enclosing coarse angular andesitic fragments from Mt. Jefferson.

24. Outerson (?) Basalt south of Pamelia Creek. Location: NE SW SE 33-10S-7E; Mt. Jefferson NW; 44°39.52'N, 121°57.15'W; 704 m (2310 ft) elev. Cut along east side of State Highway 22, 3.5 mi north of Marion Forks. Parking along west side of highway overlooking North Santiam River. About 20-m-high cut exposes thin gray phyric olivine basalt lava flows and enclosing scoria of probable Outerson Formation.

25. Mystery roadcut north of Marion Forks. Location: SW NW NE 10-11S-7E; Mt. Jefferson NW; 44°38.18'N, 121°56.24'W; 719 m (2360 ft) elev. Roadcut along east side of State Highway 22, 1.7 mi north of Marion Forks. Parking along west side of highway at north end of cut. About 20-m-section of interstratified basaltic lava flow, conglomeratic breccia, and 2-3 m of light-colored tephra and volcaniclastic beds. Lava and breccia are of probable Outerson Basalt; light-colored beds are of the Rhododendron Formation. Section is cut by several faults most of which trend northwestward paralleling the valley. Movement on these faults has been generally down on the south side.

Overview of upper Clackamas River area

Estacada lies at the head of a series of broad alluvial fans, now dissected to form terraces, which grade to the Willamette River (Fig. 1). The oldest terrace, underlain by the Springwater Formation of Trimble (1963), lies at the higher elevation and is inclined more steeply than the younger terraces, indicating uplift of this part of the range since its formation.

The Rhododendron Formation is the bedrock at Estacada. From here the tour proceeds southeastward up the Clackamas River. The canyon walls rise gradually, eventually exposing the underlying Columbia River Basalt Group at North Fork Reservoir, 7.5 mi above Estacada (Figs. 3 and 4). From the North Fork Reservoir southward, the basalt forms steep canyon walls, capped locally by Rhododendron Formation and overlying intracanyon basalt lava flows of the High Cascade Group. Stops 26 through 36 look at the stratigraphy and structures of the Columbia River Basalt Group. Starting at Three Lynx, the Clackamas River valley is widened by landsliding of the middle part of the Western Cascade Group. The basalt overlies beds of Bull Creek (probably equivalent to the Eagle Creek Formation) and Nohorn Andesite (Fig. 4, Table 1). South of the extent of the Columbia River Basalt Group, in the headwaters of Memaloose and Fish Creeks south of the Clackamas River (Figs. 3 and 4), strata of the middle Western Cascade Group are also exposed.

Columbia River basalt forms steep canyon walls at the northern end of Fish Creek. Stops 51, 52 and 53 are near the southern extent of the basalt. At stop 51, the basalt has been cut out by one of the northwest-trending faults. Farther south in Fish Creek (stop 54), the Camelsback intrusion and radial dike system are examined. Columbia River basalt lava flows interfinger with beds of Bull Creek and thin out. None of the basalt lava flows is cut by the Camelsback intrusion.

The Collawash River area south of its junction with the Clackamas River (Figs. 3 and 4) is characterized by extensive landsliding, several intrusions, and warped and faulted strata of the Western Cascade group. Stops 37 through 43 examine the geology in this area. Bagby Hot Springs is located along Hot Springs Creek, about 1 mi south by trail, from road 70 (S-70). The springs are located along the intersection of north-south and northwest-trending faults which are exposed at stop 40.

The north-trending Rhododendron Ridge separates the Collawash River from the uppermost Clackamas River. The ridge is underlain, in descending order, by High Cascade basalt, Rhododendron Formation, beds of Bull Creek, Nohorn Andesite, Breitenbush Formation, and "Sardine" Formation, forming almost a complete section of this part of the Oregon Cascade Range (Fig. 4, Table 1), and cut by several northwest-trending faults. Stops 42 through 46 reveal some of the geologic relations in Rhododendron Ridge.

The uppermost Clackamas River valley, dominated by symmetrical Sisi Butte cone, follows north-south fault zones in which the High Cascade basalt and Rhododendron Formations are juxtaposed (Figs. 3 and 4). Stops 47 through 50 cover part of the geology exposed along the Clackamas River, including small intrusions, one of which is hydrothermally altered (stop 48), and Austin Hot Springs (stop 49), located 6.8 mi above the Oak Grove Fork. Austin Hot Springs occurs along the Oak Grove Butte-Lake Harriet fault zone examined at stop 36. During the last major glaciation, a glacier descended the upper Clackamas River valley to Big Bottom, 4.9 mi above Austin Hot Springs (Figs. 3 and 4).

Stops in the upper Clackamas River Area

Stops are listed numerically, 26-54 (Figs. 3 and 4). Each is titled and briefly described. Location of each is given by ¼¼¼ section, township, range; 15-min. quadrangle quarter; latitude, longitude; and elevation, in this order. Access to each is given via road number, old U.S. Forest Service road number in parentheses, and distance from nearest main road junction.

26. Contact relationship between Rhododendron Formation and Columbia River Basalt Group along North Fork Reservoir. Location: SE NE NE 13-4S-4E; Colton NE; 45°13.5'N, 122° 15.1'W; 218 m (715 ft) elev. On USFS highway 46 (224), 0.5 mi northwest of junction with road S-403. The top of the Frenchman Springs Member of the Wanapum Basalt can be seen along the south shore of the reservoir. Rocks on the north side at the same elevation are intracanyon Rhododendron Formation volcaniclastics and lava flows.

27. Promontory Park fault (Fig. 7). Location: NE SW NW 20-4S-5E; Fish Creek Mtn. NW; 45°12.7'N, 122°14.7'W; 219 m (717 ft) elev. Along USFS highway 46 (224), 1 mi southeast of junction with road S-403. This fault offsets the section more than 150 m down to the northwest, exposing flows of the Grande Ronde Basalt on the southeast side. Many flow structures characteristic of flood basalts can be seen in the road cuts. A prominent bench can be seen approximately 120 m above the south side of the river. This bench persists throughout the Clackamas River canyon area and is a major landslide surface.

28. Prineville and Grande Ronde Basalt flows at Big Cliff (Fig. 8). Location: NW NE NW 29-4S-5E; Fish Creek Mtn. NW; 45°12'N, 122°14.6'W; 220 m (720 ft) elev. Along the north side of USFS highway 46 (224), 1 mi northwest of junction with road 45 (S-561). The overlying Grande Ronde flows have well-developed colonnade and entablature in contrast to the underlying Prineville flows which consist entirely of broad columns. The Big Cliff fault (Fig. 7) does not offset units at this locality, but controls the direction of the Clackamas River from Promontory Park. Numerous en echelon shears can be seen cutting the cliff face.

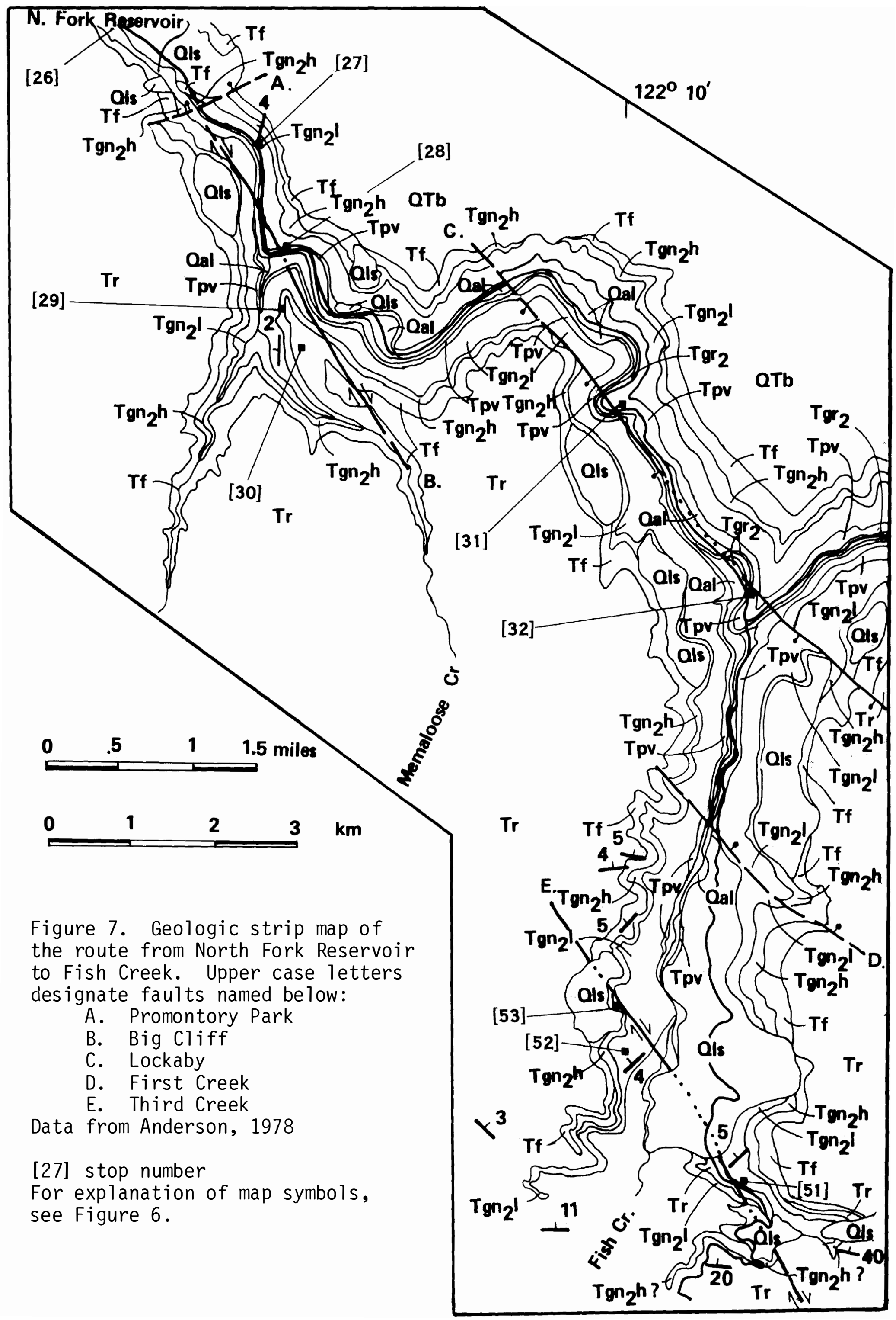

Figure 7. Geologic strip map of the route from North Fork Reservoir to Fish Creek. Upper case letters designate faults named below:

A. Promontory Park
B. Big Cliff
C. Lockaby
D. First Creek
E. Third Creek

Data from Anderson, 1978

[27] stop number
For explanation of map symbols, see Figure 6.

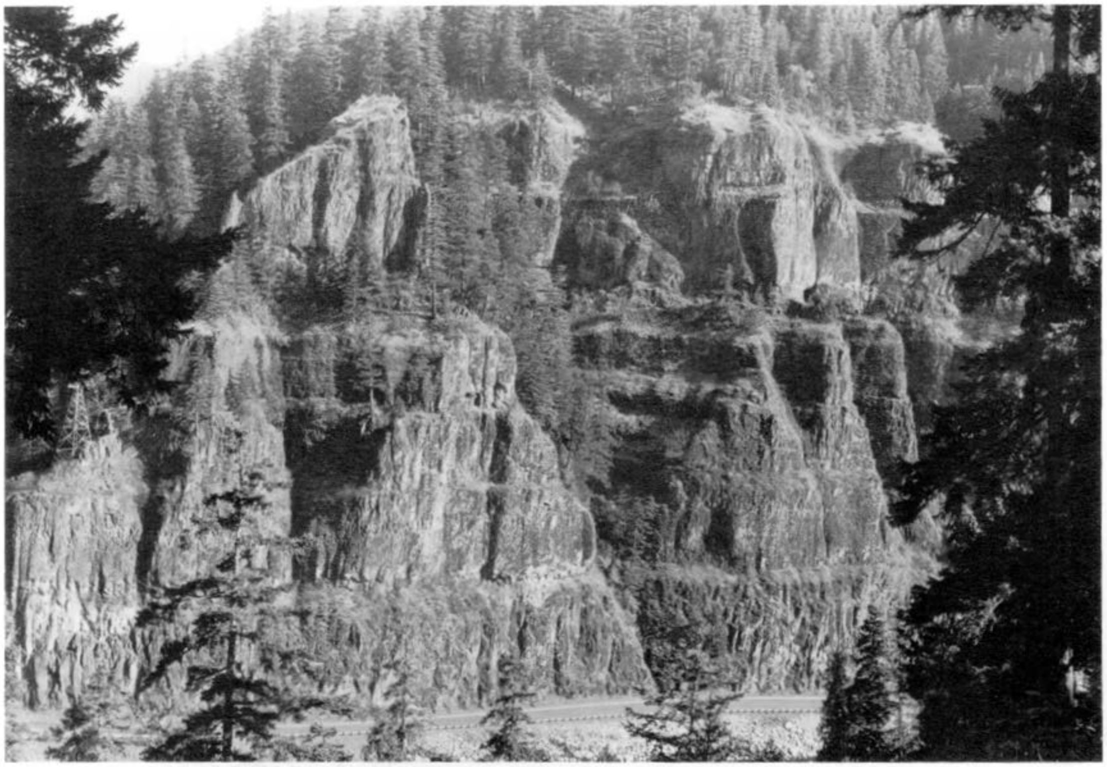

Figure 8. Normally magnetized Grande Ronde Basalt (Tgn_2h and Tgn_2l) overlying reversely magnetized Prineville basalt flow (Tpv) at road level at Big Cliff. A northwest-trending strike-slip fault, in forested ravine at center, cuts cliff without visible offset of flow contacts (stop 28).

Figure 9. Interbed at top of the Grande Ronde Basalt, considered to be lithostratigraphic equivalent of the Vantage Member of the Ellensburg Formation (stop 29).

29. Sedimentary interbed at the top of the Grande Ronde Basalt (Fig. 9). Location: SW SE NW 29-4S-5E; Fish Creek Mtn. NW: 45°11.8'N, 122°14.6'W; 366 m (1200 ft) elev. On the east side of road 45 (S-561), 1 mi from highway 46 (224) junction (Memaloose Bridge). This interbed is a lithostratigraphic equivalent of the Vantage Member of the Ellensburg Formation. The underlying flow top is deeply weathered contributing to block gliding involving overlying Frenchman Springs flows. Like other interbeds in the upper half of the basalts, this unit compositionally resembles the overlying Rhododendron Formation.

30. Frenchman Springs flows above the Vantage horizon. Location: SE NE SW 29-4S-5E; Fish Creek Mtn. NW; 45°11.5'N, 122°14.6'W; 427 m (1400 ft) elev. On the east side of road 45 (S-561), 1.5 mi from highway 46 (224) junction. Plagioclase glomerocrysts, up to 3.5 cm in size, are present in hand specimen, distinguishing these flows from the underlying aphyric Grande Ronde basalts. A four-flow sequence is exposed in relatively continuous outcrop extending uphill from this stop.

31. Prineville basalt at Big Eddy. Location: NW SW NW 35-4S-5E; Fish Creek Mtn. NW; 45°11.0'N, 122°10'W; 256 m (840 ft) elev. On the north side of highway 46, adjacent to Big Eddy campground. A hackly-jointed Grande Ronde flow is exposed beneath columns of two Prineville flows, clearly demonstrating the interfingering of these two units (Fig. 7).

32. Northwest-trending Lockaby fault in Clackamas River. Location: NW NW SW 1-5S-5E; Fish Creek Mtn. NW; 45°9.5'N, 122°5.75'W; 278 m (912 ft) elev. East side of Clackamas River channel, 0.25 mi north of junction of highway 46 and road 54 (S-54). Like the en echelon Big Cliff fault, the Lockaby fault controls the orientation of the river over a distance of several miles. Blocky-jointed Prineville basalt can be seen against hackly jointed Grande Ronde Basalt along the fault.

33. Interbed in Grande Ronde Basalt (Tgr_2). Location: SW SW SW 9-5S-6E; Fish Creek Mtn. NE; 45°8.5'N, 122°5.0'W; 348 m (1140 ft) elev. On the north side of highway 46, 4.5 mi east of junction with road 54 (S-54). Interbeds in the Columbia River Basalt increase in abundance and thickness to the south. The interbed exposed at this stop is near the base of the Grande Ronde Basalt and is compositionally similar to the older beds of Bull Creek. Fluvial gravels and a lahar are nested against these older rocks at the west end of the road cut. At The Narrows (Fig. 3) strike-slip faulting (Fig. 12) controls this reach of the river, between stops 36 and 37.

34. Base of the Columbia River Basalt. Location: NE NE NE 16-5S-6E; Fish Creek Mtn. NE; 45°7.5'N, 122°4.5'W; 344 m (1130 ft) elev. Along the north side of highway 46, 0.5 mi north of junction with road 55 (S-55). The road cuts here reveal the base of the Grande Ronde Basalt, the underlying beds of Bull Creek, the rarely seen N_1 (normal magnetic polarity) basalt flow, an interbedded lahar, and two intersecting faults. The Dinner Creek fault (Fig. 12) trends at an oblique angle to the road exposing tectonic breccia as a broad swath along the road cut. Abundant dip-slip slickensides and two minor offsets are visible. The base of the Columbia River Basalt Group lies above the Three Lynx power house and flume (Fig. 3). Lowest exposed flows occur at the top of the pipeline; the N_1 flow exposed at stop 34 has thinned out.

35. Overview of complete Columbia River Basalt Group section. Location: SW SW NW 27-5S-6E; Fish Creek Mtn. NE; 45°7'N, 122°4.5'W; 366 m (1200 ft) elev. Looking northwest from highway 46, 0.5 mi south of road 53 (S-53) at Sandstone Creek bridge crossing. The entire Columbia River Basalt Group section (less N_1) is exposed in the cliffs to the southwest (Fig. 6). A broad landslide bench caps the basalt and marks the contact with the overlying Rhododendron Formation. To the south of this stop are over 10 sq mi of landslide debris.

36. Grande Ronde Basalt in fault contact with Wanapum Basalt along Lake Harriet fault (Fig. 12). Location: NE SE NW 5-4S-7E; High Rock NW; 45°4.5'N, 121°59'W; 612 m (2040 ft) elev. On the south side of road 57 (S-57), about 4.5 mi east of junction with highway 46. A northwest-trending fault is exposed in road cuts above an abandoned cinnabar mine. Rocks in the vicinity of the fault are altered; consequently, plagioclase glomerophenocrysts of the Frenchman Springs Member are difficult to identify. A

Figure 10. Interbed within Grande Ronde Basalt (Tgn_2l) at stop 52 is compositionally similar to overlying Rhododendron Formation. A second interbed at base of trees, above, contains leaf fossils.

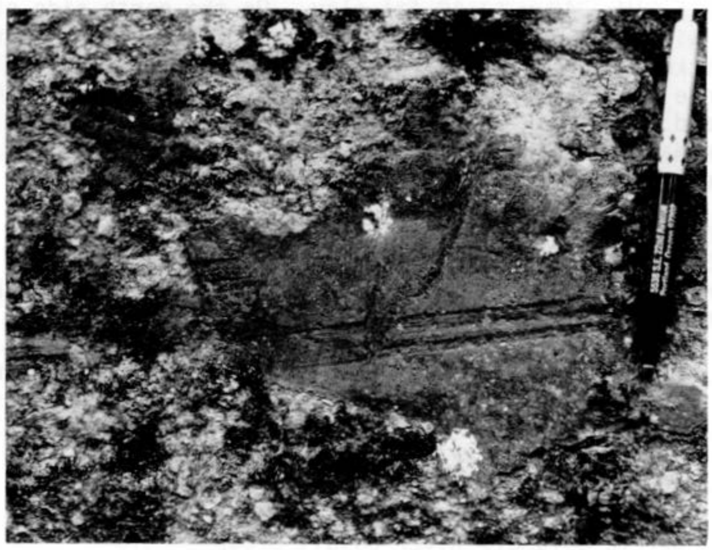

Figure 11. Horizontal and sub-horizontal slickensides at Third Creek fault (stop 53).

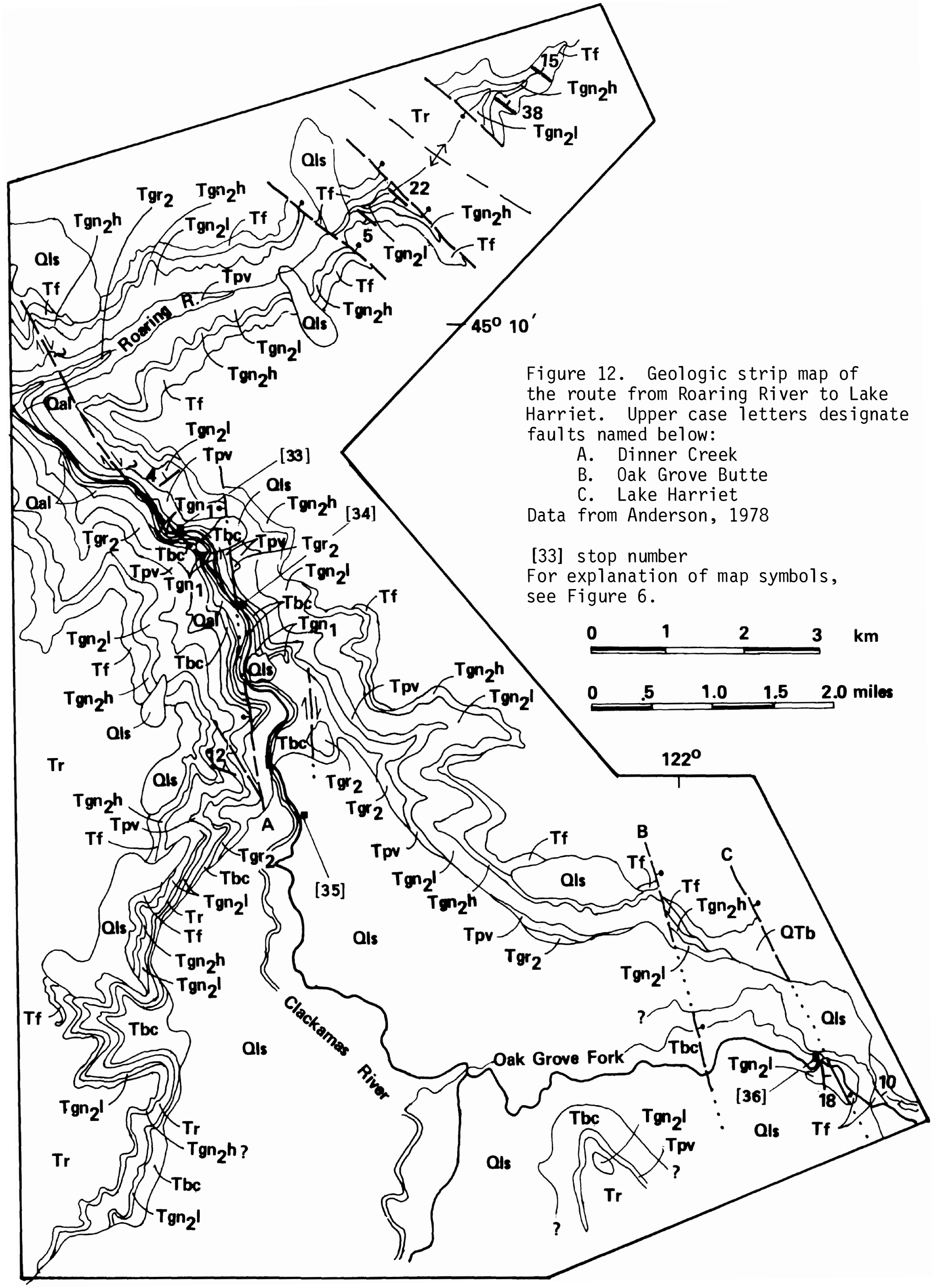

Figure 12. Geologic strip map of the route from Roaring River to Lake Harriet. Upper case letters designate faults named below:
A. Dinner Creek
B. Oak Grove Butte
C. Lake Harriet
Data from Anderson, 1978

[33] stop number
For explanation of map symbols, see Figure 6.

Grande Ronde flow and thick pillow complex overlies a volcaniclastic interbed on the southwest side of the fault; the Frenchman Springs Member lies to the northeast side of the fault. The offset on this fault is at least 150 m down to the northeast and the collective throw across the Lake Harriet fault zone is more than 300 m.

37. Warped strata of Breitenbush Formation across Collawash River from Raab Campground. Location: SW NW NW 27-6S-6E; Fish Creek Mtn. SE; 45°1.28'N, 122°4.28'W; 457 m (1500 ft) elev. View from west side of campground off USFS highway 46 (224), 0.8 mi south of junction of roads 63 (S-63) and 46. This junction is 3.7 mi south of junction of Oak Grove Fork road 57 (S-57) with 46. Stream cut is accessible by walking about 0.25 mi from stop 38. Cut exposes about 40-m section of interstratified pyroclastic flow deposits and fluvially deposited volcaniclastic strata, dipping 45°NW. A coarse mudflow breccia underlies the section to the south and is exposed about 100 m along the east river bank to the north of the viewpoint.

38. Basal contact of Austin Point intrusion (sill) with Breitenbush Formation. Location: SE SW NW 27-6S-6E; Fish Creek Mtn. SE; 45°1.28'N, 122°4.11'W; 502 m (1680 ft) elev. Take quarry road (S-63P) to west immediately south of Collawash River bridge on road 63 (S-63) 1.1 mi south of junction of roads 63 and 46 (224). Over 30-m thick sill-like intrusion of porphyritic microdiorite atop purplish thin-bedded volcaniclastic deposits. Contact is a sharp plane, dipping 30°SE. Intrusion is brecciated and zeolitized in lower 6 m; lower meter is a glassy chill zone with aligned plagioclase phenocrysts. Jointing in intrusion suggests two episodes of emplacement and cooling.

39. Shear planes in Austin Point intrusion and Collawash landslide. Location: NW SW NE 34-6S-6E; Fish Creek Mtn. SE; 44°0.39'N, 122°3.57'W; 469 m (1540 ft) elev. Along USFS road 63 (S-63), 2.7 mi south of junction of roads 63 and 46 (224). Parking along west side below steep face just north of bend. Northwest-trending shears occur in microdiorite intrusion along 100-m zone. Basal contact of sill, dipping 30°W, lies to northeast across Collawash River. Active Collawash landslide, easily recognized by its hummocky terrain and "drunken" forest, has heaved river sediments against west bank of intrusion.

40. Faults and andesite porphyry dike cutting interstratified lava flows and tuff beds of probable lower Nohorn Andesite. Location: NW NW SW 22-7S-5E; Battle Ax NW; 44°56.8' N, 122°11.5'W; 732 m (2400 ft) elev. Road cuts along south side of USFS road 70 (S-70), the Hot Springs Fork road, 7.8 mi west of junction of roads 70 and 63 (S-63) and 1.9 mi west of trail head to Bagby Hot Springs (Table 4). Road 70 lies 4.0 mi south of junction of roads 63 and 46 (224). Parking along north shoulder of road. About 200 m of road cut and the slope below expose about a 75-m stratigraphic section of the Nohorn Andesite. A 5-m thick interbed of volcaniclastic sandstone, bearing coaly partings, dipping 10°SE, along with lava flows and breccia, underlie the road. The eastern part of the road cut exposes at least two 5-10 m thick dark-colored lava flows of pyroxene andesite porphyry, volcaniclastic interbeds, and a 10-m thick pale green tuff, similar to the tuffs of the Breitenbush Formation. Units are offset by at least 12 northwest-trending shear zones, showing oblique-slip displacement. The zone strikes toward Bagby Hot Springs (Fig. 4), probably forming there the channelways for the springs. The 40-m thick lava flow at the west end of the cut is the probable continuation of the Hugh Creek flow, exposed about 0.5 mi to the southwest, dated at 13 to 16.5 Ma (Table 2). It is intruded by a tapering 9-12 m wide dike of altered andesite porphyry similar to the intrusions of the Bull-of-the-Woods complex.

41. Silicic lava flows of the Nohorn Andesite along Hot Springs Fork. Location: SE SE SW 4-7S-6E; Battle Ax NE; 44°59.02'N, 122°4.93'W; 530 m (1740 ft) elev. Along north side of USFS road 70 (S-70), the Hot Springs Fork road, 1.0 mi west of junction of roads 63 (S-63) and 70. This junction is located 4.0 mi south of junction of roads 63 and 46 (224). Parking along south shoulder overlooking creek. Eastern end of 0.8 mi stretch of discontinuous road cuts exposes very light to pinkish gray, possibly deuterically altered, fluidal layered, phyric feldspar silicic lava flow, locally brecciated and containing abundant lithic inclusions, less than 15 cm in size, which where weathered out form voids. Flow is cut by several northwest-trending shear fractures.

42. Happy-Blitzen Creeks section of Breitenbush Formation. Location: SW SW SE 24-7S-6E; Battle Ax NE; 44°56.39'N, 122°1.26'W; 799 m (2620 ft) elev. Along east side of USFS road 63 (S-63), the Collawash River road, 1.9 mi south of junction of roads 63 and 6350 (S-701) This junction is 5.1 mi south of junction with road 70 (S-70) and 9.1 mi south of junction with highway 46 (224). Parking along west shoulder of road. Stop is at top of 315-m section of Breitenbush Formation, dipping 20-40°N, and is composed of at least 9 pyroclastic flows of chiefly lithic-pumice crystal (pyroxene-quartz-plagioclase)-vitric tuff, 10-40 m thick, with interbeds of volcaniclastic sandstone, 3-13 m thick. Section is cut by two or more northwest-trending faults, but no tuff is repeated, indicating that section is possibly thicker. Tuffs are distinguishable on color, thickness, degree of welding, abundance and size of lithic and pumice fragments, and proportion of three mineral components . No attempt has yet been made to trace or correlate these tuffs with other outcrops of the Breitenbush Formation. The section is exposed southward along road for 1.3 mi and is easily examined on foot or from vehicle.

43. Lapilli-breccia and sill of nearby possible volcanic center of Rhododendron Formation, west side of Rhododendron Ridge. Location: NW NW NW 20-7S-7E; Breitenbush Hot Springs NW; 44°57.09'N, 122°59.25'W; 1219 m (4000 ft) elev. At end of USFS spur road 6350/240 (S-701D), 1.2 mi north of junction with road 6350 (S-701). Spur road is located 4.2 mi south of junction of roads 6350 and 63 (S-63). Turn-around space for bus lies 0.9 mi north of junction with road 6350. Smaller vehicles can proceed to 1.0 mi. Walk 0.2 mi over boulder-strewn road. More than 12 m of nearly white lithic lapilli-breccia is intruded by a 50-m sill of dark-gray lineated pyroxene andesite porphyry. Sill is probable off-shoot of plug immediately to east. Float on road from plug consists of light-gray pyroxene andesite porphyry with abundant rounded inclusions, averaging 5 cm in size, of darker gray andesite porphyry.

44. Older High Cascade basalt and dike of Hawk Mountain, southern Rhododendron Ridge. Location: NW NE SW 27-8S-7E; Breitenbush Hot Springs SW; 44°51.01'N, 121°56.48'W; 1390 m (4560 ft) elev. Along west side of USFS road 6350 (S-701), 6.2 mi south of Graham Pass, 11.7 mi south of junction with road 63 (S-63), and 1.0 mi north of junction with road 4671 (S-756). Parking along east shoulder of road. Cut exposes 7-m section of interstratified aa lava flows 2-4 m thick, a narrow intracanyon flow, and palagonitized breccia, 5 m thick, dipping 5-10°N. Two northwest-trending dikes, 1-2 m wide, of basalt are exposed to the south. Dike of Hawk Mtn., about 60 m wide, lies to north of cut and consists of coarsely crystalline basalt with about equal amounts of olivine and plagioclase phenocrysts. A parallel, northwest-trending dike of basalt, similar to Outerson Basalt, is exposed along road 6350 about 0.9 mi to the north, cutting strata of breccia, volcaniclastic sandstone, and white tuff of Rhododendron Formation. Cuts to south of stop expose thicker section, lacking breccia, of older High Cascade lava flows.

45. Faults and dikes cutting older High Cascade basalt along Hunter Creek, east slope of Rhododendron Ridge. Location: NE NE NE 11-8S-7E; Breitenbush Hot Springs NW; 44° 54'N, 121°54.42'W; 1045 m (3430 ft) elev. Along north side of USFS road 4671 (S-756), 6.9 mi northeast of junction with Graham Pass road 6350 (S-701), 4.0 mi southwest of junction with Lowe Creek road 4670 (S-702), and 5.4 mi southwest of junction of roads 4670 and 46 (224). Road cut exposes 36-m section of interstratified, platy and blocky jointed olivine basalt aa lava flows, and bedded varicolored volcaniclastic beds, including two very light-gray to white salic tephra beds, dipping 25°E. Section is cut by two basalt dikes, one 3-m wide with chill margins and faulted east contact. Complex faulting in west part of road cut shows normal displacement with east side up and one slidkensided, left-lateral strike-slip fault of unknown displacement. Faults and dikes strike northwestward. Part of Section is repeated. Section is underlain by more volcaniclastic beds exposed along road 4671, 0.25 mi to southwest, and capped by 1-4 m of youngest till. Lava flows are discontinuously exposed northward along road for about 1.5 mi.

46. Faulted Rhododendron Formation adjacent to High Cascade Group, northern Rhododendron Ridge. Location: NE SW NW 9-7S-7W; Breitenbush Hot Springs NW; 44°58.62'N, 121°57.83'W; 1329 m (4360 ft) elev. Along north side of USFS road 4670 (S-702), 6.5 mi northwest of junction with road 4671 (S-756) and 7.9 mi northwest of junction with highway 46 (224). Parking along south shoulder of road. Over 400 m of road cut exposes about 50-m section

of faulted and repeated Rhododendron Formation, consisting of interstratified gray coarsely porphyritic pyroxene andesite lava flows, and varicolored lithic and pumice breccia and tuff. Strata dip 20°SW on west side and lie horizontally in middle of cut. Most faults strike northwest with the east side displaced downward. High Cascade basalt lies immediately to the east. Stratigraphic relation between these formations indicates that they are separated by faulting with probably over 100 m displacement, east side down. Stop lies within southeast-trending Lake Harriet-Oak Grove Butte fault zone (Fig. 4; stops 36 and 49).

47. Older High Cascade basalt along Clackamas River north of Pinhead Creek. Location: NE NW SW 16-7S-8E; Breitenbush Hot Springs NW; 44°59.29'N, 121°52.92'W; 732 m (2400 ft) elev. Along east side of USFS highway 46 (224), 10.8 mi southeast of junction with road 63 (S-63), 2.1 mi southeast of Austin Hot Springs, and 1.4 mi north of junction with road 4670 (S-702). Parking on west shoulder of road overlooking Clackamas River. Stop lies near south end of about 1.0 mi of continuous road cuts in older High Cascade Basalt. Road cut exposes lower beds of compacted yellowish-brown to gray lithic and pumice lapilli and coarse-grained tuff and upper interstratified 2-4-m thick basalt aa lava flows, capped by youngest till, 1-2 m thick. Road cuts to north and south expose undulating layering, truncations, intracanyon lava-flow fillings, more salic tuff interbeds, and several faults striking N10-15°E. Section lies within a narrow graben; the north-south fault, along which these rocks are down-dropped into contact with Rhododendron Formation, lies just east of highway (Fig. 4).

48. Argillically altered pyroxene andesite intrusion along Clackamas River east of Austin Hot Springs. Location: NE SW NW 26-6S-7E; High Rock SW; 45°1.29'N, 121°55.58'W; 683 m (2240 ft) elev. Along north side of Clackamas River on USFS highway 46 (224), 4.1 mi east of Austin Hot Springs, 6.2 mi east of junction of roads 46 and 63 (S-63), and 0.8 mi west of junction with Pot Creek road 4660 (S637). Parking on south shoulder of highway overlooking Clackamas River. Roadcut exposes soft, very light- to pinkish-gray argillically altered pyroxene andesite. That the rock is intrusive is indicated by its massive character, still preserved although completely replaced by clay. Less altered greenish-gray pyroxene andesite occurs within spherically eroded blocks at the northwest end of the road cut. Two thin intracanyon flows of vesicular High Cascade olivine basalt are exposed at the top of the cut.

49. Austin Hot Springs. Location: SE SE NW 30-6S-7E; Fish Creek Mtn. SE; 44°1.15'N, 122°0.12'W; 509 m (1670 ft) elev. Along Clackamas River and USFS highway 46 (224), 2.1 mi east of junction with road (S-63). Parking at picnic area along river. Springs extend along river for 100 m east of picnic grounds. See Table 4.

50. Sill of Austin Point intrusion along Clackamas River. Location: NW NW SW 23-6S-6E; Fish Creek Mtn. SE; 44°1.88'N, 122°3.04'W; 500 m (1640 ft) elev. Along north side of USFS highway 46 (224), 0.4 mi east of junction with road 63 (S-63), and 4.1 mi south of junction with Oak Grove Fork road 57 (S-57). High cut of columnar-jointed microdiorite sill, over 100 m thick, dipping 20°NE, overlie interstratified lithic breccia, 12 m thick, and platy jointed pyroxene andesite porphyry lava flows, 2 to 10 m thick, of Nohorn Andesite. A 1.5-m thick chill zone occurs at base of sill. Intrusion and host rock are zeolitized. Northwest-trending faults offset contact at base of sill about 2 m, southwest side down. A probable fault extends along river bed, separating knob of sill to south from main mass to morth.

51. Third Creek fault cutting lahar (Fig. 7). Location: NE NE NE 35-5S-5E; Fish Creek Mtn. SW; 45°6'N, 122°9'W; 610 m (2000 ft) elev. On north side of road 5420 (S-505), 5.2 mi south of junction with road 5410 (S-504), which is 0.1 mi from road 54 (S-54). Outcrop is just past road 5420/170 (S-505-T) on road 5420. Watch for road junctions. Strike-slip fault trending N30° E, offsets a lahar of the Rhododendron Formation and the overlying Grande Ronde Basalt (Tgn_2l) flows. Shears cut boulder and cobbles in lahar.

52. Sedimentary interbeds in Grande Ronde Basalt (Tgn_2l). Location: NW NW NW 26-5S-5E; Fish Creek Mtn. SW; 45°7'N, 122°10'W; 494 m (1620 ft) elev. On the north side of road 5430 (S-562), 1.0 mi north of junction with road 54 (S-54). Two volcaniclastic interbeds represent interfingering Rhododendron Formation (Fig. 10). The upper interbed,

18.5 m thick, contains a 6-m layer of sandstone, containing leaf fossils, sandwiched between layers of volcanic breccia. The lower interbed, 15.4 m thick, is exposed at road level.

53. Right-lateral strike-slip fault, Third Creek fault cutting Grande Ronde Basalt (Tgn_2l and Tgn_2h). Location: NE SW SW 23-5S-5E; Fish Creek Mtn. SW; 45°7.5'N, 122°10.5'W; 506 m (1660 ft) elev. On the west side of road 5430 (S-562), 1.5 mi north of junction with road 54 (S-54). Pillow palagonite complex at road level is cut by numerous parallel shears with horizontal slickensides (Fig. 11). Step structures indicate right-lateral movement.

54. Camelsback diorite intrusion and cutting basalt dike. Location: SE SW NE 23-6S-5E; Fish Creek Mtn. SW; 45°2'N, 122°9'W; 811 m (2660 ft) elev. On the west side of road 5440 (S-647), 2.5 mi south of junction with road 54 (S-54). This junction is 7.5 mi south of junction of road 54 and highway 46. Parking on west side below talus slope. Excavation at the base of talus slope exposes 1.5-m wide basaltic dike, trending N16°W, intruding diorite of Camelsback pluton. Two sets of dikes occur in the upper Fish Creek area. The earlier consists of aphanitic to coarsely porphyritic andesite, most of which form a radial dike swarm about Camelsback. The younger dikes, one of which is exposed at the stop, trends northwestward following the regional fault structure.

REFERENCES CITED

Anderson, J.L., 1978, The stratigraphy and structure of the Columbia River Basalt in the Clackamas River drainage: Portland, Oreg., Portland State University master's thesis, 136 p.

Barnes, F.F., and Butler, J.W., 1930, Structure and stratigraphy of the Columbia River Gorge and Cascade Mountains in the vicinity of Mount Hood, Oregon: Eugene, Oreg., University of Oregon master's thesis, 136 p.

Beeson, M.H., Bentley, R.D., and Moran, M.R., 1976, Preliminary correlation of lower Yakima Basalt flows in western Oregon with the type area in central Washington: Geological Society of America Abstracts with Programs, v. 8, no. 3, p. 355.

Beeson, M.H., and Moran, M.R., 1979, Columbia River Basalt Group stratigraphy in western Oregon: Oregon Department of Geology and Mineral Industries, Oregon Geology, v. 41, no. 1, p. 11-14.

Beeson, M.H., Moran, M.R., and Olson, F.L., 1976, Geochemical data on Columbia River basalt stratigraphy in western Oregon: Geological Society of America Abstracts with Programs, v. 8, no. 3, p. 354.

Bowen, R.G., Peterson, N.V., and Riccio, J.F., 1978, Low- to intermediate-temperature thermal springs and wells in Oregon: Oregon Department of Geology and Mineral Industries Geological Map Series GMS-10.

Brock, M.R., and Grolier, M.J., 1973, Chemical analyses of basalt samples from the Columbia Plateau, Washington, Oregon, and Idaho: U.S. Geological Survey open-file report, 35 p.

Clayton, C.M., Geology of the Breitenbush Hot Springs area, Cascade Range, Oregon: Portland, Oreg., Portland State University master's thesis, 80 p.

Crandell, D.R., and Miller, R.D., 1974, Quaternary stratigraphy and extent of glaciation in the Mount Rainier region, Washington: U.S. Geological Survey Professional Paper 847, 59 p.

Dyhrman, R.F., 1975, Geology of the Bagby Hot Springs area, Clackamas and Marion Counties, Oregon: Corvallis, Oreg., Oregon State University master's thesis, 78 p.

Greene, R.C., 1968, Petrography and petrology of volcanic rocks in the Mount Jefferson area, High Cascade Range, Oregon: U.S. Geological Survey Bulletin 1251-G, 48 p.

Hammond, P.E., 1979, A tectonic model for evolution of the Cascade Range, in Armentrout, J.M., Cole, M.R., and TerBest, H., Jr., eds., Cenozoic paleogeography of the western United States: Pacific Section, Society of Economic Paleontologists and Mineralogists, 335 p.

____1980, Reconnaissance geologic map and cross sections of the southern Washington Cascade Range: Portland, Oreg., Portland State University, Publication of the Department of Earth Sciences.

Jackson, J.S., 1980, Petrology of the Bull-of-the-Woods intrusive complex: Portland, Oreg., Portland State University master's thesis (in progress).

Laursen, J.M., and Hammond, P.E., 1978, Summary of radiometric ages of Oregon rocks - supplement 1: July 1972 through December 1976: Isochron/West, no. 23, p. 3-28.

____1979, Summary of radiometric ages of Washington rocks - supplement 1: July 1972 through December 1976: Isochron/West, no. 24, p. 3-24.

Lawrence, R.D., 1976, Strike-slip faulting terminates the Basin and Range province in Oregon: Geological Society of American Bulletin, v. 87, no. 6, p. 846-850.

McBirney, A.R., Sutter, J.F., Naslund, H.R., Sutton, K.G., and White, C.M., 1974, Episodic volcanism in the central Oregon Cascade Range: Geology, v. 2, p. 585-589.

Mariner, R.H., Rapp, J.B., Willey, L.M., and Presser, T.S., 1974, The chemical composition and estimated minimum thermal reservoir temperatures of selected hot springs in Oregon: U.S. Geological Survey open-file report, 27 p.

Nathan, S., and Fruchter, J.R., 1974, Geochemical and paleomagnetic stratigraphy of the Picture Gorge and Yakima basalts (Columbia River Group) in central Oregon: Geological Society of America Bulletin, v. 85, p. 63-76.

Olson, J.P., 1978, Geology and mineralization of the North Santiam Mining District, Marion County, Oregon: Corvallis, Oreg., Oregon State University master's thesis,

135 p.
Peck, D.L., Griggs, A.B., Schlicker, H.G., Wells, F.G., and Dole, H.M., 1964, Geology of the central and northern parts of the western Cascade Range in Oregon: U.S. Geological Survey Professional Paper 449, 56 p.
Porter, S.C., 1976, Pleistocene glaciation in the southern part of the North Cascades Range, Washington: Geological Society of America Bulletin, v. 87, p. 61-75.
Portwood, B.B., 1979, Geology of a portion of the Fish Creek Mountain 15' quadrangle, Clackamas County, Oregon: Portland, Oreg., Portland State University bachelor's thesis, 33 p.
Pungrassami, T., 1969 (1970), Geology of the western Detroit Reservoir area, Quartzville and Detroit quadrangles, Linn and Marion Counties, Oregon: Corvallis, Oreg., Oregon State University master's thesis, 76 p.
Rollins, A., 1976, Geology of the Bachelor Mountain area, Linn and Marion Counties, Oregon: Corvallis, Oreg., Oregon State University master's thesis, 83 p.
Scott, W.E., 1977, Quaternary glaciation and volcanism, Metolius River area, Oregon: Geological Society of America Bulletin, v. 88, no. 1, p. 113-124.
Sutter, J.F., 1978, K/Ar ages of Cenozoic volcanic rocks from the Oregon Cascades west of 121°30': Isochron/West, no. 21, p. 15-21.
Sutton, K.G., 1974, Geology of Mount Jefferson: Eugene, Oreg., University of Oregon master's thesis, 119 p.
Swanson, D.A., Wright, T.L., Hooper, P.R., and Bentley, R.D., 1979, Revisions in stratigraphic nomenclature of the Columbia River Basalt Group: U.S. Geological Survey Bulletin 1457-G, 59 p.
Taylor, H.P., 1971, Oxygen isotope evidence for large-scale interaction between meteoric ground waters and Tertiary granodiorite intrusions, western Cascade Range, Oregon: Journal of Geophysical Research, v. 76, p. 7855-7874.
Thayer, T.P., 1936, Structure of the North Santiam River section of the Cascade Mountains in Oregon: Journal of Geology, v. 44, p. 701-716.
____1937, Petrology of later Tertiary and Quaternary rocks of the north-central Cascade Mountains in Oregon: Geological Society of American Bulletin, v. 48, p. 1611-1651.
____1939, Geology of the Salem Hills and the North Santiam River basin, Oregon: Oregon Department of Geology and Mineral Industries Bulletin 15, 40 p.
Trimble, D.E., 1963, Geology of Portland, Oregon, and adjacent areas: U.S. Geological Survey Bulletin 1119, 119 p.
Uppuluri, V.R., 1974, Prineville chemical type: a new basalt type in the Columbia River Group: Geological Society of America Bulletin, v. 85, p. 1315-1318.
Waitt, R.B., Jr., 1977, Guidebook to Quaternary geology of the Columbia, Wenatchee, Peshastin, and upper Yakima Valleys, west-central Washington: U.S. Geological Survey Open-File Report 77-753, 25 p.
Walker, G.W., Greene, R.C., and Pattee, E.C., 1966, Mineral resources of the Mount Jefferson Primitive Area, Oregon: U.S. Geological Survey Bulletin 1230-D, p. D1-D32.
Wise, W.S., 1969, Geology and petrology of the Mount Hood area: a study of High Cascade volcanism: Geological Society of America Bulletin, v. 80, p. 969-1006.
Wolfe, J.A., 1954, The Collawash flora of the upper Clackamas River basin, Oregon: Geological Society of the Oregon Country Geological News Letter, v. 20, no. 10, p. 89.
Wright, T.L., Grolier, M.J., and Swanson, D.A., 1973, Chemical variation related to the stratigraphy of the Columbia River basalt: Geological Society of America Bulletin, v. 84, p. 371-386.

BEACH PROCESSES AND EROSION PROBLEMS ON THE OREGON COAST

Paul D. Komar
School of Oceanography
Oregon State University

Herb Schlicker
Oregon Department of Geology and Mineral Industries

INTRODUCTION

The coast of Oregon provides an environment for the study of beach processes and erosion under high wave energy conditions. The purpose of this trip is to examine three areas that are fairly representative of the coast with respect to the nature of the beach deposits and processes, and to erosion problems experienced by the coastal communities. The first stop, Newport (Figure 1), is a classic example of large-scale slumping of sea cliffs resulting from sliding down seaward-dipping strata. The beach there is also typical of the fine sand beaches, those most prevalent on the Oregon coast. Stop 2 will principally examine the considerable erosion problems that have been experienced on Siletz Spit since its development in the 1960's. The beach there is much coarser than at Stop 1, and the resulting beach morphology and processes will be contrasted. Stop 3 at Taft will demonstrate the problems associated with gradual sea cliff erosion where large slumps are not involved, more typical of the Oregon coast than Stop 1.

GEOMORPHOLOGY AND PROCESSES OF THE OREGON COAST

The Oregon coast consists of a series of sandy beaches separated by large rocky headlands such as Yaquina Head and Cape Foulweather (Figure 1). The stretches of beach vary in length from small pocket beaches nestled amongst the rocky headlands to the 50-mile long beach extending from Heceta Head south to Cape Arago near Coos Bay. Because the beach sand is not able to pass around these large headlands, each of the beaches can be considered as a pocket beach. One consequence of this is that the net littoral drift within each "pocket" must be zero. Deposition and erosion patterns due to jetty construction also substantiate this (Komar et al., 1976). There appears to be an annual cycle of sand drift along the beaches, moving northward during winter storms from the southwest, but then returning southward during the summer months, yielding a net zero transport when averaged over the years.

Like most other continental beaches, the beaches of Oregon are composed mainly of quartz and feldspar grains. The finer sand beaches can contain appreciable amounts of heavy minerals, principally hornblende, augite, garnet and epidote. At many locations there are heavy-mineral concentrations buried within the beach, which become exposed during winter months of general beach erosion. Thus certain beaches are distinctly finer during the winter than during the summer, and are a distinct greenish-black. The beach sands generally have median grain diameters in the range 0.2 to 0.5 mm (fine to medium sand on the Wentworth scale). Small pocket beaches in headland areas usually consist of basalt pebbles and cobbles.

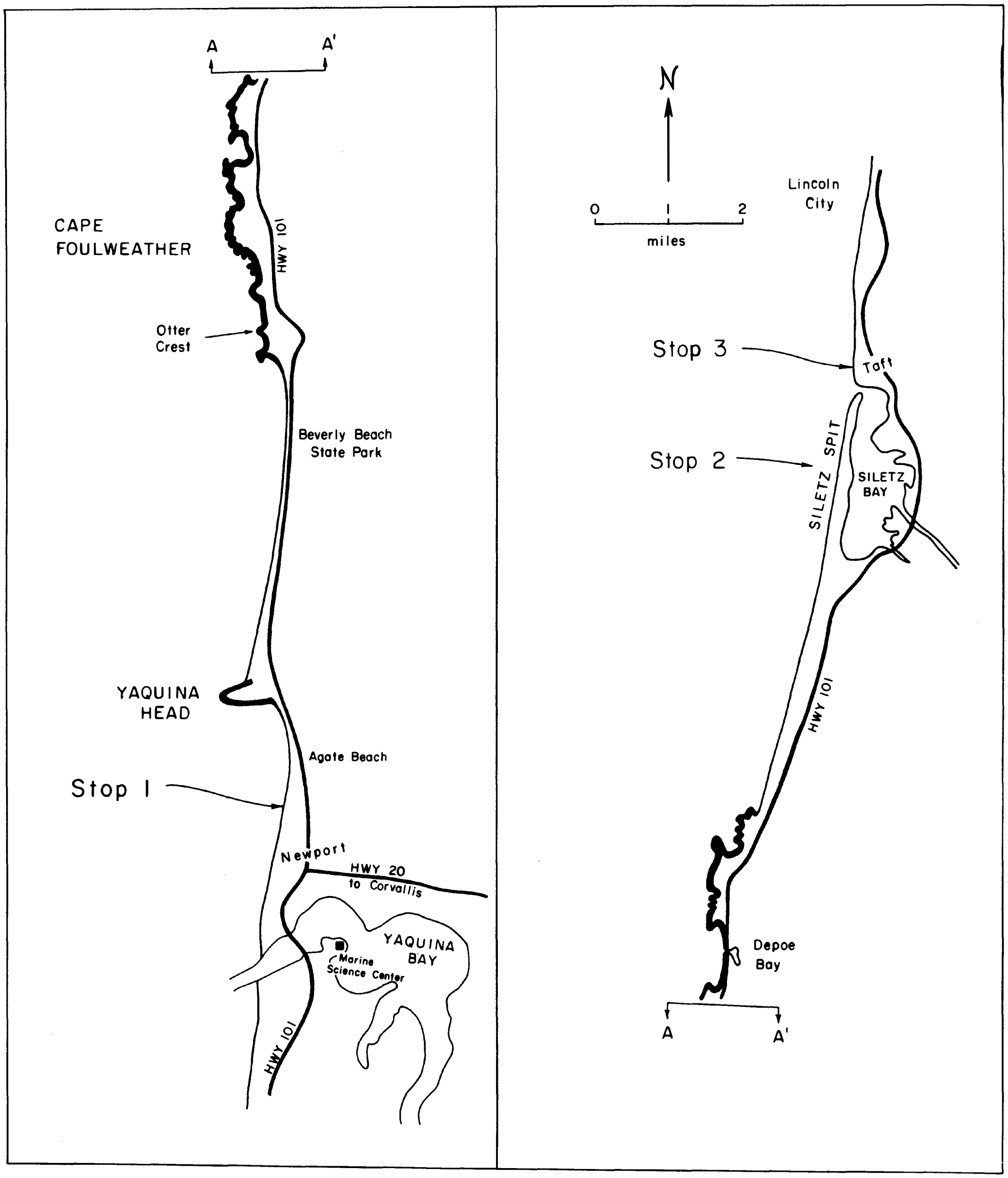

Figure 1: General location of field trip stops.

The major source of sand to most Oregon beaches comes from erosion of sea cliffs, especially those composed of Pleistocene terrace sands. Sands transported down the major rivers are deposited in the estuaries rather than reaching the ocean beaches (Kulm and Byrne, 1966; Scheidegger et al., 1980). This will be discussed more at Stop 3. Sand carried down the Columbia River moves northward when it reaches the ocean, and so is a major contributor to the Washington beaches rather than to Oregon. Only the Clatsop Plains area immediately south of the Columbia, and basically a part of the delta of the Columbia, has that river as its major sand source.

The Oregon coast is noted for the severity of its wave climate. Wave conditions follow a seasonal pattern in response to the changing weather patterns, with the largest waves occurring during the winter storms (Figure 2). Waves from exceptional storms have been measured with significant breaker heights up to 7 meters (23 feet) on several occasions since 1971 (Komar et al., 1976; Creech, 1977). One such storm is shown in the measurements contained in Figure 2, having occurred on 24-26 December 1972. That storm caused appreciable erosion on Siletz Spit (Stop 2). Ocean wave conditions are measured four times daily at the Marine Science Center in Newport by a seismic recording system that detects microseisms produced by the waves (Enfield, 1973; Quinn, et al., 1974; Bodvarsson, 1975).

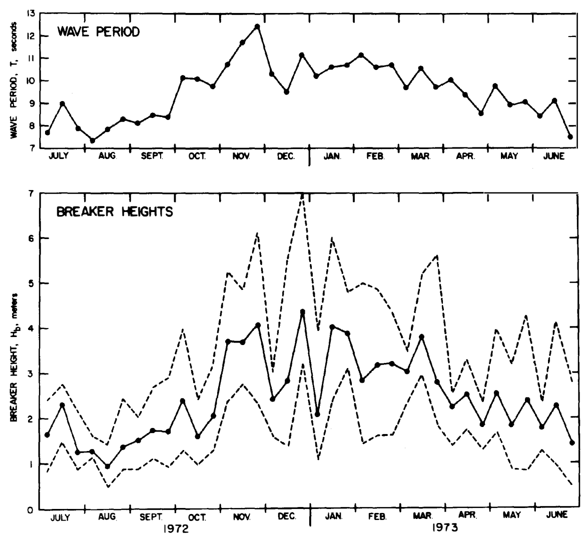

Figure 2: Significant wave breaker heights and periods, each datum point giving the average for one-third month interval. The dashed lines give the maximum and minimum breaker heights during those same intervals.

Beaches respond to the seasonally changing wave conditions. During the stormy winter months of high waves, sand is eroded from the exposed berm and shifted offshore to be deposited in the bars. During the summer months of low waves the sand shifts back onshore into the berm. Such seasonal cycles of the beach profiles occur on most beaches, and have been documented by Aguilar and Komar (1978) on Oregon beaches. One important consequence of this cycle is that there is a wide beach during the summer months that helps prevent coastal property erosion. Nearly all of our erosion occurs during the winter months when the width of the beach is reduced and the waves are able to directly attack the coastal property. Byrne (1963) has also shown that landsliding is much more common during the winter months, in part for this reason and in part due to increased rains.

Tides on the Oregon coast are moderate with a maximum spring tidal range of about 13 feet and an average range of 6 feet. The tides are mixed, with two highs and two lows each day, with successive highs generally differing in level.

Tidal records on the Oregon coast indicate that within the past 34 years the sea level has been constant with respect to the land. This contrasts with the East Coast where there is an apparent sea level rise, and cases such as Alaska where the land is tectonically emerging, giving an apparent sea level drop. The Oregon coast has been a tectonically emergent coast, being on a convergent boundary of the Juan de Fuca and North American plates. Evidence for this emergence is the terraces visible at many locations along the coast. The deposits of these terraces have been dated as late Pliocene to Pleistocene (Schlicker, et al., 1973). The absence of any present-day apparent sea level rise should limit the erosion problems on the Oregon coast, not experiencing erosion under a transgressing sea as does the East Coast. Much of the sea cliff erosion present today on the Oregon coast is probably still something of a remnant of the rapid sea-level rise ending the last glacial advance.

STOP 1: JUMPOFF JOE AREA OF NEWPORT

At this location (Figure 3) the Pleistocene marine terrace is particularly evident, as are the well-sorted sands that compose the terrace deposits. The terrace sands overlie unconformably the Astoria Formation, marine sandstones and siltstones of middle Miocene age (Snavely, 1969; Schlicker, et al., 1973). The contact between the two deposits represents the wave-cut base of the late Pliocene to early Pleistocene transgression.

The strata of the Astoria Formation dip steeply seaward at this location, producing a classic example of massive landsliding along bedding planes (Figure 4). Sliding began here in 1922, but major displacements occurred in 1942-43 at which time an area of about six acres progressively slid seaward, dropping down 20 feet in the process. More than a dozen homes and other structures were lost (North and Byrne, 1965; Stembridge, 1975). The long-term sea cliff retreat is documented in Figure 3, compiled by Stembridge (1975) from old maps (1868) and aerial photos (1939, 1967).

This is also the former site of Jumpoff Joe, an example of sea cliff and stack erosion documented by the many tourist photos of the feature taken over the years (Figure 5). Today Jumpoff Joe has been reduced to an insignificant rock nub, observable only at low tide.

The beach here is typical of the major beaches of the Oregon coast. It is fine-grained (Md = 0.2 mm) quartz sand, derived principally from erosion of the terrace sands. Because of the fine grain size, the beach slope is low and if any rip current embayments are present, they are not cut back far into the beach so as to be a threat to the coastal properties. This is in contrast to the coarse sand beach that will be seen at Siletz Spit (Stop 2). The beach here has a high content of dark heavy minerals, and for this reason is a good location to observe the formation of a variety of sedimentary structures under the wave action on the beach (rhomboid ripples, backwash ripples, laminations, etc.). The observations of backwash ripple formation by Broome and Komar (1979) were made just to the north of this location.

STOP 2: SILETZ SPIT

Access out onto Siletz Spit is through a key-operated gate (Figure 6), so that permission must first be obtained at the brown building immediately adjacent to the gate. The development of Siletz Spit began in the 1960's with the construction of an access road and the cutting of "lagoons" into the bay-side of the spit. Many of the homes date from that period, although construction continues at present. Soon after development, the spit suffered a series of erosion episodes, principally during the winters of 1972-73, 1976-77, and 1977-78 (Komar, 1978; Komar and Rea, 1976; Komar and McKinney, 1977; McKinney, 1977; Rea, 1975). The erosion reached its maximum extent in different areas of the spit at different times, rather than the entire spit eroding all at once. The response has been to place rock riprap (basalt), and today nearly the entire length of the spit has been so protected.

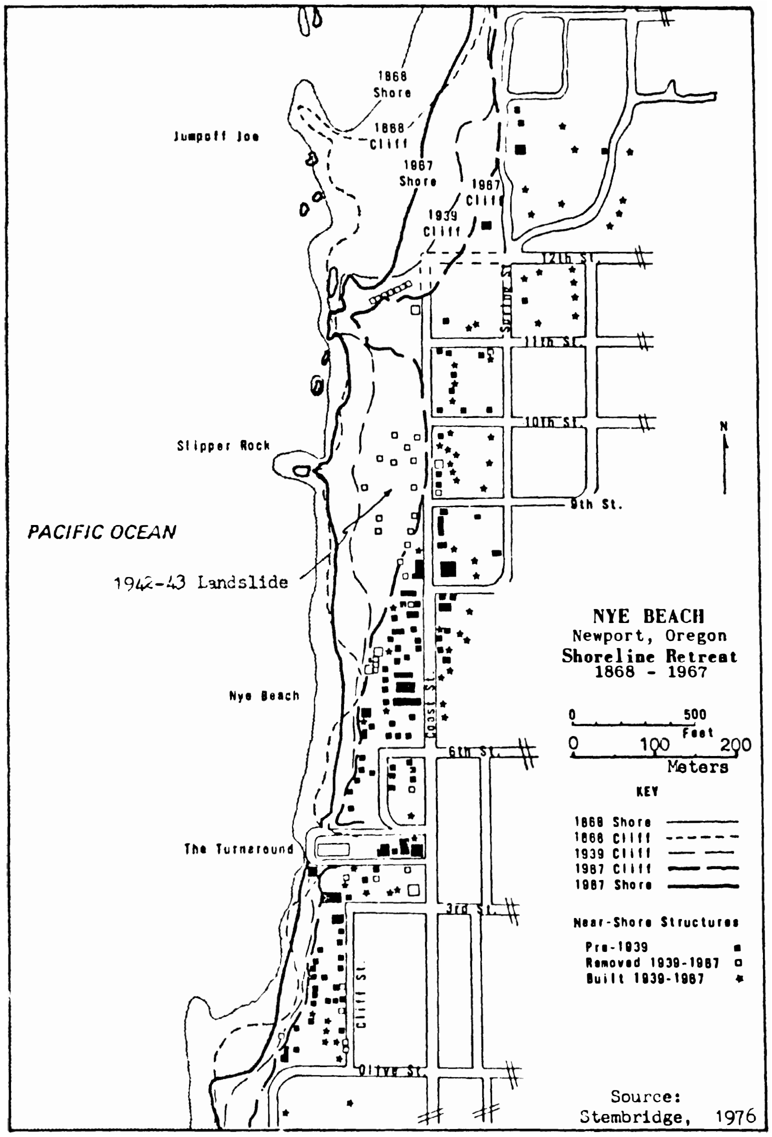

Figure 3: The sea cliff retreat in the Jumpoff Joe area of Newport (Stop 1) as documented by Stembridge (1976) from aerial photographs. The property losses here are due almost entirely to large landslides.

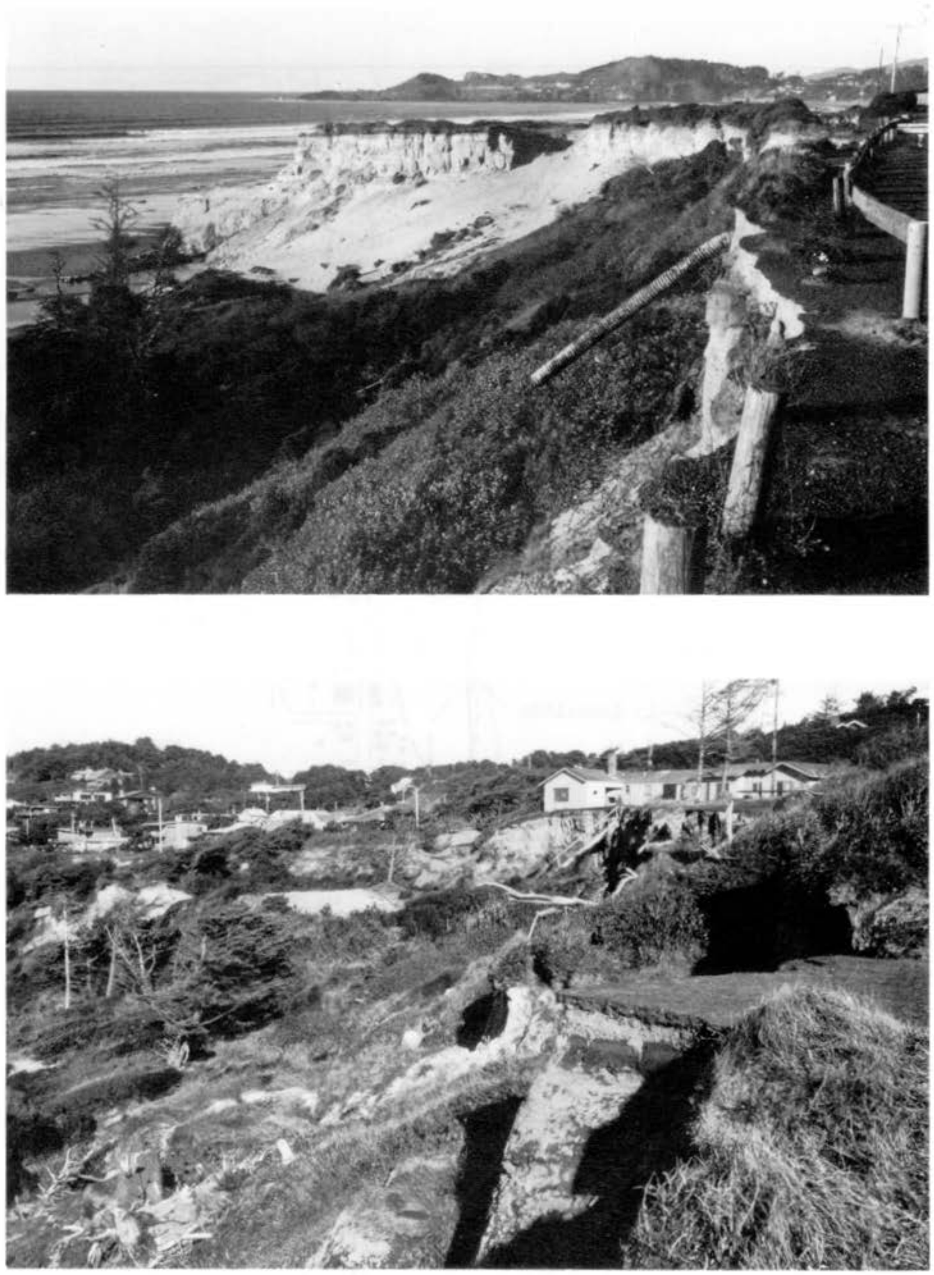

Figure 4: Large landslides in the Jumpoff Joe area of Stop 1 (Figure 3).

Figure 5: Progressive erosion of Jumooff Joe (Stop 1). Top photo (c.1880) shows it still attached to the land as part of the sea cliff. The lower photo (c.1925) shows Jumpoff Joe as a sea stack. Today little remains of the stack.

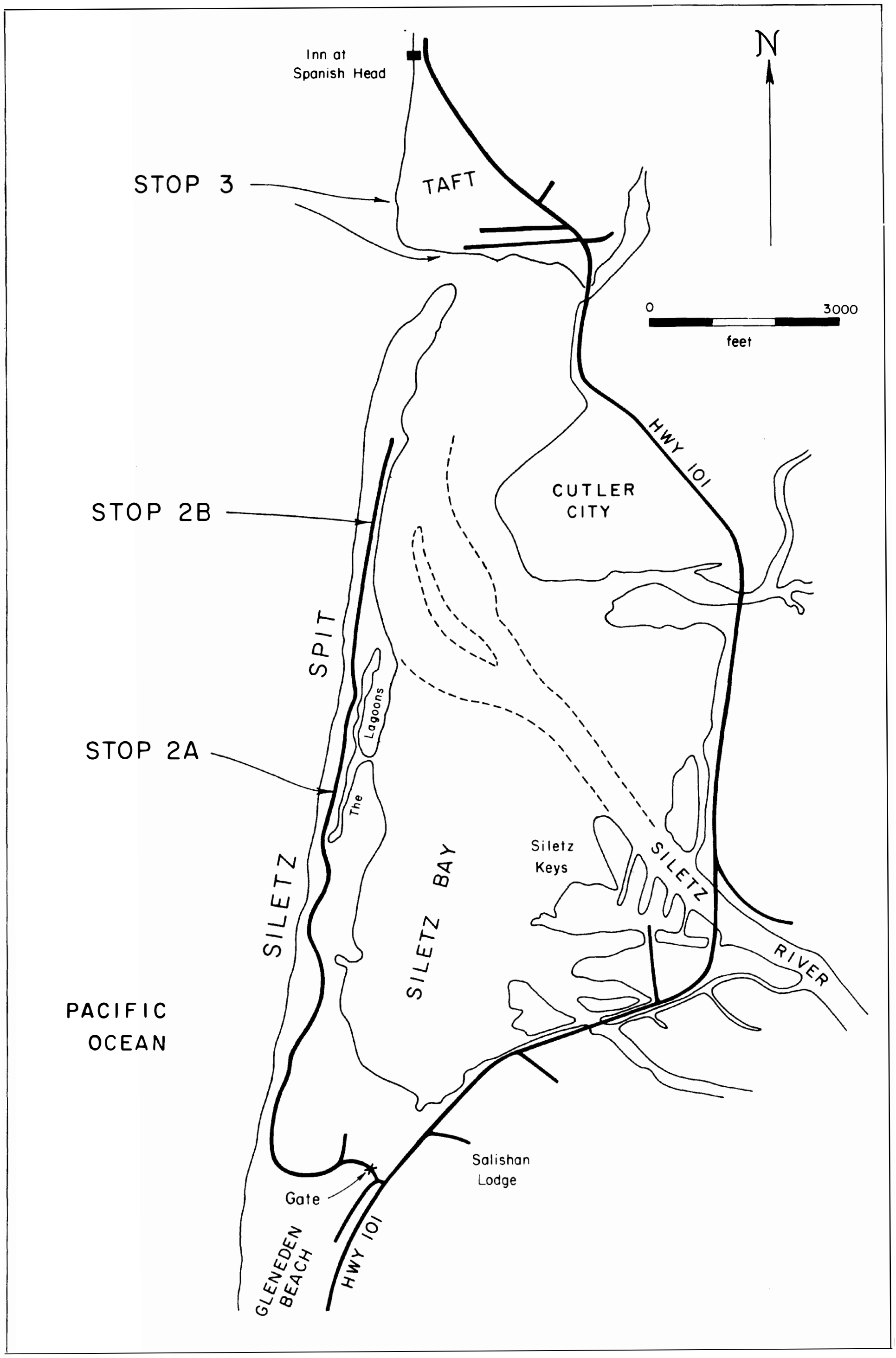

Figure 6: Locations of stops on Siletz Spit (Stop 2) and at Taft to the immediate north (Stop 3).

Figure 7: Erosion of Siletz Spit during a storm of 24-26 December 1972.

Figure 8: Embayments cut into Siletz Spit by rip currents causing erosion shown in Fig. 7.

The main stop (Stop 2A of Figure 6) is in an area that was eroded principally during the storm of 24-26 December 1972, one of the storms that generated 23-foot high breakers (Figure 2). One house under construction was lost, the only home on the spit that has been lost due to erosion, and several others were saved only by the rapid placement of riprap (Figure 7). Riprap was initially installed only along the seaward sides of the homes, and adjacent empty lots were left unprotected. The erosion of course continued in the empty lots, flanking the riprap by the homes, necessitating that the houses be protected on their sides as well. Several of the homes thereby ended up on promentories of riprap extending out into the surf (Figure 7). The erosion proceeded to within a few feet of the access road and the utility lines, at which time riprap was finally placed in those areas as well. These lots were subsequently restored by scooping sand up from the beach. Recently (1979) a new house has been constructed on one of these restored lots, to the immediate south of the house shown in Figure 7.

The beach here is much coarser than at Newport (Stop 1), and there are many obvious resulting morphological differences. Commonly present is a considerable irregularity of the shoreline trend, there being a series of embayments separated by large cusps (called rhythmic topography). The embayments are cut by rip currents, which may be visible from the ground but are best seen from the air or in aerial photographs (Figure 8). These rip embayments have played an important role in the erosion of the spit. During the winter time of general beach retreat, exceptionally large rip embayments may cut entirely through the beach width, extending back to the foredunes. This condition is seen in Figure 8, the erosion occurring in the landward edge of the largest embayment corresponding to the erosion area of Figure 7. Maximum erosion takes place when a major storm occurs, the large waves proceeding up the deeper water of such rip embayments with little energy dissipation. But the erosion is largely confined to the shoreward area of the embayments rather than extending for the entire spit length.

In a study of aerial photographs (Rea, 1975, Komar and Rea, 1976), such erosion of the foredunes due to the combined effects of rip embayments and storms was found to have occurred repeatedly in the past. It was also found that following the erosion episode, drift logs would wash into the eroded areas, helping to trap sand blown around by the winds. In this way the foredunes were naturally restored within a few years. This cycle of foredune erosion and reformation occurred repeatly in the past, and the only difference in the erosion that has taken place since the 1960's is that homes were constructed in this unstable area. The placement of riprap to protect the homes has of course interfered with this natural cycle.

Driving farther north along the spit, there is an area of bay-side erosion where the flow of the Siletz River impinges on the spit (Stop 2B of Figure 6). Riprap has been placed here to protect the road and one house to the south. This erosion is largely natural, but may have been accelerated by the placement of the Siletz Keys landfill in the bay to the south of the bridge (Figure 6). That landfill prevents river flood waters from spilling over into the south bay, instead directing all of the flow toward the spit.

STOP 3: TAFT

Siletz Bay is a classic example of a drowned-river estuary, and the bay inlet is typical of those without jetties. Beach sand carried into the bay under flood currents slightly exceeds that transported back out under the ebb currents. Thus beach sand is permanently deposited in the bay, representing a long-term net loss of sand from the beach. At the same time, sands transported down the river are trapped in the bay, not reaching the ocean beaches. The source of beach sands is instead mainly from sea cliff erosion, especially of cliffs composed of Pleistocene terrace sands. This is indicated by the heavy mineral contents of the various source sands, and the degree of rounding of the quartz grains (being much higher in the beach sands than in the river sands) [Scheidegger, et al., 1980)].

The sea cliff here is made up of a thick section of terrace sands, mainly of dune origin. Up until 1976 this beach was covered with a mass of drift logs which may have given some protection to the sea cliff (Figure 9). But it was difficult for people to

Figure 9: Sea cliff erosion in Taft (Stop 3). Upper photo (1976) shows area before most recent erosion with extensive drift log accumulation. Lower photo (1978) shows effects of the erosion. Inn at Spanish Head in background.

use the beach, so in 1976 many of the logs were removed. During the winter of 1977-78 high spring tides combined with storm waves of 23-foot breaker heights to cause erosion all along the coast, including the sea cliff here at Taft (Figure 9). It is difficult to determine whether the log removal played any role in the resulting erosion, or whether it was due entirely to the unusual severity of the storm.

The Inn at Spanish Head (Figure 9) at the north end of this beach is partly based on a basalt dike so there is little likelihood of it being undermined. But during large winter storms, the lower floor commonly becomes awash, with drift logs causing considerable destruction.

REFERENCES CITED

Aguilar-Tunon, N.A., and P.D. Komar. 1978. "The Annual Cycle of Profile Changes of Two Oregon Beaches." The Ore Bin. Department of Geology and Mineral Industries, Portland, Oregon. 40(2):25-39.

Bodvarsson, G.M. 1975. Ocean Wave-Generated Microseisms at the Oregon Coast. M.S. thesis, Oregon State University, Corvallis, 83 pp.

Broome, R., and P.D. Komar. 1979. "Undular Hydraulic Jumps and the Formation of Back-Wash Ripples on Beaches." Sedimentology. 26:543-559.

Byrne, J.V. 1963. "Coastal Erosion, Northern Oregon." Essays in Marine Geology in Honor of K.O. Emery. University of Southern California Press, Los Angeles, Ca. 11-33.

Creech, H.C. 1977. "Five Year Climatology (1972-1976) of Nearshore Ocean Waves off Yaquina Bay, Oregon." Oregon State University Sea Grant Program Ref. ORESU-T-27-001, Corvallis, Oregon. 17 pp.

Enfield, D.B. 1973. Prediction of Hazardous Columbia River Bar Conditions. Ph.D. thesis, Oregon State University, Corvallis, 204 pp.

Komar, P.D. 1978. "Wave Conditions on the Oregon Coast during the Winter of 1977-78 and the Resulting Erosion of Nestucca Spit." Shore and Beach. American Shore and Preservation Association, Miami, Florida. 46(4):3-8.

Komar, P.D., and C.C. Rea. 1976. "Erosion of Siletz Spit, Oregon." Shore and Beach. American Shore and Beach Preservation Association, Miami, Florida. 44(1):9-15.

Komar, P.D., J.R. Lizarraga, and T.A. Terich. 1976a. "Oregon Coast Shoreline Changes due to Jetties." Journal of Waterways, Harbors and Coastal Engineering Division.

Komar, P.D., W. Quinn, H.C. Creech, C.C. Rea, and J.R. Lizarraga-Arciniega. 1976b. "Wave Conditions and Beach Erosion on the Oregon Coast." The Ore Bin. Department of Geology and Mineral Industries, Portland, Oregon. 38(7):103-112.

Komar, P.D., and B.A. McKinney. 1977. "The Spring 1976 Erosion of Siletz Spit, Oregon, with an Analysis of the Causative Storm Conditions." Shore and Beach. American Shore and Beach Preservation Association, Miami, Florida. 45(3):23-30.

Kulm, L.D., and J.V. Byrne. 1966. "Sedimentary Response to Hydrology in an Oregon Estuary." Marine Geology. Elsevier Publishing Company, Amsterdam. 4:85-118.

McKinney, B.A. 1977. "The Spring 1976 Erosion of Siletz Spit, Oregon, with an Analysis of the Causative Wave and Tide Conditions." M.S. thesis, Oregon State University, Corvallis, 66 pp.

North, W.B., and J.V. Byrne. 1965. "Coastal Landslides in Northern Oregon." The Ore Bin. Department of Geology and Mineral Industries, Portland, Oregon. 27(11):217-241.

Quinn, W.H., H.C. Creech, and D.E. Zopf. 1974. "Coastal Wave Observations Via Seismometer." Mariners Weather Log. 18:367-369.

Rea, C.C. 1975. "The Erosion of Siletz Spit, Oregon." M.S. thesis, Oregon State University, Corvallis, 105 pp.

Scheidegger, K.F., C. Peterson, and P.D. Komar. 1980. "Sources and Depositional Patterns of Sands in Oregon Estuaries." American Society of Civil Engineers National Conference, Portland, Oregon, April 14-18 (Abstract).

Schlicker, H.G., R.J. Deacon, G.W. Olcott, and J.D. Beaulieu. 1973. Environmental Geology of Lincoln County, Oregon. Department of Geology and Mineral Industries, Bulletin 81, Portland, Oregon. 121 pp.

Snavely, P.D., N.S. MacLeod, and W.W. Rau. 1969. "Geology of the Newport Area." The Ore Bin. 31(2&3):25-72.

Stembridge, J.E. 1975. "Shoreline Changes and Physiographic Hazards on the Oregon Coast." Ph.D. dissertation, University of Oregon, Eugene, 202 pp.

FIELD TRIP NO. 9

CENOZOIC STRATIGRAPHY OF COOS BAY AND CAPE BLANCO, SOUTHWESTERN OREGON

BY

JOHN M. ARMENTROUT

Figure 1. Aerial View of Cape Arago Area. a) Assembly area - Stop 1: Flagpole View Point. b) Middle Cove. c) South Cove overlook - Stop 2. d) North Cove overlook - Stop 3. e) Channel-fill sequence of figure 11. f) Sea Lion View Point - Stop 4. g) Shore Acres State Park - Stop 5. h) Sunset Bay State Park - Stop 6. i) Gregory Point. j) Mouth of Coos Bay. Photograph courtesy of Oregon State Highway Division.

FIELD TRIP ROAD LOG FOR THE
CENOZOIC STRATIGRAPHY OF COOS BAY AND CAPE BLANCO,
SOUTHWESTERN OREGON

John M. Armentrout
1107 Wiltshire Drive
Carrollton, Texas 75006

INTRODUCTION

This two-day field trip is concerned with the Cenozoic stratigraphy of the southwestern Oregon Coast at Coos Bay and Cape Blanco (Fig. 2). The log is presented as two separate mileage sequences. Twelve rock units of early Eocene to Pleistocene age will be examined (Fig. 3).

The reader is referred to Baldwin (1966, 1974) and Baldwin and others (1973) for a description of the Cenozoic formations of Coos Bay and to Beaulieu (1971), Roth (1979), and Addicott (in preparation) for Cape Blanco. The molluscan paleontology of Coos Bay is discussed by Dall (1909), Turner (1938), Weaver (1945), and Armentrout (1967). Foraminiferal paleontology of Coos Bay is reviewed by Bird (1967), Rooth (1974), and Tipton (1975). The molluscan paleontology of Cape Blanco has recently been restudied by Addicott (in preparation) and Roth (1979). Foraminiferal paleontology of Cape Blanco is being restudied and initial results are presented in this paper.

CAUTION: Several of the stops are intertidal areas along sea cliffs. Participants are urged to be aware of the time of high and low tides. Caution is urged as onshore winds can significantly alter the timing and amplitude of the tide and the size of individual waves. The stop sequence should be adjusted to fit the tide and weather situations at the time of the field excursion. Many of the stops are at sea cliff view points. These areas are underlain by Pleistocene terrace sands and are often undercut. Approach all bluffs with great caution.

Overnight accommodations are available at Coos Bay, Bandon, and Port Orford. Campgrounds at Sunset Bay, Bullard's Beach near Bandon, and Cape Blanco are operated by the State of Oregon. Contact the State Parks and Recreation Section, 525 Trade Street, S.E., Salem, Oregon 97310, for information on the seasonal schedule and availability of camp sites.

ACKNOWLEDGEMENTS

The author is indebted to those Pacific Northwest geologists who shared their ideas and field data, in particular: Ewart Baldwin, University of Oregon; Ken Bird, Warren Addicott, Kristin McDougall, and Richard Janda, U.S. Geological Survey; Barry Roth, California Academy of Sciences; and Bruce Welton, Los Angeles County Museum of Natural History. Time has not permitted review of this guide by the above geologists: all interpretations as presented are the responsibility of the author.

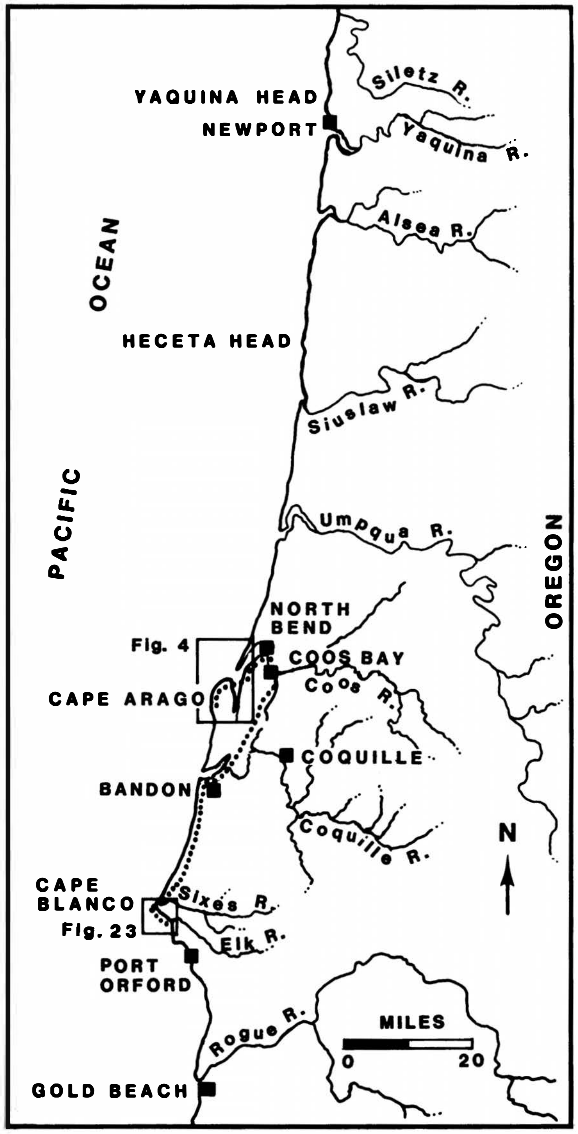

Figure 2. Index map to the field trip area.

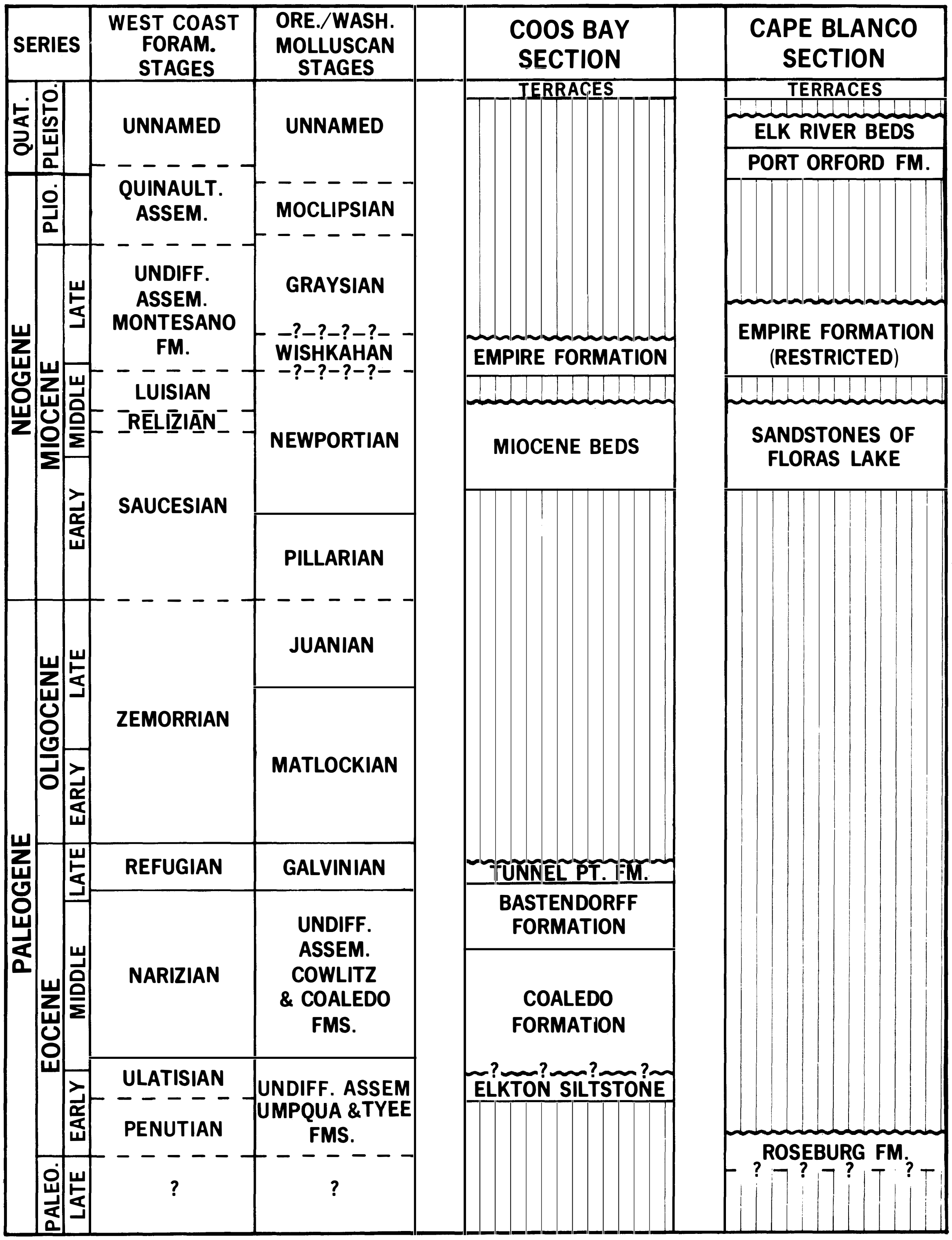

Figure 3. Correlation of provincial time scale, biochronologies and formations at Coos Bay and Cape Blanco. Usage of Foraminiferal Stages follows W. W. Rau (pers. commun., 1979); molluscan stages follows Armentrout (1975) and Addicott (1976).

COOS BAY SEGMENT

The Coos Bay field trip segment consists of a one-day excursion of 9.8 miles with 13 stops (Figs. 1, 4, and 11).

The Cenozoic geology of Coos Bay consists of Paleocene to Pleistocene continental margin marine rocks which were folded into the Coos synclinorium during Oligocene and early Miocene time (Baldwin and others, 1973). Subsequent Neogene deposition in the area was confined to the axis of this synclinorium, along the South Slough Syncline (Figs. 4 and 5). The Coos Bay Cenozoic section measures more than 12,000 feet thick (Fig. 6). Paleocene units crop out in the Coast Range around the perimeter of the Coos synclinorium but will not be visited on the field trip. The Seven Cenozoic units that will be visited are separated into four unconformity bound sequences of rocks: (1) Eocene to lower Oligocene (Elkton Siltstone, Coaledo Formation, Bastendorff Formation, and Tunnel Point Formation); (2) upper lower to middle Miocene (Miocene Beds); (3) upper Miocene (Empire Formation); and (4) Pleistocene (terrace deposits).

MILEAGE DESCRIPTION

Cumulative (Interval)

Drive to Cape Arago State Park from either North Bend or Coos Bay. The route is well marked. Cumulative mileage will be started at Stop 4.

0.0 Begin interval mileage at the entrance to Cape Arago State Park. Drive counterclockwise around the park road.

(0.5)

0.0 STOP 1: FLAG-POLE AREA: Cape Arago State Park. Park along the roadway and walk out to the stone observation area at the western edge of the Cape overlooking Middle Cove on the south (Fig. 1-a).

Cape Arago consists of Eocene sedimentary rocks folded into a north-trending anticline which is now truncated by a coastal terrace. The anticline extends from North Cove to South Cove, and is cut by a normal fault with downdroped strata on the west. A secondary fault trends through Middle Cove and may intersect the primary fault in North Cove. Resistant sandstone of the downfaulted middle Eocene Coaledo Formation form the seaward face of Cape Arago. North Cove and South Cove are eroded into the early Eocene Elkton Siltstone Member of the Tyee Formation (Beaulieu, 1971). The Elkton Siltstone is discordantly overlain by the Coaldeo Formation (Dott and Bird, 1979). The Elkton Siltstone is abundantly microfossiliferous (Bird, 1967; Dott and Bird, 1979). Sandstone of the Coaledo Formation contains megafossils, particularly at Middle Cove where sand dollars are moderately abundant along with numerous mollusks (Turner, 1938). Shale interbeds of the Coaledo Formation are microfossiliferous (Rooth, 1974).

Return to the roadway and proceed eastward.

(0.4)

0.0 STOP 2: SOUTH COVE OVERLOOK: Park along the road and walk southwest on the terrace surface to the bluff overlooking South Cove.

South from Cape Arago the coastline follows the cliff area of the Seven Devils area southward along Sacchi Beach, Agate Beach, and Merchant's Beach to Five Mile Point. Beyond Five Mile Point is the long sandy area near Whisky Run and Bullard's Beach and finally the rocky headland of Coquille Point at Bandon. On a very clear day Cape Blanco can also be seen far to the south.

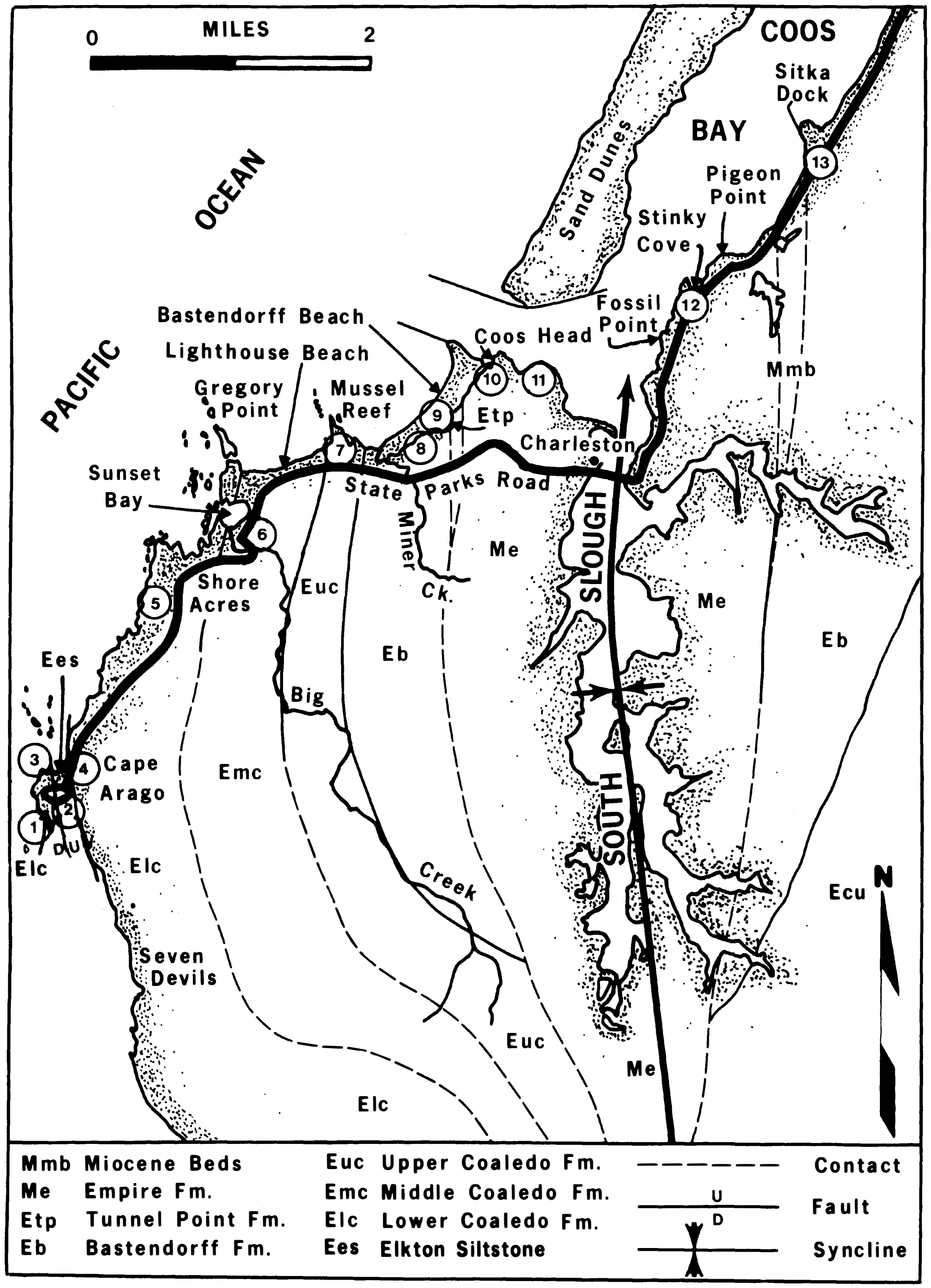

Figure 4. Geologic map for Coos Bay area (modified from Baldwin and others, 1973). Circled numbers indicate field trip stops.

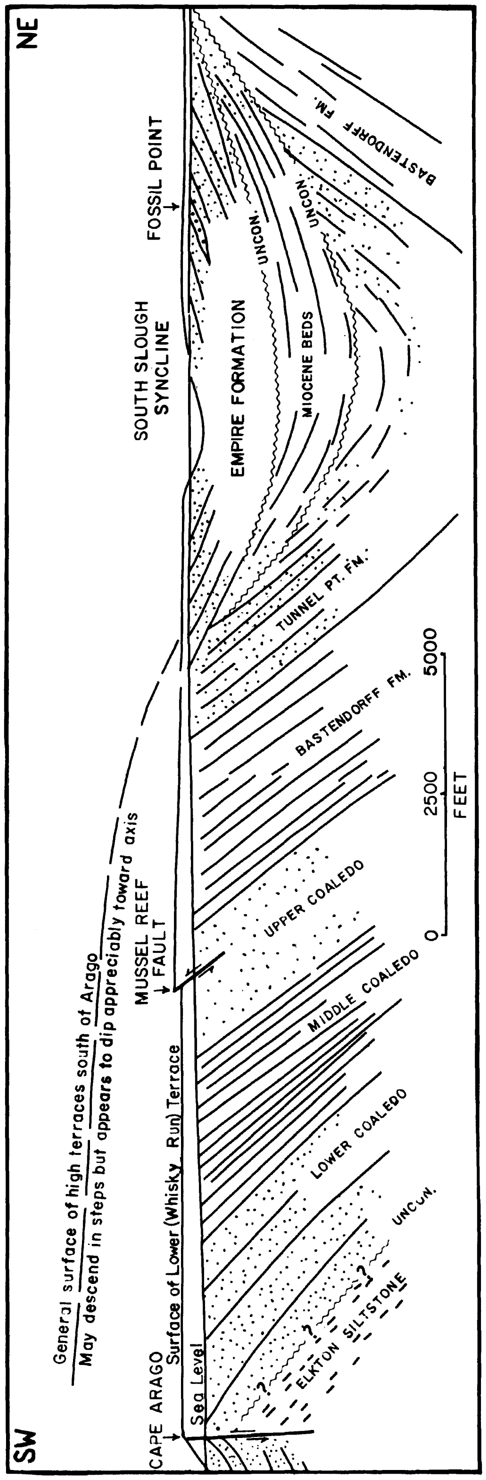

Figure 5. Geologic cross section of South Slough Syncline (modified from Baldwin 1966).

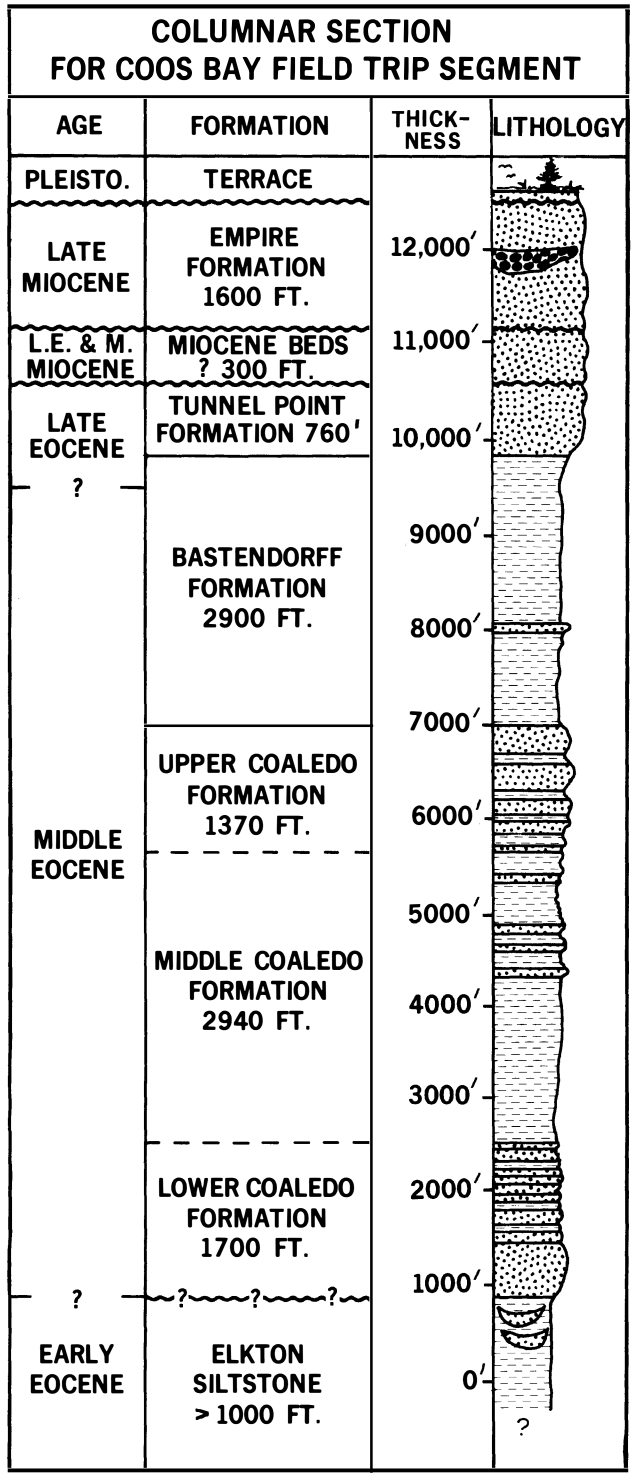

Figure 6. Stratigraphic column for Coos Bay Cenozoic formations.

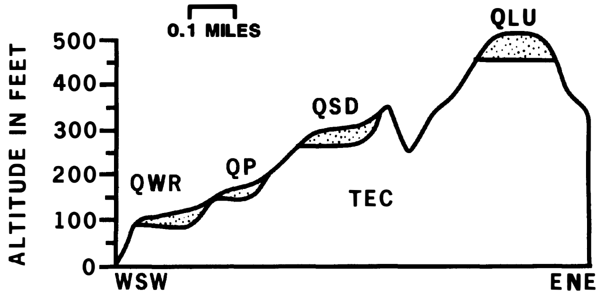

QWR WHISKY RUN TERRACE

QP PIONEER TERRACE

QSD SEVEN DEVILS TERRACE

QLU LOWER UNNAMED TERRACE

TEC EOCENE COALEDO FORMATION

Figure 7. Coastal Terrace Sequence: STOP 2. Griggs (1945) has mapped five coastal terraces in the vicinity of Cape Arago. This diagram shows the relative relationship of the four lower and more visible terraces which can be seen from STOP 2. The cross section is drawn trending east-northeast.

A sequence of five coastal terraces can be seen from this vantage point (Fig. 7). Griggs (1945) mapped, named, and cursorily described these terraces. Baldwin (1945, 1966) and Armentrout (1967) have made observations at selected key localities. Cape Arago is capped with 10 to 40 feet of colluvium and marine sands and gravels of the Whisky Run terrace. At Cape Arago the paleoshoreline of the Whisky Run terrace is at an altitude of about 95 feet. Southward along the Seven Devils area the prominent bench of the Seven Devils terrace occurs at an altitude of about 300 feet. Farther south, the Pioneer terrace is well developed at about 150 feet above the valley at Two Mile Creek which is just north of Five Mile Point. The Whisky Run terrace at 100 feet elevation forms the flat surface of Five Mile Point. The break between the Pioneer and Whisky Run terraces is visible in the coastal bluffs between Five Mile Point and Two Mile Creek. Two prominent high terraces at altitudes of 730 and 500 feet were unnamed by Griggs (1945), and are difficult to identify at Cape Arago.

Large channels filled with lenticular sequences of massive sandstone and mudstone can be seen in the eastern cliffs of South Cove (Figs. 8-9). These rocks of the Elkton Siltstone are transitional stratigraphically from thick-bedded, mid-fan sandy turbidites of the underlying Tyee Formation to the overlying coal-bearing deltaic Coaledo Formation (Dott and Bird, 1979). Foraminifers suggest a shoaling sequence from upper bathyal Tyee faunas to inner neritic, upper Elkton faunas. Channel fills are either laminated mudstone-siltstone identical with the channelized deposits or massive to faintly parallel-laminated and rarely graded light-colored sandstones.

Dott and Bird (1979) interpret the Elkton Siltstone at Cape Arago as shelf and slope deposits cut by an array of sea gullies which range in size up to 300 feet wide and 75 feet deep. These gullies may have acted as conduits of sand from a sandy littoral and deltaic zone (Coaledo Formation-like facies) across a narrow shelf and slope feeding deeper marine turbidity currents and other gravity flows (Tyee Formation-like facies), which built subsea fans (Dott and Bird, 1979).

Return to roadway and proceed north and west back through the main entrance of Cape Arago State Park, stopping at the drinking fountain at the north end of the main parking area.

(0.3)

0.0 STOP 3: NORTH COVE OVERLOOK: Walk along the paved trail to the north end of the picnic area. (Fig 1-d). From vantage points along this trail the geology of North Cove can be seen.

The geology of North Cove is similar to that of South Cove. The eastern cliffs of the Cove are Elkton Siltstone while the seastacks farthest to the west are Coaledo Formation sandstone. The traverse along the North Cove beach is passable even at normal high tide. The trail from the Cape Arago-North Cove picnic area descends to the beach. A major Elkton Siltstone channel crops out at the eastern margin of North Cove (Figs. 1-e and 10). The channel axis has been reoccupied by a modern stream which cascades down a prominent rib of sandstone. The sandstone rib stands in marked relief compared to exposures of the same sandstone on either side of the waterfall. The constantly wet sandstone may be more erosionally resistant than alternately wet and dry cliff faces to either side (Ehlen, 1967). The major "waterfall" channel is only one of several Elkton Siltstone channels which occur along the cliffs to the north of the waterfall. Sedimentary structures in the Elkton Siltstone are exposed on the wave-cut terrace just north of the lobate beach north of the waterfall. Primary sedimentary structures include flame structures, rill-type solemarks, load features, groove and flute casts, interclast conglomerates, climbing ripple laminations, flaser bedding, cross-trough stratification, laminated mudstone and sandstone, and clastic dikes. Paleocurrents are to the northwest. Northward, past the area of Sea Lion View Point (STOP 4), the Elkton Siltstone is overlain by massive tan conglomeratic sandstones of the Coaledo Formation.

Return to the North Cove parking area and leave Cape Arago State Park on State Parks Road.

(0.4)

0.0 STOP 4: SEA LION VIEW POINT: From this view point (Fig. 1-f) one can see the seastacks of North Cove and Simpson's Reef. Shell Island is the largest sea stack of the North Cove group.

Simpson's Reef, the farthest offshore and most elongate reef, dips landward. Most of the North Cove sea stacks dip seaward. These structural attitudes define Simpson's Reef Syncline (Ehlen, 1967).

0.0 START CUMULATIVE MILEAGE. Continue north on State Parks Road. Road cuts along this area are in alluvium and colluvium on the back of Whisky Run terrace.

(1.0)

1.0 Shore Acres State Park: turn left into the park. Proceed to and park in the main viewpoint parking area. Walk out to the view area at the sea cliff.

(0.2)

1.2 STOP 5: SHORE ACRES STATE PARK: Shore Acres (Fig. 1-g) was developed as an estate by the Louis Simpson family, prominent in lumbering and shipbuilding in the Coos Bay area. The manor house burned in the late 1930's and the estate (including the land of Cape Arago State Park) was donated by the Simpson family to the State of Oregon in 1942.

Shore Acres is underlain by the lower sandstone member of the Coaledo Formation. These strata dip eastward at about 40° and are part of the east limb of the Cape Arago Anticline (Ehlen, 1967). Numerous down to the south normal faults trend northwest. The five coves in the park area are eroded along zones of weakness associated with faults. The lower sandstone member of the Coaledo Formation is about 1,300 feet thick in the coastal section (Ryberg, 1978) and thickens to 1,800 feet to the southeast (Allen and Baldwin, 1944) where the outcrop area of the Coaledo Formation wraps around the south end of the South Slough Syncline. The lower sandstone member is predominantly fine- to medium-grained, cross-bedded and

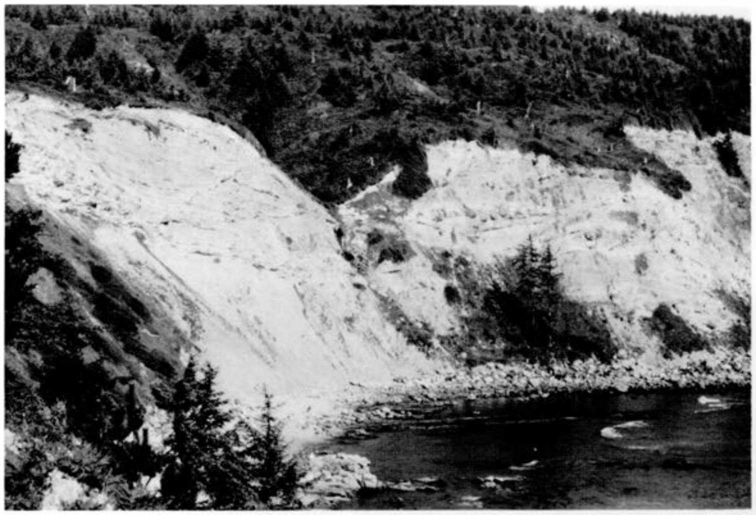

Figure 8. Elkton Siltstone: STOP 2. Channel complexes of the Elkton Siltstone crop out along the eastern wall of South Cove. This photo shows three channels: one at the upper left; a second lower channel cut by the center gully; and a third just to the right of the center gully (see Fig. 9).

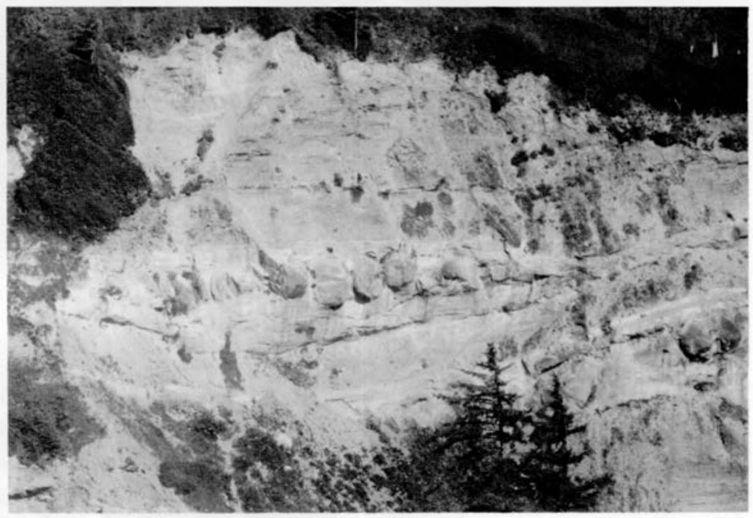

Figure 9. Elkton Siltstone: STOP 2. This telephoto view is of the lenticular channel-fill sandstone in the channel sequence shown in Figure 8 just to the right of the center gully.

Figure 10. Elkton Siltstone: STOP 3. This photo shows a predominantly siltstone channel-fill in the Elkton Siltstone along the east wall of North Cove. The waterfall at the right of the photo cascades down a rib of a sandstone bed within the same channel-fill sequence.

Figure 11. Aerial View of Coos Bay Area. a) Sunset Bay Sunset Park - Stop 6. b) Gregory Point. c) Lighthouse Beach - Stop 7b. d) Yoakam Point - Stop 7a. e) Miner Creek - Stop 7c. f) Bastendorff Beach - Stop 8. g) Tunnel Point - Stop 9. h) Coos Head-South Jetty - Stop 10. i) Coast Guard Cove - Stop 11. j) Charleston. k) South Slough. l) Fossil Point. m) Stinky Cove - Stop 12. n) Miocene Rocks - Stop 13. o) North Spit sand dunes. p) Empire. q) North Bend. r) Coos Bay. Photograph courtesy of Delano Photographics, Portland, Oregon.

laminated sandstones with minor interbeds of siltstone and mudstone. At Shore Acres the sandstones stand out as erosionally resistant, concretionary ribs where the interbedded fine-grained rocks have been differentially eroded. Large iron-cemented concretions are characteristic features of the lower Coaledo Formation. Fossils are abundant in some intervals of the lower Coaledo. Ophiuroids (brittle stars) are moderately common within one bed which crops out in both the northern and southern coves at Shore Acres State Park.

Shore Acres State Park is developed upon the Whisky Run terrace (Fig. 7). Four to nine feet of littoral sand rest upon this terrace platform. Whisky Run terrace sands can best be viewed from the north end of the viewpoint area.

Proceed back to State Parks Road.

(0.4)

1.6 Turn left toward Sunset Bay State Park.

(0.4)

2.0 View at 11:00 o'clock of Gregory Point and Cape Arago Lighthouse (Fig. 1-i and 11-b). Gregory Point is underlain by lower Coaledo Formation sandstone. These sandstones dip northeastward and strike increasingly more westward around the northern end of the Cape Arago Anticline (Ehlen, 1967).

(0.5)

2.5 Bridge across Big Creek. Big Creek heads in shales of the Bastendorff Formation to the east and cuts through the upper and middle Coaledo Formation.

(0.2)

2.7 <u>STOP 6</u>: <u>SUNSET BAY STATE PARK</u>: Park in the beach parking area. Traverses along either the north or south margins of Sunset Bay afford access to outcrops of lower Coaledo sandstone and middle Coaledo siltstone and mudstone. Access is best at low tide when outcrops of the surf-cut terrace are exposed over large areas along the north side of the cove. Trails along the north bluff of the bay provide excellent views of the faulting of the wave-cut terrace (beware of undercutting of the trails along the bluff).

Sunset Bay is an arcuate bay formed along a complex set of northwest-trending faults transverse to the strike of bedding (Fig. 11-a). Sunset Bay is offset 450 feet in a right lateral sense, between the north side and south side of the bay. Whether this displacement is along a single fault, or a series of smaller faults such as those exposed along the bay margins, is unknown. Orientation of drag folds suggests that the fault motion was oblique slip (Ehlen, 1967) (Fig. 12).

Ryberg (1978) identified several lithofacies in coarsening upward sequences within the lower Coaledo Formation. Outcrops exposing these coarsening upward sequences occur along the shores of Sunset Bay. The top of each sequence is generally identified by dark-brown, concretionary, coarse pebbly sandstone which forms erosionally resistant ribs. The typical sequence from bottom to top includes interdistributary siltstone and fine-grained sandstone, overlain by coarser distributary channel (and possibly fluvial) sandstone with interbedded lagoon or swamp coal and carbonaceous siltstone. These coarsening upward sequences are interpreted by Ryberg (1978) as representative of the outbuilding of individual distributary channels during progradation of a delta. This agrees with Dott's (1966) deltaic model for the Coaldeo Formation.

Sedimentary structures are well developed and beautifully exposed in outcrops along the north side of Sunset Bay and on the cliffs and terraces beyond the southwest edge of the bay entrance. Primary sedimentary structures include tabular, trough, wedge and hummocky cross-stratification, ripple cross-stratification, and rare flute and groove sole marks. Secondary

Figure 12. Coaledo Formation: STOP 6. View of drag-folds along faults in the Coaledo Formation. Photo taken at low tide from bluffs above the north side of Sunset Bay.

structures resulting from gravity deformation of the sediments include contorted bedding and flare, and ball and pillow structures. Clastic dikes and isolated sandstone "load-balls" represent liquification structures. Bioturbation includes both vertical and horizontal burrows.

The lower Coaledo is abundantly fossiliferous (Turner, 1938; Rooth, 1974). Mollusks and Foraminifera dominate the fauna but echinoids, shark teeth, and rare crustacean fossils also occur. The mollusks suggest deposition in middle to lower neritic depths (Rooth, 1974).

Paleocurrents are predominantly to the northwest and mineralogic studies suggest a mixed andesitic (e.g., Cascade-like) and metaplutonic (e.g., Klamath Mountains-like) provenance (Dott, 1966; Ryberg, 1978). This fits well with Dott's (1966) paleogeographic reconstruction for middle Eocene time which consists of a broad coastal plain prograding westward across a narrow shelf and slope. The coastal plain was flanked by highlands on the southeast. The highland included both volcanic and metaplutonic terrains.

Outcrops of the middle member of the Coaldeo Formation in Sunset Bay consist of interbedded laminated siltstone and mudstone with minor amounts of sandstone. Ryberg (1978) considered this lithofacies to represent intertidal flat and delta front deposits. The abundant molluscan (Turner, 1938) and foraminiferal faunas (Detling, 1946; Cushman and others, 1947; Rooth, 1974) represent deepening conditions from outer neritic just above the lower Coaledo sandstones to upper bathyal conditions above. The best outcrops and a complete section of the middle Coaledo siltstones and mudstones occurs along Lighthouse Beach at STOP 7.

The steeply dipping beds of the Coaledo Formation are truncated by the Pleistocene Whisky Run terrace. The Whisky Run terrace platform and presumably the shoreline angle are at an altitude of about 50 feet at the rear of the north side of Sunset Bay. The terrace platform along the south side of the bay is at 70 feet. The terrace has probably been offset by movement along a fault hidden beneath the water of Sunset Bay.

Tree stumps with root spreads up to 35 feet are exposed along Big Creek and in the intertidal zone of Sunset Bay beach. One set of root systems occurs in association with peat toward the north end of the beach. The trees could have been growing on the Holocene flood plain of Big Creek and drowned as the sea carved out the Sunset Bay amphitheater long after sea level attained its present position. Previously unpublished carbon

14 data on one root from along Big Creek yields an estimated age of about 1,200 years B.P. (Southern Methodist University Radiocarbon Laboratory Sample 593-B8/12-Count 1439: 10/11/78; Armentrout, unpub. data).

Return to the parking area and proceed north on State Parks Road. The road climbs from the Big Creek Holocene flood plain to the top of the Pleistocene Whisky Run terrace.

(0.4)

3.1 Road to the left provides access to the Cape Arago Lighthouse on Gregory Point. Steeply dipping beds of the lower Coaledo sandstone underlie the point.

(0.6)

3.7 STOP 7: YOAKAM POINT - MUSSEL REEF: Park along State Parks Road and walk northwest along a dirt road; about 150 feet from the main road, bear right (north) at the Y-junction, and continue to the sea cliff overlook area.

STOP 7A: Looking westward from Yoakam Point the three members of the Coaledo Formation can be observed. The lower sandstone member underlies Gregory Point to the west (Fig. 11-b). The middle mudstone and siltstone member has been eroded back forming Lighthouse Beach (Fig. 11-c). Yoakam Point and its seaward extension, Mussel Reef, consists of the upper sandstone member of the Coaledo Formation (Fig. 11-d). The cove immediately east of Yoakam Point is eroded in a siltstone of the upper sandstone member of the Coaledo Formation. The small point at the east side of this cove is the uppermost Coaledo Formation sandstone.

The platform of the Gregory Point-Yoakam Point area is formed by the Whisky Run terrace and is veneered by about 11 feet of littoral sand. At Yoakam Point the terrace is faulted with the eastern block offset about 10 feet above the western block. The fault trends north-northwest, parallel to the strike of the underlying Coaledo Formation and appears to be a high-angle reverse fault (Baldwin, 1966) (Fig. 5). The fault is best observed from the beach where the offset of a coal seam delineates the fault motion.

Griggs (1945) has mapped the eastward continuation of the Whisky Run terrace at the back of Bastendorff Beach where it forms the platform as far northeast as Tunnel Point (Fig. 11-g). The Pioneer terrace surface forms the platform at Coos Head, the northernmost point at the mouth of Coos Bay (Griggs, 1945) (Fig. 11-h).

Descend to Lighthouse Beach along the trail just south of Yoakam Point and walk to Gregory Point. Stop 7B consists of a traverse from Gregory Point to Yoakam Point.

STOP 7B: Gregory Point is formed of uppermost lower Coaledo sandstone interpreted to be deltaic distributary channel deposits (Ryberg, 1978). The sandstone is conformably overlain by middle Coaledo siltstone, mudstone and thinly bedded sandstone interpreted by Ryberg (1978) as intertidal flat to delta front deposits. Thick channelized massive sandstone occurs at several intervals within the finer grained sequence and is interpreted as prodelta front slump deposits (proximal turbidite or grainflow gravitite). A white tuff 3- to 6-feet-thick occurs just above the middle part of the middle Coaledo member at Lighthouse Beach.

At several points along Lighthouse Beach the truncated ends of middle Coaledo sandstone beds at the abrasion surface of Whisky Run terrace are bored by rock-boring clams. These features will be examined in detail at STOP 11.

The middle Coaledo Formation mudstone and siltstone is gradational with the overlying upper Coaledo sandstone. Upper Coaledo sandstone units are very similar to those of the lower Coaledo, representing fluvial and distributary channel deposits interbedded with finer grained muddy units of lagoon and tidal flat deposits. A single ten-foot-thick coal crops out between thick sandstone ribs at Yoakam Point and represents coaly swamp deposits. Just above this coal seam is a sandy interval with molluscan fossils including the brackish-water oyster Ostrea (Rooth, 1974). Ryberg (1978) suggests that these fossiliferous, poorly sorted, cross-stratified sandstones with irregular basal and top contacts are estuarine deposits. Several coarsening upward sequences occur within the upper Coaledo sandstone sequence near Yoakam Point.

Benthic foraminiferal and molluscan assemblages from the Coaledo Formation suggest neritic depths for the lower and upper sandstone members and lower neritic to bathyal depths for the middle siltstone/mudstone member (Rooth, 1974).

STOP 7C: Return to State Parks Road. Walk downhill to the north and west along the cliff at the southwestern end of Bastendorff Beach. Enter the cove at the northeast end of Yoakam Point.

The uppermost units of the Coaledo Formation crop out above Yoakam Point as a deep reentrant cove and a narrow sandstone point. The cove is eroded in mudstones and siltstones of marine origin. Prodelta foreset and tidal flat-lagoonal deposits coarsening upward into fluvial and distributary channel sandstones form the uppermost Coaledo sandstone point (Ryberg, 1978).

Traverse back toward State Parks Road along the cliffs at the south end of Bastendorff Beach. Along this traverse is the gradation from Coaledo Formation sandstone to Bastendorff Beach shale. The Coaledo sandstones are principally well-bedded barrier bar or beach deposits interbedded with silty prodelta, foreset sandstone and siltstone couplets (Ryberg, 1978). These units are poorly exposed and the overlying Bastendorff Formation shale has been largely eroded out along the valley of Miner Creek (Fig. 11-e).

Return to the parking area and drive northwest along State Parks Road. The road descends from the platform of Whisky Run terrace to the Holocene flood plain of Miner Creek. The broad valley of Miner Creek is formed in the easily eroded shales of the Bastendorff Formation.

(0.2)
3.9 Ahead at 1:00 o'clock the hillside exhibits active slumping or slump-earthflow typical of areas underlain by the Bastendorff Formation.

(0.1)
4.0 Turn left onto Bastendorff Beach Road.

The road ascends to the Whisky Run terrace surface.

(0.3)
4.3 STOP 8: BASTENDORFF BEACH VIEWPOINT: Park at the viewpoint across the road from Bastendorff Beach County Park Campground (Fig. 11-f).

From this viewpoint one looks west to Yoakam and Gregory Points formed upon sandstones of the Coaledo Formation and east to the bluff of Tunnel Point. Bastendorff Beach has accreted for the most part since construction of the South Jetty at the mouth of Coos Bay.

The lowermost outcrops of the Bastendorff Formation are to the southwest of the viewpoint and can be reached along the base of the bluff. These outcrops consist of middle Bastendorff Formation interbedded sandstone and shale.

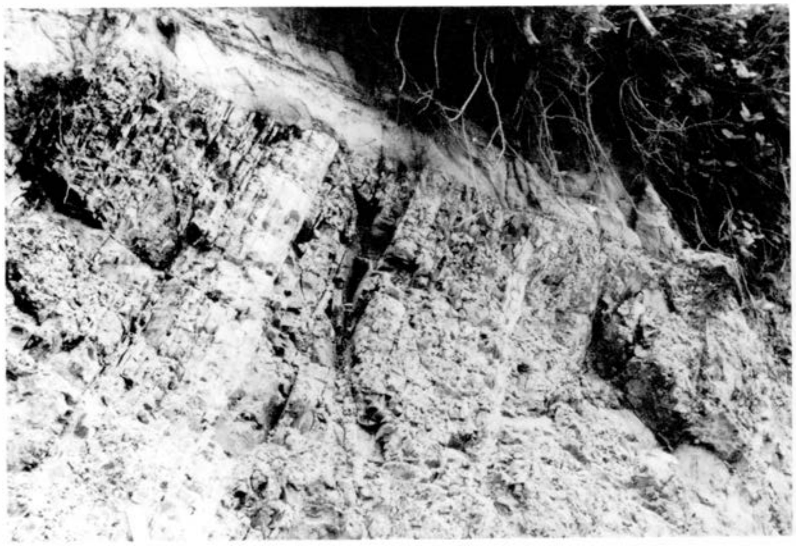

Figure 13. Bastendorff Formation: STOP 8. Interbedded claystones, siltstones and ash layers of the Bastendorff Formation are truncated and weathered at the abrasion surface of the Whisky Run Terrace.

Upper Bastendorff Formation shale crops out along the Bastendorff Beach road about 50 yards north of the viewpoint (Fig. 13). The road cut outcrop exposes the interbedded, finely laminated, dark-gray siltstones and mudstones with thin yellowish-grey-weathering tuff beds. Microfossils and rare small mud-pectens occur within these rocks. Foraminiferal faunas suggest bathyal to abyssal depositional environments shallowing upsection to upper bathyal to neritic environments toward the top of the Bastendorff Formation (Rooth, 1974; Tipton, 1975).

At the top of the outcrop the Bastendorff Formation shales are truncated by the wave-cut platform of the Whisky Run terrace. The terrace surface was bored by clams. The borings can be found in several locations along the outcrop bluff where the borings in the Bastendorff shale are filled by terrace sands.

Return to the beach overlook and continue driving north along Bastendorff Beach Road.

(0.2)

4.5 View ahead is of Tunnel Point to the immediate right and Coos Head and the South Jetty at the inlet to Coos Bay in the distance (Figs. 11-g and 14).

(0.2)

4.7 STOP 9: TUNNEL POINT: Park in the turnout to the left. The Tunnel Point Formation forms the old sea cliff to the southeast of the parking area. A trail along the base of the bluff provides access to the outcrops.

The basal sandstone of the Tunnel Point Formation forms the strikewall at the contact between the Bastendorff and Tunnel Point Formations. The point formed in this basal sandstone is supported by a 10-inch-thick, highly fossiliferous concretionary bed. Upsection from this basal sandstone the Tunnel Point Formation consists of poorly bedded, fine-grained, tuffaceous sandstone and sandy siltstone. The formation is fossiliferous throughout with a molluscan fauna dominated by pelecypods. The fauna is indicative of the Galvinian Stage (Armentrout, 1975a) and suggests deposition within the neritic zone.

The dipping strata of Tunnel Point are truncated by the abrasion platform of the Whisky Run terrace. Griggs (1945) mapped the Whisky Run terrace continuously to the west as far as Cape Arago. East of Tunnel Point, he mapped the terrace platform capping Coos Head as the Pioneer terrace.

Figure 14. Tunnel Point Formation. STOP 9. This view of Tunnel Point is toward the northeast across Bastendorff Beach. The cliff face is formed in the basal sandstone of the Tunnel Point Formation.

Figure 15. Tunnel Point Cave: STOP 9. The Tunnel Point sea cave formed prior to the accretion of Bastendorff Beach. The sea cave has maximum dimensions of 118 feet deep, 49 feet wide, and 23 feet high.

Tunnel Point received its name from the occurrence of a large sea cave within the main point of the lower Tunnel Point Formation (Fig. 15). The cave was formed by sea cliff erosion prior to the construction of the South Jetty at the mouth of Coos Bay which initiated the accretion of Bastendorff Beach. The sea cave can be entered at the southeast end of the western face of Tunnel Point. A second entrance eroded along a shaly interval within Tunnel Point was blocked about 1963 by blocks of rock falling from the passage roof. Blocks of sandstone frequently fall from the ceiling and extreme caution is urged upon entering the cave.

Return to the parking area and proceed northeast on Bastendorff Beach Road.

(0.1)

4.8 Late Miocene Empire Formation sandstone forms the bluff ahead. The densely vegetated valley to the right, down which Coos Head Road descends, is formed on a slumped, faulted interval in the upper Tunnel Point Formation (Weaver, 1945). The contact between the 70° east-dipping Tunnel Point Formation and the 30° northeast-dipping Empire Formation occurs somewhere in this valley.

(0.1)

4.9 Junction of Bastendorff Beach Road and Coos Head Road. Turn left.

(0.1)

5.0 The cliffs to the right are concretionary sandstones of the Empire Formation.

(0.2)

5.2 STOP 10: COOS HEAD AND SOUTH JETTY: Park at the landward end of the jetty and walk to the east end of the concrete core of the jetty. The view from this point includes the North Jetty and North Jetty Dunes Area across the mouth of Coos Bay, and to the east, Coos Head (Figs. 11-h and 11-o). An old (and very dangerous) railroad tunnel can be seen at the southeast corner of the cove at the end of the jetty. Building rock and other materials were brought to the jetty area via this tunnel.

Some of the South Jetty is constructed of blocks of volcanic breccia. This breccia is from quarries east and north of Coos Bay where local centers of volcanism formed during deposition of the Roseburg Formation of the Umpqua Group (Baldwin, 1974). The volcanics are characteristically fine-grained, pillowed or brecciated calc-alkalic basalts (Baldwin and others, 1973). These local Roseburg Formation basalts are compositionally and age equivalent to the early Eocene Siletz River Volcanics to the north. The basalts generally have a chloritized groundmass and cavity-filling zeolites.

The rocks of the Empire Formation forming Coos Head are massive bioturbated fossiliferous sandstone with abundant fossiliferous concretions. At the upper left corner of the railroad tunnel and northwest along the cove wall is a single waterlaid tuff bed. This tuff crops out in the Empire Formation only along the west limb of South Slough Syncline.

Sandstone of the Empire Formation is truncated by the Pioneer terrace platform at an elevation of about 72 feet above sea level.

Return to the vehicles and proceed back along Coos Head Road.

(0.2)

5.4 Pass the juncton of Coos Head and Bastendorff Beach Roads, continuing on Coos Head Road.

(0.4)

5.8 Pass Coos Head Naval Facility and turn left onto the gravel-surfaced road paralleling the fenced perimeter of the Naval Facility. The road is on the Pioneer terrace.

(0.2)

6.0 Bear right at Y in the road. The road to the left of the Y goes to Coos Head Lookout, overlooking the mouth of Coos Bay.

(0.5)

6.5 Junction at Boat Basin Drive. University of Oregon Institute of Marine Biology on right - Oregon State Fish and Wildlife Commission facility on left. Turn left.

(0.1)

6.6 STOP 11: COOS HEAD - COAST GUARD HOUSING FACILITY: Park in the area of the junction of Boat Basin Drive and Alaska Packers Road. Walk north along the extension of Boat Basin Drive for about 100 yards to a small cove with a concrete jetty, just past some University of Oregon research laboratory buildings. Permission for access should be obtained from the Director, Oregon Institute of Marine Biology, Charleston, Oregon 97420.

Walk to the seaward end of the concrete jetty. From this vantage point the wave-cut platform can be seen on the truncated Empire Formation at Coos Head (Fig. 16). At the northern points of Coos Head, the terrace platform is at an elevation of about 72 feet above sea level. The platform descends to an elevation of about 10 feet above sea level at the landward end of the jetty. The terrace deposits, littoral and aeolian sands, thicken to the east as the wave-cut platform descends, keeping the top of the terrace deposits at nearly the same elevation. This relationship

Figure 16. Coos Head: STOP 11. This view, from the end of the jetty at the old Coast Guard dock at Coos Head, shows the terrace surface descending from an elevation of about 72 feet to the right at Coos Head, to about 10 feet at the landward end of the jetty.

Figure 17. Bored Terrace Surface: STOP 11. The abrasion surface of the marine terrace at STOP 11 is bored by the pelecypods Penitella (large conical borings) and Adula (small cylindrical borings with a heart-shaped cross section.

suggests deformation after platform erosion and before terrace deposition, or differential terrace fill on original topography of the wave-cut platform. Terrace stratigraphy along the axis of South Slouth Syncline is complex reflecting a history of warping, tectonic uplift, sea level fluctuation and paleotopography. This stop provides one example of the complexity. Griggs (1945) considered the terrace surface at the landward end of the jetty to be the Whisky Run terrace. The terrace surface at the top of Coos Head is mapped as Pioneer terrace (Griggs, 1945). The wave-cut platform at Coos Head appears to ascend continuously from the Whisky Run terrace to the Pioneer terrace. Obviously further work is required to unravel the terrace sequence stratigraphy.

At the landward end of the jetty the terrace abrasion platform is exposed revealing a densely bored surface (Fig. 17). Large spindle-shaped borings of pholad clams (Penitella) and smaller cross-sectionally heart-shaped date-mussel borings (Adula) are abundant. The boring pholads penetrate

Figure 18. Empire Formation-Fossil Point: STOP 12. Fossil Point consists of a fossiliferous intraformational conglomerate within the Empire Formation. This view to the southwest is of the updip side of the conglomerate where the erosional basal contact is well exposed.

eroded rock surfaces creating a host of small cavities. These cavities provide living space for an endolithic community of organisms. Modern communities of this type have been studied at Coos Bay (Evans, 1967), and analogous late Pleistocene fossil assemblages are known at several localities along the Oregon coast (Armentrout, 1975b).

Return to vehicles and drive southeast on Boat Basin Drive past the Oregon Institute of Marine Biology into Charleston.

(0.6)

7.2 Charleston, junction of Boat Basin Drive and State Parks Road at west end of South Slough Bridge. Turn left onto bridge (Fig. 11-j).

(0.1)

7.3 Center of South Slough Bridge - axis of South Slough Syncline.

(0.2)

7.5 Bluff outcrop to the right of the road is 8 feet of strongly weathered aeolian sand, overlying a well-preserved, weakly developed podzol. The soil is developed on complexly cross-stratified fine to medium sand. The sand occurs in 8- to 16-inch-thick sets that have foreset bedding dipping both north and south, parallel to the axis of South Slough. Some of the sets are separated from one another by two- to four-inch-thick, laterally persistent beds of fine gravel. The cross-strata were probably produced by alternating tidal currents along the axis of a "paleo-slough" (R. Janda pers. commun., 1979). Exposures farther to the east and south show that these sediments extend at least to present sea level.

(0.7)

8.2 To the left of the road is a small cove (difficult to see through the dense vegetation). It is along the southwest side of this cove that the upper conglomerate of the Empire Formation crops out. The outcrops can be reached along the beach.

(0.3)

8.5 Fossil Point (Fig. 11-l) is located along the bay opposite the side road intersection just north of the Barview grocery. One must go through private property to reach the point from here, or walk the beach at low tide from the Pigeon Point area to the north (STOP 12).

(0.4)

8.9 STOP 12: STINKY COVE - FOSSIL POINT AREA: Park off the main road and walk out to the point at the southwest margin of the small cove, locally known as "Stinky Cove" for the abundant accumulations of seaweed (Fig. 11-m). Pigeon Point is the low point to the north of the cove. The stop consists of a half-mile traverse south along the beach to Fossil Point (Fig. 18). The traverse takes about an hour and a half and is best taken at low tide.

Once Fossil Point is reached a small "scramble" trail at the east end of the Point provides access to the top of the outcrop.

Outcrops from Stinky Cove southward are massive sandstones of the Empire Formation. The exposures consist of a wave-cut platform, exposed at low tide, which is grooved by numerous drainage channels following fractures in the sandstone. Concretionary intervals roughly depict bedding. The strata strike N. 5° W. and dip west at about 12°. Molluscan and vertebrate fossils are common along this interval. The sands are extensively bioturbated and trace fossils include siltstone cored vertical burrows and oblique grazing traces. The fossiliferous conglomerate at Fossil Point is known as the Coos Conglomerate (Dall, 1909). The Coos Conglomerate is 36 feet thick, has an erosional base, and has been traced bayward and upsection where it grades into the typical sandstone of the Empire Formation (Armentrout, 1967, 1973).

Armentrout (1967) compared the Coos Conglomerate to modern beach deposits along the Fossil Point-Pigeon Point area and noted the following common characteristics: channeled basal contacts; interfingering with beach sands; cobbles and boulders of fossiliferous lower Empire Formation sandstones; rounded beach pebbles and cobbles of chert, basalt, and quartzite in a lithic feldspathic sand matrix; and fossils eroded from the Empire Formation mixed with broken shells of the contemporaneous shallow-water fauna. Armentrout (1973) interpreted the Coos Conglomerate, and a similar conglomerate higher in the Empire Formation south of Fossil Point, as intraformational deposits formed in littoral to sublittoral tidal channels just seaward of a paleoshoreline, essentially parallel with the modern eastern margin of Coos Bay.

The molluscan fauna of the Empire Formation was originally studied by Dall (1909). Recent biostratigraphic analysis of the Empire fauna assigns it to the Wishkahan Stage of late Miocene age (Addicott, 1976). The fauna is interpreted as being deposited in inner sublittoral environments (Armentrout, 1967). Vertebrate fossils from the Empire Formation are discussed by Ray (1976).

The shoreline bluffs between Stinky Cove and Fossil Point are truncated by a marine terrace refered to as the Whisky Run terrace by Baldwin (1966). The erosional platform of this terrace has been bored by pholads. The spindle-shaped borings of these clams can be seen at several locations along the traverse, especially just southwest of the top of the Coos Conglomerate at Fossil Point, and at the point forming the southwest side of Stinky Cove.

Return to the Stinky Cove parking area and proceed northeast on State Parks Road toward Coos Bay.

(0.2)

9.1 Pigeon Point road on the left. Pigeon Point is formed of Empire Formation sandstone.

(0.3)

9.4 Pleistocene dune outcrop on the right.

(0.3)

9.7 Immediately below this point along the beach are outcrops of the basal Empire Formation.

(0.1)

9.8 STOP 13: MIOCENE BEDS: Park along the shoulder of the roadway and descend to the beach via any one of the several steep trails (Fig. 11-n). This stop must be made at low tide.

Once at the beach, look north toward Sitka Dock. In the immediate foreground, at low tide, are several rows of barnacle and seaweed-covered concretions exposed between the sand beach and bay mud (Fig. 19). These

Figure 19. Miocene Beds: STOP 13. Outcrops of upper lower to middle Miocene concretionary sandstones, shown in this low tide photo, occur as bay bottom exposures between the sand beach and bay bottom muds. The pulp plant in the distance at Sitka Dock is currently abandoned.

Figure 20. Miocene Beds: STOP 13. This closeup photo shows Patinopecten oregonensis cancellosus (Moore) a fossil commonly found in the concretions of the Miocene Beds of Coos Bay.

concretions and the enclosing sandstone, which crop out on the bay bottom, are the "Miocene Beds" of Coos Bay (Armentrout, 1967, 1978; Baldwin, 1966). The "Miocene Beds" are highly fossiliferous with a molluscan fauna assigned to the late early to middle Miocene Newportian Molluscan Stage (Addicott, 1976; Armentrout, 1978). The concretions often have very large pectens within (Fig. 20). Paleoecologic analysis suggests deposition in warm-temperate waters of less than 180-foot depth (Armentrout, 1967, 1978; Moore, 1963).

Along the beach southeast of this outcrop area are basal beds of the late Miocene Empire Formation. About 10 feet of crossbedded sandstone crop out below a prominent highly fossiliferous concretionary zone. The lowermost Empire Formation sandstone overlies the upper lower and middle Miocene beds with slight angular discordance.

Return to the vehicles. This completes Day 1 of the field trip. Day 2 begins at the Cape Blanco Road turn off on Highway 101, 46 miles south of Coos Bay and 4.5 miles south of Port Orford.

Figure 21. Aerial View of Cape Blanco Traverse. a) Jurassic Otter Point Formation. b) Late Miocene Empire Formation. c) Cape Blanco Coast Guard facility. d) Eocene Shales - Stop 4. e) Miocene Sandstones - Stop 6. f) Fin Rock Miocene Sandstones - Stop 7. g) Terrace Fossil Beds - Stop 3. h) View Point - Stop 2. i) Cape Blanco State Park Campground. j) Goldwasher's Gully - Stop 11. k) Cliff at Stop 12. l) Cliffs at Stops 13-15. m) Mouth of Elk River. n) Port Orford. o) Humbug Mountain. Photograph courtesy of Oregon State Highway Division.

CAPE BLANCO SEGMENT

The Cape Blanco field trip segment consists of a one-day excursion. This segment starts on Highway 101, 46 miles south of Coos Bay at the junction with the Cape Blanco Road (Fig. 2). The road log is 4.4 miles long with one stop and is followed by a two mile beach traverse with 14 cliff exposure stops (Figs. 21-23). Tides are not a problem along the beach traverse. An access road intersects the beach traverse at the half-way point: Goldwasher's Gully. This road is accessible during summer months via the paved State Park campground road system, and during the winter months via an unpaved ranch road at the point of mileage 4.0.

The Cenozoic geology of Cape Blanco consists of Eocene to Pleistocene, continental margin, marine and non-marine rocks. The section consists of six rock units and measures approximately 1,220-feet-thick (Figs. 3 and 22). The six units are separated into five unconformity-bounded sequences of rock: 1) Eocene (Roseburg Formation, Baldwin and others, 1973); 2) late early to middle Miocene (Sandstone of Floras Lake, Addicott, in preparation); 3) late Miocene (Empire Formation as restricted by Addicott, in preparation); 4) Pleistocene [Port Orford Formation, Baldwin (1945), and Elk River Beds of Baldwin (1945) as restricted by Addicott (1964) and Clifton and Boggs (1970)]; and 5) late Pleistocene [terrace deposits of Addicott (1964) and Clifton and Boggs (1970)].

MILEAGE DESCRIPTION

Cumulative (interval)

Drive Highway 101 to the Cape Blanco Road 46 miles south of Coos Bay and 4.5 miles north of Port Orford. Mileage starts at the turn-off from Highway 101 to Cape Blanco.

0.0 Heading west toward Cape Blanco the road traverses the surface of a late Pleistocene marine terrace. Ditch-cuts expose berm and back beach sediments.

(0.5)

0.5 Road descends to the back edge of another late Pleistocene marine terrace.

(0.3)

0.8 Small mounds on either side of the road are former sea stacks of the Jurassic Otter Point Formation which protrude through the terrace-surface. Surficial deposits are mostly alluvium.

(1.7)

2.5 Road descends over two alluvial terraces to the Sixes River floodplain.

(0.9)

3.4) Roadcut outcrops of dark-gray rocks are Jurassic Otter Point Formation.

(0.1)

3.5 STOP 1: TERRACE DEPOSITS: Park along the turn out to the right of Cape Blanco Road. A road-cut on the south side of Cape Blanco Road exposes an excellent sequence of foreshore and surf zone sandstone and conglomerate (R. Janda, pers. commun., 1979). These rocks occur at the top of a regressive sequence of terrace deposits resting on a surf cut platform.

Continue toward Cape Blanco.

(0.5)

4.0 A dirt road to the left provides access to the beach at Goldwasher's Gully. This is a private ranch road and care must be taken to leave all gates closed, and to drive slowly. When using this dirt road take the first right turn after the second gate to reach the beach.

(0.2)

4.2 Entrance road to Cape Blanco State Park Campground. This campground is open only during the summer season.

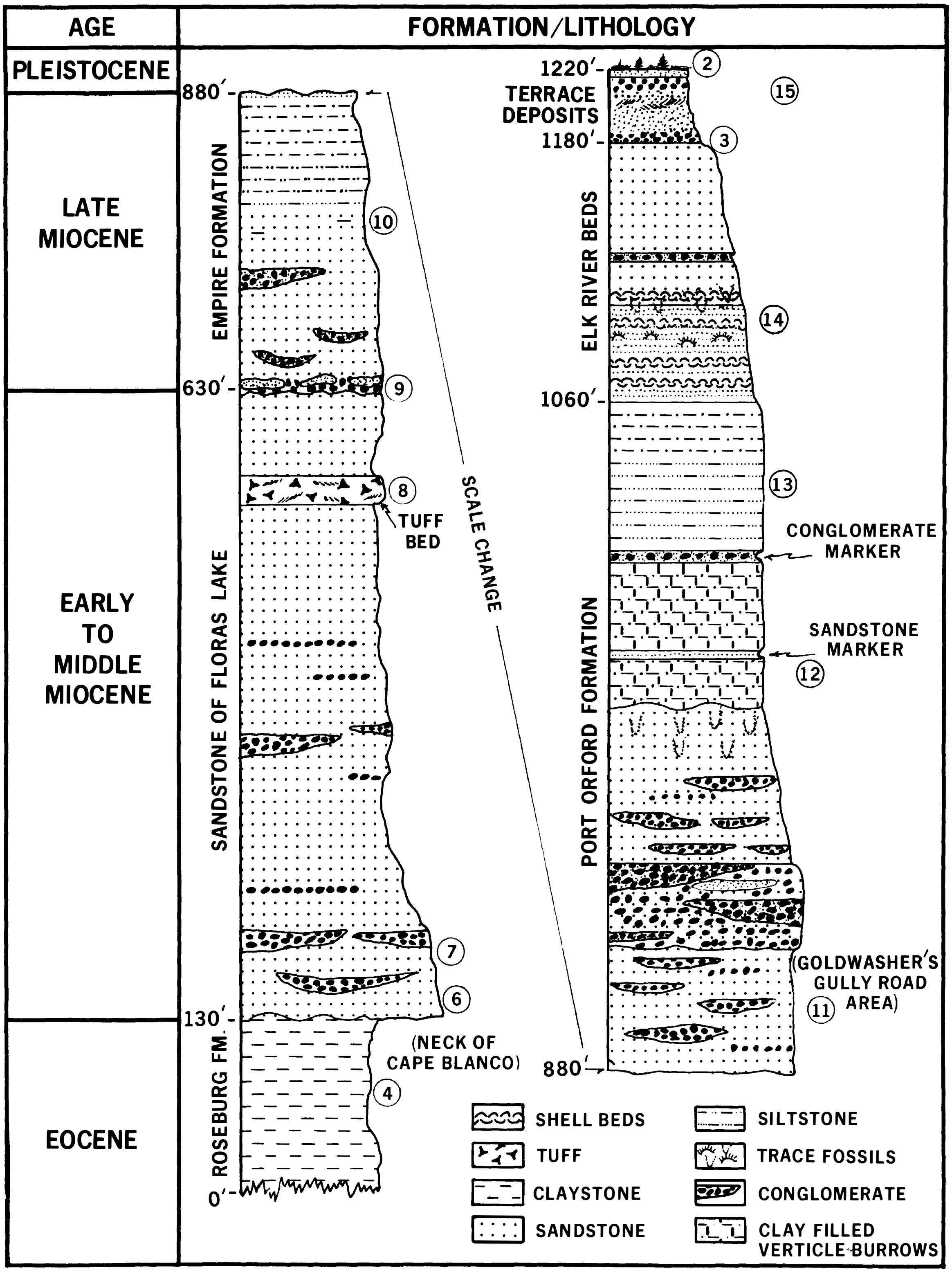

Figure 22. Stratigraphic column for Cape Blanco Cenozoic formations. Each field trip stop is indicated by a numbered circle.

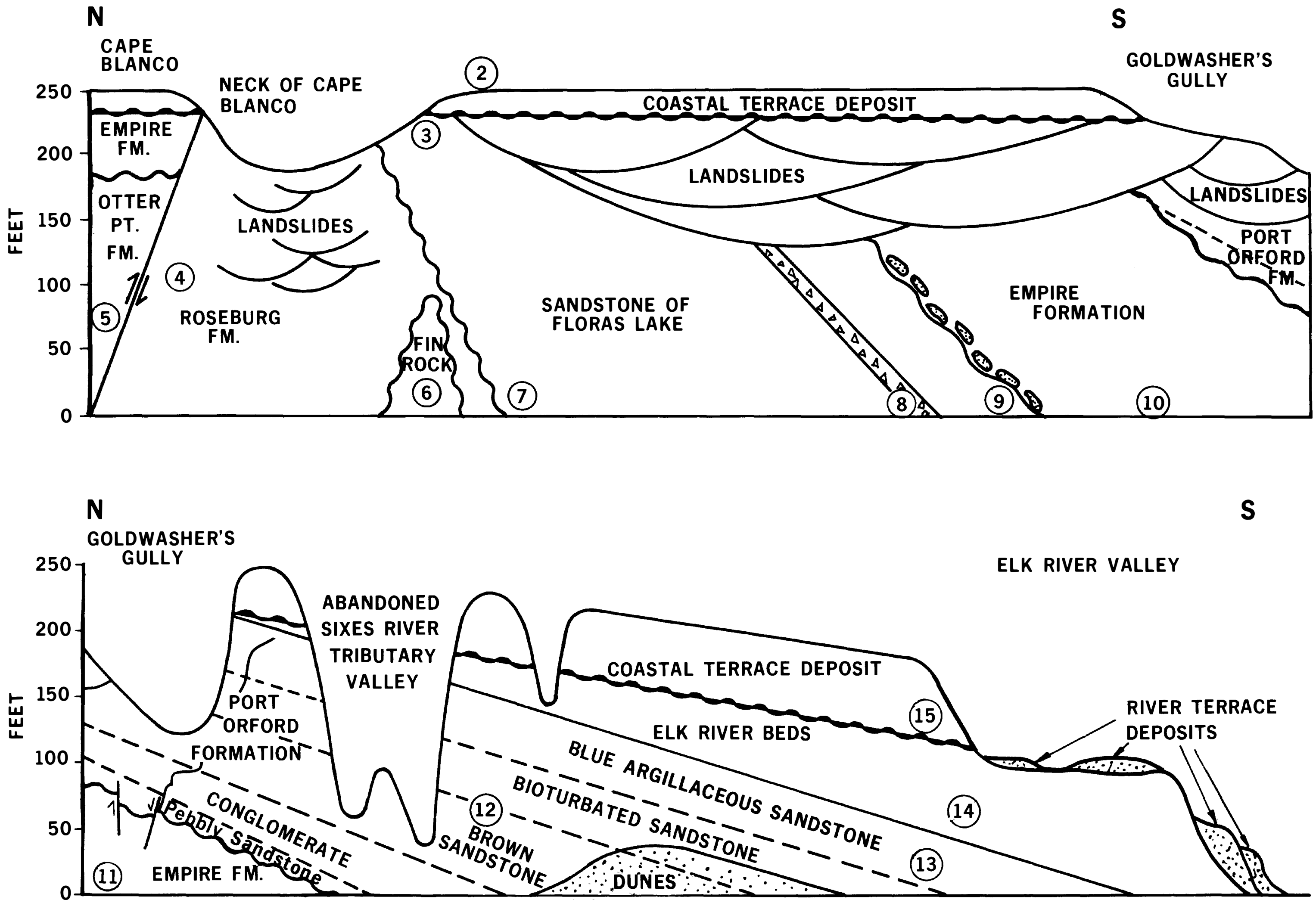

Figure 23. Schematic diagram of the Cenozoic stratigraphy of the beach traverse from Cape Blanco south to the mouth of the Elk River. Each stop is marked with a numbered circle.

(0.2)
4.4 STOP 2: CAPE BLANCO HEADLAND: VIEW POINT: Park along the dirt-turnout on the south side of the Cape Blanco Road. Walk south along the bluffs to the fenced area above the cliffs, 1/4 mile from the road, stopping at the corner of the fence (Fig. 21-h). From this vantage point, the stratigraphy of Cape Blanco is visable. Use figures 21 and 24 to identify the units. Of partucular note is the shell bed at the base of the terrace sequence. The shell bed is located off to the right, in the cliff top alcove, above the slumped area of the neck of Cape Blanco (Figs. 25-26; STOP 3).

Walk back north along the bluff and descend downward through the terrace deposit sequence to the shell beds.

STOP 3: TERRACE SHELL BEDS: Two molluscan faunal assemblages occur within the basal marine transgressive facies of a late Pleistocene coastal terrace deposit exposed in the cliffs just south of the neck of Cape Blanco (Figs. 21-g and 25-26). Initial population of the surf-cut terrace platform was by the pelecypods *Penitella penita* and *Zirfaea pilsbryi* that bored into lithified and concretionary Miocene sandstone (sandstone of Floras Lake). The borings provided niches for a subsequent fauna consisting of nestling organisms. Fossilized members of this nestling assemblage consists of the gastropod *Crepidula nummaria* and the pelecypods *Macoma inquinata*, *Protothaca staminea ruderata*, and *Hiatella pholadis*. This community of borers and nestlers suggests a shallow intertidal to inner sublittoral habitat with sufficient wave energy to prevent persistent accumulation of sediment. Subsequent erosion removed all but the deeper borings of (*Zirfaea pilsbryi* and those borings in the more erosionally resistant concretionary sandstone and sandstone boulders.

As the transgression continued, the water deepened allowing deposition of a sandy substratum and the establishment of a community of soft sediment burrowers. Sand-filled depressions on the terrace platform are locally burrowed by *Mya truncata* and *Macoma inquinata*, suggesting that these small, shallower burrowers were first to populate the sandy substrate. This early population is overlain by a densely packed shell layer of burrowing mollusks dominated by adult *Tresus capax* and *Saxidomus giganteus*. The burrowing community of the sandy substratum suggests shallow offshore waters of the inner sublittoral zone.

Foraminifera associated with the shell bed consist of an agglomeration of many thick-walled and solution resistant species that have been transported into shallower water, possibly the inner neritic zone (K. McDougall, pers. commun., 1979). Species present are representative of the inner neritic (*Elphidium frigidum* and *Elphidiella lobatulus*), middle neritic (quinqueloculinids and *Cibicides lobatulus*), and outer neritic (*Cassidulina limbata*) depth zones.

The fossiliferous transgressive terrace deposits are overlain by a regressive sequence of beach and dune sandstone, and fluvial conglomerate. The Miocene sandstones underlying the sandstone conglomerate terrace deposits will be viewed and discussed at STOPS 6 and 7.

Continue descending the south side of the Cape Blanco "neck" working northward toward the gray "Bad-lands" topography.

Figure 24. South side of Cape Blanco: STOP 2. The dark cliff-base outcrops are Jurassic Otter Point Fm. unconformably overlain by late Miocene Empire Fm. The Cape is capped by horizontally bedded late Pleistocene terrace deposits. Eocene Roseburg Fm. shales form the slumping "neck" of Cape Blanco. The sea stack (Fin Rock) is Miocene sandstone of Floras Lake.

Figure 25. Pleistocene Coastal Terrace Deposit: STOP 3. The marine to non-marine sandstone and conglomerate of the marine terrace sequence unconformably overly upper lower to middle Miocene sandstones. A shell bed (Fig. 26) marks the base of the terrace deposit.

Figure 26. Marine Terrace Fossil Bed: STOP 3. The base of the marine terrace sequence consists of an in situ shell bed of burrowing clams (large Tresus and Saxidomus) overlying the terrace abrasion surface which has been bored by clams (Zirfaea).

STOP 4: ROSEBURG FORMATION: Calcareous gray shales crop out between the Cape Blanco headland cliffs and the slumped area of the Cape Blanco "neck" (Figs. 21-d and 27). The shales are finely laminated claystone and mudstone and are interpreted as abyssal plain turbidite deposits. Locally the shales are intensely deformed. Isoclinal folds and small exotic blocks of phyllite and schist occur within the shales (R. Janda, pers. commun., 1979). In the cliffs on the north side of Cape Blanco the Jurassic Otter Point Formation appears to have been thrust over the shales (Dott, 1962, 1971).

The gray shales at Cape Blanco were originally mapped by Diller (1902) as questionably Myrtle Formation of Cretaceous age. Bandy (1944) recovered a foraminiferal fauna which he assigned to the middle Eocene. Baldwin (in Baldwin and others, 1973) has assigned the gray shales to the Roseburg Formation of latest Paleocene to early Eocene age.

The gray shales contain abundant benthic foraminifers. Agglutinated species of *Ammodiscus*, *Bathysiphon*, and *Spiroplectammina*, compose the bulk of the assemblage and calcareous foraminifers are rare. Siliceous cement is the principal component of the agglutinated tests. The benthic foraminiferal assemblage is therefore interpreted by McDougall (pers. commun., 1979) as being deposited below the CCD (Calcium Compensation Depth) in the lower bathyal or abyssal facies.

The foraminiferal assemblage described by Bandy (1944) is dominated by calcareous shelf species, and was not recovered in samples examined for this study (K. McDougall, pers. commun., 1979) or in other studies of these same rocks (R. E. Thoms, pers. commun., 1979).

Continue traversing downward and north to the beach cliff exposures at the Cape Blanco headland.

STOP 5: JURASSIC OTTER POINT FORMATION: Dark-gray massive mudstone and sandstone of late Jurassic age form the cliffs at the north end of the beach on the south side of the Cape Blanco headland (Fig. 24). These rocks have been mapped as Otter Point Formation (Dott, 1971) and occur in a fault block unconformably overlain by late Miocene Empire Formation (as restricted by Addicott, in preparation). The Otter Point Formation at Cape Blanco is principally a mélange or broken formation. Tectonically polished blocks of greenstone and blue schist occur along the fault bounding the southeast side of the Empire Formation outcrops (R. Janda, pers. commun., 1979).

Walk south along the beach to Fin Rock, a large sea stack (Figs. 21-e and 24).

STOP 6: SANDSTONE OF FLORAS LAKE: FIN ROCK: Massive brown-weathering, fine to medium-grained sandstone with interbedded pebble and cobble conglomerate lenses are well exposed at Fin Rock (Fig. 24) and in the sea cliffs immediately south of the slumping "neck" of Cape Blanco (Fig. 28; STOP 7).

The sandstone at STOPS 6 and 7 was originally included in Diller's (1902) Empire Formation. Durham (1953) recognized an unconformity (Fig. 29; STOP 9) within Diller's Empire Formation and found the molluscan fauna of the lower unit to be middle Miocene in age, and the upper unit to be late Miocene to Pliocene in age. Janda (pers. commun., 1979) found a mappable lithologic difference between the two units: the lower having pebbles

Figure 27. Roseburg Formation Shales: STOP 4. The Eocene Roseburg Formation shales form the slumping "neck" of Cape Blanco. The shales are finely laminated and highly calcareous.

Figure 28. Sandstone of Floras Lake: STOP 7. The upper lower and middle Miocene sandstone of Floras Lake form steep cliffs just south of the "neck" of Cape Blanco. Lenticular pebble conglomerates are a characteristic feature of this rock unit.

of numerous labile types; the upper having pebbles of quartz and other resistent types. To differentiate these two unconformity-bounded units Janda (pers. commun., 1979) suggests that the lower conglomeratic sandstones be informally referred to as the sandstone of Floras Lake, and that the Empire Formation be restricted to the upper Miocene unconformity-bounded sequence (STOPS 9 and 10) which is a correlative of the type Empire Formation at Coos Bay (Addicott, 1976).

Cross the beach southward to the base of the sandstone cliffs.

STOP 7: SANDSTONE OF FLORAS LAKE: These cliff outcrops expose excellent examples of the pebble and cobble lenses of the sandstone of Floras Lake (Fig. 29). The unit fines upward through the approximately 500 foot thick section exposed in the cliffs south of Cape Blanco. Correlative rocks crop out to the north of Cape Blanco from Blacklock Point to Floras Lake (R. Janda, pers. commun., 1979).

The molluscan fauna of the sandstone of Floras Lake is referable to the Newportian Molluscan Stage (Addicott, 1976) of the Pacific Northwest. Species restricted to the Newportian Stage include Molopophorus matthewi, Nassarius arnoldi, Macoma flagleri and Mytilus middendorffi. The age of the Newportian is late early to middle Miocene in terms of the European standards (Addicott, 1976).

Mytilus middendorffi is particularly abundant in the sandstone of Floras Lake. This distinctive plicate mussel is an index fossil of the Newportian and ranged from Southern California to the Gulf of Alaska and possibly Kamchatka (Allison and Addicott, 1976).

The abundant Mytilus, associated with the barnacle Balanus sp. and the pebble conglomerate lenses suggest a very shallow, possibly intertidal, depositional environment and proximity to a rocky shoreline (Addicott, in preparation). Upsection, the rocks fine to micaceous sandstones and the fauna changes to one characterized by Spisula albaria, Katherinella cf. K. angustifrons and Dentalium sp., suggesting deepening of the depositional environment to about 30 to 60 feet.

Continue south along the sea cliff to a 25-foot-thick tuff bed. Some of the outcrops along this traverse are landslide blocks from stratigraphically higher intervals within the Miocene sequence. The tuff bed crops out 400 feet upsection from STOP 7 and forms a 10-foot-high, back-beach bluff.

STOP 8: TUFF BED OF SANDSTONE OF FLORAS LAKE: This 25-foot-thick bed consists of massive fine-grained tuff and intervals of cross-stratified coarse-grained tuff. An upper interval of massive fine-grained tuff contains a floral assemblage of entire leaves assignable to the upper Seldovian (middle Miocene) Megafloral Stage (Wolfe and Hopkins, 1967; J. Wolfe, pers. commun., 1979). The sedimentary strutures, presence of entire leaves, and the abundance of tuff, suggest near-shore deposition with the leaves and tuff entering from a fluvial source.

Overlying the tuff unit are about 100 feet of sandstone of Floras Lake which are massive, carbonaceous and micaceous sandstone with scattered large concretions (Addicott, in preparation). Mollusk fossils are abundant in many of the concretions and consist mostly of Spisula albaria.

Continue south along the bluffs through the upper sandstone of Floras Lake to the unconformity shown in figure 29.

STOP 9: FLORAS LAKE/EMPIRE UNCONFORMITY: Figure 29 is a photo of the unconformity between the sandstone of Floras Lake and the overlying Empire Formation. The unconformity crops out in a northwest-facing bluff at the southeast side of a small shallow cove. The unconformity is a channelized surface, overlain by concretionary sandstone containing blocks of sandstone of Floras Lake. The reworked sandstone blocks are riddled with borings filled with shell debris (Addicott, in preparation).

The lower Empire Formation consists of medium to fine-grained yellowish-weathering sandstone with some thin, laterally persistent pebble lenses. The strata grade upward to white to tan-weathering massive, very fine-grained sandstone and siltstone. The section measures more than 250 feet in thickness. The pebble lenses in the lower part of the Empire Formation section contain abundant vein quartz and chert which are rare constituents in the conglomerates of the underlying sandstone of Floras Lake (Addicott, in preparation).

Figure 29. Late Middle Miocene Unconformity: STOP 9. The upper lower and middle Miocene sandstone of Floras Lake is unconformably overlain by late Miocene sandstones of the Empire Formation. This photo shows the unconformity (diagonally from upper left to lower right corners) with blocks of Floras Lake sandstone incorporated within the basal Empire Formation.

Mollusks are the principle fossils of the Empire Formation. Commonly occuring species include Lucinoma annulata, Macoma cf. M. calcarea, Nuculana sp., Portlandia sp., Compsomyax cf. C. subdiaphena, and Cnesterium scissurata. The molluscan fauna and sedimentary structures suggest deposition in an intertidal to shallow subtidal environment with a general deepening upsection (Addicott, in preparation).

Mollusks in the lower 100 feet of the Empire Formation are referable to the late Miocene Wishkahan Molluscan Stage (Addicott, 1976). Species from the Empire Formation at Cape Blanco that are restricted to the Wishkahan Stage include Acila blancoensis, Glycymeris gabbi, Tellinella merriami, and Opalia wishkahensis (Addicott, in preparation).

Continue southward along the cliffs to the siltstone outcrops of the Empire Formation just north of Goldwasher's Gully.

STOP 10: EMPIRE FORMATION: The upper Empire Formation fine-grained sandstone and siltstone contain a low diversity molluscan fauna characterized by Portlandia, Nuculana, Compsomyax, Lucinoma, and Cnesterium, suggesting a middle to outer sublittoral environment. The mollusks are not age diagnostic, but are correlated with the Graysian Molluscan Stage of western Washington (Addicott, 1976) based upon diatoms. Diatom florules assigned to the late Miocene, North Pacific Diatom Zone XIV of Schrader (1973) have been collected from both the upper Empire Formation at Cape Blanco and from siltstones of upper Montesano Formation of Fowler (1965) (J. Barron, written commun., 1979). The diatomaceous Montesano siltstones are within the type section of the Graysian Molluscan Stage (Addicott, in preparation).

Continue south to the mouth of Goldwasher's Gully where a paved road provides access to the beach (Figs. 21-j and 30).

STOP 11: EMPIRE/PORT ORFORD UNCONFORMITY AND LOWER PORT ORFORD FORMATION: At this stop walk seaward as far as possible to view the overall stratigraphic relationships using figures 23 and 30 for orientation.

NOTE: Considerable differences of opinion exist concerning the use of the names Port Orford Formation and Elk River Beds. The usage presented here follows that of Baldwin (1945) with the exception of Baldwin's uppermost Elk River Beds which are here considered to be a marine terrace deposit unconformably overlying the Elk River Beds (Addicott, 1964; Clifton and Boggs, 1970). For a complete discussion of stratigraphic nomenclature see Roth (1979).

In the cliff face north of Goldwasher's Gully are three rock units. The lower consists of the light colored upper Empire Formation siltstone and sandstone. Unconformably overlying the Empire Formation is the Port Orford Formation of Baldwin (1945) consisting of dark-colored conglomerate overlain by lighter-colored sandstone.

In the cliff face south of Goldwasher's Gully the full 180-foot-thick section of the Port Orford Formation is exposed and is overlain by the Elk River Beds and marine terrace deposits (Fig. 23). The Port Orford Formation represents a transgressive depositional sequence and the Elk River Beds a regressive depositional sequence. Both formations are considered to be Pleistocene in age (Roth, 1979).

The lower 30 feet of the Port Orford Formation consist of sandstone with pebble conglomerate lenses. This lower unit is unconformably overlain by a 20-foot-thick, poorly sorted, rusty-brown cobble and gravel conglomerate locally containing one- to three-foot-thick lenses of gray, carbonaceous, fine-grained clayey sandstone and siltstone. The intraformational unconformity is an angular discordance where the pebbly sandstone of the lower sequence is truncated and overlain by the cobble and gravel conglomerate. South of the gully the angular unconformity appears less marked as the cliff face swings parallel with the strike of the unconformity (Roth, 1979). These relationships are best exposed in the gully at the east side of Goldwasher's Gully road. North of the road the lower pebbly sandstone unit is preserved only in down-faulted blocks (Fig. 23). These faults do not extend upward into the conglomerate of the Port Orford Formation. Roth (1979) suggests assigning a separate formational name to the unconformity-bounded pebbly sandstone which is here included as the basal unit of the Port Orford Formation. The lenticular nature of the conglomerate within the sandstone, the lenticular bedding and imbricated cobbles of the conglomerate, and the absence of marine fossils in both units, suggests that both were deposited in fluvial environments.

Higher in the cliffs a fining upward sequence of sandstone and clayey sandstone of the upper Port Orford Formation is exposed. The sandstone forms a slope until the amount of silt becomes sufficient to make the sandstone more erosionally resistant and it forms a series of vertical faces. The two principle breaks in the vertical faces occur at a lower six-inch-thick, well-sorted, poorly consolidated sandstone and an upper six-inch-thick conglomerate (Fig. 22). These two thin units serve as marker beds for correlation of the cliff face sections south of Goldwasher's Gully (STOPS 11-13).

Figure 30. Outcrops at Goldwasher's Gully: Stop 11. The road at Goldwasher's Gully descends through the Pleistocene Port Orford Formation, and flatens and turns left (right in photo) at the contact with the unconformably underlying late Miocene Empire Formation. (See Figs. 22 and 23).

After becoming oriented to the distribution of rock types, within the cliff face exposures of the Port Orford Formation, approach the outcrops for close examination of the rock types and sedimentary structures. The lower pebbly sandstone and conglomerate crop out only at this stop. Southward they dip below beach level.

Climb the cliff face to the top of the conglomerate along the grassy landslide surfaces. Conformably overlying the conglomerate is a light-brown sandstone about 40 feet thick. Lenses of pebbles occur within this unit. Fossils are absent and sedimentary structures are generally low angle and planar suggesting beach deposition. Pebble-filled burrows occur toward the top of the brown sandstone unit. The brown sandstone is gradationally overlain by silty sandstone characterized by abundant silt-cored burrows (Fig. 31) and are suggestive of lower fore-shore deposition. The contact between the brown sandstone and burrowed silty sandstone is locally characterized by convolute bedding suggestive of dewatering processes.

The cliffs steepen at this interval and it is suggested that further observations be made at STOPS 12 and 13 where the upper units of the Port Orford Formation dip to beach level.

Returning to the beach, walk one-half mile south from Goldwasher's Gully past the valley of an old Sixes River tributary (R. Janda, pers. commun., 1979), past the small pyramidal erosional remnant of Port Orford Formation sandstone, to the north end of the next set of cliffs (Fig. 23). The units of the Port Orford Formation can be correlated by using the six-inch sandstone and six-inch conglomerate marker beds both which erode rapidly leaving small reentrants in the cliff face.

STOP 12: BIOTURBATED SILTY SANDSTONE OF THE PORT ORFORD FORMATION: The bioturbated silty sandstone unit of the Port Orford Formation crops out at beach level in rounded bluffs just north of the back beach dunes. The burrows are most typically clay-cored and about one inch in diameter. They are similar to the trace fossil Thallasinoides (Fig. 31). Casts of the pelecypods Clinocardium and Macoma, and barnacles of the genus Balanus, occur in these silty sandstones. The marker conglomerate mentioned above is exposed at the north end of the outcrop about 20

Figure 31. Port Orford Formation: STOP 12. Part of the Port Orford Formation is extensively bioturbated. The burrows, shown in this photo, are clay-cored and are similar to the trace fossil Thallasinoides.

Figure 32. Port Orford Formation and Elk River Beds: STOP 13. This bluff outcrop exposes the uppermost gray-weathering Port Orford Formation overlain by the darker gray sands of the Elk River Beds. The vertical outcrop at the bluff top is a marine terrace sequence (see Fig. 36).

feet up the bluff. The conglomerate is generally six-inches-thick and locally thickens to eighteen-inches. It is interpreted to be a storm-lag deposits. The gravel is locally fossiliferous with the most common mollusks being Clinocardium meekianum baldwini, Nassarius fossatus, and Olivella pycna with Siliqua oregonia, Fusitriton oregonensis, Nucella lamellosa, and Mitrella gausapata less common (Roth, 1979). The molluscan fauna consists of both inner sublittoral and rocky intertidal associations, suggesting transport of the intertidal elements into deeper water during storms which formed the fossiliferous storm-lag-conglomerate deposits.

Above the conglomerate, bioturbation becomes less pervasive, the clay content increases, and the occurrence of molluscan fossils increases, all as a consequence of the deepening waters of the transgression. The clayey sandstone is the blue argillaceous sandstone of Baldwin's (1945) uppermost Port Orford Formation. At this stop it forms a nearly inaccessable cliff face and will be examined more closely at STOP 13.

Continue south along the beach. This part of the traverse is best made along the wet sand area looking back at the cliffs from a distance. The cliff outcrops are partially obscured by landslides, vegetation, and dunes. The blue argillaceous sandstone of the Port Orford Formation crops out as a vertical face with little or no vegetation. It is overlain by less erosionally resistent gray sandstone of the Elk River Beds which are often densely vegetated and form stair-stepped slopes. The contact between these two units (Fig. 32) provides a good marker horizon for correlating exposures along the cliff face. The cliff top is capped by late Pleistocene terrace deposits which form a vertical face above the Elk River Beds.

STOP 13: PORT ORFORD FORMATION/ELK RIVER BEDS CONTACT: About three-tenths of a mile south of STOP 12 the blue argillaceous sandstone of the uppermost Port Orford Formation dips to beach level (Fig. 32). From this point south the cliffs retreat landward along the northern meander loop of Elk River.

The blue argillaceous sandstone marks the maximum transgression of the Port Orford Formation - Elk River Beds sequence. This is shown both by the fine-grained nature of the rocks and by the faunas. The blue argillaceous sandstone becomes finer-grained upsection and fossils become more abundant. Two major shell layers, interpreted as storm-lag-deposits, occur within the upper 20 feet of the 50-foot-thick blue argillaceous sandstone. The molluscan fauna is dominated by *Macoma lipara*, *Macoma nasuta*, *Mitrella gausapata*, *Nassarius fossatus*, and *Olivella pycna*. *Katherinella subdiaphana*, *Cryptomya californica*, and *Thracia* n. sp. are also common. The fauna suggests inner to middle neritic water depths (Roth, 1979). The associated foraminiferal fauna is of low diversity (average 6 species/sample) and is characterized by *Elphidiella nitida*, *Bucella frigida*, *Elphidium frigidam*, *Polymorphina charlottensis*, and *Trichohylus ornatissima* (K. McDougall, pers. commun., 1979). The foraminiferal fauna suggests quiet water of inner neritic depths with a slight increase in water depth upsection.

The blue argillaceous sandstone is overlain by the gray fine-grained sandstone of the Elk River Beds of Baldwin (1945). The contact forms a marked color and topographic break in the sea cliffs. Diller (1902, 1903) and Baldwin (1945) considered this contact to be an unconformity. Close examination of the contact will show that it is gradational from the clay-rich blue argillaceous sandstone below to the moderately well sorted, friable gray sandstone above. Roth (1979) discusses earlier interpretations of this contact.

Continue walking south several hundred feet to the series of cliff face amphitheaters where the Elk River Beds are well exposed and easily accessible.

STOP 14: ELK RIVER BEDS: The Elk River Beds consist of unconsolidated, gray, fine-grained sandstone which is locally highly fossiliferous. The unit is as much as 120-feet-thick and coarsens upward to unfossiliferous conglomeratic sandstone reflecting the regressive phase of the Port Orford - Elk River transgressive-regressive cycle. The Elk River Beds as used here are restricted from Baldwin's (1945) usage. The upper 30 to 50 feet of the cliff face section is considered to be part of a late Pleistocene marine terrace deposit unconformably overlying the gray sandstones of the Elk River Beds (Addicott, 1964; Clifton and Boggs, 1970). This unconformity is readily apparent in the vicinity of Goldwasher's Gully, but less so at this stop where the terrace deposits and Elk River Beds are both nearly horizontal and concordant. A color change from the gray of the Elk River Beds to the yellowish terrace deposits, and a break in slope marks the unconformity (Roth, 1979).

In the lower 30 feet of the Elk River Beds are a number of shell layers referred to as the Psephidia beds (Clifton and Boggs, 1970) (Fig. 33). These fossiliferous beds contain a molluscan fauna of over 50 species dominated by Psephidia aff. P. barbarensis, Polinices pallidus, Solariella obscura, Mitrella gausapata, Nassarius perpingius, and Propebela cf. P. fidicula (Roth, 1979). Clifton and Boggs (1970) interpreted the predominantly concave-up orientation of Psephidia shells as the result of deposition in a wave-swept shallow marine environment. Addicott (pers. commun. in Clifton and Boggs, 1970) interpreted the faunal assemblage to indicate deposition in less than 90 feet of water. These shelly beds contain abundant foraminifers. The low diversity foram. fauna (average 6 species/sample) is dominated by Elphidiella nitida and Elphidium frigidum (average 72% of specimens) (K. McDougall, pers. commun., 1979). Associated species are Brucella frigida, Buliminella elegantissima, and Cibicides lobatus. This fauna suggests inner neritic water depths probably at the deeper part of this zone (Bandy, 1950; K. McDougall, pers. commun., 1979).

The Psephidia beds are grouped into lower cross-stratified (hummocky bedding) beds and upper cross-stratified and bioturbated beds (Figs. 33 and 35). Below the lower of these two sets of Psephidia beds, and elsewhere in the sequence, are distinctive trace fossils resembling "sunbursts" (Figs. 33-34). The origin and taxonomic assignment of these "sunburst" structures is unknown.

The Psephidia beds become less abundant upsection and grade into unfossiliferous pebbly sandstone. About midway upsection within the Elk River Beds is a conglomerate about one foot thick which serves as a marker bed for correlating exposures of this unit. The remainder of the section of Elk River Beds is unfossiliferous and increasingly coarse, reflecting the final regressive phase of the Port Orford-Elk River transgressive-regressive cycle.

Continue climbing the cliff (or walking south along the cliffs) to examine the overlying marine terrace deposits.

STOP 15: TERRACE DEPOSITS: The upper 30 to 50 feet of cliff face exposures consists of sandstone and conglomerate marine terrace deposits (Fig. 36). Janda (pers. commun., 1979) has recognized a discontinuously preserved basal transgressive phase of back beach or surf zone deposits resting upon the wave cut platform, and an overlying regressive phase which includes a variety of sedimentary structures indicative of upsection shallowing: from near wave base (hummocky bedding); to surf zone (complex on-shore, off-shore, and long-shore cross stratification); to back beach berm and fore-shore (parallel stratification, thin but laterally persistent clay beds, buried soil zones, and inversely graded sands and black sands); to aeolian and alluvial deposits (well sorted cross-stratified sands and poorly sorted conglomerates). These marine terrace deposits are correlative with the terrace deposit at STOP 3, and are late Pleistocene in age (Addicott, 1964; Roth, 1979).

This stop ends the traverse and the Cape Blanco segment of the field trip.

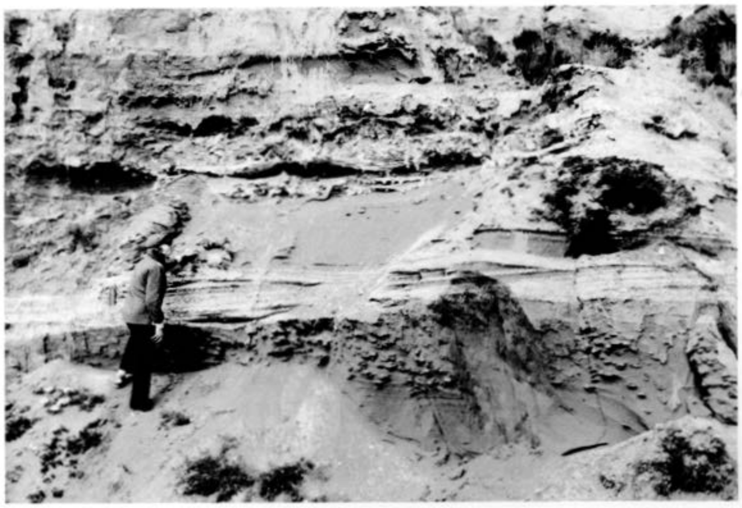

Figure 33. Elk River Beds: STOP 14. The Elk River Beds contain a large shallow marine fossil assemblage. The cross laminated shell beds are composed predominantly of the clam *Psephidia*. The upper *Psephidia* beds of this photo are bioturbated (Fig. 35). Below the lower *Psephidia* beds are numerous "sunburst" structures. (Fig. 34).

Figure 34. Elk River Beds: STOP 14. The "sunburst" structures of the Elk River Beds, shown in this photo, are considered to be biogenic.

Figure 35. Elk River Beds: STOP 14. The bioturbated upper *Psephidia* beds of Figure 33 are shown in this photo. The *Psephidia* shells line the wedge shaped burrows.

Figure 36. Coastal Terrace Deposit: STOP 15. The marine terrace abrasion surface is covered by 30 to 50 feet of marine to nonmarine sandstone and conglomerates. The unit is characterized by rapid lateral facies changes of alluvial, dune, backbeach, foreshore, and subtidal deposits.

REFERENCES CITED

Addicott, W. O., 1964, A late Pleistocene invertebrate fauna from southwestern Oregon: Journal of Paleontology, v. 38, no. 4, p. 650-661.

_____1976, Neogene molluscan stages of Oregon and Washington, in Neogene Symposium: Society of Economic Paleontologists and Mineralogists, Pacific Section, San Francisco, Calif., April 1976, p. 95-115.

_____in preparation, Biostratigraphy of the marine Neogene sequence at Cape Blanco, southwestern Oregon.

Allen, J. E., and Baldwin, E. M., 1944, Geology and coal resources of the Coos Bay quadrangle: Oregon Department of Geology and Mineral Industries Bulletin 27, 153 p.

Allison, R. C., and Addicott, W. O., 1976, The North Pacific Miocene record of Mytilus (Plicatomytilus), a new subgenus of Bivalvia: U.S. Geological Survey Professional Paper 962, 21 p.

Armentrout, J. M., 1967, The Tarheel and Empire Formations - geology and paleontology of the type sections, Coos Bay, Oregon: University of Oregon, Eugene, Oregon, Master's Thesis, 155 p., unpublished.

_____1973, Origin of the Coos Conglomerate, Coos Bay, Oregon: Geological Society of America, Abstracts with Programs, v. 5, no. 1, p. 4.

_____1975a, Molluscan biostratigraphy of the Lincoln Creek Formation, southwest Washington: in Weaver, D. E. (ed.), Paleogene Symposium and selected technical papers, Annual Meeting, Pacific Sections American Association of Petroleum Geologists, Society of Economic Paleontologists and Mineralogists, Society of Economic Geophysicists, Long Beach, California, p. 14-48.

_____1975b, Burrowing and boring molluscan faunas of the Pleistocene terraces of southwestern Oregon: American Association of Petroleum Geologists Annual Meeting Abstracts, vol. 2, p. 1-2.

_____1978, A new Miocene formation at Cods [Coos] Bay, Oregon: American Association of Petroleum Geologists, Society of Economic Geophysicists, Society of Economic Paleontologists and Mineralogists, Pacific Sections, 53d Annual Meeting, Sacramento, Calif., Program, p. 12-13.

Baldwin, E. M., 1945, Some revisions of the late Cenozoic stratigraphy of the southern Oregon coast: Journal of Geology, v. 53, no. 1, p. 35-46.

_____1966, Some revisions of the geology of the Coos Bay area, Oregon: Ore Bin, v. 28, no. 11, p. 189-203.

_____1974, Eocene stratigraphy of southwestern Oregon: Oregon Department of Geology and Mineral Industries Bulletin 83, 40 p.

Baldwin, E. M., Beaulieu, J. D., Ramp, L., Gray, J., Newton, V. C., Jr., and Mason, R. S., 1973, Geology and mineral resources of Coos County, Oregon: Oregon Department of Geology and Mineral Industries Bulletin 80, 82 p.

Bandy, O. L., 1944, Eocene Foraminifera from Cape Blanco, Oregon: Journal of Paleontology, v. 18, no. 4, p. 366-377.

_____1950, Some later Cenozoic Foraminifera from Cape Blanco, Oregon: Journal of Paleontology, v. 24, no. 3, p. 269-281.

Beaulieu, J. D., 1971, Geologic formations of western Oregon: Oregon Department of Geology and Mineral Industries Bulletin 70, 72 p.

Beaulieu, J. D., and Hughs, P. W., 1976, Land use geology of western Curry County, Oregon: Oregon Department of Geology and Mineral Industries Bulletin 90, p. 148.

Bird, K. J., 1967, Biostratigraphy of the Tyee Formation (Eocene), southwestern Oregon: University of Wisconsin, Doctoral Thesis, 209 p., unpublished.

Clifton, H. E., and Boggs, S., Jr., 1970, Concave-up pelecypod (Psephidia) shells in shallow marine sand, Elk River Beds, southwestern, Oregon: Journal of Sedimentary Petrology, v. 40, no. 3, p. 888-897.

Cushman, J. A., Stewart, R. E., and Stewart, K. C., 1947, Five papers on Foraminifera from the Tertiary of western Oregon: Oregon Department of Geology and Mineral Industries Bull. 36, pts. 111 and IV, p. 57-93.

Dall, W. H., 1909, The Miocene of Astoria and Coos Bay, Oregon: U.S. Geological Survey Professional Paper 59, 278 p.

Detling, M. R., 1946, Foraminifera of the Coos Bay lower Tertiary, Coos County, Oregon: Journal of Paleontology, v. 20, no. 4, p. 348-361.

Diller, J. S., 1902, Topographic development of the Klamath Mountains (California and Oregon): U.S. Geological Survey Bulletin 196, p. 1-69.

_____1903, Description of the Port Orford quadrangle, Oregon: U.S. Geological Survey Geologic Atlas, Folio 89, 6 p.

Dott, R. H., Jr., 1962, Geology of the Cape Blanco area, southwest Oregon: Ore Bin, v. 24, no. 8, p. 121-133.

_____1966, Eocene deltaic sedimentation at Coos Bay, Oregon: Journal of Geology, v. 74, no. 4, p. 373-420.

_____1971, Geology of the southwestern Oregon Coast west of the 124th meridian: Oregon Department of Geology and Mineral Industries Bulletin 69, 63 p.

Dott, R. H., Jr., and Bird, K. J., 1979, Sand transport through channels across an Eocene shelf and slope in southwestern Oregon, U.S.A.: Society of Economic Paleontologists and Mineralogists Special Publication no. 27, in press.

Durham, J. W., 1953, Miocene at Cape Blanco, Oregon (abs.): Geological Society of America Bulletin, v. 64, no. 12, pt. 2, p. 1504-1505.

Ehlen, Jr., 1967, Geology of State Parks near Cape Arago, Coos County, Oregon: Ore Bin, v. 29, no. 4, p. 61-82.

Evans, J. W., 1967, Relationship between Penitella penita (Conrad, 1837) and other organisms of the rocky shore: Veliger, v. 10, no. 2, p. 148-151.

Fowler, G. A., 1965, The stratigraphy, Foraminifera, and paleoecology of the Montesano Formation, Grays Harbor County, Washington: University of Southern California, Los Angeles, California, Doctoral thesis, 354 p., unpublished.

Griggs, A. B., 1945, Chromite-bearing sands of the southern part of the coast of Oregon: U.S. Geological Survey Bulletin 945-E, 150 p.

Moore, E. J., 1963, Miocene mollusks from the Astoria Formation in Oregon: U.S. Geological Survey Professional Paper 419, 109 p. (1964).

Ray, C. E., 1967, Fossil marine mammals of Oregon: Systematic Zoology, v. 25, p. 420-436.

Rooth, G. H., 1974, Biostratigraphy and paleoecology of the Coaledo and Bastendorff Formations, southwestern Oregon: Oregon State University, Corvallis, Oregon, Doctoral Thesis, 270 p., unpublished.

Roth, Barry, 1979, Late Cenozoic marine invertebrates from northwest California and southwest Oregon: University of California Berkeley, California, Doctoral Thesis, 803 p., unpublished.

Ryberg, P. T., 1978, Lithofacies and depositional environments of the Coaledo Formation, Coos County, Oregon: University of Oregon, Eugene, Oregon, Master's Thesis, 159 p., unpublished.

Schrader, H. J., 1973, Cenozoic diatoms from the northeast Pacific, Leg 18: Deep Sea Drilling Project Initial Reports, v. 18, p. 673-798.

Snavely, P. D., Jr., and Wagner, H. C., 1963, Tertiary geologic history of western Oregon and Washington: Washington Division of Mines and Geology Report of Investigations 22, 25 p.

Tipton, Ann, 1975, Foraminiferal biostratigraphy of the Late Eocene to Early Oligocene type Bastendorff Formation, near Coos Bay, Oregon: in Weaver, D.E. (ed.), Paleogene Symposium and selected technical papers, Annual Meeting, Pacific Sections American Association of Petroleum Geologists, Society of Economic Paleontologists and Mineralogists, Society of Economic Geophysicists, Long Beach, California, p. 563-585.

Turner, F. E., 1938, Stratigraphy and mollusca of the Eocene of western Oregon: Geological Society of America Special Paper 10, 130 p.

Weaver, C. E., 1945, Stratigraphy and paleontology of the Tertiary formations at Coos Bay, Oregon: University of Washington Publications in Geology, v. 6, no. 2, p. 31-62.

Wolfe, J. A., and Hopkins, D. M., 1967, Climatic change recorded by Tertiary land floras in northwestern North American, in Hatai, Kotora, ed., Tertiary correlations and climatic changes in the Pacific: Eleventh Pacific Science Congress, Tokyo, 1967, p. 67-76.

FIELD TRIP GUIDE:

GEOMORPHOLOGY AND HYDROLOGY IN THE H. J. ANDREWS

EXPERIMENTAL FOREST, WESTERN CASCADES

F. J. Swanson
R. D. Harr
R. L. Fredriksen

U.S Department of Agriculture, Forest Service
Forestry Sciences Laboratory
Corvallis, Oregon

March 1980

INTRODUCTION

The H. J. Andrews Experimental Forest comprises the entire 6,100 ha Lookout Creek drainage about 60 km east of Eugene in the McKenzie River basin (Figure 1). This area was established as an Experimental Forest in 1948 by the USDA Forest Service. Management of the Forest was carried out jointly by two arms of the U.S. Forest Service--the Willamette National Forest and the Pacific Northwest Forest and Range Experiment Station. Research activities during the first two decades of the Forest focused on problems in applied forestry such as regeneration, design of road networks, logging systems engineering, and management impacts on soil erosion and water quality. During this period about 20 percent of the Forest was clearcut and road right-of-way (20 m width) was developed over about 3 percent of the area. In the past decade, use and management of the Forest have included two aditional areas of emphasis: (1) basic research on the forest and stream ecosystems, and (2) baseline monitoring of key environmental variables and ecosystem properties.

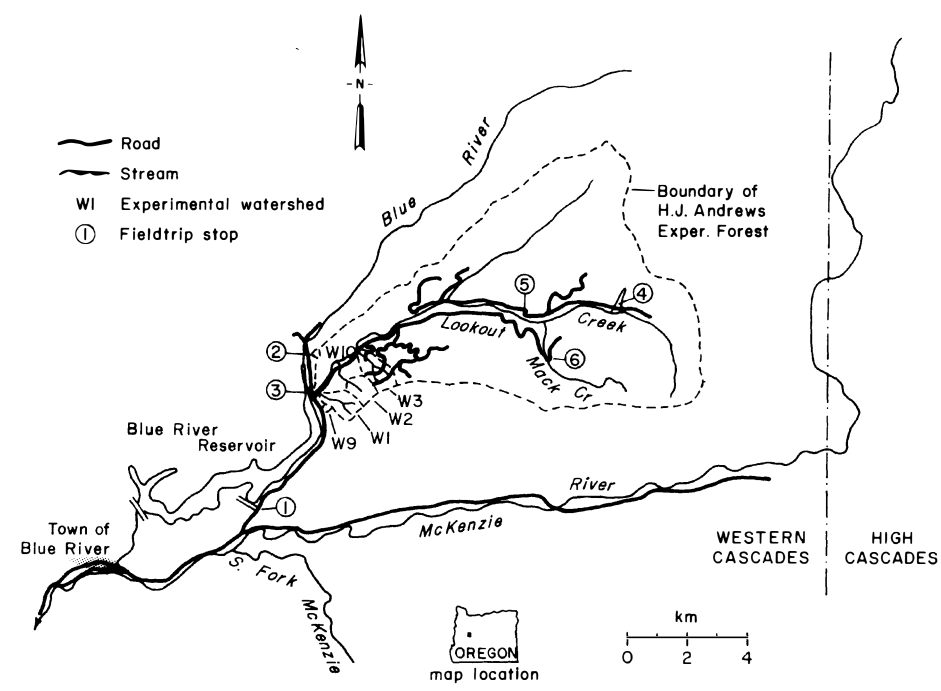

Figure 1. Location map.

Much of the basic ecosystem research has occurred since 1969 when the Forest became a primary site for research by the Coniferous Forest Biome of the U.S./International Biological Program funded by National Science Foundation. Many of the studies started under the Biome program led to the numerous ongoing research activities currently supported at a level of more than $1,000,000 per year by U.S. Forest Service, National Science Foundation, Oregon State University, and other organizations. Use of the Forest for long-term monitoring of environmental and ecological parameters has been formalized by its designation as (1) a site in UNESCO's Biosphere Reserve Program (1974) and (2) the first Experimental Ecological Reserve (1977) established by the National Science Foundation. Monitoring activities include standard meteorology observations, stream discharge and water chemistry monitoring, and periodic sampling of vegetation plots, stream organic debris, and channel cross-sections.

Although most of the basic and applied forest ecosystem research and baseline monitoring activities in the Forest are biologically oriented, geomorphology and soils research have been an important part of the studies since the early 1950's. Steep terrain, mass movement-prone soils, and dense forest vegetation set the stage for many interesting interactions among vegetation, geomorphic processes, and forest practices. Research on these interactions occurs at three scales: (1) forest-wide inventories of mass movement features, (2) small watershed studies of sediment sources and yields, and (3) measurements of rates of individual processes (Tables 1 and 2). This field trip examines geomorphic features and processes at each of these scales.

GENERAL CHARACTERISTICS OF THE ANDREWS FOREST

The Andrews Forest lies at the east margin of the western Cascade Range in terrain described on an early map as "heavily timbered ridges separated by immense ravines" (Pengra, 1863). The Forest is predominantly timbered with 400 to 500 year-old stands dominated by Douglas-fir (*Pseudotsuga menziesii*), western hemlock (*Tsuga heterophylla*), and western redcedar (*Thuja plicata*). Portions of the watershed were burned partially or fully in about 1840, and the headwaters of Mack Creek burned in about 1900. The "immense ravine" of Lookout Creek valley stretches from 420 to 1,615 m in elevation and hillslope gradients over 70 percent are common.

Annual precipitation averages 230 cm, 80 percent of which falls between October and April during long-duration, low-intensity frontal storms. Snow is common at low elevations, but rarely persists longer than 2 weeks and generally melts in several days. Permanent winter snowpack occurs above 1,000 to 1,200 m elevation. Major floods typically occur as a result of rain augmented by snowmelt.

Soils in the area have loamy surface horizons, ranging from silty-clays to sandy and gravelly loams. Because of aggregation of primary soil particles by organic matter and other agents, porosity of surface soils is 60 to 70 percent, over half of which is macropore space (Ranken 1974). Subsoil porosities are also high, ranging from 50 to 60 percent, of which about 20 percent is macropore space. The pore-size distribution of the soil accounts for two important hydrologic properties: (1) all water enters the soil and travels by subsurface flow to streams (Harr, 1977), because soil permeabilities are up to several hundred times greater than rainfall rates, and (2) soil is able to retain 30-40 cm of water in its top 120 cm (Dyrness, 1969) which is an important water source for the dense forest vegetation during the dry summers. These conditions of high soil permeability combined with steep slopes cause headwater streams to respond very quickly to changes in rainfall rate (Harr, 1977).

Bedrock at elevations below about 850 m is composed of a variety of hydrothermally altered volcaniclastic rocks of the late Oligocene to early Miocene Little Butte Formation (Peck et al., 1964, Swanson and James, 1975a). The western end of the Forest is cut by numerous steeply dipping, northwest-trending dikes. Little Butte Formation rocks are overlain by ash flow and basaltic andesite lava flows of the Miocene Sardine Formation which crop out up to elevations of about 1,220 m. Ridge crests along the eastern and southern boundaries of the Forest are capped with thick andesite lava flows with K-Ar ages in the range of about 4 to 6 million years.

Table 1. Experimental watersheds in the H. J. Andrews Experimental Forest. Forests in watersheds 1, 2, 3, 9, and 10 were 400 to 500 year old Douglas-fir--western hemlock stands. Watersheds 6, 7, and 8 were 100-130 year old Douglas-fir stands.

Watershed no.	Area (ha)	Elevation (m) Min.	Max.	Management history	Water & sediment yield, start of record W[1/]	C	S	B
1	96	460	990	100 percent clearcut (1962-1966)	1953	1962	1957	1957
2	60	530	1,070	Control	1953	1962	1957	1957
3	101	490	1,070	6 percent roads (1959) 25 percent clearcut (1963)	1973	1962	1957	1957
6	13	880	1,010	100 percent clearcut (1974)	1964	1972	1972	--
7	15	910	1,020	100 percent partial cut (1974)	1964	1972	1972	--
8	21	960	1,130	Control	1964	1972	1972	--
9	9	425	700	Control	1967	1969	1969	1973
10	10	425	700	100 percent clearcut (1975)	1967	1969	1969	1973

[1/] W = water discharge; C = water chemistry, typically N, P, K, Ca, Na, Mg; S = suspended sediment, C and S sampled with grab samples and pumping proportional sampler (Fredriksen, 1969); B = bedload sampled in ponding basin.

Table 2. Erosion process studies in the H. J. Andrews Experimental Forest

Erosion process monitoring

Process	Sites	Methods	Duration of record
Creep	Both straight and hummocky slopes	Inclinometer tubes	1969 to present and shorter
Earthflow	One site, upper Lookout Creek	Stake arrays, inclinometer tubes, crackmeter, theodolite survey	1974 to present 1974 to present 1976 to present 1976 to present
Surface erosion	Steep slopes in WS1, WS9, WS10, and other forest sites	Collector boxes, 0.5 and 2.4 m long	1974 to present and shorter
Channel changes	6 sites, small to large streams	Monumented cross-sections	1978 to present
Forest-wide inventories of mass movement processes			
Debris avalanches	All of Andrews	Ongoing inventory of events 75 m^3	1950 to present
Slump-earthflow	All of Andrews	Field and air photo analysis	Some features 6,700+ yrs.

Holocene deposition of thin tephra units completes the history of accumulation of volcanic material in the Lookout Creek drainage. Mazama ash with fragments up to about 1 cm diameter rained over the Andrews area about 6,700 radiocarbon years ago. Average thickness of initial airfall deposits was probably on the order of 1 cm. Fine-grained (<1 mm diameter) basaltic tephra erupting from the Sand Mountain area (Taylor 1968) probably fell on portions of the Forest about 3,000 radiocarbon years ago. The Mazama ash, weathered to a distinctive yellow color, fell in sufficient abundance to be a useful time marker in analysis of some geomorphic surfaces in the area.

Landscapes of the Andrews Forests have been sculptured by glacial, fluvial, mass movement, and other hillslope processes (Swanson and James, 1975a). Details of glacial history of the area have been obscured by subsequent erosion and redistribution of glacial landforms and deposits. The origin of bouldery deposits in the area is commonly ambiguous. For example, nearly identical bouldery diamictons can be produced by glacial, volcanic, and mass movement processes; and combinations of these three types of processes may all operate on a single batch of earth material. So the glacial history of these areas of the western Cascades has been poorly kept due to rapid removal of the record by other geomorphic processes and presence of anistropic rock types that do not form neat glacial landforms in the first place.

Despite these difficulties glacial processes have clearly influenced higher elevation, north aspect parts of the Lookout Creek drainage (Crandell, 1965, Swanson and James, 1975a). Cirques were formed by small alpine glaciers on the north side of ridges higher than about 1,370 m elevation. Valley wall and bottom glacial deposits derived from headwaters of the Lookout Creek drainage extend as far down valley as about 660 m elevation. The lower end of Lookout Creek drainage was also influenced by damming of lower Blue River by glacial ice in the main McKenzie River valley (Swanson and James, 1975b). The ice dam backed water up into the mouth of Lookout Creek, causing deposition of fine grained, varved quiet water sediments.

Mass movement processes have created distinctive wide spread landforms. Slump-earthflow features, produced by slow, deep-seated mass movements, cover over 25 percent of the landscape in the lower elevation half of the forest underlain by volcaniclastic rocks (Swanston and Swanson, 1976). The heads of most large earthflow features are located at geologic contacts where hard lava flow bedrock caps softer volcaniclastic rock. About a third of the slump-earthflow areas has been active in the past century based on disrupted growth of trees; and some areas are currently active during each wet season. Even the most active earthflows in the area are heavily forested.

Slump-earthflow areas typically have subdued relief, hummocky ground and deranged drainage systems. Active features have open tension and shear cracks, split and tilted trees, and very irregular drainage patterns and channel cross-section geometry. At low flow stream water goes undergound where crack systems intersect stream channels. On flows that have been dormant for progressively longer periods of time there is less evidence of disrupted vegetation and drainage systems. Some earthflows in the Forest have deposits of Mazama ash in poorly drained depressions, suggesting that the hummocky ground existed 6,700 years ago.

Steep terrain in areas of volcaniclastic bedrock and associated soils has been sculptured largely by debris avalanches. These rapid soil mass movements are initiated from the headward tips of incipient drainage depressions ("hollows" of Dietrich and Dunne, 1978), from streamside areas, and infrequently from smooth slopes. Events are commonly triggered as a result of high precipitation on wet soil conditions, and multiple windthrow of trees may also be a contributing factor on forested sites. Debris avalanches are a major mechanism for transfer of soil from slump-earthflow features to streams. Slump-earthflow movement oversteepens the toes of deep-seated failures and causes them to encroach on streams, thus aggravating bank cutting and debris avalanche potential (Swanson and Swanston, 1977). Debris avalanches also take place on the steep headwall areas of some slump-earthflow features.

Small, steep channels in the lower elevation half of the Forest area are also subject to mass movements termed debris torrents. Most debris torrents (82 percent of 38 inventoried events) are initiated as debris avalanches from hillslopes which enter channels and maintain their momentum downstream until they are stopped by obstructions or bends in the channel or simply by decreasing channel gradient (Swanston and Swanson, 1976). Some debris torrents start in channels as a result of flotation of organic debris. Many torrents move through first-order channels and can travel up to a kilometer downstream into lower second- and upper third-order channels. The scouring and exposure of bedrock by debris torrents probably contributes to the incised appearance of many first- through third-order channels in the area. Many small streams are flanked by 2 to 8 m high steep banks of colluvium and bedrock.

Other hillslope processes transport soil from slopes to channels in the Forest, but do not create large scale landforms. Sheetwash and rill erosion are trivial on all but severely disturbed sites due to low precipitation intensities and high infiltration rates. Surface erosion by dry ravel, throughfall and rain drop impact, and freeze-thaw processes is significant on steep slopes. Root throw is also an important soil transport process which does create distinctive, though small scale, landforms. Soil mantle creep and transport of material in solution are subtle, but important, pervasive processes in this terrain.

Fluvial processes, of course, have played important roles in shaping the landscape of Lookout Creek basin. Streams are steep and development of fluvial landforms has been constrained by influences of bedrock, hillslope mass movement processes, and large organic debris derived from adjacent forests. Significant development of flood plains and terraces occurs along streams larger than third-order. Remnants of alluvial fans are located at junctions of smaller streams with fourth- and fifth-order streams (Swanson and James, 1975b). The coarse scale of jointing in the volcanic bedrock produces large clasts that become the boulders and cobbles covering much of the streambed area.

Sediment yield from forested parts of this landscape are at the low end of the range for mountainous terrain. Anderson (1954) estimates 48 $T/km^2/yr$ of suspended sediment yield for the McKenzie River basin, based on samples collected in 1949 and 1950 before much development had occurred. Sediment yield from small forested watersheds in the Forest is about 40 $T/km^2/yr$ composed of dissolved, suspended, and bedload sediment in order of decreasing contribution to total yield (Fredriksen and Harr, 1979, Swanson et al., in press). Removal of vegetation by wildfire and logging results in increased soil erosion and sediment yield (Fredriksen and Harr, 1979, and others).

STOP 1. SADDLE DAM OF BLUE RIVER RESERVOIR

This stop provides an overview of the geographic, geologic, and geomorphic setting of the field trip area and environs (Figure 1). To the north we look across the Blue River Reservoir and into the Blue River drainage. We are on a low divide with the westward flowing McKenzie River south of us. The Lookout Creek drainage and the Andrews Experimental Forest meet Blue River at the head of the reservoir.

We are in the western Cascade geologic and physiographic provinces. Bedrock is comprised entirely of Pliocene and older volcanic and subvolcanic intrusive material, and landforms have been shaped by erosional processes. The boundary with the High Cascades lies about 20 km east of this spot. Steeply dipping, north-trending, normal faults which are down-dropped on the east form the boundary. The High Cascades are predominantly a constructional volcanic landscape formed during the past two million years.

During the Pleistocene, Blue River drained directly into the McKenzie River through this saddle dam area (Swanson and James, 1975b). Pre-latest Wisconsin glaciers from the High Cascade platform and from the South Fork McKenzie River basin flowed down the main McKenzie River valley and blocked the mouth of Blue River. This ice dam formed a lake 30+ m higher than maximum reservoir level and diverted the lower Blue River to its present course. Drilling in the saddle dam area by the Corps of Engineers revealed more than 60 m of glacial deposits forming a natural saddle dam below the man-made saddle dam.

Till, outwash, and varved lake sediments are exposed in the dam area. A wood sample from these deposits is more than 40,000 radiocarbon years old. Along the drive up the east side of the reservoir we pass kame terrace deposits on the valley wall above the road. Bedrock exposed in road cuts is predominantly propylitically altered, green, laharic breccias cut by numerous vertical, northwest-trending dikes.

STOP 2. WATERSHED 10

Watershed 10 (WS10) has been the principal study site of the Oregon phase of the Coniferous Forest Biome research. This 10 ha watershed is probably the most intensively studied piece of ground of this scale in the western hemisphere. Research since 1969 has examined hydrology, vegetation, nutrient cycling, aquatic biology, and geomorphology under both forested and recovering clearcut conditions. The 400 to 500 year-old stand of Douglas-fir, western hemlock, western redcedar, and other tree species (Grier and Logan, 1978) was clearcut with directional falling with jacks and yarded with a skyline system in the summer of 1975. Heavy residues were yarded to the landing and hauled away or burned there. Limb-sized material was hand-cleaned from the channel and piled above high flow line. The overall logging operation was designed to follow practices used in standard Forest Service operations at that time. Companion WS9 about 1.5 km south is maintained in the forested condition as a control.

Geomorphology research in WS10 is comparing erosion under forested and clearcut recovery conditions. We do this by developing erosion budgets, comprehensive assessments of soil and sediment movement by all significant erosion processes. The soil/sediment routing system is viewed as movement of material down slopes and channels from one temporary storage site to another. Storage sites include shallow depressions on slopes that ultimately fail by debris avalanching (Dietrich and Dunne, 1978) and wedges of sediment stored behind logs in streams. Transfer processes between storage sites range from debris avalanches that typically occur on a few percent of the watershed once every few centuries to watershed-wide persistent processes such as surface erosion and solution transfer (Table 3).

Table 3. Process characteristics and transfer rates of organic and inorganic material to the channel by hillslope processes (T/yr) and export from the channel by channel processes (T/yr) for Watershed 10.

Process	Frequency	Area influenced (% of watershed)	Material transfer: Inorganic	Material transfer: Organic
Hillslope processes				
Solution transfer	Continuous	99	3	0.3
Litterfall	Continuous, seasonal	100	0	0.3
Surface erosion	Continuous	99	0.5	0.3
Creep	Seasonal	99	1.1	0.04
Root throw	1/yr	0.1**	0.1	0.1
Debris avalanche	1/370 yr	1–2**	6	0.4
Slump/earthflow	Seasonal*	5–8%	0	0
TOTAL			10.7	1.4
Channel processes				
Solution transfer	Continuous	1	3.0	0.3
Suspended sediment	Continuous, storm	1	0.7	0.1
Bedload	Storm	1	0.6	0.3
Debris torrent	1/580 yr	1	4.6	0.3
TOTAL			8.9	1.0

*Inactive in past century in Watershed 10
**Area influenced by one event.

An erosion budget has been prepared for Watershed 10 in old-growth forest conditions (Table 3). Methods of generating these estimates are described by Swanson et al. (in press). Such a budget provides a basis for comparing processes. For inorganic matter transport the mass movement processes are very important, although they are estimated to occur less frequently than 1 per 300 years under forest conditions. (Note: there are many difficulties in making these estimates, including the dominance of the 30 year record by events triggered in a single storm of a probable return period much greater than 30 years.) The most persistent process, solution transfer, is also very important.

We are now observing changes in the rate of each erosion process during the post-clearcut recovery period. Each transfer process and storage site in the soil/sediment routing system is regulated by a different combination of vegetative factors. Root strength, for example, affects debris avalanche potential, and presence of an organic litter layer moderates surface erosion. Consequently each erosion process has a different response to clearcutting and revegetation.

Substantial increases in suspended and bedload export occurred following logging. Sediment yield is limited by (1) availability of sediment for transport and (2) availability of flowing water, the transporting medium. Snowmelt peak flows from WS10 were actually delayed and smaller the first winter after logging, but rain generated peak flows were not affected significantly (Harr and McCorison, 1979). Changes were attributed to differences in short term snow accumulation and melt. Increased sediment yield has come from increased availability of material from three sources: (1) material input to the channel during the logging operation itself, predominantly fine organics, (2) sediment that entered the channel and was stored behind large debris before logging, but was released from storage when logs were removed in the yarding operation, and (3) soil from post-logging accelerated hillslope erosion.

Erosion monitoring facilities on the watershed include inclinometer tubes, 0.5 m wide surface erosion collectors along the stream perimeter, 2.4 m wide surface erosion collectors on upslope sites, monumented channel cross-sections, sediment ponding basin, and stream gaging facility with proportional pumping sampler (Fredriksen, 1969) for water chemistry and suspended sediment sampling.

STOP 3. EXPERIMENTAL WATERSHEDS 1, 2, AND 3

These watersheds have long, documented histories of land use, research activities, and erosion (Fredriksen 1963, 1965, 1970, Fredriksen and Harr 1979). WS1 was clearcut between 1962 and 1966 using a skyline yarding system and slash was broadcast burned in a hot fire in 1966. WS3 had clearcuts of 5, 9, and 11 ha logged with high lead cable systems and slash was broadcast burned. Roads totalling 2.66 km were built at three levels in the watershed in 1959. Water and sediment yield, precipitation, and vegetation have been monitored since before logging (Table 1, Fredriksen and Harr, 1979, Dyrness, 1973). WS2 has been maintained as a control.

Vegetation removal caused several changes in streamflow characteristics. Removal of forest vegetation reduced both interception and transpiration, allowing more precipitation to leave the watershed by streamflow rather than evaporation. At WS1 initial increases in annual water yields were 45-50 cm, about 75 percent of which occurred during the winter rainy season (Rothacher 1970). Yield increases are diminishing as revegetation proceeds. Summer flows were increased 3-5 times the first few years after logging, but owing to rapid growth of riparian vegetation, such increases have disappeared (Rothacher, 1971). Changes at WS3 have been smaller because of less extensive logging in that watershed.

After logging, peak flows in fall and spring increased up to 2 times because soil water storage remained high due to reduced evapotranspiration (Rothacher, 1973). Large peak flows in winter were largely unchanged because (1) soils in logged and unlogged areas are both recharged by this time and respond similarly to precipitation, and (2) the hydrologic properties of soil were not altered to the extent that surface runoff became significant. On other experimental watersheds in western Oregon, where soil disturbance and compaction by roadbuilding and tractor yarding were much greater than on WS1, size of peak flows has been increased (Harr et al., 1975, Harr et al., 1979).

Variation of annual suspended and bedload (material trapped in sediment basin) sediment yields among watersheds has been great. In the first 14 years following cutting and burning WS1 has yielded 12 times as much particulate matter as WS2. Much of this increase has come from accelerated debris avalanche erosion after clearcutting. Seven debris avalanches (>75 m^3 each) moved soil down slope between 1964 and 1972. About 75 percent of the volume of soil moved by debris avalanches came from sites of current or past slump-earthflow activity, emphasizing the importance of interactions between these two types of processes. Surface erosion processes, particularly dry ravel, also increased substantially (Mersereau and Dyrness, 1972), but most sites of accelerated surface erosion have returned to rates more typical of forested areas. Soil which has entered the channel systems after logging has been routed slowly downstream through the numerous large logs and alder (Alnus rubra) and willow (Salix spp.) riparian vegetation. Despite burning and some physical removal of sediment-trapping organic matter from the main channel, much of the soil eroded from slopes after logging is still stored in the channel system.

WS3, on the other hand, experienced very rapid release of sediment. Most debris avalanche activity in the watershed was related to roads, principally fill slope failures (Fredriksen, 1963, 1965, 1970). The masses of fill material entered steep headwater channels and moved rapidly downstream sweeping up alluvium, colluvium, and streamside vegetation along the way. This series of debris torrents in the major December 1964 storm moved about two-thirds of the total particulate matter export from WS3 over the first 17 years after logging and road construction. About 80 percent of export for the period occurred in two days. Total post-logging yield has been about 90 times that of control WS2.

The debris torrent histories of WS1 and WS3 have determined the contrasts in their sediment yield histories. The road fill failures at the heads of long, steep, straight channels initiated debris torrents which flushed the WS3 channel system. No torrents have flushed the WS1 channels because of a variety of factors, including debris avalanche location in the watershed. WS1 debris avalanches have not had sufficient velocity, volume, and straight down-channel trajectory to trigger debris torrents. Annual sediment yield from WS 1 now exceeds yield from WS3 as sediment is slowly released from storage in the lower WS1 main channel and as soil is eroded from an active earthflow in the upper part of the watershed.

STOP 4. LOOKOUT CREEK EARTHFLOW

This 900 m long and 150 m wide earthflow is moving south into Lookout Creek at an average rate of about 10 cm/yr (Figure 2, Swanson and Swanston, 1977). Bedrock is a variety of volcaniclastic materials capped by a basalt flow which is the source of blocks forming the talus slope at the headscarp. Except for two small clearcut areas, the earthflow is forested, mainly with 400 to 500 year-old trees in the lower half while most trees on the upper half were established following a wildfire in the mid-1800's.

The earthflow landscape is irregular with scattered steep (>60%) slopes, which probably represent vegetated scarps, and many low relief areas, including poorly drained depressions. Drainage pattern and channel cross-sectional geometry are very irregular. The earthflow can be divided into three active blocks in the lower half of the whole earthflow. Each block is bounded by open, lateral shear cracks and a tension crack system across the head (Figure 2). The upper half of the earthflow does not appear to have been active in the last century or so, based on straight growth of trees in that area.

Earthflow movement is monitored with (1) stake arrays (strain rhombs) across active cracks to measure relative surface movement between blocks, (2) inclinometer tubes for

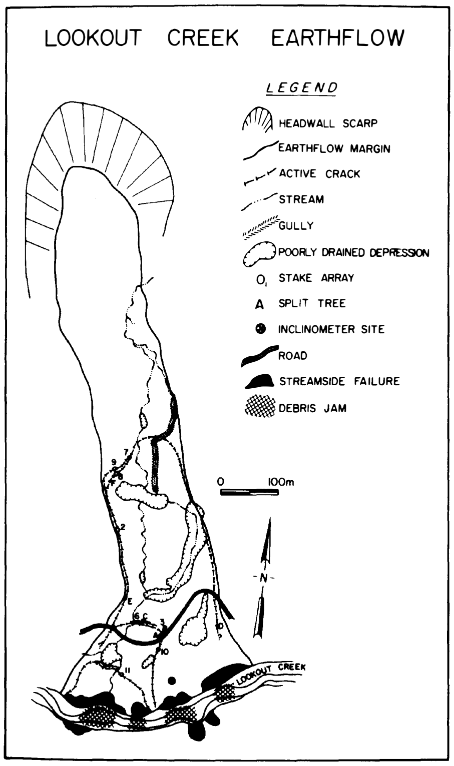

Figure 2. Map of Lookout Creek earthflow. Mapped by G. W. Lienkaemper (from Swanson and Swanston, 1977).

monitoring vertical velocity profiles, (3) crackmeters to record continuously the opening of crack systems, (4) theodolite surveys of points on the earthflow from stable reference points off the earthflow, and (5) analysis of tree rings in scar tissue on live trees being split up the middle because they straddle an active crack (Swanson and Swanston, 1977). Water inputs in rain and snowmelt and groundwater levels are also continuously recorded, so that movement-water input relations can be examined. The purpose of the work is to gain a basic understanding of earthflow behavior so we can better assess impacts of management activities on this erosion process.

The five year record of annual movement from repeat surveys of stake arrays reveals large year-to-year differences in movement, determined by water inputs during current and previous years (Table 4). Very little movement occurred in the 1976-1977 drought year, and this dry period appears to have also caused low total movement rate in the next year. Movement in 1978-1979 was twice that in 1977-1978, although the more recent period had 20 percent less precipitation.

Table 4. Stake array measurements of movement of Lookout Creek earthflow. Stake array 2 measures movement relative to stable ground. Arrays 3 and 6 measure relative movement between two moving blocks. Precipitation data are from WS2 meteorology station.

Stake array	1974-1975	1975-1976	1976-1977	1977-1978	1978-1979**
	Earthflow Movement (cm/yr)				
2	9.6	14.2	0.2	6.1	13.1
3	5.0	8.6	0.7	3.9	9.2
6	no data	5.9	0.7	2.8	5.9
Total precipitation (mm) Oct. 1-June 1	2225	2361	1049	2125	1707

*Located on Fig. 3
**Movement data for this year are preliminary

Comparison of crackmeter and precipitation records indicates tight control of movement rate by water availability (Figure 3). Movement at this site does not begin in the fall until nearly 90 cm of rain has fallen. Once the system is primed with water, movement continues at a slow rate until spring except for periods of accelerated movement in response to storm periods of water input in excess of about 12 cm/24 hr.

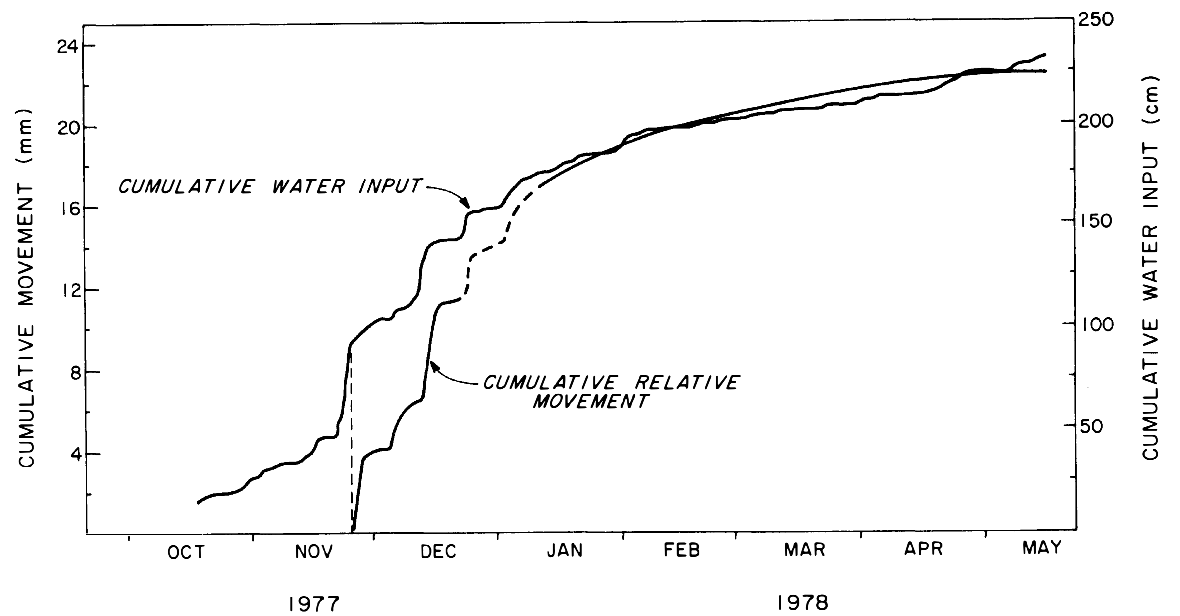

Figure 3. Cumulative water input and relative movement at crackmeter located at site 6 (Fig. 2). Movement curve is dashed for period when only total movement is known.

Sediment delivery to Lookout Creek occurs by bank cutting and streamside slides after long periods of earthflow movement constricting the channel. The last major episode of sediment input to Lookout Creek from this earthflow was during the December 1964 and January 1965 floods.

Earthflow movements can affect the structure and species composition of forest ecosystems. For example, differential movement near stake arrays 7, 8, and 9 (Figure 2) has tipped and split trees, leading to much windthrow, many holes in the canopy, and a multileveled forest with abundant understory vegetation. Close upslope, in areas of no recent earthflow movement, the canopy of Douglas-fir and western hemlock is complete, heavily shading lower levels of the forest and, thereby, greatly limiting understory development.

STOP 5. REVEGETATING DEBRIS AVALANCHES AND TORRENT SITES

This road backslope failed in 1957, entered the channel below the road, and this material moved as a debris torrent downstream to Lookout Creek. The slide scar was planted with Douglas-fir seedlings many of which survived; but they have stunted growth and a chlorotic condition from growing in the nutrient deficient subsoil. The torrent track is now a lush stand of alder overtopped by a few black cottonwood (*Populus trihcocarpa*).

More than 140 such debris avalanches moving greater than 75 m^3 of soil have occurred from forested, clearcut, and road right-of-way sites since 1950 (Dyrness, 1967, Swanson and Dyrness, 1975). All but two events began in soil derived from volcaniclastic bedrock, indicating the strong control of bedrock and soil types on slope stability. In the debris avalanche-prone part of the Forest, rates of debris avalanche erosion from clearcuts and road right-of-way exceed the forest rate by 2.8 and 31 times respectively, based on rates calculated by dividing soil volume moved by 28 years and by the area in each land status at the end of the record. This estimate of management impact on debris avalanche erosion is similar to results of other studies in the Pacific Northwest (Swanston and Swanson, 1976).

This method of measuring management impacts can result in substantial under- or overestimates. Management impacts may be overestimated because (a) forest rates are used as the natural debris avalanche erosion rate, but the actual natural rate should include periods of accelerated erosion following natural disturbances such as wildfire, (b) in the case of roads, analysis on this time scale assesses impacts of some road construction, site location, and maintenance practices no longer employed, and (c) management impacts are only temporary and there may be a one to two decade period of accelerated erosion followed by a long interval of debris avalanche erosion at rates lower than in older forested areas. If (c) is true, cutting may affect the timing of debris avalanche erosion more than the overall long term rate. On the other hand, management impacts for general National Forest land may be underestimated by Andrews Forest data, because logging and roading have generally been conducted with the highest contemporary standards. Furthermore, intensity of timber harvest activities in the Forest has declined markedly since the mid-1960's. These estimates of impact are also conservative because the calculation method uses area in each land status at the end of the inventory period. This is the time of smallest forested area and largest clearcut and road right-of-way areas. Since we divide total volume of soil moved by debris avalanches for the period by these area terms, the forest debris avalanche erosion rate is overestimated and road and clearcut rates are underestimated.

There is need for assessment of debris avalanche impact on long term timber productivity. This involves determining both landscape area impacted by debris avalanches and the recovery of productivity on these sites. General observations suggest that area affected is less than a few percent of the landscape, even in debris avalanche-prone areas; but recovery rate may be so slow that at least one rotation of timber production may be lost.

STOP 6. MACK CREEK

The adjacent clearcut and forested reaches of Mack Creek have been sites of intensive stream ecosystem research since the early 1970's, including studies of conditions and roles of large organic debris in streams. Large woody debris derived from the adjacent forest shapes aquatic habitats, provides nutrients, cover, and substrate for aquatic organisms, and regulates movement of sediment, particulate organic matter, and water through the stream system. Consequently, natural or man-imposed changes in debris conditions affect physical and biological functions of streams.

Debris conditions vary with stream size. Concentrations of coarse woody debris (>10 cm diameter) generally decrease downstream where wider channels have greater transport capability and the canopy is open over the stream, so input of large woody debris is lower. Large debris in first- and second-order streams is randomly distributed along streams, and is generally located where it initially fell, because the stream is too small to move it. Intermediate-sized streams, such as this third-order section of Mack Creek, can move some large pieces of debris at flood flows, but not whole down trees. Therefore, these streams have scattered, distinct accumulations, many of them affecting the full channel width. Large rivers can transport all debris that enters them and they deposit this material high on the banks and on upstream ends of islands. This material then affects the stream only at high flow.

We have studied the history of large debris in Mack Creek by dating log input to the stream with tree-ring analysis (Swanson et al., 1976) and by following changes in debris conditions through time. Generally we have observed scattered inputs during wind storms and this material moves and accumulates on the large, stable debris jams during very high flow events. Maps made in 1975 of Mack Creek above the road crossing (Figures 4 and 5) can be compared with the distribution of logs today to get a measure of variability of debris conditions. Much of the change occurred during a high flow event in November 1977. The main accumulations which were keyed on large, down, old growth trees (MA-13 and MA-16) have remained intact with minor modification. Accumulation MA-14 appears to have washed out because the main piece had decayed and partially collapsed under its own weight. It was, therefore, hit directly, broken up, and washed downstream by the high flow. So in streams of this size, debris conditions change as a result of new inputs, redistribution during high flows, and the slow, continual process of wood decomposition.

Monitoring of this site will continue on a long term basis. Changes are observed by annually mapping any new or moved pieces and by repeat surveys of monumented channel cross-sections. Changes in the adjacent forest will be followed by annual checks of a map showing standing and down live and dead trees in a 2-ha area straddling the creek. Debris conditions in streams of other sizes of the same forest type, and some flowing through younger stands, are being monitored at other sites in the area.

Reprints of cited papers and other literature on research in the H. J. Andrews Experimental Forest are available through the authors or the Resident Manager, H. J. Andrews Experimental Forest, P.O. Box 300, Blue River, Oregon 97413.

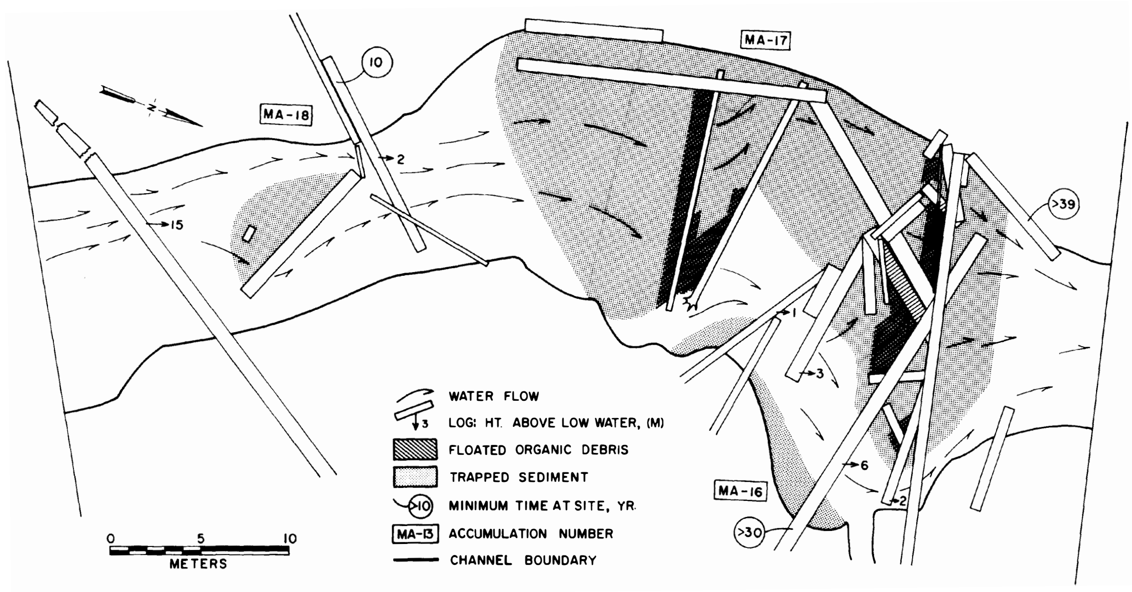

Figure 4. Map of large organic debris and other material in 1975 in section of Mack Creek upstream from section in Figure 5.

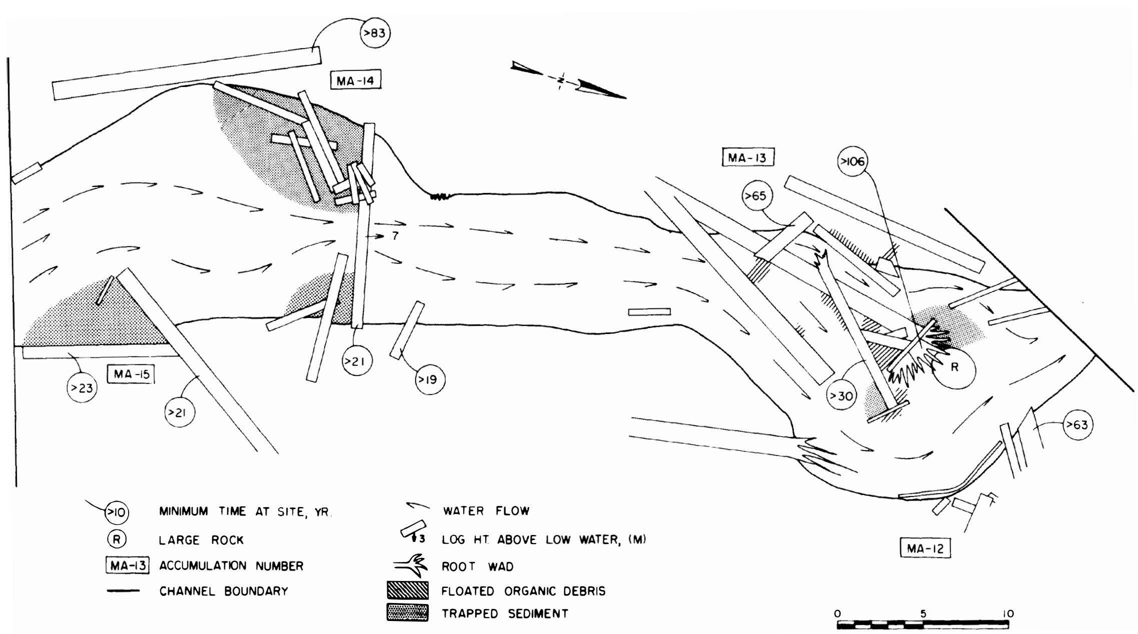

Figure 5. Map of stream section downstream of section in Figure 4. Maps by G. W. Lienkaemper (from Swanson et al., 1976).

REFERENCES

Anderson, H. W., 1954, Suspended sediment discharge as related to streamflow, topography, soil, and land use: Trans. Am. Geophys. Union, v.35, p. 268-281.

Crandell, D. R., 1965, The glacial history of western Washington and Oregon, In The Quaternary of the United States, Wright, H. E., and Frey, D. G. (eds.) Princeton Univ. Press, Princeton, N.J.: p. 341-353.

Dietrich, W. E., and Dunne, T., 1978, Sediment budget for a small catchment in mountainous terrain: Zeit. f. Geomorph., Suppl. Bd. 29, p. 191-206.

Dyrness, C. T., 1967, Mass soil movements in the H. J. Andrews Experimental Forest: USDA For. Serv. Res. Pap. PNW-42, 12 p.

______________, 1969, Hydrologic properties of soils on three small watersheds in the western Cascades of Oregon: USDA For. Serv. Res. Note PNW-111, 17 p.

______________, 1973, Early stages of plant succession following logging and burning in the western Cascades of Oregon: Ecol., v. 54, p. 57-69.

Fredriksen, R. L., 1963, A case history of a mud and rock slide on an experimental watershed: USDA For. Serv. Res. Note PNW-1, 4 p.

______________, 1965, Christmas storm damage on the H. J. Andrews Experimental Forest: USDA For. Serv. Res. Note PNW-29, 11 p.

______________, 1969, A battery powered proportional stream water sampler: Water Resour. Res., v.5, p. 1410-1413.

______________, 1970, Erosion and sedimentation, following road construction and timber harvest on unstable soils in three small western Oregon watersheds: USDA For. Serv. Res. Pap. PNW-104, 15 p.

Fredriksen, R. L., and Harr, R. D., 1979, Soil, vegetation, and watershed management. In Forest soils of the Douglas-fir Region, Heilman, P. E., Anderson, H. W., and Baumgartner, D. M. (eds), Wash. State Univ., Coop. Ext., Pullman: p. 231-260.

Grier, C. C., and Logan, R. S., 1978, Old-growth Pseudotsuga menziesii communities of a western Oregon watershed: biomass distribution and production budgets: Ecol. Monogr., v. 47, p. 373-400.

Harr, R. D., 1977, Water flux in soil and subsoil on a steep forested slope: J. Hydrology, v. 33, p. 37-58.

Harr, R. D., Fredriksen, R. L., and Rothacher, J., 1979, Changes in streamflow following timber harvest in southwestern Oregon: USDA For. Serv. Res. Pap. PNW-249, 22 p.

Harr, R. D., Harper, W. C., Krygier, J. T., and Hsieh, F. S., 1975, Changes in storm hydrographs after roadbuilding and clearcutting in the Oregon Coast Range: Water Resour. Res., v. 11, p. 436-444.

Harr, R. D., and McCorison, F. M., 1979, Initial effects of clearcut logging on size and timing of peak flows in a small watershed in western Oregon: Water Resour. Res., v. 15, p. 90-94.

Mersereau, R. C., and Dyrness, C. T., 1972, Accelerated mass wasting after logging and slash burning in western Oregon: J. Soil and Water Conserv., v. 27, p. 112-114.

Peck, D. L., Griggs, A. B., Schlicker, H. G., Wells, F. G., and Dole, H. M., 1964, Geology of the central and northern parts of the western Cascade Range in Oregon. U.S. Geol. Surv. Prof. Pap. 449, 56 p.

Pengra, B. J., 1863, A diagram of public surveys in Oregon, Surveyor General's Office, Eugene City, reprod. in Oreg. Hist. Quart., v. 79, n. 1.

Ranken, D. W., 1974, Hydrologic properties of soil and subsoil on a steep, forested slope: M.S. thesis, Oreg. State Univ., Corvallis, 117 p.

Rothacher, J., 1970, Increases in water yield following clearcut logging in the Pacific Northwest: Water Resour, Res., v. 6, p. 653-658.

______________, 1971, Regimes of streamflow and their modification by logging, In Forest land uses and the stream environment, symposium proceedings, Morris, J., (ed.), Cont. Educ. Publ., Oreg. State Univ., Corvallis: p. 40-54.

______________, 1973, Does harvest in west slope Douglas-fir increase peak flow in small forest streams?: USDA For. Serv. Res. Pap. PNW-163, 13 p.

Swanson, F. J., and Dyrness, C. T., 1975, Impacts of clearcutting and road construction on soil erosion by landslides in the western Cascade Range: Oregon, Geology, v. 3, p. 393-396.

Swanson, F. J., Fredriksen, R. L., and McCorison, F. M., in press, Material transfer in a western Oregon forested watershed: Chap. in Synthesis Volume, U.S./Internat. Biol. Prog., Conif. For. Biome.

Swanson, F. J., and James, M. E., 1975a, Geology and geomorphology of the H. J. Andrews Experimental Forest, western Cascades, Oregon: USDA For. Serv. Res. Pap. PNW-188, 14 p.

______________, 1975b, Geomorphic history of the lower Blue River-Lookout Creek area, western Cascades, Oregon: Northwest Sci., v. 49, p. 1-11.

Swanson, F. J., Lienkaemper, G. W., and Sedell, J. R., 1976, History, physical effects and management implications of large organic debris in western Oregon streams: USDA For. Serv. Gen. Tech. Rep. PNW-56, 15 p.

Swanson, F. J., and Swanston, D. N., 1977, Complex mass-movement terrains in the western Cascade Range, Oregon: Rev. in Eng. Geol., Geol. Soc. Am., v. 3, p. 113-124.

Swanston, D. N., and Swanson, F. J., 1976, Timber harvesting, mass erosion, and steepland forest geomorphology in the Pacific Northwest, In Geomorphology and Engineering, Coates, D. R. (ed.), Dowden, Hutchinson, and Ross, Inc., Stroudsburg, Pa.: p. 199-221.

Taylor, E. M., 1968, Roadside geology Santiam and McKenzie Pass Highways, Oregon, In Andesite Conference Guidebook, Oreg. Dep. Geol. Min. Ind. Bull. 62,: p. 3-33.